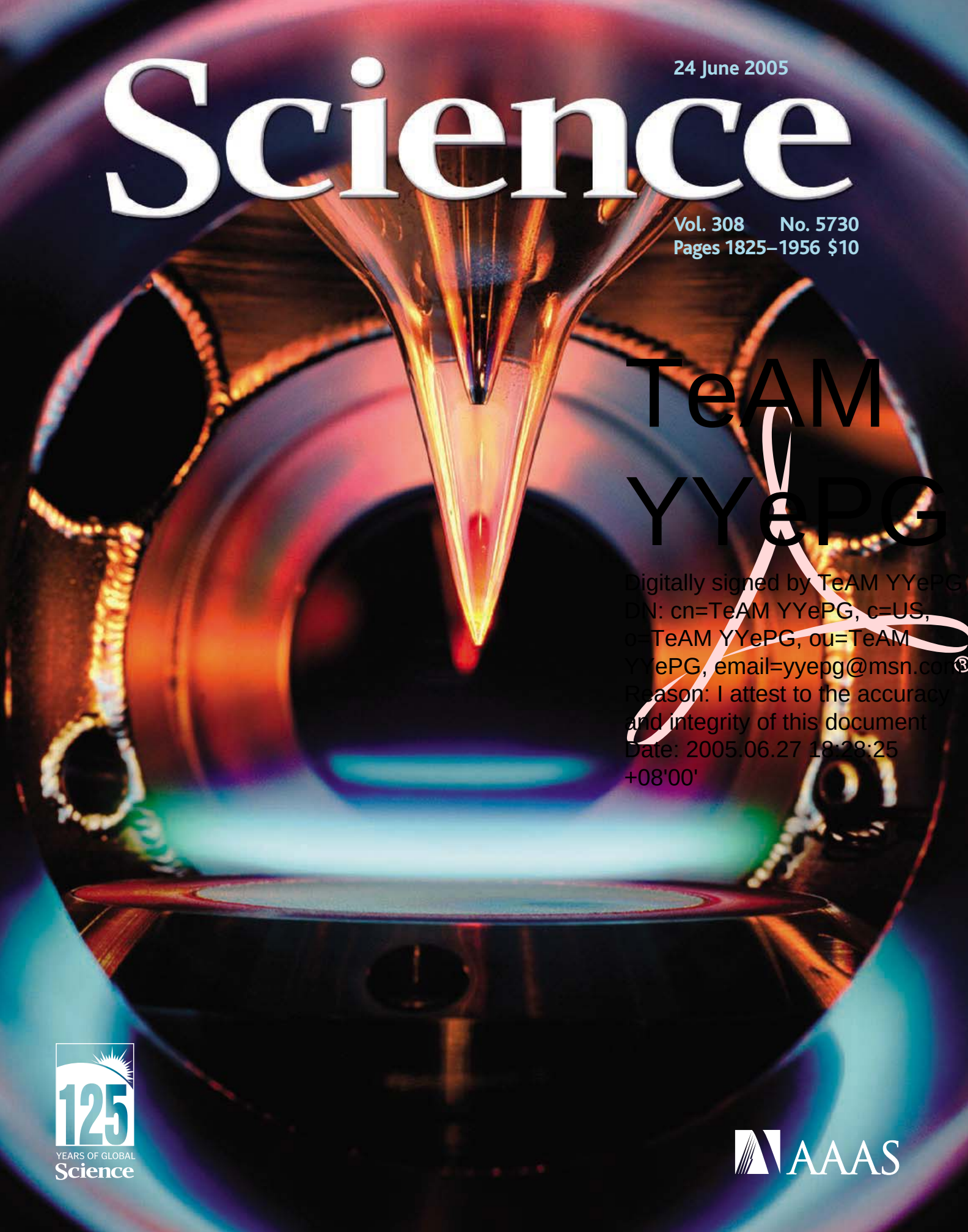

24 June 2005

Science

Vol. 308 No. 5730
Pages 1825–1956 $10

125 YEARS OF GLOBAL Science

AAAS

Now The Right Side Knows What The Left Side Is Doing.

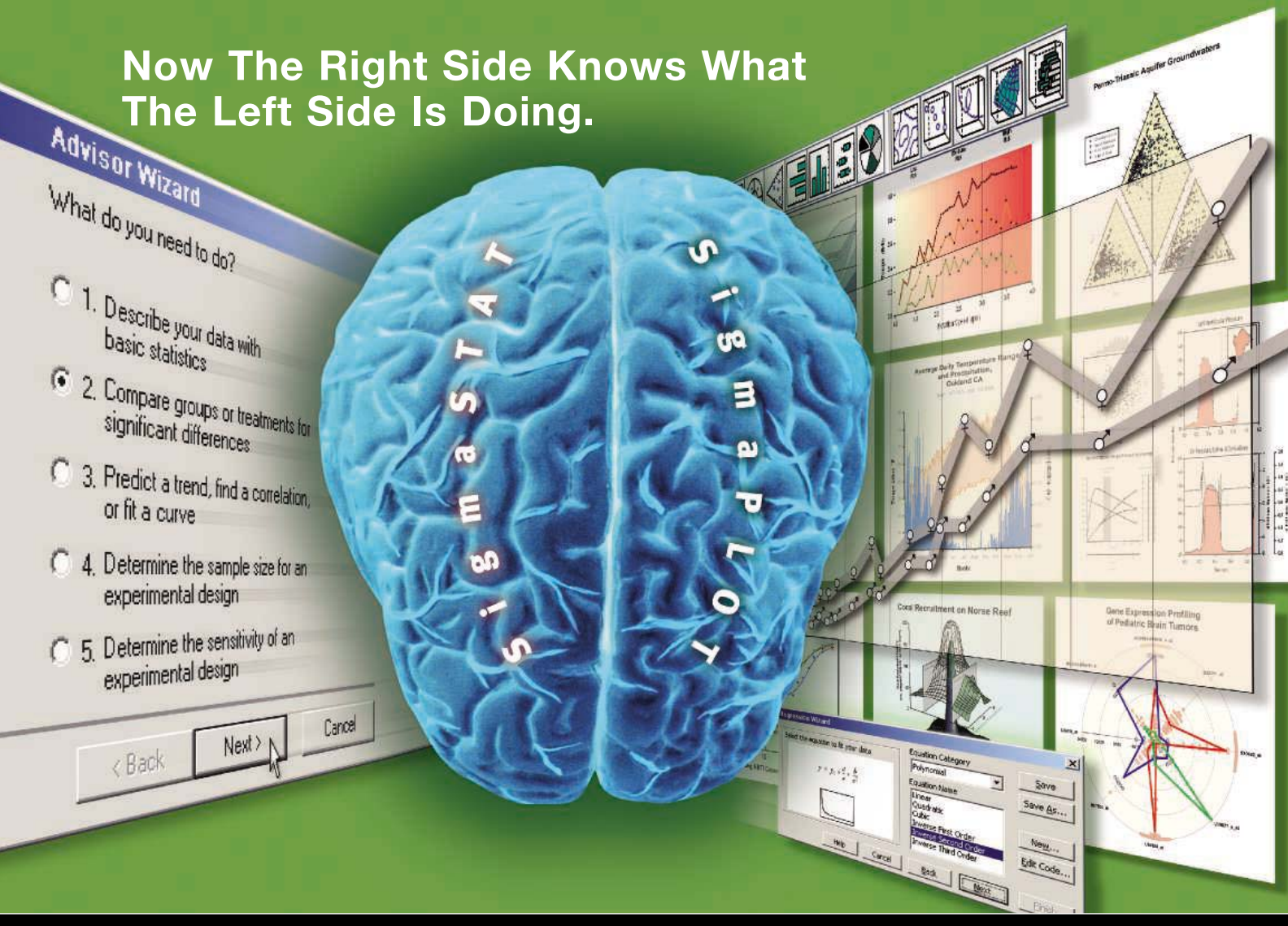

Combine the Powerful Statistical Output of SigmaStat with the Publication-quality Graph Creation of SigmaPlot

SigmaPlot is the award-winning technical graphing and data analysis software package used by more than 100,000 researchers worldwide who need to produce defensible research and create compelling graphs that clearly present their results for technical publications, presentations or the web. SigmaStat 3.1 now seamlessly integrates with SigmaPlot 9.0 for deeper statistical analysis within SigmaPlot's statistics menu.

SigmaPlot allows you to:

> Create graphs easily and publish your work anywhere
> Analyze and manage your data quickly and easily
> Choose over 80 different 2-D and 3-D graph types
> Customize every element of your graphs
> Instantly access SigmaPlot from Microsoft® Excel
> Streamline your work by automating repetitive tasks

SIGMAPLOT
Exact Graphs for Exact Science

Add SigmaStat 3.1 to get easy-to-use, expert statistical analysis within SigmaPlot!

SigmaStat guides you through your analysis:

> Suggests the appropriate statistical test
> Checks assumptions in the data to avoid statistical error
> If your data violates any of those assumptions, the Advisor Wizard suggests another test
> Generates an intelligent report that explains your results in plain English – not statistical jargon
> Even handles messy data with missing values

SIGMASTAT
Advisory Statistics for Scientists

With SigmaStat you'll have the expertise of a professional statistical consultant at your fingertips!

FREE ONLINE TUTORIALS & 30-DAY TRIAL SOFTWARE AVAILABLE AT WWW.SYSTAT.COM

SigmaScan®
Automated Image Analysis

TABLECurve 2D
Automated Curve Fitting Analysis

TABLECurve 3D
Automated Surface Fitting Analysis

PeakFit
Automated Peak Separation Analysis

SYSTAT®
Comprehensive Statistical Analysis

adsci

WHEN ACCURACY IS THE NAME OF THE GAME.

Achieve up to six times higher reverse transcription accuracy with AccuScript™ RT from Stratagene

Reverse transcriptases (RT) exhibit significantly higher error rates than other known DNA polymerases, introducing errors at frequencies of one per 1,500 to 30,000 nucleotides during cDNA synthesis[1]. Our new AccuScript™ RT delivers 3- to 6-fold fewer reverse transcription errors than other reverse transcriptases, creating more accurate copies of RNA.

- **Greatly reduce sequence errors during first-strand cDNA synthesis**
- **Produce high yields of full-length cDNA**
- **Excellent RT-PCR sensitivity with low RNA amounts**

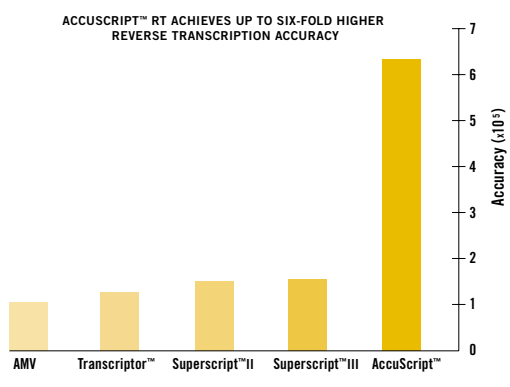

Need More Information? Give Us A Call:

Stratagene USA and Canada
Order: (800) 424-5444 x3
Technical Services: (800) 894-1304

Stratagene Europe
Order: 00800-7000-7000
Technical Services: 00800-7400-7400

Stratagene Japan K.K.
Order: 03-5159-2060
Technical Services: 03-5159-2070

www.stratagene.com

Ask us about these great products:

AccuScript™ Reverse Transcriptase System	50 rxns	600089
	200 rxns	600090
AccuScript™ First Strand cDNA Synthesis System		200820
AccuScript™ High Fidelity RT-PCR Kit with *PfuUltra*™ DNA Polymerase*		600180

STRATAGENE®

1. Roberts, J.D., Bebenek, K., Kunkel T.A. The Accuracy of Reverse Transcriptase from HIV-1. Science 1988 (242) 1171-1173.

Transcriptor is a trademark of Roche Applied Science. Superscript is a trademark of Invitrogen.

* Purchase of these products is accompanied by a license to use them in the Polymerase Chain Reaction (PCR) process in conjunction with a thermal cycler whose use in the automated performance of the PCR process is covered by the up-front license fee, either by payment to Applied Biosystems or as purchased, i.e., an authorized thermal cycler.

Amersham Biosciences

Part of GE Healthcare

Before you put our radionucleotides to the test

We put them to the test

Radionucleotides from GE Healthcare are made to perform. Our ^{32}P and ^{33}P nucleotides are tested in DNA-labeling experiments before shipping, so you can be confident they'll work in your application. But what's more, they're manufactured frequently and dispensed from local sites, so you can always rely on rapid delivery of the freshest material. For your convenience, they're available in a variety of pack sizes and formats, which can be customized to your specific needs. All of which adds up to a refreshingly easy way to ensure the best results in your research.

Visit www.amershambiosciences.com/radiochemicals

imagination at work

Science

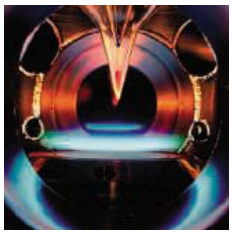

COVER Molecular-beam flame sampling. A flat flame (blue) from a sintered metal burner (bottom) produces gases that are sampled through a small aperture in a quartz cone. These gases can then be analyzed by synchrotron-photoionization mass spectrometry, which has revealed previously undetected combustion intermediates. See page 1887. [Photo: Sandia National Laboratories]

Volume 308
24 June 2005
Number 5730

DEPARTMENTS

1856

NEWS OF THE WEEK

1873

NEWS FOCUS

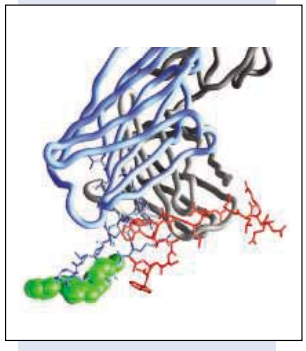

1878 & 1906

LETTERS

BOOKS *ET AL.*

POLICY FORUM

PERSPECTIVES

Contents continued

Systems Biology — RNAi and Gene Expression Analysis

GeneGlobe — the world's largest database of matching siRNAs and RT-PCR assays

New

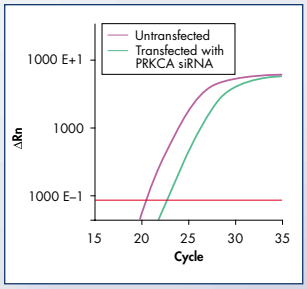

Reliable quantification after knockdown.

Visit www.qiagen.com/GeneGlobe .

New genomewide solutions from QIAGEN provide potent, specific siRNAs and matching, ready-to-use, validated primer sets for SYBR® Green based real-time RT-PCR assays.

- **One database** — easy online access to RNAi and gene expression solutions at the GeneGlobe™ Web portal
- **Two matching solutions** — siRNAs and matching real-time RT-PCR assays you can rely on
- **Three complete genomes** — siRNAs and RT-PCR assays are available for the entire human, mouse, and rat genomes

For matched siRNAs and real-time RT-PCR assays, go to www.qiagen.com/GeneGlobe !

QIAGEN

WWW.QIAGEN.COM

SCIENCE EXPRESS www.sciencexpress.org

TECHNICAL COMMENT ABSTRACTS

BREVIA

REPORTS

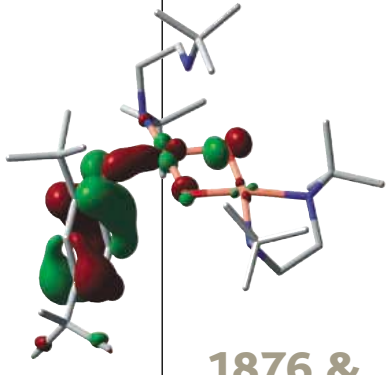

1876 & 1890

Contents continued

Systems Biology — Whole Genome Amplification

REPLI-g — perfection in DNA replication: unlimited and precise throughout the whole genome

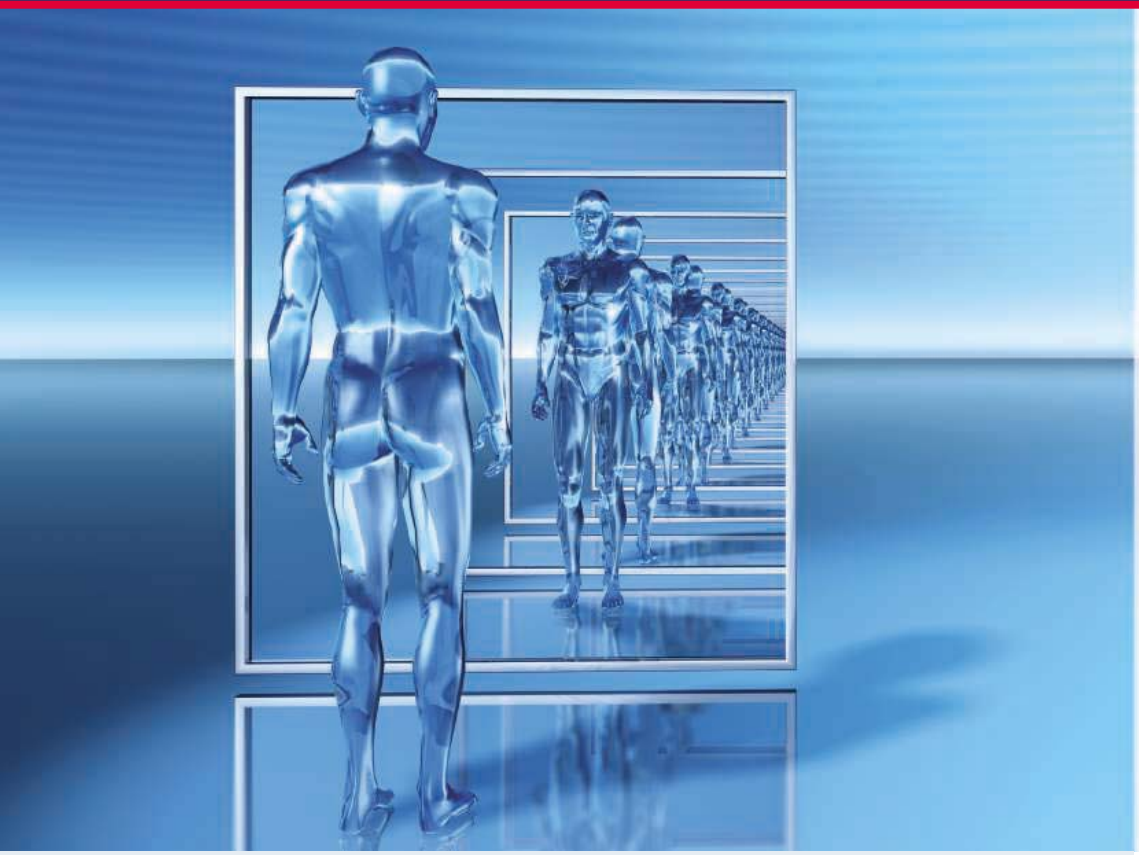

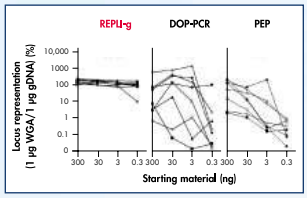

Superior locus representation compared to PCR-based techniques

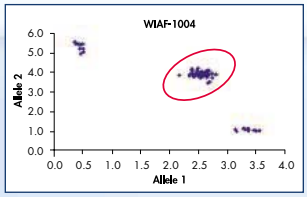

Reliable SNP genotyping

REPLI-g® Kits and Services provide unlimited and precise replication of genomic DNA, allowing precious samples to be expanded, shared, and banked.

- **Reproducible amplification from a variety of starting materials** — including genomic DNA, fresh or dried blood, buccal swabs, fresh or frozen tissue, and cells
- **Highly uniform amplification** — across the whole genome with minimal sequence bias
- **Get more data from your samples** — unlimited DNA for all your downstream applications including SNP genotyping, STR analysis, PCR, sequencing, and arrays
- **Standardized and consistent DNA yields** — enabling direct use in downstream applications without quantification

For perfect and reproducible results, use REPLI-g technology.
Find out more at www.qiagen.com/goto/wholegenomeamplification !

QIAGEN

Reports continued

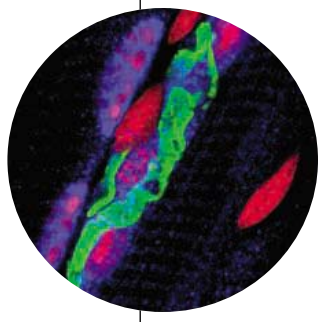

1920

1853 &1934

AAAS
ADVANCING SCIENCE, SERVING SOCIETY

SCIENCE (ISSN 0036-8075) is published weekly on Friday, except the last week in December, by the American Association for the Advancement of Science, 1200 New York Avenue, NW, Washington, DC 20005. Periodicals Mail postage (publication No. 484460) paid at Washington, DC, and additional mailing offices.

Domestic individual membership and subscription (51 issues): $135 ($74 allocated to subscription). Domestic institutional subscription (51 issues): $550; Foreign postage extra: Mexico, Caribbean (surface mail) $55; other countries (air assist delivery) $85. First class, airmail, student, and emeritus rates on request. Canadian rates with GST available upon request, GST #1254 88122. Publications Mail Agreement Number 1069624. **Printed in the U.S.A.**

Change of address: allow 4 weeks, giving old and new addresses and 8-digit account number. **Postmaster:** Send change of address to *Science*, P.O. Box 1811, Danbury, CT 06813–1811. **Single copy sales:** $10.00 per issue prepaid includes surface postage; bulk rates on request. **Authorization to photocopy** material for internal or personal use under circumstances not falling within the fair use provisions of the Copyright Act is granted by AAAS to libraries and other users registered with the Copyright Clearance Center (CCC) Transactional Reporting Service, provided that $15.00 per article is paid directly to CCC, 222 Rosewood Drive, Danvers, MA 01923. The identification code for *Science* is 0036-8075/83 $15.00. *Science* is indexed in the *Reader's Guide to Periodical Literature* and in several specialized indexes.

Contents continued ▶

TaKaRa

High Speed Real Time PCR

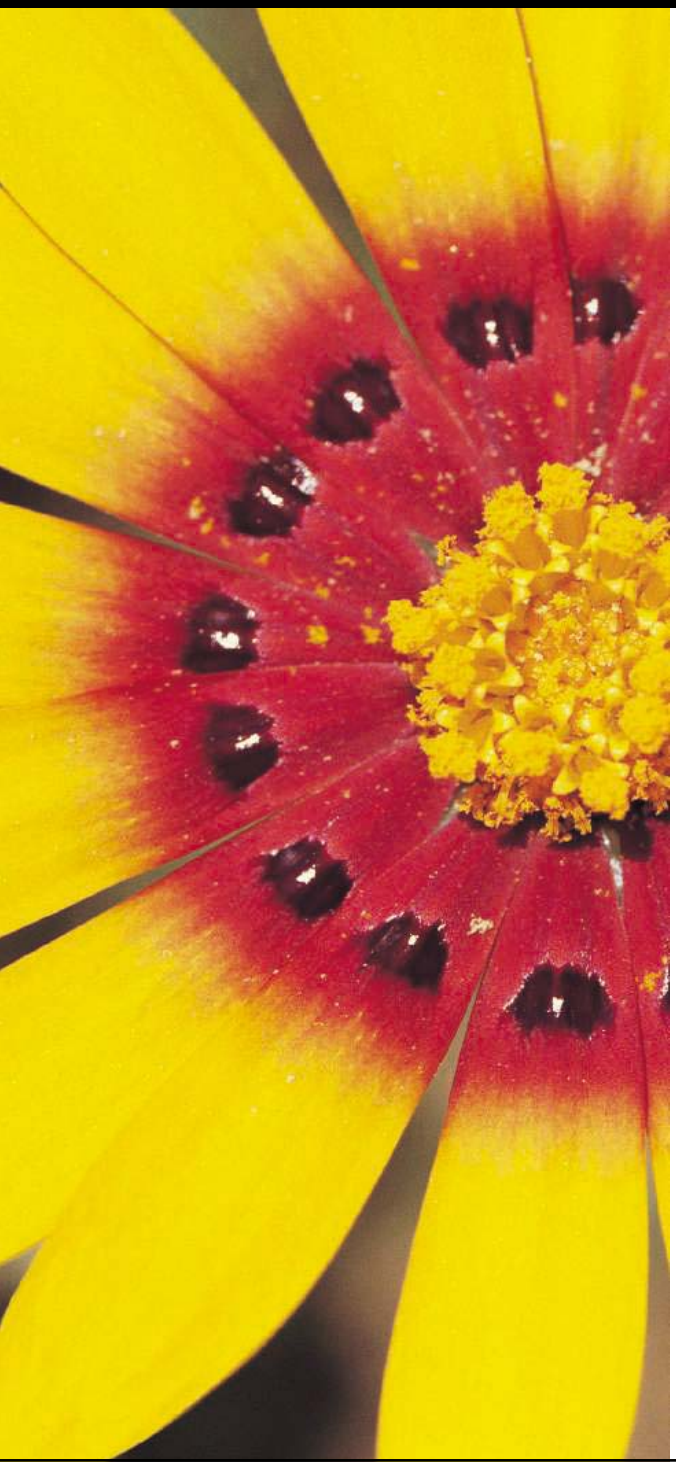

Premix Ex Taq™ (Perfect Real Time)

Premix Ex Taq™ (Perfect Real Time) is a 2X premix, specially designed for high speed, high sensitivity real time PCR using either detection probes (e.g. TaqMan®) or SYBR® Green I (not included). This premix combines high-performance Takara *Ex Taq*™ Hot Start DNA Polymerase, which uses antibody-mediated Hot Start technology to prevent non-specific amplification, with a newly formulated real time PCR buffer that provides increased amplification efficiency and further improved specificity for high speed real time PCR. The results are exceptional real time PCR quickly and easily.

- **Fast:** Reaction can be completed in 50 minutes.
- **Versatility**: Compatible with Smart Cycler®, LightCycler®, ABI PRISM® 7000/7700/7900 HT, Applied Biosystems 7500 Real-Time PCR Systems, and other real time PCR instruments.

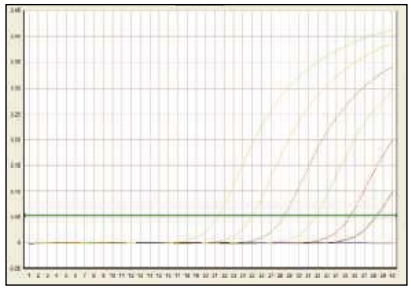

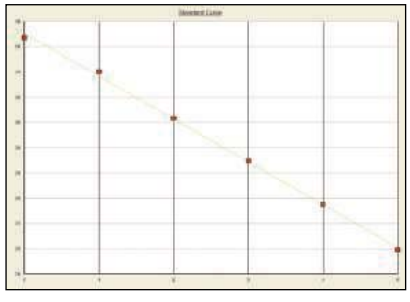

- **High Sensitivity:** Detects as few as 10 copies.
- **Convenient:** Two tubes of ROX reference dyes are supplied.
- **Wide Dynamic Range:** Refer to graphs (left).

Amplification curve (upper panel) and **Standard curve** (lower panel) for *Premix Ex Taq*™ (Perfect Real Time) using the TaqMan® Gene Expression Assay on the Applied Biosystems 7500 Real-Time PCR system.

Target: Mouse GAPD gene.

TAKARA BIO INC.
The Biotechnology Company™

Otsu, Shiga, Japan
Phone: +81 77-543-7247 Fax: +81 77-543-9254

USA: Takara Mirus Bio Inc. Phone: 888-251-6618 Fax: 608-441-2845
Europe: Takara Bio Europe S.A. Phone: +33 1 41 47 2370 Fax: +33 1 41 47 2371
Korea: Takara Korea Biomedical Inc. Phone: +82 31 739 3300 Fax: +82 31 739 3311
China: Takara Biotechnology (Dalian) Co., Ltd. Phone: +86 411 8764 1681 Fax: +86 411 8761 9946

For more information and a list of Takara distributors worldwide, please visit our website today!

www.takara-bio.com

sciencenow www.sciencenow.org Daily News Coverage

Fat Under Attack
Researchers engineer mice that kill their own fat cells.

Maldives Experience That Sinking Feeling
Indian island chain could be underwater within 100 years, but skeptics aren't convinced.

A Nano-Sized Trojan Horse
Tiny polymers trick cancer cells into eating poison.

Funding cuts in computer science research.

science's next wave www.nextwave.org Career Resources for Young Scientists

US: DARPA Changes Reverberate in the Computer Science World *J. Kling*
Changes in the priorities of the Defense Advanced Research Projects Agency have led to decreased funding for basic computer science research.

US: Educated Woman, Chapter 40—Directions Anyone? *M. P. DeWhyse*
Searching for a job requires networking and a willingness to ask questions and explore possibilities.

Canada: It's a Small World—Canada's Hub for Nanotech *A. Fazekas*
The National Institute for Nanotechnology offers opportunities for early-career researchers.

UK: Beyond the Great Unknown *P. Dee*
Now receiving his welfare benefit, Phil Dee is using his time to seek out new career opportunities.

MiSciNet: Spelman Students "Score" Using Advanced Technology *C. Parks*
Undergraduates program robots to compete in RoboCup, a soccer tournament for autonomous robots.

science's sage ke www.sageke.org Science of Aging Knowledge Environment

Perspective: Endothelial Progenitor Cell Therapy for Atherosclerosis—The Philosopher's Stone for an Aging Population? *J. Kravchenko, P. J. Goldschmidt-Clermont, T. Powell, E. Stallard, I. Akushevich, M. S. Cuffe, K. G. Manton*
Effect of therapy on human life span is predicted to be comparable to that caused by eliminating cancer.

News Focus: Sticking It to Parkinson's Disease *M. Leslie*
Vaccination spares mice from brain damage.

News Focus: Releasing the Pressure *R. J. Davenport*
Eliminating kidney protein in mice relieves swelling spurred by diabetes drugs.

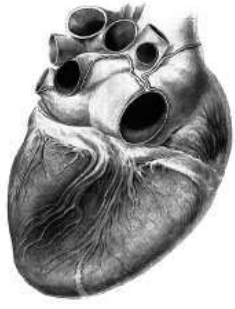

Improving cardiovascular health.

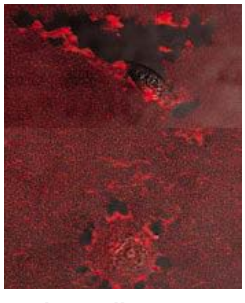

Tracking cell movement.

science's stke www.stke.org Signal Transduction Knowledge Environment

Perspective: Wrestling with SUMO in a New Arena *V. G. Wilson and G. Rosas-Acosta*
Sumoylation of a plasma membrane channel results in complete inactivation.

Protocol: Quantum Dot–Based Cell Motility Assay *W. Gu, T. Pellegrino, W. J. Parak, R. Boudreau, M. A. Le Gros, D. Gerion, A. P. Alivisatos, C. A. Larabell*
Cells leave a nonfluorescent trail when plated on nanocrystals.

Teaching Resource: Glial Intercellular Waves *A. Charles*
The animation shows propagation of sequential signaling in glia.

Teaching Resource: Sensory Systems—Taste Perception *R. F. Margolskee*
Prepare a lecture for a graduate-level class on taste receptors and transduction.

Separate individual or institutional subscriptions to these products may be required for full-text access.

Believe it!

DNA Sequencing for $2.50 per reaction.

- Read length up to 900 bases.
- High quality electropherograms.
- Fast turnaround.
- Plasmid and PCR purification available.

$2.50 per reaction!

POLYMORPHIC
Polymorphic DNA Technologies, Inc.℠

Polymorphic exclusively uses ABI 3730XL sequencers.
Data delivered via secure FTP, email or CD.
No charge for standard sequencing primers.
96 sample minimum order.
96 well plates only- no tubes.

www.polymorphicdna.com
info@polymorphicdna.com

1125 Atlantic Ave., Ste. 102
Alameda, CA 94501

888.362.0888

For more information please visit
www.polymorphicdna.com

edited by Stella Hurtley and Phil Szuromi

Paleocene Warming at Depth

The Paleocene-Eocene Thermal Maximum (PETM) was a geologically brief period of warming that occurred about 55 million years ago. During this episode, the global carbon cycle was significantly perturbed, as reflected by a large and sudden change in the carbon isotopic composition of the global active carbon pool. This perturbation may have been caused by a massive release of methane hydrates from the sea floor, but the cause of such a release is not understood. **Tripati and Elderfield** (p. 1894) present benthic ocean temperature records from intermediate-depth waters in both hemispheres and near the equator which show that all of those locations warmed roughly equally, by 4° to 5°C, slightly ahead of the corresponding changes in the carbon system. These data are consistent with the idea that destabilization of methane clathrates in marine sediments were involved as a source of the isotopically anomalous carbon during the event.

Thicker in the Middle

The mass balance of Antarctica's ice sheets is a critical parameter in any evaluation of the potential sea level rise that would accompany global warming. **Davis *et al.*** (p. 1898, published online 19 May 2005; see the Perspective by **Vaughan**) report results, derived from measurements made by satellite radar altimetry conducted from 1992 to 2003, which show that large parts of the interior of Antarctica gained mass during that time. They attribute this increase to a rise in precipitation in East Antarctica, an effect that has been suggested to accompany global warming. The mass balance of the entire ice sheet is still uncertain, however, because mass loss in areas near the coast that are not accessible to this technique could be even greater than the gains seen in the interior.

Assessing a Hydrogen Future

The pollution reductions and health gains that would follow from powering cars and trucks with hydrogen are well understood in principle, but a detailed analysis of those benefits would be useful. **Jacobson *et al.*** (p. 1901) present such a model study of the effects of converting the entire United States vehicle fleet to hydrogen fuel cells or fossil fuel–electric hybrid vehicles. The use of hydrogen fuel cell vehicles reduces pollution and adverse health effects in all cases, but to what extent depends on how the hydrogen is produced. In the best case, the generation of hydrogen by wind power may make it a more economical fuel than gasoline when all costs are considered.

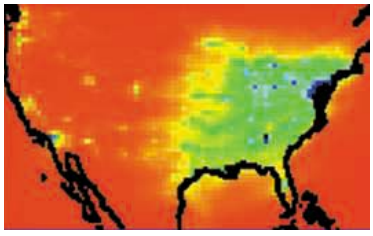

CREDITS (TOP TO BOTTOM): PERRY *ET AL.*; JACOBSON *ET AL.*

Weighing Earth's Core

Seismic velocities and comparisons with experiments have been used to infer the density of Earth's interior, often through a linear extrapolation known as Birch's Law. This analysis has indicated that Earth's inner core is mostly an iron-nickel alloy that must contain some light elements, such as sulfur or oxygen. However, this inference requires knowledge of how seismic velocities vary, not just with density but also temperature. **Lin *et al.*** (p. 1892) directly measured seismic velocities in iron at high pressure and at several temperatures. Temperatures comparable to those in the deep Earth reduce the sound velocity relative to the inferred density. Thus, Earth's core requires more light elements than indicated from a linear relation with density, a finding more consistent with other inferences.

A Changing Climate for Fish and Chips

Climate change is well established as a potential threat to biodiversity and the services and benefits that people gain from ecosystems. **Perry *et al.*** (p. 1912, published online 12 May 2005) examined the effects of climate change on a key ecosystem service, marine fisheries. Many species have exhibited a strong northward shift during the last 25 years in the North Sea. Many commercially important fish such as cod, whiting, and anglerfish have shifted from 50 to 800 kilometers northward. If current climate trends continue, some species may have withdrawn completely from the North Sea by 2050.

Burning Up

Understanding fire is one of the oldest challenges in chemistry. Spectroscopy studies of flames can identify molecular fragments, which then serve as input for kinetic models that sort out the many steps whereby hydrocarbons are oxidized into water and CO_2. In these models, carbonyl compounds are well-established intermediates, but their less stable enol tautomers, which bear an OH group bound to a C=C double bond, are not. **Taatjes *et al.*** (p. 1887, published online 12 May 2005; see the cover) have now observed significant amounts of two-, three-, and four-carbon enols in flames burning commercial gasoline constituents. A clean, low-temperature hydrocarbon oxidation is achieved by tyrosinase enzymes, in which two copper ions in the active site bind O_2 and catalyze the formal insertion of an O atom into an aromatic C–H bond in phenol. Synthetic chemists have assumed that the hydrocarbon interacts with the bound O_2 before it cleaves. **Mirica *et al.*** (p. 1890; see the Perspective by **Reedijk**) present evidence from a model complex that suggests a different pathway. Spectroscopic studies of a compound in which a copper dimer mimicks the O_2 binding site of the enzyme reveal a reactive intermediate at –120°C in which the O_2 bond is broken before oxygen transfer to a phenol derivative. These results suggest that the enzymatic oxidation could likewise involve phenol attack on an electrophilic copper (III) bridging oxo species.

Absent Allies

A major difficulty in developing a vaccine against human immunodeficiency virus (HIV) is the high level of escape by the virus when it encounters antibodies within each host. Nevertheless, a small handful of monoclonal antibodies broadly specific for HIV can neutralize the virus, and they have been studied carefully

CONTINUED ON PAGE 1839

PIERCE

Grasp the Proteome™

NEW!

- **Mitochondria** — Mitochondria Isolation Kit* for Tissues
- **Mitochondria** — Mitochondria Isolation Kit* for Mammalian Cells
- **B-PER®*** — Bacterial Protein Extraction Reagents
- **NE-PER®** — Nuclear Protein Extraction Reagents
- **Mem-PER®** — Eukaryotic Membrane Protein Extraction Reagent (Works for tissues too!)
- **M-PER®** — Mammalian Cell Lysis Reagent
- **T-PER®** — Tissue Lysis Reagent
- **Y-PER®** — Yeast Cell Lysis Reagents
- **GST & 6xHIS** — Purification Kits for Bacterial and Yeast Cells
- **HALT™** — Protease Inhibitor Cocktails

Incredibly convenient ways to pop open cells and extract proteins!

Poppers™

Cell Lysis Solutions

[easier, faster, safer, gentler]

Poppers™ Liquid Cell Lysis Reagents come pre-mixed and ready to use. They're the new wave of cell lysis! No hit-or-miss homemade recipes, no glass beads, no sonicators, no or reduced Douncing, no French presses, and no freezing and thawing! Just pour and explore!

Highlights:

- Speed – isolates intact mitochondria from tissue in ~60 minutes
- A choice of two isolation methods – reagent-based method allows for concurrent preparations of multiple samples; traditional Dounce homogenization method allows for single-sample processing with higher yields
- Bench-top compatibility – isolation performed in a microcentrifuge tube
- Convenience – all isolation reagents are provided ready to use with complete and easy-to-follow instructions

NEW! Mitochondria Isolation Kit for Tissues (Product # 89801), the latest addition to the Poppers™ Cell Lysis Solutions line!

Providing two convenient methods for the quick and efficient isolation of intact mitochondria from hard or soft mammalian tissue – reagent-based and Dounce.

New! Poppers™ Cell Lysis Solutions Handbook. Request yours today!

www.piercenet.com/poppers/pop22f

PIERCE

Tel: 815-968-0747 or 800-874-3723 • Fax: 815-968-7316 • Customer Assistance E-mail: CS@piercenet.com

Outside the United States, visit our web site or call 815-968-0747 to locate your local Perbio Science branch office (below) or distributor

Belgium & Dist.: Tel +32 53 85 7184 euromarketing@perbio.com
China: Tel +86 10 8049 9033 support@perbio.com.cn
France: Tel 0800 50 82 15 euromarketing@perbio.com
Germany: Tel 0228 9125650 de.info@perbio.com
Hong Kong: Tel 852 2753 0686 SalesHK@perbio.com
The Netherlands: Tel 076 50 31 880 euromarketing@perbio.com
United Kingdom: Tel 0800 252185 uk.info@perbio.com
Switzerland: Tel 0800 56 31 40 euromarketing@perbio.com

*U.S. patent pending on Mitochondria Isolation Kit Technology. B-PER® Technology is protected by U.S. patent # 6,174,704.

PERBIO

with the hope of understanding why similar antibodies are not generated easily during a normal immune response. **Haynes *et al.*** (p. 1906, published online 28 April 2005; see the Perspective by **Nabel**) find that two of the monoclonal antibodies possess a range of specificities and react against the human phospholipid, cardiolipin. Thus, broadly neutralizing antibodies may be seen so rarely in HIV infection because the very features that endow anti-HIV properties also make them self-reactive and, as such, they are not tolerated by the body's immune system.

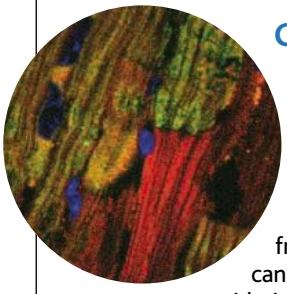

CREDIT: SCHRINER *ET AL.*

Catalase for Longer Life

Cell and tissue damage caused by free radical oxygen molecules have been linked to aging pathologies, yet the idea that antioxidant defenses can prolong life has been controversial. **Schriner *et al.*** (p. 1909, published online 5 May 2005; see the Perspective by **Miller**) generated transgenic mice that overexpress catalase in mitochondria, a major source within the cell of oxygen free radicals. Catalase removes damaging hydrogen peroxide that can generate reactive oxygen species. In the transgenic mice, cellular oxidative damage and age-related decline in heart function were reduced and cataract formation was delayed. In addition, life span increased by nearly 20%. Thus, antioxidant enzymes can promote mammalian longevity.

Calling New Neurons

Most neurogenesis in the brain occurs in the context of early development. However, even through adulthood, a steady stream of newly generated neurons supplies the olfactory bulb. Neuronal progenitors from the subventricular zone of the brain migrate together as a chain to the olfactory bulb. **Ng *et al.*** (p. 1923) have now identified prokineticin 2 (PK2) as one of the signals that calls the neurons to their destination. Prokineticin proteins are secreted, and in other locations also regulate processes such as gastrointestinal motility and pain sensitization. The mammalian retina, like other regions of the brain, develops in a sequential manner. Cells of a given function are born earlier, whereas those born later are dedicated to other functions. **Kim *et al.*** (p. 1927) have clarified how one signaling molecule, growth and differentiation factor 11 (GDF11), affects this trajectory of differentiation in the retina differently than in the olfactory epithelium. In the developing retina, GDF11 does not affect proliferation of progenitor cells, as it does in the olfactory epithelium, but signals to the progenitor cells competence to produce certain types of differentiated cells

Alarming the Mob

Although there has been much interest in the function and evolution of alarm signals in animals, few studies have been able to control the presentation of predators to prey species and elucidate any complexity of meaning that might be encoded in these signals. **Templeton *et al.*** (p. 1934; see the news story by **Miller**) exposed black-capped chickadees, a common North American songbird, to various different species and sizes of predator. Chickadees living in small flocks responded to alarm calls by mobbing the threatening predator. Spectrographic analyses showed striking differences in chickadee alarm calls that correlating strongly with the size and threat of the potential predators. Furthermore, the chickadees responded to recordings of the different alarm calls by varying their mobbing behavior.

Agrin Yes, Neuregulin No

Neuromuscular junctions develop through a series of reciprocal interactions between the muscle fiber and the incoming motor neuron. Both agrin and neuregulin have been implicated in neuromuscular junction development. **Escher *et al.*** (p. 1920) use targeted gene ablations to clarify which molecules act when. It seems that neuregulins are not critical for neuromuscular junction formation, but agrin is. The previously observed effects of neuregulin signaling disruptions on neuromuscular junction formation may well have been mediated indirectly through the effects of neuregulins on Schwann cells, which surround the neuromuscular junction.

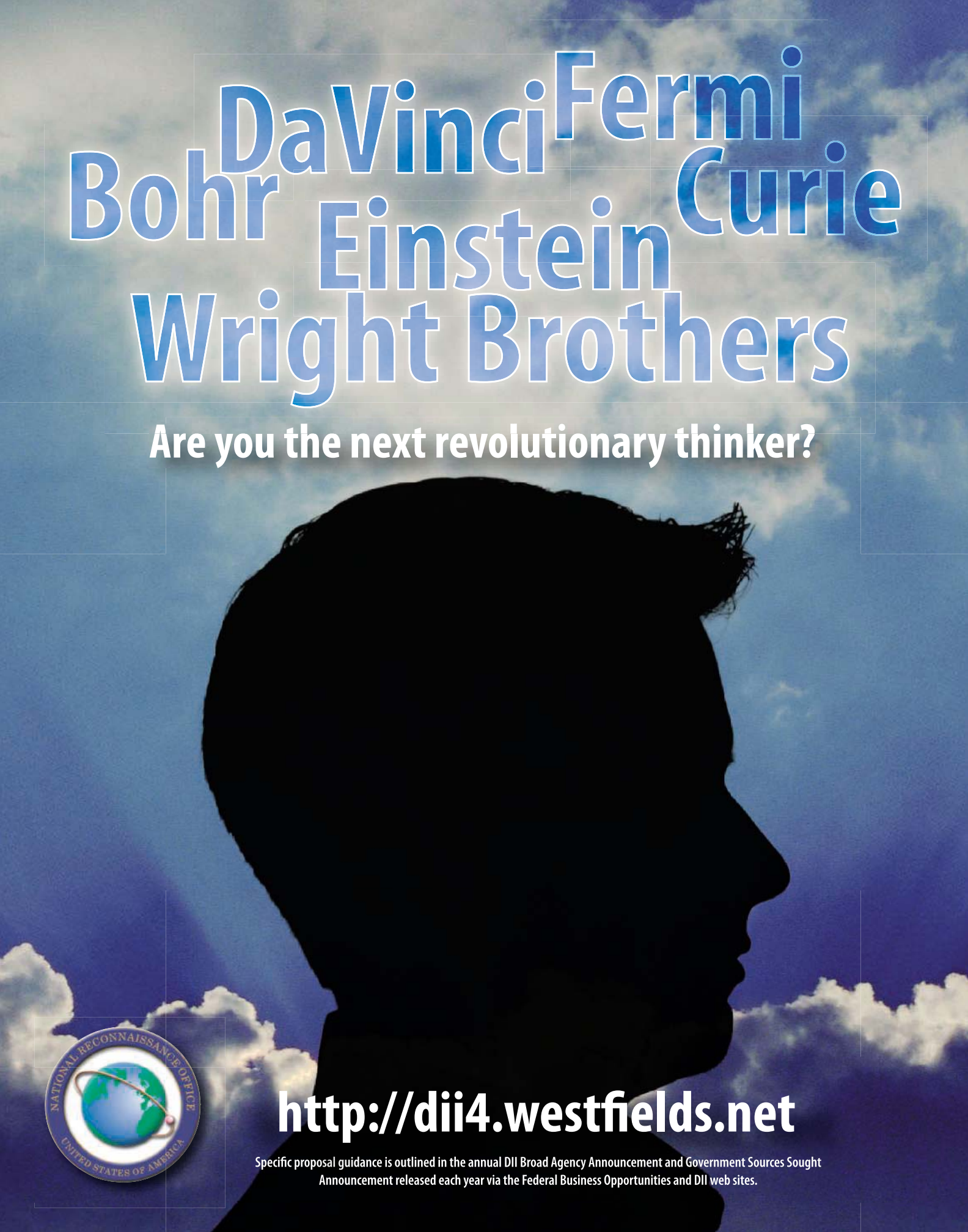
DaVinci
Fermi
Bohr
Curie
Einstein
Wright Brothers
Are you the next revolutionary thinker?
NATIONAL RECONNAISSANCE OFFICE
UNITED STATES OF AMERICA
http://dii4.westfields.net
Specific proposal guidance is outlined in the annual DII Broad Agency Announcement and Government Sources Sought Announcement released each year via the Federal Business Opportunities and DII web sites.

Science and Prohibited Weapons

This year, on 17 June, the Geneva Protocol, an international treaty prohibiting the use of asphyxiating or poisonous gases and bacteriological methods of warfare, turned 80 years of age. It was fostered in part by a 1918 appeal in which the International Committee of the Red Cross (ICRC) described the use of poisonous gas against soldiers as a "barbarous invention which science is bringing to perfection." Great peacetime advances in chemistry before the First World War made possible the manufacture and use of chlorine, phosgene, and mustard gas on the battlefield. The ICRC foresaw "a struggle the ferocity of which will exceed the greatest barbarity the world has known."

The 20th century witnessed a continuous accumulation of potential biological and chemical weapons in many nations. Some of these weapons were deployed; for example, in Abyssinia in the 1930s, in China in World War II, in Yemen in 1963, and in the Iran-Iraq war of the 1980s. This gave the impetus to two important international legal regimes: the 1972 Biological Weapons Convention (BWC) and the 1993 Chemical Weapons Convention (CWC). These treaties extended the Geneva Protocol's prohibition beyond mere use to include the development, production, and transfer of all such weapons.

The scientific community now faces difficult questions. Major advances in chemistry, microbiology, and nuclear physics have, regrettably, led to hostile use of the knowledge and materials from these scientific domains; a use that the original scientist-discoverers would have deplored. What will be the outcome for humanity if the results of the research explosion in life sciences and biotechnology are also turned to hostile use? What are the associated responsibilities of scientists?

Scientists in academia and government recognize that advances in the life sciences and biotechnology could make biological weapons more effective, safer to use, more difficult to detect, and therefore more attractive options for would-be users. The dangers lie in both bioterrorism and in government-backed programs, and robust international mechanisms are required to deter the development, production, transfer, and use of these weapons. This provides the background to the numerous conferences this year discussing biosecurity and for the meeting of experts at the BWC this month in Geneva that is examining proposed codes of conduct for scientists.

These discussions take place against a history of societal norms against biological and chemical weapons that reaches back much further than the 1925 Geneva Protocol. The current treaties represent the development and codification of rules and taboos that for thousands of years have protected people from poisoning and the deliberate spreading of disease. Both Greek and Roman civilizations customarily observed a prohibition on the use of poisons. In 500 B.C., the Manu treaty in India banned such weapons. A millennium later, regulations on the conduct of war drawn from the Koran by the Saracens forbade poisoning. These examples demonstrate that recent treaties banning chemical and biological warfare find a deeper resonance in human history, psychology, and morality.

The ICRC has a mandate to assist and protect victims of war, and for that reason it promotes and strengthens international humanitarian law. Prompted by scientists' concerns about the future, the ICRC issued an appeal in September 2002 to governments and anyone working in the life sciences or biotechnology. It aimed to create a culture of responsibility that is coherent with current developments in scientific ethics and existing law.

Scientists must be aware of the importance of their own work in upholding and developing international law; in particular, the BWC and the CWC. They should make every effort to ensure that the outcome of their research serves only to advance humanity. Scientists have a special responsibility to advise governments objectively and to collaborate with others—lawyers, diplomats, and the military—to secure a world in which nobody risks being subject to poisoning and the deliberate spreading of disease.

Robin Coupland and Kobi-Renée Leins

Robin Coupland is medical adviser and Kobi-Renée Leins is project manager in the Mines/Arms Unit, Legal Division, International Committee of the Red Cross.

10.1126/science.1115436

CREDIT: BETTMANN/CORBIS

MOVE BEYOND TRADITIONAL PCR LIMITATIONS

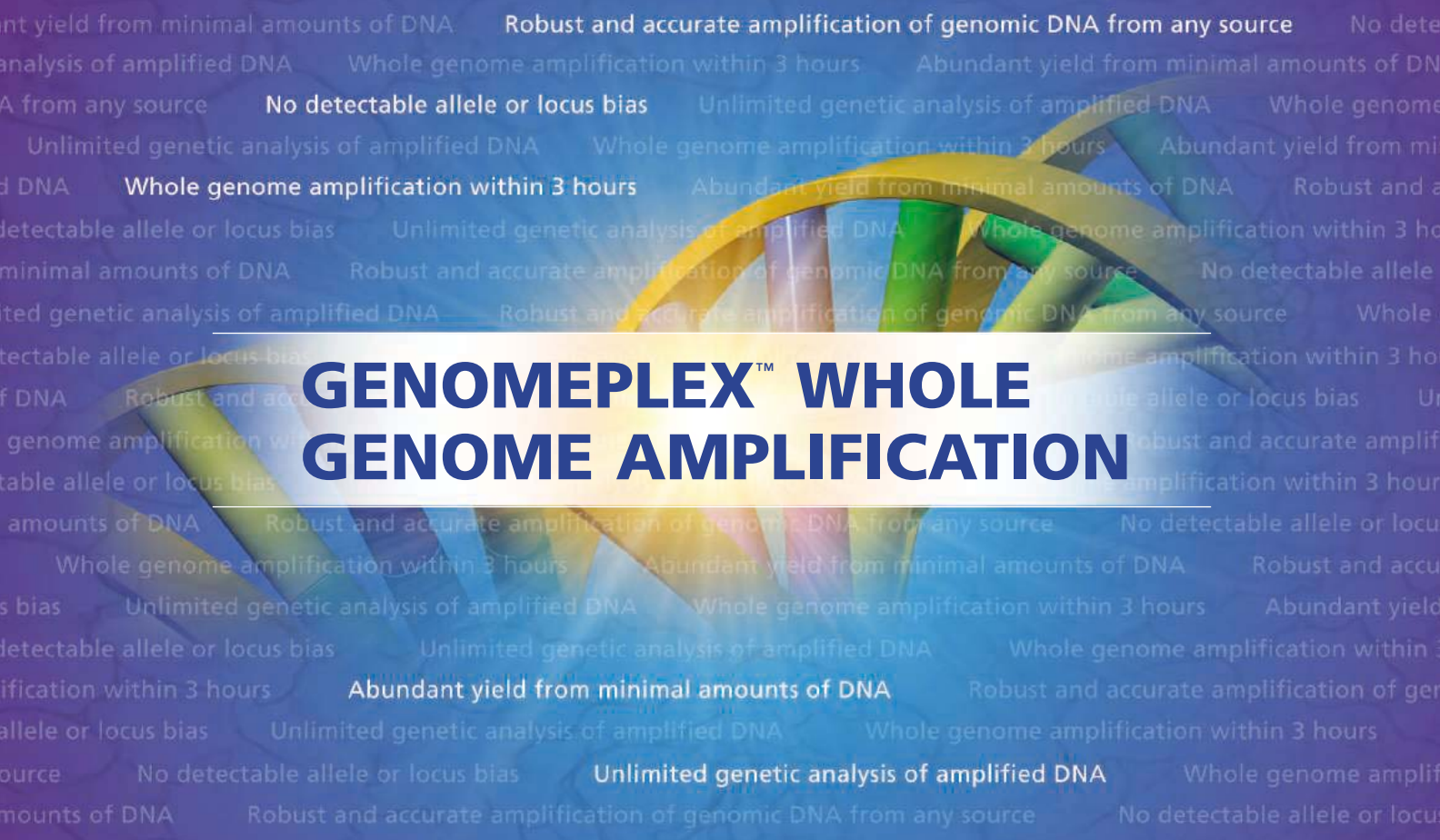

GENOMEPLEX™ WHOLE GENOME AMPLIFICATION

UNSURPASSED YIELD, UNLIMITED POTENTIAL

Sigma's GenomePlex Whole Genome Amplification (WGA) kit provides a rapid and straightforward method to preserve and expand very small amounts of precious DNA.

- **Robust and Accurate Amplification**
  Whole genome amplification with no detectable allele or locus bias within 3 hours
- **Ultimate Flexibility**
  Amplify DNA from virtually any source including blood, buccal swabs, cell culture, plants, and bacteria
- **Unlimited Genetic Analysis**
  GenomePlex WGA DNA is suitable for use with common downstream applications including TaqMan® and BeadArray® or may be stored at -20°C.

Product Code	Description
WGA-1	GenomePlex WGA Kit

Call **800-325-3010** to order or visit us on the web at **sigma-aldrich.com/swga.**

sigma-aldrich.com

LEADERSHIP IN LIFE SCIENCE, HIGH TECHNOLOGY AND SERVICE

SIGMA-ALDRICH CORPORATION • BOX 14508 • ST. LOUIS • MISSOURI 63178 • USA

SIGMA®

EDITORS' CHOICE

edited by Gilbert Chin

CHEMISTRY

With a Double Twist

The design of small-molecule oligomers that adopt conformations resembling the double-stranded helical structure of nucleic acids in solution has been challenging. Two strategies tried to date are to replace the phosphate ester backbone of nucleic acids with amides and to use metal ions to direct assembly of the strands.

Tanaka *et al.* describe how to build a double helix structure that relies on the formation of amidinium-carboxylate salt bridges to couple crescent-shaped backbones, which consist of *m*-terphenyl groups joined by a dialkyne linker. The right- or left-handedness of the double helices, which were characterized by circular dichroism and nuclear magnetic resonance of organic solutions and x-ray diffraction of crystals, is dictated by the chirality of the phenylethyl groups attached to the amidine. The presence of reactive trimethylsilylethynyl groups on the ends of these short strands should allow longer helices to be synthesized. — PDS

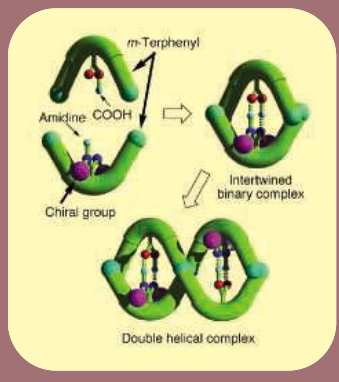

Schematic for double helix construction.

Angew. Chem. Int. Ed. **44**, 3867 (2005).

OCEAN SCIENCE

The Means of Production

The equating of new production (marine primary production fueled by nutrients supplied externally, rather than by nutrients derived from recycled organisms) to export production (primary production lost to recycling through removal to deep waters and sediments) is a common assumption in many studies of marine chemistry. This assumption has allowed numerous estimates of the hard-to-measure quantity of export production to be made, using the more easily measured new production. These quantities are then used to calculate how much CO_2 marine organisms might remove from the atmosphere, a central question in climate studies.

Plattner *et al.* investigate the strength of this assumption for annually integrated new and export production in the central Californian marine upwelling system, using an eddy-resolving, coupled physical-ecosystem-biogeochemical model. They find that new and export production can decouple on a local scale (hundreds of kilometers), because of horizontal transport by persistent meso- and submesoscale circulation patterns, as well as by offshore flow caused by Ekman transport. Thus, although these results do not pertain to global estimates over long periods of time, they do illustrate that the concept of the equality of new and export production has to be used with care, particularly over short spatial and temporal scales. — HJS

Geophys. Res. Lett. **32**, 10.1029/2005GL022660 (2005).

MICROBIOLOGY

Of Coats and Pockets

The protozoan parasite *Trypanosoma brucei* is responsible for African sleeping sickness. One of the interesting features of its biology is that while multiplying in the bloodstream, the parasite evades immune detection and clearance by expressing on its cell surface a dense coat of variant surface glycoprotein (VSG); this coat is doffed periodically (internalized via the flagellar pocket) and replaced with an antigenically distinct version of VSG.

Sheader *et al.* examined how trypanosomes respond when the turnover of VSG is blocked by RNA interference. In vitro, trypanosomes deficient for VSG synthesis stalled before the cytokinesis stage of the cell cycle, when the two daughter cells normally would separate. In vivo, arrested trypanosomes were rapidly cleared from the bloodstream of infected mice, even though the total amount of surface VSG had not decreased. It appears that the ongoing manufacture of VSG is monitored by the parasite to maintain a dense surface coat. However, at least in these experiments, the RNAi-treated parasites appeared to be trapped in a slightly compromised coat that can be targeted successfully by the host immune system. — SMH

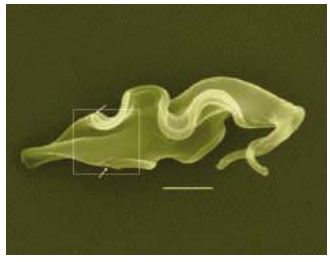

A trypanosome that has stalled before cytokinesis has opposing flagellar pockets.

Proc. Natl. Acad. Sci. U.S.A. **102**, 8716 (2005).

PSYCHIATRY

Correlating Variants and Variation

Genetic factors are widely believed to play a role in the etiology of schizophrenia, a debilitating psychiatric disorder that affects about 1% of the population. However, identifications of specific contributory genes and of critical sequence variants in those genes have not been unambiguous, because the disorder likely arises through the interactions of multiple genes, each exerting a weak effect.

To distinguish critical sequence variants in the *DISC1* (*disrupted-in-schizophrenia*) candidate gene from background noise, Callicott *et al.* studied whether any of the putative risk-conferring variants correlated with biological features of schizophrenia. Intriguingly, they found that in healthy people, one particular disease-associated variant of *DISC1* appears to adversely influence the anatomical structure and cognitive functioning of the hippocampal formation, which has long been a focal point of pathological studies of schizophrenia. These results thus support the hypothesis that variation in the *DISC1* gene is a contributing factor in the development of schizophrenia and likely acts, at least in part, through its effects on the hippocampus. — PAK

Proc. Natl. Acad. Sci. U.S.A. **102**, 8627 (2005).

CONTINUED ON PAGE 1845

CREDITS: (TOP) TANAKA *ET AL.*, *ANGEW. CHEM. INT. ED.* **44**, 3867 (2005); (BOTTOM) SHEADER *ET AL.*, *PROC. NATL. ACAD. SCI. U.S.A.* **102**, 8716 (2005)

WIN A $250 GIFT CHEQUE!

Download the conference brochure by August 1 at www.drugdisc.com/us and you will automatically entered in the American Express Gift Cheque drawing.

Optimizing the Discovery & Development Interface to *Improve Productivity*

Enhance Safety & Efficacy

Develop New Business

Explore New Markets

10th Anniversary DRUG DISCOVERY TECHNOLOGY® & Development

Keynote Sessions

Lester M. Crawford, D.V.M., Ph.D.
Acting Commissioner, FDA

John L. LaMattina, Ph.D.
President, Pfizer Global R&D

Keynote Panel Discussion

Exploring the Industry and Regulatory Interface in Drug Development

Moderator:

Robert R. Ruffolo, Jr., Ph.D.
President, R&D, Wyeth

The Boston Convention & Exhibition Center, Boston, MA

Conference: **August 8-11, 2005**

Exhibition: **August 9-11, 2005**

Visit www.drugdisc.com/us

- ✔ **Review the 150+ conference session options**
- ✔ **Create a customized schedule**
- ✔ **Participate in an industry survey & "quiz"**
- ✔ **Download the brochure & enter the drawing**

Presidential Sponsors:

CAS · ELSEVIER · MDL

Executive Sponsor:

INGENUITY® SYSTEMS

Supporting Publications:

DRUG DISCOVERY TODAY · SCRIP World Pharmaceutical News · Science AAAS · CHEMICAL & Engineering News · BioTechniques

Association Sponsor:

MBC Massachusetts Biotechnology Council

Organized by:

ibc Life Sciences

PHYSICS

Confined to One Dimension

In most instances, atoms in free space, either in the gas or liquid phase, can bind to form molecules only if the scattering length between the atoms is positive—that is, if the atoms attract. When the scattering length is negative, the atoms repel each other, and molecule formation does not occur. In the case of cold atoms, the scattering length can be tuned between positive and negative values by an external magnetic field.

Moritz *et al.* show that confining the atoms to a one-dimensional optical trap gives rise to quite different behavior. The reduced dimensionality in which the atoms move strongly affects the two-particle physics that subsequently determines the scattering length. They find two-particle bound molecular states irrespective of the field-tuned scattering length. This work illustrates the power of cold atoms to provide a tunable system that describes and mirrors the behavior of complex solid-state systems in which the analysis may not be as tractable. — ISO

Phys. Rev. Lett. **94**, 210401 (2005).

MOLECULAR BIOLOGY

RNA Traffic

Both yeast and mammalian cells exhibit a handful of cytoplasmic sites referred to as processing bodies (P bodies), where enzymes that catalyze hydrolytic reactions, such as decapping and deadenylation, in the process of mRNA degradation can be found. Three groups have extended the list of components that congregate at these foci.

Andrei *et al.* show that eukaryotic initiation factor 4E (eIF4E), which binds to the cap at the 5′ end of the mRNA, and one of its binding partners (eIF4E-T) localize to P bodies. They suggest that these two factors combine to inhibit translation (the initiation stage of translation depends on eIF4E being free to interact with eIF4G) of mRNAs residing in P bodies. Sen and Blau, and Liu *et al.*, report that

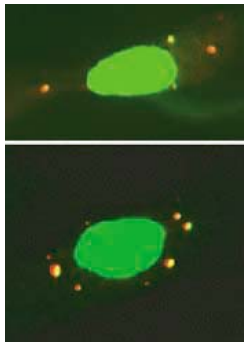

Colocalization of an miRNA-targeted mRNA (green) and Argonaute 2 (red) in P bodies.

P bodies contain Argonaute 2, the endonuclease of the RNA-induced silencing complex (RISC), and the latter group find microRNAs (miRNAs) in complex with their target mRNAs there, too. These observations suggest that both the cleavage of mRNAs triggered by small interfering RNAs (siRNAs) and the translational repression of mRNAs induced by miRNAs may depend on trafficking of protein-RNA complexes into P bodies. — GJC

RNA **11**, 717 (2005); *Nat. Cell Biol.* **7**, 633; 10.1038/ncb1274 (2005).

HIGHLIGHTED IN *SCIENCE*'S SIGNAL TRANSDUCTION KNOWLEDGE ENVIRONMENT

Science's STKE www.stke.org

Reducing Tolerance and Dependence

Although morphine is highly effective against pain, long-term use is problematic because it leads to tolerance and dependence—both of which are likely associated with up-regulation of cAMP signaling and adaptive changes in the expression of target genes. Morphine analgesia and tolerance are mediated through the μ opioid peptide (MOP) receptor, which is also activated by endogenous opiates and methadone; however, unlike these other ligands, morphine does not stimulate endocytosis of the MOP receptor. He and Whistler found that a concentration of methadone that did not stimulate endocytosis by itself nevertheless resulted in MOP receptor endocytosis when administered with a saturating amount of morphine. The authors propose that joint occupation of a dimeric MOP receptor by morphine and methadone can engage the endocytic machinery with much reduced activation of the cAMP pathway. In rats, this mix inhibited the development of morphine tolerance (assessed by tail-flick) and dependence (assessed by the behavioral response to pharmacologically induced opiate withdrawal) without reducing the potency of morphine analgesia. — EMA

Curr. Biol. **15**, 1028 (2005).

CREDITS: LIU *ET AL.*, *NAT. CELL BIOL.* **7** 10.1038/NCB1274 (2005)

www.sciencemag.org

Science

1200 New York Avenue, NW
Washington, DC 20005
Editorial: 202-326-6550, FAX 202-289-7562
News: 202-326-6500, FAX 202-371-9227

Bateman House, 82-88 Hills Road
Cambridge, UK CB2 1LQ
+44 (0) 1223 326500, FAX +44 (0) 1223 326501

SUBSCRIPTION SERVICES For change of address, missing issues, new orders and renewals, and payment questions: 800-731-4939 or 202-326-6417, FAX 202-842-1065. Mailing addresses: AAAS, P.O. Box 1811, Danbury, CT 06813 or AAAS Member Services, 1200 New York Avenue, NW, Washington, DC 20005

INSTITUTIONAL SITE LICENCES please call 202-326-6755 for any questions or information

REPRINTS Ordering/Billing/Status 800-635-7171; Corrections 202-326-6501

PERMISSIONS 202-326-7074, FAX 202-682-0816

MEMBER BENEFITS Bookstore: AAAS/BarnesandNoble.com bookstore www.aaas.org/bn; Car purchase discount: Subaru VIP Program 202-326-6417; Credit Card: MBNA 800-847-7378; Car Rentals: Hertz 800-654-2200 CDP#343457, Dollar 800-800-4000 #AA1115; AAAS Travels: Betchart Expeditions 800-252-4910; Life Insurance: Seabury & Smith 800-424-9883; Other Benefits: AAAS Member Services 202-326-6417 or www.aaasmember.org.

science_editors@aaas.org (for general editorial queries)
science_letters@aaas.org (for queries about letters)
science_reviews@aaas.org (for returning manuscript reviews)
science_bookrevs@aas.org (for book review queries)

Published by the American Association for the Advancement of Science (AAAS), *Science* serves its readers as a forum for the presentation and discussion of important issues related to the advancement of science, including the presentation of minority or conflicting points of view, rather than by publishing only material on which a consensus has been reached. Accordingly, all articles published in *Science*—including editorials, news and comment, and book reviews—are signed and reflect the individual views of the authors and not official points of view adopted by the AAAS or the institutions with which the authors are affiliated.

AAAS was founded in 1848 and incorporated in 1874. Its mission is to advance science and innovation throughout the world for the benefit of all people. The goals of the association are to: foster communication among scientists, engineers and the public; enhance international cooperation in science and its applications; promote the responsible conduct and use of science and technology; foster education in science and technology for everyone; enhance the science and technology workforce and infrastructure; increase public understanding and appreciation of science and technology; and strengthen support for the science and technology enterprise.

INFORMATION FOR CONTRIBUTORS

See pages 135 and 136 of the 7 January 2005 issue or access www.sciencemag.org/feature/contribinfo/home.shtml

EDITOR-IN-CHIEF **Donald Kennedy**
EXECUTIVE EDITOR **Monica M. Bradford**
DEPUTY EDITORS **R. Brooks Hanson, Katrina L. Kelner**
NEWS EDITOR **Colin Norman**

EDITORIAL SUPERVISORY SENIOR EDITORS Barbara Jasny, Phillip D. Szuromi; SENIOR EDITORS Gilbert J. Chin, Lisa D. Chong, Pamela J. Hines, Paula A. Kiberstis (Boston), Beverly A. Purnell, L. Bryan Ray, Guy Riddihough (Manila), H. Jesse Smith, Valda Vinson, David Voss; ASSOCIATE EDITORS Marc S. Lavine, Jake S. Yeston; ONLINE EDITOR Stewart Wills; CONTRIBUTING EDITOR Ivan Amato; ASSOCIATE ONLINE EDITOR Tara S. Marathe; BOOK REVIEW EDITOR Sherman J. Suter; ASSOCIATE LETTERS EDITOR Etta Kavanagh; INFORMATION SPECIALIST Janet Kegg; EDITORIAL MANAGER Cara Tate; SENIOR COPY EDITORS Jeffrey E. Cook, Harry Jach, Barbara P. Ordway; COPY EDITORS Cynthia Howe, Alexis Wynne Mogul, Sabrah M. n'haRaven, Jennifer Sills, Trista Wagoner; EDITORIAL COORDINATORS Carolyn Kyle, Beverly Shields; PUBLICATION ASSISTANTS Chris Filiatreau, Joi S. Granger, Jeffrey Hearn, Lisa Johnson, Scott Miller, Jerry Richardson, Brian White, Anita Wynn; EDITORIAL ASSISTANTS Ramatoulaye Diop, E. Annie Hall, Patricia M. Moore, Brendan Nardozzi, Michael Rodewald; EXECUTIVE ASSISTANT Sylvia S. Kihara; ADMINISTRATIVE SUPPORT Patricia F. Fisher

NEWS SENIOR CORRESPONDENT Jean Marx; DEPUTY NEWS EDITORS Robert Coontz, Jeffrey Mervis, Leslie Roberts, John Travis; CONTRIBUTING EDITORS Elizabeth Culotta, Polly Shulman; NEWS WRITERS Yudhijit Bhattacharjee, Jennifer Couzin, David Grimm, Constance Holden, Jocelyn Kaiser, Richard A. Kerr, Eli Kintisch, Andrew Lawler (New England), Greg Miller, Elizabeth Pennisi, Charles Seife, Robert F. Service (Pacific NW), Erik Stokstad; Amitabh Avasthi (intern); CONTRIBUTING CORRESPONDENTS Marcia Barinaga (Berkeley, CA), Barry A. Cipra, Adrian Cho, Jon Cohen (San Diego, CA), Daniel Ferber, Ann Gibbons, Robert Irion, Mitch Leslie (NetWatch), Charles C. Mann, Evelyn Strauss, Gary Taubes, Ingrid Wickelgren; COPY EDITORS Linda B. Felaco, Rachel Curran, Sean Richardson; ADMINISTRATIVE SUPPORT Scherraine Mack, Fannie Groom BUREAUS: Berkeley, CA: 510-652-0302, FAX 510-652-1867, New England: 207-549-7755, San Diego, CA: 760-942-3252, FAX 760-942-4979, Pacific Northwest: 503-963-1940

PRODUCTION DIRECTOR James Landry; SENIOR MANAGER Wendy K. Shank; ASSISTANT MANAGER Rebecca Doshi; SENIOR SPECIALISTS Vicki J. Jorgensen, Jessica K. Moshell; SPECIALISTS Jay R. Covert, Stacey Ferebee; **PREFLIGHT** DIRECTOR David M. Tompkins; MANAGER Marcus Spiegler; SPECIALIST Jessie Mudjitaba;

ART DIRECTOR Joshua Moglia; ASSOCIATE ART DIRECTOR Kelly Buckheit; ILLUSTRATOR Katharine Sutliff; SENIOR ART ASSOCIATES Holly Bishop, Laura Creveling, Preston Huey, Julie White; ASSOCIATE Nayomi Kevitiyagala; PHOTO RESEARCHER Leslie Blizard

***SCIENCE* INTERNATIONAL**

EUROPE (science@science-int.co.uk) EDITORIAL: INTERNATIONAL MANAGING EDITOR Andrew M. Sugden; SENIOR EDITOR/PERSPECTIVES Julia Fahrenkamp-Uppenbrink; SENIOR EDITORS Caroline Ash (Geneva: +41 (0) 222 346 3106), Stella M. Hurtley, Ian S. Osborne, Peter Stern; ASSOCIATE EDITOR Stephen J. Simpson; EDITORIAL SUPPORT Emma Westgate; Deborah Dennison ADMINISTRATIVE SUPPORT Janet Clements, Phil Marlow, Jill White; NEWS: INTERNATIONAL NEWS EDITOR Eliot Marshall DEPUTY NEWS EDITOR Daniel Clery; CORRESPONDENT Gretchen Vogel (Berlin: +49 (0) 30 2809 3902, FAX +49 (0) 30 2809 8365); CONTRIBUTING CORRESPONDENTS Michael Balter (Paris), Martin Enserink (Amsterdam and Paris); INTERN Mason Inman

ASIA Japan Office: Asca Corporation, Eiko Ishioka, Fusako Tamura, 1-8-13, Hirano-cho, Chuo-ku, Osaka-shi, Osaka, 541-0046 Japan; +81 (0) 6 6202 6272, FAX +81 (0) 6 6202 6271; asca@os.gulf.or.jp JAPAN NEWS BUREAU: Dennis Normile (contributing correspondent, +81 (0) 3 3391 0630, FAX 81 (0) 3 5936 3531; dnormile@gol.com); CHINA REPRESENTATIVE Hao Xin, + 86 (0) 10 6307 4439 or 6307 3676, FAX +86 (0) 10 6307 4358; haoxin@earthlink.net; SOUTH ASIA Pallava Bagla (contributing correspondent +91 (0) 11 2271 2896; pbagla@vsnl.com); CENTRAL ASIA Richard Stone (+7 3272 6413 35, rstone@aaas.org)

EXECUTIVE PUBLISHER **Alan I. Leshner**
PUBLISHER **Beth Rosner**

FULFILLMENT & MEMBERSHIP SERVICES (membership@aaas.org) DIRECTOR Marlene Zendell; MANAGER Waylon Butler; SYSTEMS SPECIALIST Andrew Vargo SENIOR SPECIALIST Pat Butler; SPECIALISTS Laurie Baker, Tamara Alfson, Karena Smith

BUSINESS OPERATIONS AND ADMINISTRATION DIRECTOR Deborah Rivera-Wienhold; BUSINESS MANAGER Randy Yi; SENIOR BUSINESS ANALYST Lisa Donovan; BUSINESS ANALYST Jessica Tierney; FINANCIAL ANALYST Farida Yeasmin; RIGHTS AND PERMISSIONS: ADMINISTRATOR Emilie David; ASSOCIATE Elizabeth Sandler; MARKETING: DIRECTOR John Meyers; MEMBERSHIP MARKETING MANAGER Darryl Walter; MARKETING ASSOCIATE Julianne Wielga; RECRUITMENT MARKETING MANAGER Allison Pritchard; ASSOCIATES Mary Ellen Crowley, Amanda Donathen, Catherine Featherston; DIRECTOR OF INTERNATIONAL MARKETING AND RECRUITMENT ADVERTISING Deborah Harris; INTERNATIONAL MARKETING MANAGER Wendy Sturley; MARKETING/MEMBER SERVICES EXECUTIVE: Linda Rusk; JAPAN SALES AND MARKETING MANAGER Jason Hannaford; SITE LICENSE SALES: DIRECTOR Tom Ryan; SALES AND CUSTOMER SERVICE Mehan Dossani, Catherine Holland, Adam Banner, Yaniv Snir; ELECTRONIC MEDIA: INTERNET PRODUCTION MANAGER Lizabeth Harman; ASSISTANT PRODUCTION MANAGER Wendy Stengel; SENIOR PRODUCTION ASSOCIATES Sheila Mackall, Amanda K. Skelton, Lisa Stanford; PRODUCTION ASSOCIATE Nichele Johnston; LEAD APPLICATIONS DEVELOPER Carl Saffell

PRODUCT ADVERTISING (science_advertising@aaas.org); MIDWEST Rick Bongiovanni: 330-405-7080, FAX 330-405-7081 • WEST COAST/W. CANADA B. Neil Boylan (Associate Director): 650-964-2266, FAX 650-964-2267 • EAST COAST/E. CANADA Christopher Breslin: 443-512-0330, FAX 443-512-0331 • UK/SCANDINAVIA/FRANCE/ITALY/BELGIUM/NETHERLANDS Andrew Davies (Associate Director): +44 (0)1782 750111, FAX +44 (0) 1782 751999 • GERMANY/SWITZERLAND/AUSTRIA Tracey Peers (Associate Director): +44 (0) 1782 752530, FAX +44 (0) 1782 752531 JAPAN Mashy Yoshikawa: +81 (0) 33235 5961, FAX +81 (0) 33235 5852 ISRAEL Jessica Nachlas +9723 5449123 • TRAFFIC MANAGER Carol Maddox; SALES COORDINATOR Deiandra Simms

CLASSIFIED ADVERTISING (advertise@sciencecareers.org); U.S.: SALES DIRECTOR Gabrielle Boguslawski: 718-491-1607, FAX 202-289-6742; INTERNET SALES MANAGER Beth Dwyer: 202-326-6534; INSIDE SALES MANAGER Daryl Anderson: 202-326-6543; WEST COAST/MIDWEST Kristine von Zedlitz: 415-956-2531; EAST COAST Jill Downing: 631-580-2445; LINE AD SALES Emnet Tesfaye: 202-326-6740; SENIOR SALES COORDINATOR Erika Bryant; SALES COORDINATORS Rohan Edmonson, Christopher Normile, Joyce Scott, Shirley Young; INTERNATIONAL: SALES MANAGER Tracy Holmes: +44 (0) 1223 326525, FAX +44 (0) 1223 326532; SALES Christina Harrison, Suitlana Barnes; SALES ASSISTANT Helen Moroney; JAPAN: Jason Hannaford: +81 (0) 52 789 1860, FAX +81 (0) 52 789 1861; PRODUCTION: MANAGER Jennifer Rankin; ASSISTANT MANAGER Deborah Tompkins; ASSOCIATE Amy Hardcastle; SENIOR TRAFFICKING ASSOCIATE Christine Hall; SENIOR PUBLICATIONS ASSISTANT Robert Buck; PUBLICATIONS ASSISTANT Natasha Pinol

AAAS BOARD OF DIRECTORS RETIRING PRESIDENT, CHAIR Shirley Ann Jackson; PRESIDENT Gilbert S. Omenn; PRESIDENT-ELECT John P. Holdren; TREASURER David E. Shaw; CHIEF EXECUTIVE OFFICER Alan I. Leshner; BOARD Rosina M. Bierbaum; John E. Burris; John E. Dowling; Lynn W. Enquist; Susan M. Fitzpatrick; Richard A. Meserve; Norine E. Noonan; Peter J. Stang; Kathryn D. Sullivan

AAAS
ADVANCING SCIENCE, SERVING SOCIETY

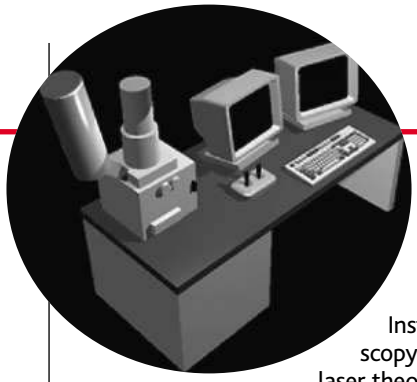

NetWatch

edited by Mitch Leslie

EDUCATION

Sharing the Spectrum

Instructors who've devised a new x-ray spectroscopy lab or have some good pointers for teaching laser theory can pass on that know-how to their peers through this new Web site. OpenSpectrum lets college teachers take part, Wikipedia-style, in revamping an existing tutorial, Science of Spectroscopy (NetWatch, 13 September 2002, p. 1775). Created by Stewart Mader of Emerson College in Boston and Michael Rooke of Long Island University in New York, OpenSpectrum encourages teachers to collaborate and share specialized knowledge as they tailor the content for their classes, says Mader. In addition, Mader has teamed with NASA to include space and satellite images that illustrate uses of spectroscopy.

scienceofspectroscopy.info/wiki

EDUCATION

Standing Up for Darwin

Evolution is under attack again, as school boards in Kansas and other states consider whether to mandate teaching of "intelligent design," a glorified version of creationism (*Science*, 29 April, p. 627). To help teachers and other visitors better understand evolution, the U.S. National Academies have released this collection* of previously published reports, position statements, and other documents. The offerings include a synopsis of the evidence for evolution and a guide to using it to help students learn how science works.

Two other sites previously reviewed in NetWatch brim with helpful information. In a section on obstacles to teaching Darwinism, this primer† from the University of California, Berkeley, profiles different strains of anti-evolutionism. Part of the Talk.Origins Archive, this page‡ offers a clear take on human ancestry and debunks creationist views on the subject.

* nationalacademies.org/evolution
† evolution.berkeley.edu
‡ www.talkorigins.org/faqs/homs

EXHIBITS

Trial of the (17th) Century

On 22 June 1633, an elderly and frail Galileo Galilei appeared before a tribunal of the Roman Inquisition, clad in a white shirt signifying contrition. Arraigned for advocating the heresy that Earth wasn't the center of the universe, Galileo took a plea bargain and vowed to "abjure, curse, and detest the aforesaid errors and heresies, and generally every other error and sect whatsoever contrary to the said Holy Church." Read more about the famous clash between religion and science at this site from law professor Douglas Linder of the University of Missouri, Kansas City. Along with an account of the trial (left) and its background, Linder marshals a wealth of documents from the case. You can study Galileo's *Dialogue Concerning the Two Chief World Systems*—the work that prompted the Church to take action against him—the papal condemnation, and part of his recantation. The Galileo pages are part of Linder's site summarizing famous trials, including two others with a scientific angle: the 1925 Scopes trial and the 1951 nuclear espionage case against Julius and Ethel Rosenberg.

www.law.umkc.edu/faculty/projects/ftrials/galileo/galileo.html

IMAGES

Moth Parade

To identify a salamander or warbler, just crack open one of the many available field guides. Researchers vexed by a mysterious moth don't have that luxury because there's no comprehensive catalog for the nearly 11,000 species fluttering around North America. However, entomologist John Snyder of Furman University in Greenville, South Carolina, has compiled a virtual field guide* that links to photos of more than 4000 moth species scattered around the Internet. Snyder says that he made an effort to corral caterpillars, such as this plump tomato hornworm (*Manduca quinquemaculata*), which are often hard to find in other references. A similar site,† hosted by three Italian scientists and insect enthusiasts, covers some 1450 kinds of European and North African moths and butterflies.

* facweb.furman.edu/~snyderjohn/leplist
† www.leps.it

RESOURCES

The E-Print Files

If you're looking for online theses or electronic manuscripts, visit this archive compiled by grad student Tim Brody of the University of Southampton, U.K. It lists more than 430 sites that stow open-access dissertations and papers, including unreviewed manuscripts. The collections cover topics from agricultural and applied economics to wind power.

archives.eprints.org

Send site suggestions to netwatch@aaas.org. Archive: www.sciencemag.org/netwatch

This Week

PAGE 1853
Chickadees' alarming repertoire

1855
Photosynthesis in the abyss

EUROPEAN UNION

Political Crisis Puts Europe's Research Ambitions in Doubt

The marathon summit that failed and plunged the European Union into disarray last week also dealt a severe blow to aspirations for European science policy, unveiled just 2 months ago by the European Commission—most notably to its plan to double the E.U.'s science budget. Disappointed researchers say the fiasco shows that politicians are only paying lip service to the so-called Lisbon strategy, which aims to revamp Europe's economy through research, innovation, and economic reforms.

"What a nightmare," says French biologist Frédéric Sgard, vice president of Euroscience, an organization of European researchers that has lobbied for major new investments in science. The failure could spell the end of the plan, hailed by many scientists, for a European Research Council (ERC) to fund basic research.The 2-day meeting in Brussels, aimed at hashing out an E.U. budget for 2007–13, ended in bitter acrimony primarily because the United Kingdom refused to pay more into the E.U.'s coffers if negotiations on the union's agricultural subsidies weren't reopened—a condition unacceptable to France, the subsidies' main beneficiary. The stalemate deepened a crisis opened 3 weeks ago by the French and Dutch "no" votes on the proposed European Constitution.

In April, the European Commission had rolled out its proposal for Framework 7 (FP7), the most ambitious of the E.U.'s research programs yet. At €73 billion, the 7-year program would have more than doubled the E.U.'s annual expenditure on research and innovation. But disagreements about the broader budget clouded the plan's future from the start (*Science*, 15 April, p. 342). In an attempt to solve the looming crisis, Luxembourg, which currently holds the E.U. presidency, recently proposed growing the entire "competitiveness" budget—which includes research—at a much slower pace, which would result in €43 billion or less for FP7.

The Luxembourg compromise failed last week, but few countries protested the cuts that it would have made in research and innovation, Sgard says, making it very unlikely they will reserve more money for science in any future agreement. What's more, with Britain assuming the rotating presidency for 6 months on 1 July, any compromise on member contributions and farm subsidies seems unlikely. That will, in turn, hamstring the discussion about FP7 in the European Parliament, which has just started, says Giles Chichester, chair of the Committee on Industry, Research, and Energy: "It would be extremely difficult if we don't know how much money we're talking about. We're in uncharted territory here."

No love lost. Britain's Tony Blair and France's Jacques Chirac disagreed bitterly at last week's summit meeting.

The European Commission doesn't have a plan B, says a spokesperson for Research Commissioner Janez Potočnik. Until an agreement is reached on a new budget, the commission will continue preparing for FP7 based on the original proposal, she says. Member states' unwillingness to pay for the ambitious science policy they say they support has been "a huge disappointment" for Potočnik, who had tried hard to rally leaders behind FP7, according to a source close to the commissioner.

Potočnik's predecessor Philippe Busquin, the architect of the commission's current science policy, is equally dismayed. Busquin, now a member of the European Parliament, calls the Luxembourg plan "unacceptable"—all the more so because it would leave agricultural subsidies almost intact. "That's a budget of the past instead of the future," Busquin ▶

CONDENSED MATTER PHYSICS

Tiny Whirlpools Prove Atoms Flow Freely

Most researchers would rather not poke holes in their own experiments, but a team of physicists is happy to have done just that. Stirring a cloud of ultracold atoms, the physicists produced an array of tiny whirlpools that pierced the cloud and proved that the atoms in it had formed a "superfluid," a strange quantum-mechanical soup that flows without any resistance and refuses to rotate. The observation confirms that atoms can join in pairs and behave much like the free-flowing electrons in a superconductor, an effect that physicists have been racing to witness (*Science*, 8 August 2003, p. 750).

"It's a fantastic experiment, really heroic," says Deborah Jin, a physicist at JILA, a laboratory run by the National Institute of Standards and Technology and the University of Colorado, Boulder. Last year, Jin and her team showed that atoms in a gas could pair like the electrons in a superconductor (*Science*, 6 February 2004, p. 741), but experimenters had not proved that the paired atoms actually flowed without resistance. The new results provide "conclusive evidence for superfluidity," Jin says.

To generate the vortices, Martin Zwierlein, Wolfgang Ketterle, and colleagues at the Massachusetts Institute of Technology in Cambridge first used laser beams and magnetic fields to chill atoms of the isotope lithium-6 to within billionths of a degree of absolute zero. The atoms hovered in a vacuum chamber, trapped in a laser beam, and the researchers applied a magnetic field to make them interact. Tuning the strength of the field, the physicists coaxed the atoms to pair to form a "Fermi condensate." The subtle pairing occurs even though the atoms cannot bind to form molecules.

The researchers then tried to rotate the ▶

CREDIT: THIERRY ROGE/REUTERS

1856
Missing connections in autism

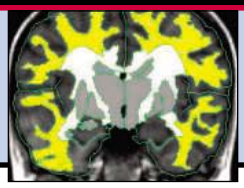

1858
The rocky road to personal medicines

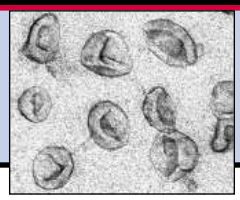

1862
What role do exosomes play?

says. "This way, Europe will stagnate."

Experts can only speculate about what might be sacrificed in a science budget that falls far short of the commission's €73 billion proposal. One "prime target" would be the European Research Council, a new body to fund basic, investigator-driven research in a Europe-wide competition, Chichester predicts. "It's always easier to cut something if you haven't started it yet," he says. But doing so would risk demoralizing and alienating the scientific community, which fought hard for the ERC; even major cuts in its proposed €1.7 billion annual budget would rob the council of its credibility, says Danish mathematician Mogens Flensted-Jensen, vice chair of the expert group that proposed the ERC in 2003.

Still, Helga Nowotny, chair of the European Research Advisory Board, does see some hope. The crisis will force politicians to rethink what European unification is all about; research, innovation, and education may well benefit if scientists keep pressing their case. What's more, she notes that the United Kingdom is a strong proponent of shifting E.U. funds from farms to labs. Even if the British cannot foster a new agreement when they chair the union during their presidency, "they will certainly put research back on the map," Nowotny says.

–MARTIN ENSERINK

INFECTIOUS DISEASES

Lapses Worry Bird Flu Experts

Global health experts trying to stave off a deadly pandemic of avian flu are alarmed by recent actions they see as counterproductive and even dangerous. Vietnam has been slow to report 10 new human cases, and farmers in China have reportedly been giving an antiviral drug to chickens that may have made the virus resistant to one of the few drugs available to fight human flu. If confirmed, China's actions would be "very, very dangerous," says Ilaria Capua of the Istituto Zooprofilattico Sperimentale della Venezie in Legnaro, Italy.

Drug habit. Chinese farmers routinely administered an antiviral drug to poultry, according to a news report.

Vietnam has found another possible case of human-to-human transmission of the H5N1 virus among a total of 10 new cases it reported in a 1-week period—6 weeks or more after they were originally detected. The Ministry of Health officially notified the World Health Organization (WHO) of three new human H5N1 cases on 8 June, but the most recent of those had been detected on 26 April. On 14 June, Vietnam reported three more human cases that had turned up during the last 2 weeks of May. And on 17 June, the ministry reported four additional cases that had emerged between 1 and 17 June.

Peter Horby, an epidemiologist in WHO's Hanoi office, says Vietnamese officials have quickly asked for help when there were obvious changes in the virus's behavior, as when numerous mild cases of the disease emerged this spring. But he says it has been frustrating that these same officials have been less forthcoming in reporting the details of what they apparently see as more routine cases.

Some bird flu experts are equally alarmed by China's veterinary use of the human antiviral drug amantadine, as reported in the 18 June *Washington Post*. According to the article, drugmakers and other sources in China admitted that the drug has been sold cheaply to farmers and given to poultry both as a treatment and a prophylactic since the late 1990s.

Most of the H5N1 strains isolated in the current outbreak in Asia are resistant to amantadine, but establishing a firm link with China's use of the drug would require extensive data on where, when, and how much of the drug was used, notes Klaus Stöhr, WHO's global influenza coordinator. K. Y. Yuen, a virologist at the University of Hong Kong, says the misuse of antivirals, such as amantadine, does raise the risk of fostering resistance. But he says the genetic mutation associated with amantadine resistance has been reported in viruses not exposed to the drug, which suggests that ▶

cloud by tickling it with another laser, much as one might set a golf ball spinning by brushing it with a feather, as they report this week in *Nature*. Had the lithium-6 been an ordinary fluid, the cloud would have rotated as a whole, just as water will rotate along with a slowly turning drinking glass. A superfluid resists rotation, however, because it is essentially a quantum wave that can possess only quantized amounts of rotation. Turn its container fast enough, and a superfluid admits one quantum of rotation in the form of a tiny whirlpool, or "vortex." Turn faster still, and the vortices proliferate and form a triangular array. That is what Zwierlein and Ketterle observed in the cloud of atoms, although not without a lot of work. "It was bloody difficult," Ketterle says. "We were actually close to giving up."

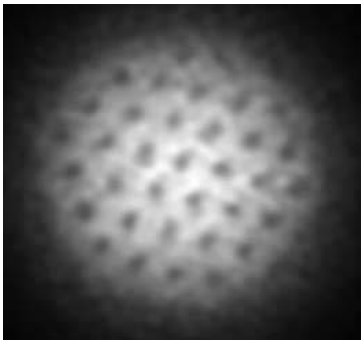

Smoking gun. Array of vortices proves that paired atoms form a superfluid.

A Fermi condensate is a cousin of a Bose-Einstein condensate, a superfluid that forms when, instead of pairing, particles pile into a single quantum wave. By changing the magnetic field, physicists can now transform a Fermi condensate of atoms into a Bose-Einstein condensate of loosely bound molecules and probe the connection between the two superfluids, says Henk Stoof, a theorist at Utrecht University in the Netherlands: "How you go from one limit to the other is very important." The tunable superfluid could even mimic more exotic superfluids, such as the paired-up neutrons coursing through the hearts of neutron stars.

–ADRIAN CHO

CREDITS (TOP TO BOTTOM): GREG BAKER/AP PHOTO; ANDRE SCHIROTZEK/MIT

eppendorf PhysioCare Concept criteria 3 and 4

- 30% less weight
- Single handed volume setting
- Ergonomic studies
- Ergonomics approved by TÜV

Less strain – more efficiency.

Optimized form and function – Perfectly balanced

PhysioCare Concept pipettes.
The more strain you experience, the less energy you have. And because energy is a very precious and exhaustible resource, we try to use it as efficiently as possible.

So why aren't more manufacturers doing it?
Probably because it's not that easy.

TÜV Rheinland approved our manual pipettes as: ergonomic, user-friendly and user tested.

PhysioCare concept

Check out how good your pipette really is!
PhysioCare Concept™ website
www.physiocare-concept.info

eppendorf

In touch with life

Your local distributor: www.eppendorf.com/worldwide · Application Hotline: +49 180-3 66 67 89
Eppendorf AG · Germany · +49 40 538 01-0 • Eppendorf North America, Inc. 800-645-3050

other factors might be at work as well.

Still, given the threat of a pandemic and the dearth of flu drugs—the only alternative to amantadine and a cousin is oseltamivir, or Tamiflu, which is more expensive and harder to produce—antivirals should probably not be used for animal flu infection at all, Stöhr says. They aren't licensed for use in poultry and would do little to contain the virus anyway if not accompanied by strict biosecurity measures, adds Capua.

Xu Shixing, a Chinese Ministry of Agriculture official, says the ministry never approved the use of amantadine for poultry, as was claimed in the *Post* article.

In yet another reminder of the virus's expanding geographical grip, Indonesia confirmed its first human case of H5N1 infection last week, the fourth country to do so.

–DENNIS NORMILE AND MARTIN ENSERINK

With reporting by Gong Yidong of *China Features* in Beijing.

EUROPEAN PATENTS

BRCA2 Claim Faces New Challenge

A patent on the breast cancer gene *BRCA2*—a symbol of assertive U.S. biotechnology—faces a major challenge in the European Patent Office (EPO) in Munich, Germany, on 29 June. European clinical groups say the patent—licensed to Myriad Genetics of Salt Lake City, Utah—should be dismissed for legal and ethical reasons, including the fact that it is limited to diagnoses in Ashkenazi Jewish women. They hope this will stall the company's licensing push in Europe. The case is being watched as a test of how enforceable human gene patents will be in Europe.

Opposed. Gert Matthijs says the *BRCA2* patent is "not acceptable."

The controversial patent is a fragment of what was once a broad package of Myriad claims covering the genes *BRCA1* and *BRCA2*. Although Myriad has exclusive rights to commercialize tests based on *BRCA1* and *BRCA2* in the United States, European clinics have resisted signing up for licenses. (The patents are owned by an array of groups, including the University of Utah Research Foundation.) European opponents have chipped away at Myriad's claims; their challenge based on sequence errors in a description of *BRCA1*, for example, helped scuttle that patent in Europe.

In January, EPO approved a whittled-down version of the patent request on *BRCA2*, awarding the company "use of an isolated nucleic acid" on chromosome 13 "for diagnosing a predisposition to breast cancer in Ashkenazi Jewish women in vitro." Continuing an anti-Myriad campaign already 5 years old, the Institut Curie in Paris and 19 other groups interested in gene testing have contested the new *BRCA2* patent. (EPO is following standard practice in letting opponents argue against the patent after it has been awarded.) Many clinics have resisted the company's efforts to sell licenses because they seemed one-sided and based on weak claims, says geneticist Gert-Jan van Ommen of the Center of Human and Clinical Genetics at Leiden University Medical Center in the Netherlands. He says doctors object to paying Myriad for something they could do themselves. (A test now costs about $2800.) Myriad requires physicians to send patients' DNA samples to Utah, where the company keeps them. This does "not sit well," says van Ommen, because Europeans had contributed a great deal to *BRCA* research.

Last week the opponents recruited a new ally, the European Society for Human Genetics (ESHG) in Vienna, Austria. It has asked EPO to dismiss Myriad's *BRCA2* patent because it explicitly claims a mutation in Ashkenazi Jewish women. The chair of ESHG's patenting and licensing committee, human geneticist Gert Matthijs of the University of Leuven, Belgium, says that seeking ownership of a mutation in an ethnic group "is not acceptable to most geneticists."

Dominique Stoppa-Lyonnet of the Institut Curie adds that it would compel a doctor to ask a woman about her ancestry before offering a consultation: "This is discrimination," she believes. Besides, Stoppa-Lyonnet says, it is impractical: Many people of Ashkenazi descent don't know their ancestry.

Myriad declined to comment because the matter is under legal review. However, a legal brief filed last year on the company's behalf by the firm Vossius & Partner in Munich argues that Myriad and collaborators spent "millions of dollars" to characterize *BRCA2* and released the data freely for public use. Women across the globe have benefited, the brief says. It further argues that focusing on the Ashkenazi population makes testing for breast cancer risk more efficient and affordable.

If the past is a guide, the EPO technical group will make its decision known quickly, says spokesperson Rainer Osterwalder. Either side can appeal for a final high-level EPO review.

–ELIOT MARSHALL

CREDIT: F. REINHOLD

ScienceScope

The Gods Must Be Angry

Astrophysicists are anxiously awaiting a federal court decision on a lawsuit that threatens a planned gamma ray telescope near Kitt Peak in Arizona. The Tohono O'odham tribe brought suit against the scope this spring, arguing that the deity they believe created the world resides near where the array is to be built.

The National Science Foundation (NSF), which is funding the $13.1 million project with the Department of Energy, has already spent $1 million at the site. Construction was halted after the lawsuit was filed. Under federal law, NSF must seek alternative locations for the Very Energetic Radiation Imaging Telescope Array System, which was due to be completed by next fall and would be operated by the Smithsonian Astrophysical Observatory in Cambridge, Massachusetts. "If other sites are not available, then not building [the system] is a possibility," says NSF lawyer Amy Northcutt, although she adds that offsite work on telescope components continues.

NSF last month filed a motion to dismiss the lawsuit, and the tribe is expected to respond this week. Then it will be up to the court to make a decision.

–ANDREW LAWLER

Vessel Makes Waves in New Ranking

Ocean scientists have a sinking feeling about the new lineup of proposed large facilities at the National Science Foundation (NSF).

Last year, the National Science Board, NSF's oversight body, put a $269 million network of instruments called the Ocean Observatories Initiative (OOI) at the top of its list of projects for fiscal year 2007. But late last month, the science board put the Alaska Region Research Vessel on top and slid OOI down to third place, behind a network of ecological observatories called NEON that NSF has been trying for years to make pass congressional muster. Third is a perilous position because NSF has said it plans to propose only two new projects in 2007.

Board president Warren Washington says "all of the projects are well worth doing" but that the need for scientists to monitor the rapid warming in the Arctic guided the board. Senator Ted Stevens (R–AK) is also a big fan of the ship, although Washington says that Stevens's support was not a factor. OOI's steering committee will discuss the reshuffling at a meeting next week.

–JEFFREY MERVIS

NUCLEAR SCIENCE

RHIC Gets Nod Over JLab in Worst-Case DOE Scenario

Earlier this year, the Department of Energy posed an agonizing question to a panel of nuclear physicists: If its budget doesn't get any better, which of two major DOE facilities should be shut down? Last week the panel delivered a verdict, showing a "slight preference" for the Relativistic Heavy Ion Collider (RHIC) at Brookhaven National Laboratory in Upton, New York, over the Thomas Jefferson National Accelerator Facility (JLab) in Newport News, Virginia. But adopting that choice, it warned DOE officials, would create a damaging rift within the nuclear science community.

At risk. A continued tight budget could force DOE to shut its Thomas Jefferson National Accelerator Facility.

"It would be a dagger in the heart of international nuclear physics if this would happen," says Tony Thomas, JLab's chief scientist. "It would create a deep chasm within the U.S. nuclear science community as well as an international chasm." And the so-called winner is barely more joyful. "It would be really bad if we succumbed to the temptation to break into camps," says Sam Aronson, associate director for high-energy and nuclear physics at Brookhaven. "We've always managed to get past difficult budget situations; we should not take the opportunity to fight with each other."

The trouble began in February after President George W. Bush proposed cutting nuclear physics at DOE by more than 8%, to $371 million. That drop would translate into a drastic reduction in run times for the two main nuclear physics facilities in the United States, RHIC at Brookhaven and CEBAF at JLab. And although Congress seems inclined to restore the cuts this year, DOE is expecting lean times for at least the rest of the decade. So in March, DOE asked its nuclear science advisory committee for help in dealing with such a scenario (*Science*, 29 April, p. 615).

The budget outlook gave the panel little flexibility, says Texas A&M physicist Robert Tribble, who chaired the subcommittee that made the call: "There's simply no way we can sustain JLab and RHIC operations at meaningful levels and still have a future." The panel's "slight preference" for keeping RHIC alive was based on the fact that the instrument was still in the "discovery phase" after creating the quark-gluon plasma (*Science*, 22 April, p. 479).

The potential for a schism is based on the fact that RHIC and CEBAF do very different types of nuclear-physics experiments. The former uses heavy ions to probe the conditions of nuclear matter in the early universe, whereas the latter uses electron beams to look at things such as the structure of the proton. Shutting down one would deprive a large chunk of the U.S. nuclear science community of a place to do research, dividing it into haves and have-nots. Picking one branch of research at the expense of another is divisive, says JLab's Thomas. ▶

TAIWAN

New University President Has Links to Paranormal Research

JINAN, CHINA—The Taiwan government has chosen a devotee of research into paranormal phenomena to lead its premier university. Lee Si-chen, a semiconductor physicist at National Taiwan University (NTU), says he plans to end his current experiments of parapsychology once he takes office this week as NTU's 16th president. But faculty members are worried that those experiments, prominently displayed on Lee's CV and Web site, will undermine his efforts to make NTU, founded in 1928, a world-class institution.

Lee, 52, previously dean of academic affairs at NTU, is well regarded for his work in solid state physics. "Professor Lee has certainly made several important contributions to semiconductor heterojunction device physics," says James Harris, a semiconductor physicist at Stanford University in California. Trained at Stanford and a fellow of the Institute of Electrical and Electronics Engineers (IEEE), the leading international society for electrical and electronics engineers, Lee says he wants to make NTU one of the world's top 100 universities by wooing top-ranked scientists from around the globe and building new research and teaching facilities.

In conjunction with his administrative and scientific labors, however, Lee has maintained an active interest in the paranormal. His research into *Qigong* (a Chinese practice combining meditation and breathing exercises) has favorably examined claims that so-called external *Qi* is capable of altering the nature of materials without any physical contact. He has also explored the phenomenon of "finger-reading," which purports that school-aged children can be trained to visualize numbers, Chinese characters, and symbols written on paper that is wadded up and placed in their hands.

That work bothers some of his colleagues. This spring, Yang Shin-nan, a physicist and delegate to the university's faculty senate, wrote an open letter expressing his fear that Lee's appointment could damage the university's reputation. NTU physicist Kao Yeong-Chuan, a longtime critic of Lee's paranormal research, says that he was "shocked that Professor Lee could get enough votes to become one of the two finalists." Kao is willing to cut Lee some slack, but he says that "extraordinary claims must be backed up by extraordinary evidence."

Lee, who was appointed to a 4-year term, defends his line of investigation. "Everybody is welcome to reasonably challenge other people's research, but not to reject all unusual phenomena bluntly and arrogantly," he says, adding that most of his studies on finger-reading were done to confirm the work of others. "Scientists should not be forbidden from exploring the unknown frontier."

Lee acknowledges, however, that findings have been inconsistent because human beings are "unsteady." And although he would like to find more quantifiable metrics for studying such phenomena, he says he plans to terminate his experiments "for the sake of a peaceful campus."

–LEI DU

Lei Du is a freelance writer in Shandong Province, China.

CREDIT: PHOTO COURTESY OF JEFFERSON LAB

The silver lining in the dark clouds gathering over nuclear science is a positive reaction from Congress so far this year. The House of Representatives has approved a 2006 spending bill that brings much of DOE's nuclear science budget close to current levels (*Science*, 27 May, p. 1241). Last week, a Senate panel added back even more, according to Dennis Kovar, DOE's associate director in charge of nuclear physics. At those funding levels—appropriately adjusted for inflation—Tribble says that DOE need not shut down a facility, although he warns that run times at the facilities would still suffer. And level funding won't help a major new experiment being planned. The Rare Isotope Accelerator, says the panel, "can proceed only with a significant influx of new money."

An anemic budget would have ramifications for the next generation of U.S. nuclear scientists, too, say physicists. "If you close either [RHIC or JLab] at this time," says David Armstrong, a nuclear physicist at the College of William and Mary in Williamsburg, Virginia, "I in good conscience could not advise my students to pursue a career in nuclear science." –CHARLES SEIFE

BEHAVIOR

Bird Alarm Calls Size Up Predators

A great horned owl may look like a more fearsome predator than a puny pygmy owl, but for small, agile birds such as chickadees, the maneuverable pygmy owl is probably the more lethal threat. Now, on page 1934, researchers report that black-capped chickadees have a sophisticated system of alarm calls that conveys information about the size of potential predators. The calls appear to help the chickadees mount a coordinated defense that is calibrated to the predatory threat.

Chickadees are social birds, and they gang up to "mob" predators and drive them away. "They dive-bomb the predator and make a lot of noise," says study author Christopher Templeton, currently a Ph.D. student at the University of Washington, Seattle. While Templeton was working at the University of Montana, he and his adviser, behavioral ecologist Erick Greene, noticed that chickadees responded differently to the sight of different predators. "They really harassed some predators and just ignored others," Templeton says.

The researchers suspected that the chickadees' calls might organize their defense. The birds make two different alarm calls: a soft, high-pitched "seet" call and the louder namesake "chick-a-dee" call. A previous study found that the "seet" call indicates the presence of predators flying overhead. The "chick-a-dee" call is used in a variety of situations, from signaling the presence of stationary predators to identifying flockmates.

The researchers recorded more than 5000 calls that birds made when various predators—including owls, hawks, and falcons from a local wildlife rehabilitation center—were placed in their woodsy outdoor enclosure. The recordings showed that, among other changes, the birds made more "chick-a-dee" calls and incorporated more "dee" syllables into each call when they saw a small raptor with a short wingspan. A 70-gram pygmy owl, for instance, might elicit four "dees" at the end of a call, whereas a 1.4-kilogram great horned owl might elicit only two. But not all small birds elicited more "dees": A harmless quail elicited fewer than two "dees" per call, on average. The researchers hypothesize that more "dees" mean more danger.

On guard. Black-capped chickadees vary their alarm calls according to the size of the predator that has been spotted.

Next, the team played back recorded alarm calls through a hidden speaker and watched the chickadees' reaction. The birds mounted a more vigorous mobbing response when ▶

CREDIT: C. N. TEMPLETON *ET AL.*, *SCIENCE*

ScienceScope

Science Education Review

The board that oversees the National Science Foundation is hoping that a new study of U.S. math and science education will help make the case for a bigger NSF education budget. The study, commissioned by the National Science Board, comes as the White House has proposed shifting precollege science and math instruction funds from NSF to the Department of Education. But many education researchers say NSF has a better track record on science-based reforms.

Although the study's exact focus is still unclear, board president Warren Washington says he'll be looking for outside education experts who have the political savvy to sell the report's conclusions. –JEFFREY MERVIS

Auger Team Picks Colorado

A 15-nation consortium that studies ultrahigh-energy cosmic rays expects to announce its first results next week from the half-completed Pierre Auger Observatory in western Argentina. And this month, the physicists selected a site in Colorado where they hope to build its northern twin.

Each $50 million observatory would consist of 1600 water tanks and 24 ultraviolet telescopes. A 3000-square-kilometer track on the high plains of southeastern Colorado won out over a site in western Utah because of easier access to private lands and better potential for expansion. The researchers hope agencies in their respective countries will provide enough money to complete the northern array by 2012. –ROBERT IRION

Kennewick Man, Finally

Next month, after 9 years of litigation between scientists and the federal government, a dozen researchers will begin preliminary studies on the 9400-year-old remains of Kennewick Man. Access to the bones, now at the Burke Museum in Seattle, Washington, was arranged this spring, says Alan Schneider of Portland, Oregon, the scientists' lawyer.

The first round of study will examine what happened to the bones, found along the Columbia River in 1996, after the man's death. Schneider says further studies could be threatened by a proposed revision of the Native American Graves Protection and Repatriation Act that would broaden the definition of "native American." The bill (S. 536), he says, would allow tribes to block access to any such remains even if no connection with an existing tribe can be established. –CONSTANCE HOLDEN

Science

AAAS

AFFYMETRIX®

AAAS Newcomb Cleveland Prize

Supported by

AFFYMETRIX

CALL FOR NOMINATIONS

This $25,000 prize is awarded to the author or authors of an outstanding paper published in the Research Articles or Reports sections of *Science*.

Readers are invited to nominate papers published during the period 1 June 2004 – 31 May 2005. An eligible paper is one from the relevant sections that includes original research data, theory, or synthesis or one that presents a fundamental contribution to basic knowledge or a technical achievement of far-reaching consequence. Reference to pertinent earlier work by the author may be included to give perspective.

DEADLINE: 30 JUNE 2005

Phone ..... +1 (202) 326 6507

E-mail ..... skihara@aaas.org

Additional information about the prize and the nomination procedure can be found at:
www.aaas.org/about/awards/

they heard a small predator alarm call. More birds got involved, and they approached closer to the speaker and kept up the mobbing for a longer period of time in response to a small predator alarm call than in response to a large predator call.

"The work … shows us that even very common species that we may take for granted have evolved to have very elaborate and exacting systems of communication," says James Hare, who studies ground squirrel alarm calls at the University of Manitoba in Winnipeg, Canada. Historically, researchers have thought alarm calls signaled information about either the type of predator or the degree of threat, says Daniel Blumstein of the University of California, Los Angeles, who studies marmot communication. The new study helps break down this "false dichotomy" by showing that chickadee calls tell of both, Blumstein says.

It also adds to evidence that complex communication arises in the animal kingdom wherever there's a need. "These results should begin to redress the still-pervasive bias that sophisticated signaling can only arise amongst our primate kin," says Christopher Evans, an animal behavior researcher at Macquaire University in Sydney, Australia. **–GREG MILLER**

MARINE BIOLOGY

Microbe May Push Photosynthesis Into Deep Water

The announcement this week of a bacterium that appears to derive energy from light despite living in the inky depths of an ocean threatens to overthrow the dogma that photosynthesis depends on the sun. The microbe may also offer clues about life on early Earth—or on other planets.

Not everyone is convinced yet that the bacterium, discovered in 2003, is a natural resident of the deep sea. But if true, it could be a crucial piece of the puzzle of how photosynthesis evolved. "The results break new ground and are indeed surprising," says Bob Buchanan, a microbiologist at the University of California, Berkeley.

Since their discovery in 1977, deep-sea hydrothermal vents have offered up a surprising menagerie, including 2-meter tubeworms and eyeless crabs, that thrives near the caustic 350°C effluent that burps out. In the late 1980s, Cindy Van Dover, a marine biologist at the College of William and Mary in Williamsburg, Virginia, found a vent-dwelling eyeless shrimp with a light-sensitive patch on its back. Because of the superheated water, vents glow with infrared radiation, but the shrimp's light-gathering pigments seemed geared for much higher frequencies of light.

The explanation came in 1996 when a team led by Alan Chave, an oceanographer at the Woods Hole Oceanographic Institution (WHOI) in Massachusetts, proved that the water around the vents produces additional light. The extra glow is too weak to be detected by human eyes but has a frequency well into the visible spectrum. Researchers still don't agree on the mechanism by which the vents make this deep-sea illumination, but its discovery prompted another question: Does the phenomenon sustain any life?

Bacteria 80 meters below the surface of the Black Sea eke out a living from similarly dim light. These so-called green sulfur bacteria have the most efficient photosynthesis known, sponging up every stray photon that penetrates the water column. So, in an effort partly funded by NASA's Astrobiology Institute, Van Dover teamed up with Thomas Beatty, a microbiologist at the University of British Columbia in Vancouver, Canada, Robert Blankenship, a biochemist at Arizona State University in Tempe, and others to see if similar bacteria were living off the vent light. In 2003, they descended 2.4 kilometers in the WHOI research submarine *Alvin* to retrieve samples from a pair of vents that lie along the volcanically active Pacific Ridge. Back on the ship, they added the samples to various nutrient media to see what might grow.

Defying the long odds, the team now describes the first example of an organism that seems to live off a light source other than the sun. The bacterium—known as GSB1 for the time being—requires light, sulfur, and CO_2 to grow, the team reports online 28 June in the *Proceedings of the National Academy of Sciences*.

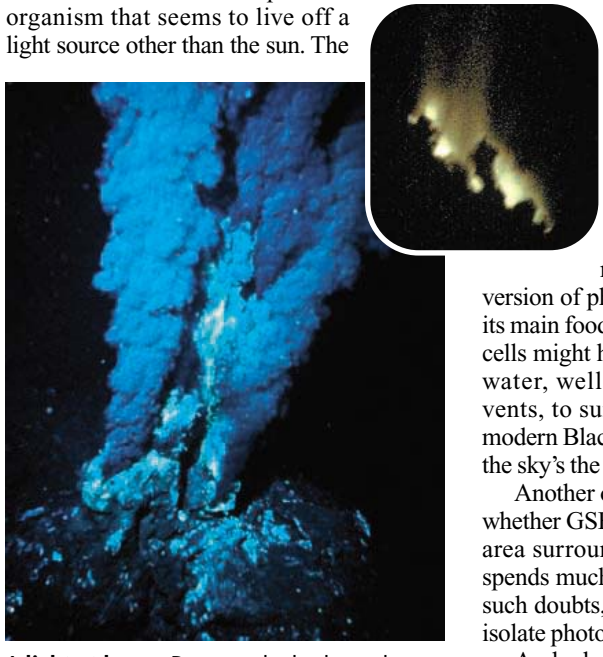

A light at home. Deep-sea hydrothermal vents such as this one emit a mysterious glow (*inset*) that may support photosynthetic bacteria.

To help culture the exotic bacterium, the team recruited Jörg Overmann, a microbiologist at the University of Munich, Germany, and discoverer of the Black Sea green sulfur bacteria. Although oxygen is thought to be toxic to all green sulfur bacteria, they unexpectedly found that GSB1 seems unbothered by it. The team proposes that the turbulent vent environment makes exposure to oxygen-rich water unavoidable for the bacterium, requiring it to adapt.

The big question, according to Euan Nisbet, an Archaean geologist at Royal Holloway, University of London, U.K., is whether GSB1 is a missing link in the evolution of photosynthesis. "Of what use is half of photosynthesis?" he asks, referring to Darwin's puzzle of how evolutionary change through baby steps can create complex structures such as eyes that require multiple parts to function. Nisbet argues that a deep-sea microbe on the early anoxic Earth could have developed a primitive method for detecting the direction of the vents through infrared radiation, setting the stage for a later vent microbe to develop an inefficient version of photosynthesis as a supplement to its main food. Then, "one of these preadapted cells might have drifted into rather shallower water, well away from the hydrothermal vents, to survive by using sunlight just as modern Black Sea bacteria do. And after that, the sky's the limit," Nisbet says.

Another open question, says Buchanan, is whether GSB1 "is a long-term resident in the area surrounding the vent or whether it … spends much of its life elsewhere." To quash such doubts, Beatty is planning a mission to isolate photosynthesizers from other vents.

And what about the vent glow that may power such microbes? Its source remains "quite a speculative issue," says Chave, with explanations ranging from chemical reactions in the vent effluent to sonoluminescence, the flash produced by imploding bubbles. Little work has been done on the phenomenon since its discovery, "both because defining the mechanism would require some difficult measurements … and because interest has waned," says Chave. He hopes, however, that GSB1's discovery "will regalvanize the interest." **–JOHN BOHANNON**

John Bohannon is a science writer based in Berlin.

CREDITS: NOAA; (INSET) DELANEY, SMITH, VAN DOVER, CANN & FOSTER

Autism researchers are hot on the idea that autism results from abnormal communications between brain regions rather than a broken part of the brain

Autistic Brains Out of Synch?

Fourteen-year-old Benjamin Garbowit memorizes long lists of ingredients from food labels but has trouble understanding the point of even simple storybooks. The eighth grader from Short Hills, New Jersey, struggles through a conversation with a stranger, offering mostly one-word utterances. And he is confused by common gestures such as a pat on the head from his mother. "What does it mean?" he wants to know. "Is it love?"

Benjamin has autism, a disorder that has long mystified parents, doctors, and scientists alike because of the diverse deficits, and occasional talents, that accompany it. Although the most glaring problems appear in social interactions, serious shortcomings also show up in reasoning tasks that require integrating different types of information. Autistic individuals may memorize facts easily but find complex concepts elusive.

Researchers have struggled to find an overarching conception of the disorder. And in the past 3 years, they have accumulated tantalizing data suggesting that the problems in autism result from poor connections in the brain areas rather than from defects in a specific brain region. "A confluence of investigations point to a model of autism in which different brain regions are not talking to each other very well," says Martha Herbert, a pediatric neurologist at Harvard Medical School in Boston. "This is a big paradigm shift, because people have been looking for the 'brain address' of the problem in autism."

Imaging experiments show a lack of cooperation between different brain areas, as well as abnormalities in the volume and distribution of the white matter that insulates neuronal signals. Other studies have found oddities in the organization, number, and size of neurons in certain brain regions that could give rise to connectivity problems. "It's the most exciting set of developments in the field to date," comments Helen Tager-Flusberg, an autism researcher at Boston University School of Medicine.

So far, the studies are largely suggestive, and skeptics say that connectivity theory does not get to the bottom of autism. Yet if the theory is correct, it suggests a new approach to molecular studies of the disease. For instance, researchers might look for genes that perturb the development of neural connections rather than genes that map to specific behaviors.

Meanwhile, the work may enable more precise diagnosis of the disorder and a new way to test the efficacy of behavioral therapies or future drugs. "We're very close to finding a biological marker for autism using brain morphology and activation," says Marcel Just, a cognitive neuroscientist at Carnegie Mellon University in Pittsburgh, Pennsylvania.

Just the facts. Benjamin Garbowit, 14, knows the populations of many nations but struggles with the point of even simple stories.

Incommunicado

The idea that faulty connections are at the core of autism is implied in a psychological theory proposed in the 1980s by developmental neuropsychologist Uta Frith of University College London. Frith noted that many autistic behaviors can be explained by a person obsessing with details and not integrating the particulars—whether they be words, facts, or visual details—to determine their broader meaning. Frith theorized that this tendency resulted from a lack of "top-down" mental processing. In the autistic brain, the theory went, the brain's frontal lobes—which play a central role in organizing, planning, directing attention, and guiding behavior—are not communicating properly with the more detail-oriented areas at the back of the brain.

It was not until 2002 that Frith and her colleagues reported the first evidence for connectivity problems in autism. The researchers used positron emission tomography (PET) to scan the brains of 10 high-functioning autistic people and 10 controls while they tried to interpret the actions of two triangles on a computer screen. Under different conditions, the triangles moved randomly, interacted in straightforward ways such as dancing or chasing, or appeared to use mental strategies such as coaxing or tricking that autistic people typically do not recognize.

As expected, the autistics did not describe the triangles' "intentions" as well as the normal subjects did, and they showed less activation in frontal brain regions involved in understanding the mental states of others. In addition, the scientists found that a visual region was not in synch with the mental-strategy network in the autistic brains, "as if there were some sort of bottleneck" in communications, Frith says.

The latest data, from functional magnetic resonance imaging (fMRI), suggest that other parts of the brain are on nonspeaking terms as well. (Unlike PET, in which brain activation in each area is averaged over the course of a task, fMRI samples activation levels as often as once a second, enabling researchers to correlate the patterns of activation of different brain regions in time.) Just's lab at Carnegie Mellon, along with Nancy Minshew at the University of Pittsburgh School of Medicine, imaged the brains of 17 high-functioning autistic people and 17 controls as they answered questions about sentences. During this task, the activated brain areas showed far less synchrony in the autistic brains than in the brains of controls, they reported last August in *Brain*. "Some of the regions aren't linked up," Minshew concludes.

When the Pittsburgh teams used fMRI to test the ability to remember faces, they saw more varied connectivity abnormalities. In the

CREDITS (TOP TO BOTTOM): RON LEVINE/GETTY IMAGES; J. WICKELGREN

autistic brains, links were weak between the front of the brain and the parietal lobe, between frontal regions and posterior perceptual brain areas, and between the face-processing brain region and other areas, the team reported in May at the International Meeting for Autism Research in Boston. They also described connectivity abnormalities in the brain network involved in the triangle task. "In study after study, we see a lower degree of synchronization in autistic brains," Just says.

This phenomenon could explain why autistic people have trouble carrying out certain actions. Ralph-Axel Müller, a cognitive neuroscientist at San Diego State University in California, and his colleagues recently scanned the brains of eight autistic males and eight controls while they watched an image of a hand on a computer screen. Each time a blue dot appeared on a finger, the subject tried to press a button with the same finger on his hand. As expected, the autistic males performed worse than controls. Their brains also showed a lack of synchrony between visual areas in the back of the brain and the inferior frontal cortex, which governs action planning and other functions. The results suggest that neural circuits for action plans may not be fully intact in autism, the researchers reported in the 15 April issue of *Neuroimage*.

Part of the communication failure could be with so-called mirror neurons, which are heavily involved in imitating behaviors (*Science*, 13 May, p. 945). "It appears that the mirror-neuron system is impaired in autism because the long fiber tracts that connect to the mirror neurons are not as well organized," Müller speculates. If so, that could explain the failure to imitate spoken words, for example, and might account for some of the language delays in autism.

Faulty wiring

Anatomical evidence is also bolstering the idea that disparate brain regions do not communicate efficiently in autism. For instance, Harvard's Herbert and her colleagues saw a large excess of white matter, which contains the nerve fibers insulated with myelin, in the brains of 14 autistic boys aged 5 to 11 compared to 14 normal boys in a structural MRI study reported in the April 2004 *Annals of Neurology*. Frontal areas showed the greatest excesses. The prefrontal lobe, the area devoted to the most complex processing, had 36% more white matter in the autistic brains compared to a 22% enlargement in the occipital lobe at the back of the brain, indicating that autistic brains sport irregularities in their white matter and particularly in the lobes that integrate different types of information.

This surfeit of white matter was concentrated at the brain's surface, where short- and medium-range nerve fibers abound. Deeper, longer stretches of white matter, such as the nerve fibers that connect the two halves of the brain, were not enlarged in the autistic boys they examined. This suggests that individual brain regions—particularly the prefrontal cortex, devoted to complex processing—may have hyperefficient internal communications but don't interact well with distant brain regions, such as those in the other hemisphere.

Herbert thinks the culprit may lie in the white matter itself, but it's too early to decide, she says, whether the abnormality relates to myelin production, neuronal fibers, or some other white-matter component. Herbert did not see any evidence of additional gray matter, which is dense with neurons, in the school-age autistic brains she studied.

But others have found gray-matter abnormalities in autism, suggesting that the excess white matter might reflect a normal amount of wrapping on a larger number of nerve fibers. Autistic toddlers have on average 12% more gray matter in their cerebral cortex, according to a 2001 study by neuroscientist Eric Courchesne of the University of California, San Diego, and his colleagues. In unpublished postmortem studies, Courchesne's group has found a large excess of a special class of pyramidal neurons in the frontal cortex.

Courchesne sees an imbalance in neuronal numbers between the front and back of the brain as a potential root cause of autism. If neurons that process sensory signals at the rear of the brain try to communicate with too many frontal neurons, their connections to that lobe may be too diffuse and lose their impact. That would greatly impair the ability of the frontal cortex to integrate sensory information, direct attention, plan, organize, and perform its other functions.

The theory that autism results primarily from a gray-matter imbalance is also consistent with findings from the lab of neuroscientist Manuel Casanova, now at the University of Louisville School of Medicine in Kentucky. In 2002, Casanova and his colleagues published data showing abnormalities in postmortem autistic brains in cortical minicolumns. These are groups of 80 to 100 cells that extend inward from the brain's surface and function as information processing units. The nine autistic brains that Casanova's team examined had many more—but much smaller—minicolumns than nine control brains had in certain portions of the frontal and temporal lobes, the researchers reported in *Neurology*. Having more minicolumns would create an abundance of short connective fibers relative to

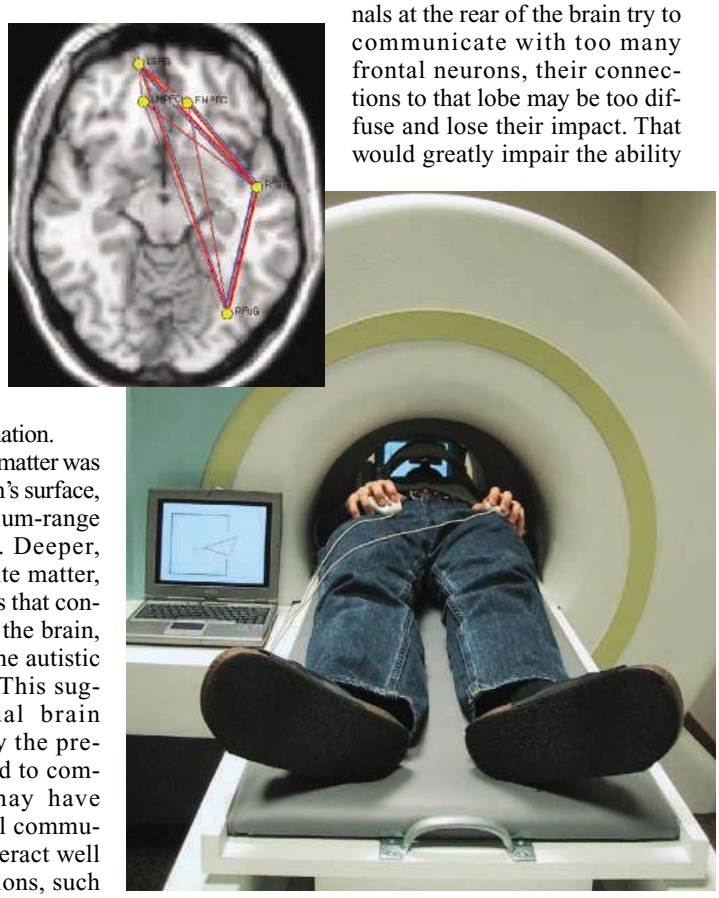

Dancing triangles. A volunteer tries to interpret the motives of two interacting triangles in an MRI simulator. (*Inset*) Autistic people show lower synchrony between areas of a brain network (blue lines) during this task than do controls (red lines).

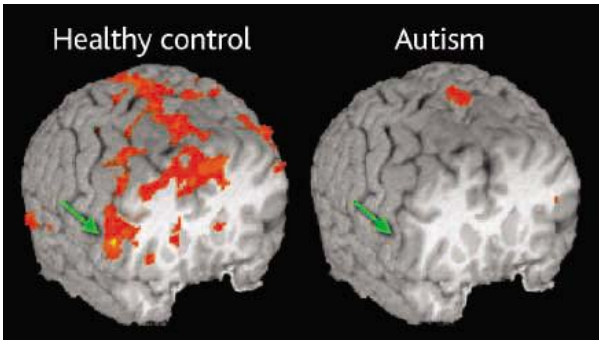

Copycat smarts. The autistic brain (*right*) shows very little cooperation between brain areas when volunteers try to perform copycat finger movements. In controls (*left*), various brain regions, including the site of "mirror neurons" (*arrow*), work together during the exercise.

CREDITS (TOP TO BOTTOM): MARCEL JUST/CARNEGIE MELLON UNIVERSITY; MICHELE VILLALOBOS AND RALPH-AXEL MÜLLER/SAN DIEGO STATE UNIVERSITY

long ones, perhaps accounting for the disproportionate increase in white matter relative to gray matter in autistic brains.

And in unpublished findings from seven autistic and seven control brains, Casanova and Christoph Schmitz of the University of Maastricht in the Netherlands and their colleagues found that the autistic brains also had smaller cells in their minicolumns. Smaller cells carry shorter axons, bolstering the hypothesis that autism results from too many short-range connections and not enough long ones.

Even if a neuronal imbalance is to blame, no one knows how it arises. Courchesne and others hypothesize that it might result from a problem in the pruning, or elimination, of neurons and synapses early in life. Work from Courchesne's lab from 2003 suggests that most of the abnormal brain growth in autism occurs from birth to age 3. This may leave an unruly excess of neurons and circuitry in certain brain regions.

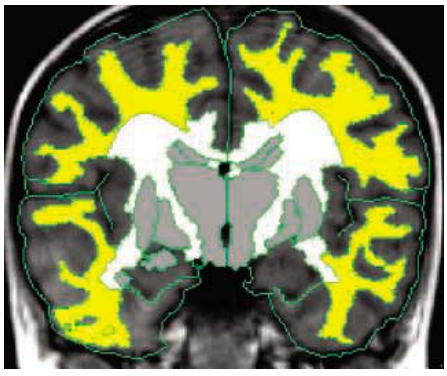

Not too deep. Autistic brains contain an excess of surface white matter (yellow), which contains relatively short neuronal fibers, but do not show an enlargement of deeper white matter (white), where the longest fibers reside.

More questions than answers

Despite the converging evidence, not everyone is convinced that faulty connections lie at the heart of autism. Geraldine Dawson, an autism researcher at the University of Washington, Seattle, suggests that connectivity problems in autism might be an effect—rather than a cause—of an earlier dysfunction in the brain, such as a defect in brain systems that govern social reward and affect an infant's attention to faces and speech. Such a defect, Dawson says, "will influence the development of speech and face perception, which ultimately will affect the development of the complex, integrated brain circuitry that underlies language and social development."

Even if connectivity problems are at the root of autism, the theory needs fleshing out. Abnormalities in brain connectivity have also shown up in attention deficit hyperactivity disorder (ADHD), schizophrenia, and dyslexia. To get to the heart of autism, researchers now need to pinpoint which particular white matter—or gray matter—abnormalities are the problem in autism versus, say, dyslexia or ADHD, skeptics point out.

Even so, proponents argue that the theory at least points researchers in the right direction. "It's a much more valid way of looking at impairments in autism. It's where the field of autism has to go," Müller says. And no matter where connectivity theory leads, the autism field is energized by the concept. Says Courchesne: "People smell something really exciting. They are seeing that there is a very interesting, if complex, story emerging."

–INGRID WICKELGREN

Pharmacogenomics

Going From Genome to Pill

A new medicine for African Americans with heart failure hints at what the drug industry sees as the enormous payoff from pharmacogenomics

Last week an advisory panel to the U.S. Food and Drug Administration (FDA) took an unprecedented step in recommending approval of a drug for a single racial group. The drug, a combination pill called BiDil that contains two heart-failure medications, had failed to help patients in the general population live longer. But in a clinical trial last year, BiDil decreased the risk of death among African Americans by 43%. That was sufficient evidence to convince the panel that BiDil should be approved to treat African-American patients with heart failure. FDA was widely expected to follow the recommendation this week.

By backing BiDil, the FDA panel gave another push to pharmacogenomics, an approach that promises to revolutionize both drug discovery and patient care. African Americans have a higher likelihood of developing hypertension and other conditions related to heart failure. However, whether that's due to genes, the environment, or some complex interplay isn't yet known. Still, BiDil represents the latest example of the industry's push to target drugs to subgroups of patients who, based largely on their genetic makeup, are most likely to benefit (*Science*, 24 October 2003, p. 594). In recent months studies have shown potential benefits of medicines targeted to patients with specific genotypes for treating cancer and heart disease. Other studies have helped doctors properly dose a wide variety of compounds already on the market. "I think that the use of pharmacogenomics will have a profound effect," says Gary Peltz, head of genetics and genomics research at Roche's Palo Alto, California, lab. "It hasn't hit yet. [But] we're clearly on the road."

To date, pharmacogenomic therapies represent a trifling portion of pharmaceutical sales, some $3.65 billion in a $550 billion market. That won't change unless scientists overcome an array of challenges, from untangling the genetics behind complex diseases such as diabetes to altering practices that could disqualify patients for health insurance based on their genes. There are also concerns that approval of drugs based on race, a sociological trait, will increase racial stereotypes and bolster the discredited notion that there are fundamental genetic differences between races. But those problems, say drug industry officials, pale in comparison to the projected benefits to patients—and to the industry. "Every major pharmaceutical company is reorganizing or has reorganized their clinical paradigm" to test drugs in conjunction with tracking genes or other molecular markers of disease, says Ronald Salerno, who directs regulatory affairs for Wyeth Pharmaceuticals in Collegeville, Pennsylvania. "This is the way drugs will be developed in the future."

Improving the odds

Although pharmacogenomics only recently entered the lexicon, the notion of treating populations based on the genes involved in health and disease dates from the 1950s. That's when researchers caught an initial glimpse that the speed at which different people metabolized drugs in their system was linked to genetics. But it took another 40 years to progress from those hints to medicines. In 1997, Genentech's Herceptin was approved to fight a form of breast cancer in which cancer cells overexpressed a protein

CREDITS (TOP TO BOTTOM): MGH/CENTER FOR MORPHOMETRIC ANALYSIS; PHOTO BY MATT MCKEE

called the HER2 receptor. In 2001, Novartis won approval for Gleevec to treat a form of cancer called chronic myeloid leukemia, in which an aberrant gene triggers a proliferation of white blood cells. And last year, ImClone's Erbitux went on sale to fight colon cancer by targeting a growth factor receptor on tumor cells. Since 1996, doctors have also genotyped the HIV viruses present in AIDS patients to help them select the best combination of drugs to treat the disease. The completion of the human genome project in 2001 allowed drugmakers to scan humanity's entire genetic sequence for links to a wide swath of diseases.

Although pharmacogenomics is expected to be useful throughout the drug development pipeline, its greatest effect at present is on how clinical trials are conducted. In particular, it's helping researchers identify which patients are most likely to benefit from a drug. Better screening of novel compounds for efficacy, toxicity, and side effects should mean fewer compounds falling by the wayside once they enter late-stage trials, the biggest component of the $1-billion-plus cost of bringing the average drug to market. "If we can get the attrition rate down, even the most reluctant managers will shift," says Mitch Martin, who heads genomic research at Roche's Nutley, New Jersey, R&D center.

Having a better idea of the likely beneficiaries of a drug also increases the odds of identifying the best therapeutic dose. Take the example of warfarin, a blood-thinning compound used by 2.1 million Americans every year to lower the risk of heart attack and stroke. Too little of the drug can be ineffective, but too much of it can cause dangerous internal bleeding and other potentially fatal consequences. Moreover, there is a 120-fold difference in the dosages given to different patients depending on the suite of enzymes each patient carries that break down the compound. Finding the right dose depends largely on repeated blood tests and a lot of trial and error.

That may soon change. This month, researchers at the University of Washington, Seattle, and Washington University in St. Louis, Missouri, reported in the *New England Journal of Medicine* that as much as 25% of this dosage difference can be explained by variations in a gene encoding an enzyme involved in blood clotting called vitamin K epoxide reductase complex, subunit 1 (VKORC1). After examining medical records and blood samples from more than 550 patients and sequencing their *VKORC1* genes, the researchers found 10 common variants of the gene. Patients clustered into three groups requiring high, medium, or low dosages. These clusters, it turned out, were closely linked to racial heritage. African Americans were most likely to have a genetic makeup requiring a large dose of the drug, whereas Asian Americans more often required a low dose and European Americans were split between the two groups.

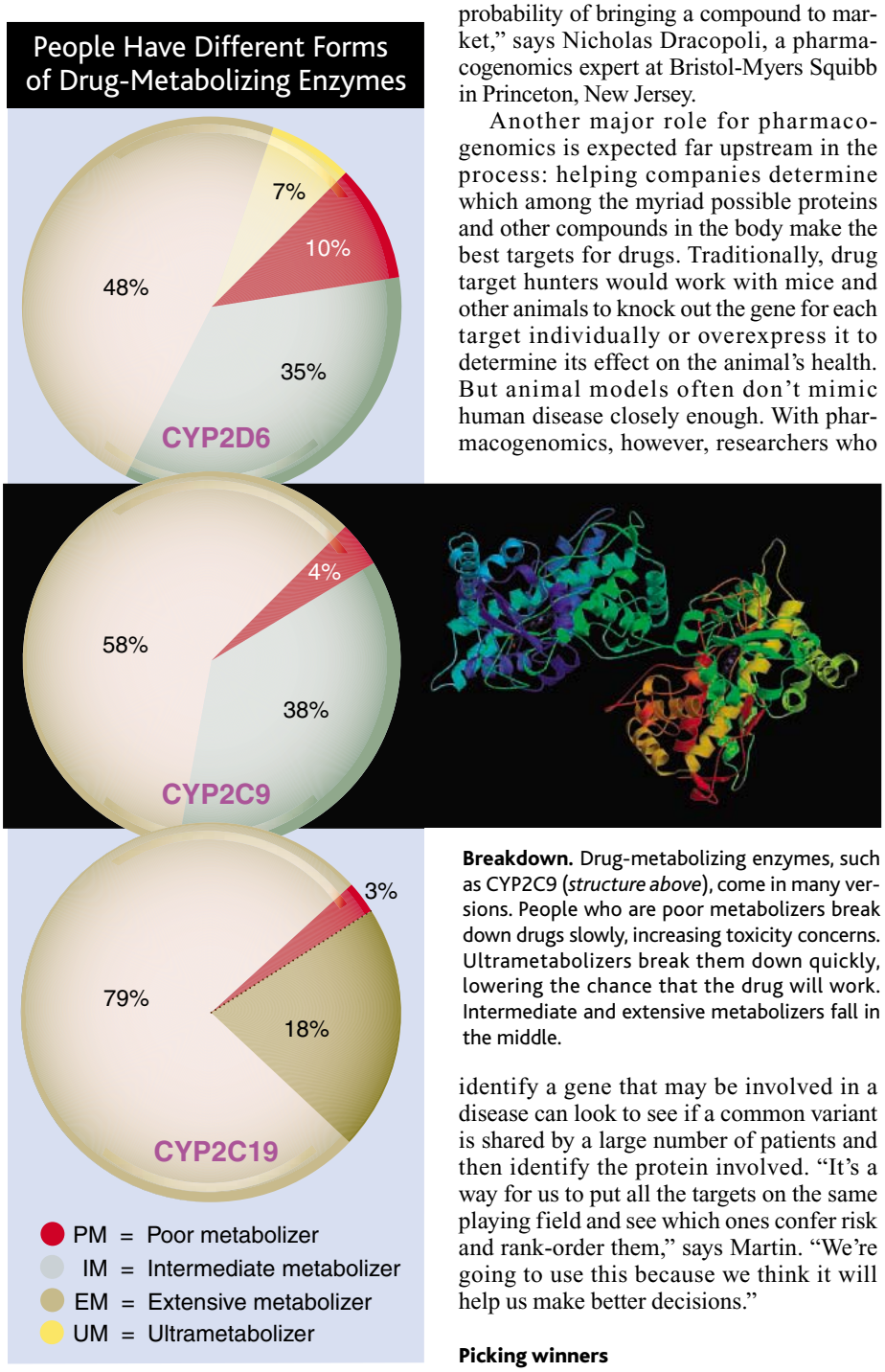

Breakdown. Drug-metabolizing enzymes, such as CYP2C9 (*structure above*), come in many versions. People who are poor metabolizers break down drugs slowly, increasing toxicity concerns. Ultrametabolizers break them down quickly, lowering the chance that the drug will work. Intermediate and extensive metabolizers fall in the middle.

The bottom line for physicians is both obvious and subtle, Martin says: Genotyping patients can save lives, and finding the right dosage may help get a drug through clinical trials. A traditionally run clinical trial will select a dosage that ensures safety for all participants, Peltz points out. If 10% of patients can tolerate only a low dose of a particular drug, that dosage will become the standard of care. That means 90% of patients won't receive an optimal dose, decreasing the chance that the drug will be shown to be effective. "The real value is in increasing the probability of bringing a compound to market," says Nicholas Dracopoli, a pharmacogenomics expert at Bristol-Myers Squibb in Princeton, New Jersey.

Another major role for pharmacogenomics is expected far upstream in the process: helping companies determine which among the myriad possible proteins and other compounds in the body make the best targets for drugs. Traditionally, drug target hunters would work with mice and other animals to knock out the gene for each target individually or overexpress it to determine its effect on the animal's health. But animal models often don't mimic human disease closely enough. With pharmacogenomics, however, researchers who identify a gene that may be involved in a disease can look to see if a common variant is shared by a large number of patients and then identify the protein involved. "It's a way for us to put all the targets on the same playing field and see which ones confer risk and rank-order them," says Martin. "We're going to use this because we think it will help us make better decisions."

Picking winners

Even so, most industry experts agree that the technology is not yet ripe for a complex disease such as diabetes, which is triggered by a wide range of genetic and environmental causes. That's also true for conditions such as hypertension, in which doctors can already get a rapid readout on the effectiveness of a drug just by performing a simple test, such as checking a patient's blood pressure.

SOURCE: GENELEX CORPORATION; (STRUCTURE) RESEARCH COLLABORATORY FOR STRUCTURAL BIOINFORMATICS

By contrast, cancer seems a promising target. "In oncology patients, it's very important to treat with an optimal therapy in the first cycle," Dracopoli says. "Every time it fails, the tumor becomes more systemic, more drug-resistant, and harder to treat."

The fact that cancer is typically initially examined with a biopsy and, in some cases, surgery gives doctors tissue samples that can be used to genotype the cells present. In theory, says Dracopoli, the next step would be to select a drug most appropriate for combating that form of cancer. Last month, for example, researchers led by Michael Heinrich of Oregon Health and Science University in Portland reported new evidence of Gleevec's ability to treat a form of gastrointestinal cancer, abbreviated GIST. Gleevec works by inhibiting a protein called KIT, which is abnormally expressed in GIST and fuels tumor growth by signaling cancer cells to keep growing. The majority of GIST patients initially respond well to Gleevec. But after 2 years, more than half develop resistance to the drug.

In a previous study, Heinrich's team found that patients with a mutation on a region of the KIT gene called exon 11 were far more likely to respond well to Gleevec over time than were patients with a different mutation on exon 9. In a paper he presented at the American Society for Clinical Oncology (ASCO) meeting in May, Heinrich confirmed this result with a much larger set of patients and also revealed the best dosing for GIST patients. Meanwhile, in another study at the same meeting, researchers led by George Demetri of the Dana-Farber Cancer Institute in Boston, Massachusetts, reported that a Pfizer compound called Sutent was more likely to improve the outcome among GIST patients with a KIT mutation on exon 9.

Another major push for pharmacogenomics research is deciphering the genetics behind the metabolism of different drugs in the body. A classic example is a compound known as 6-mercaptourine, or 6-MP. The drug has long been used to treat children with a form of blood cancer known as childhood acute lymphocytic leukemia (ALL). But one in every 300 children has a variant of a gene for an enzyme called thiopurine methyltransferase that prevents 6-MP from being metabolized. In those patients, the drug builds up and in many cases has proven fatal. Beginning in the 1980s, researchers led by Richard Weinshilboum at the Mayo Clinic in Rochester, Minnesota, flagged the genetic link to the slow metabolism of 6-MP. Now doctors increasingly run genetic tests on ALL patients before giving them 6-MP to weed out the patients who shouldn't receive the drug.

That same strategy is also being used to unravel the genetics behind a broad range of drug-metabolism enzymes, known as cytochrome P450s, that are present primarily in the liver and kidneys. The impact could be dramatic: Variations in just one of these enzymes, known as CYP2D6, have a broad effect on drug metabolism, according to a report this month in *Nature Reviews Drug Discovery* by health policy experts Kathryn Phillips and Stephanie Van Bebber of the University of California, San Francisco. "The most commonly used drugs metabolized by CYP2D6 account for 189 million prescriptions and $12.8 billion annually in expenditures in the U.S., which represent approximately 5% to 10% of total utilization and expenditures for outpatient prescription drugs," the authors conclude.

Whether researchers can tie patients' responses to all these drugs to variations in *CYP2D6* genes remains to be seen. But they have made some progress. Researchers led by Matthew Goetz, a medical oncologist at the Mayo Clinic in Rochester, Minnesota, reported at the ASCO meeting that genotyping drug-metabolism enzymes can drastically reduce the risk of toxic side effects from a standard chemotherapy regimen containing three cancer drugs, called irinotecan, oxaliplatin, and capecitabine. Despite the drugs' antitumor benefits, their combined use can be lethal for some patients. But Goetz's team found that genetic variants of an enzyme abbreviated UGT1A1 determined what dose of irinotecan could be tolerated, as well as whether the drug works with the others.

Finally, pharmacogenomics is also opening up new markets for biomarker companies with the tests needed to draw the link. Last December, for example, FDA approved a new gene chip from Roche called the AmpliChip, which tests for common variants of two important genes for drug metabolism, *CYP2D6* and *CYP2C19*. A Seattle, Washington, company called Genelex recently started marketing an alternative test directly to consumers.

Despite these and other enticing results, even pharmacogenomics proponents warn against expecting a medical revolution. "It's not something that's going to change the world in 3 years," says Scott Weiss, a pharmacogenomics researcher at Harvard Medical School in Boston. Among the hurdles, Weiss and others say, is that studies linking genes to disease outcome are time-consuming and expensive. That means higher costs in the short run.

Doctors also must be trained to use and properly interpret genetic tests. "Doctors have to buy in," says Wyeth's Salerno. One reason they might resist, Salerno suggests, is a fear of being second-guessed by lawyers. "If someone gets injured from an adverse event [from taking a drug], will that person ask why the doctor didn't check my genotype?" Salerno asks. Finally, patients must become comfortable with the notion not only of having their genomes tested but also with the possibility that insurance companies might exclude coverage for a particular disease, arguing that a genetic link makes it a preexisting condition.

Many of these changes will take time. But that's fine, Salerno says, because the field of pharmacogenomics is still young. "This is not a fad," Salerno says. "This is going to be a cornerstone of future medicine."

–ROBERT F. SERVICE

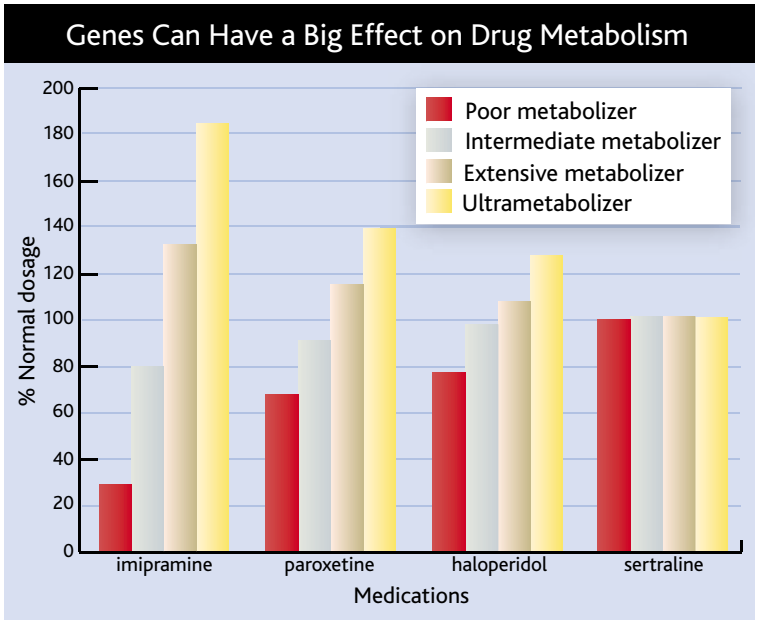

Not so simple. People with different forms of the enzyme CYP2D6 respond differently to some antidepressants, such as imipramine, but similarly to others, such as sertraline. In the graph above, the normal dose is 100%. Poor metabolizers of imipramine, for example, can only tolerate 25% of that amount.

SOURCE: GENELEX CORPORATION

Visions of a Biotech Empire On the Kazakh Steppe

Kazakhstan has enlisted a U.S.-trained biologist to clear out the cobwebs and create a modern biotechnology industry

ASTANA, KAZAKHSTAN—When Erlan Ramanculov moved from Colorado to Kazakhstan in 2004, he and his wife had one main objective: to raise their daughters in his native land. He took a position managing four struggling biological institutes in Almaty, the largest city in this oil-rich Central Asian country. Sometimes, though, as the 38-year-old molecular biologist dealt with a stultifying bureaucracy, he wondered whether he'd erred in leaving the United States. He'd spent 11 years at Texas A&M University in College Station and the U.S. Centers for Disease Control and Prevention in Fort Collins, Colorado, becoming a topflight researcher on phages, viruses that infect bacteria.

Then in February, Ramanculov was tapped to build a national biotech program with resources far beyond anything he could have imagined back in the States. The government has approved plans and is now reviewing financing for a $50 million Life Science and Biotech Center of Excellence, supported in part by the World Bank, with a flagship research facility to be built in Astana, the nation's capital. Ramanculov, director of the new center, has enlisted an advisory board to set research directions and has begun wooing top Kazakh expatriate and foreign scientists. "The center will be a testing ground for new principles, fully integrated into the world scientific community," says Kazakhstan's reform-minded deputy science minister Azamat Abdimomunov, who has championed the project.

The challenges are formidable. The most obvious is acquiring hardware: Kazakh researchers are mostly making do with Soviet-era equipment. They also must overcome Western concerns about proliferation. Subsumed in Ramanculov's center is an institute in Stepnogorsk that was once the world's largest biological weapons production facility; U.S. State Department officials have urged Kazakh officials not to let its weapons experts get lost in the shuffle.

Young Turkics

The driving force behind Kazakhstan's planned biotech revolution is Abdimomunov, a 29-year-old political scientist trained at Harvard University's John F. Kennedy School of Government. Since his appointment in January, the blunt-spoken Abdimomunov, keen on flow charts and Venn diagrams, has floated plans for stricter evaluations of institutes. He also wants to infuse fresh blood by expanding a popular program, Bolashak (for "the future"), which pays tuition and stipends for elite university students to study abroad.

The new biotech center is his boldest move yet, in part because it is a rebuke to Stepnogorsk. The "Progress" Technopark established in Stepnogorsk in 2002 was supposed to usher in a biotech marvel, producing everything from amino acids to vodka. But a science ministry document says that despite large cash infusions, it has "failed to produce any result." "Unfortunately, we have been more successful at dismantling equipment than putting things together," acknowledges Progress president Valeriy Shimanayev. The science ministry plans to dissolve Technopark this month.

Abdimomunov faults local managers and a U.S. assistance effort that he claims paid short shrift to commercialization. He vented his frustrations to one U.S. State Department official in what both sides called an "uncomfortable" encounter this spring. "The American side should have expressed a greater desire to assist us," Shimanayev says. Comments a U.S. official: "You can't just keep pouring aid in forever."

State will keep a close eye on the new biotech center because, the official says, "there are people in Stepnogorsk who we don't want to see go without work." The United States, Canada, and other countries have thrown a lifeline to a few dozen key weaponeers at Stepnogorsk, primarily through the International Science and Technology Center (ISTC), a multilateral fund. How to balance nonproliferation concerns and Kazakhstan's biotech aspirations is to be discussed at a meeting this month between U.S., ISTC, and Canadian officials.

Ramanculov aims to make the most of Kazakhstan's decaying infrastructure. He plans to seek World Bank help to raise standards across a wide front. "Every research group in Kazakhstan is a monopolist in its own small field. Nobody in the country can judge their work," Ramanculov says, adding that a lack of competitiveness has fostered poor science and a dearth of investment. The science ministry plans to rate scientists by citation index. "We're changing the rules of the game: People are going to have to work harder," Ramanculov says. Still, he says, "we cannot produce a cutting-edge research facility from our local cadres. We have to bring people in here."

Dark past, bright future? The former bioweapons complex at Stepnogorsk is part of a radical overhaul of Kazakhstan's biotech program led by Erlan Ramanculov (*inset*).

That will be no mean feat. Winters on the steppe here are fiercely cold, windy, and snowy, whereas summers are hot and buggy. Ramanculov hopes six-figure salaries will lure talent. "We need to bring in a few big guys," he says. Ramanculov will also be able to rope in 40 Bolashak-trained biologists in a few years when they return home from their studies. His former Ph.D. supervisor thinks he can succeed. Ramanculov "is a risk taker" with "tremendous drive and resolve," says Ry Young, a phage biologist at Texas A&M. "If this project *can* be successfully done, it will get done. Few people can resist his personality."

Having secured land on the Ishim River, Ramanculov has hired a Singapore-based firm, Jurong Consultants, to draw up designs for the research center and apartments for scientists. Construction is slated to begin next year. By next month, Ramanculov says, outside advisers will recommend areas in which the center might compete globally. "Whatever we do will be good," he says, "because not enough has been done in Kazakhstan." The changes sweeping Kazakh science have convinced Ramanculov that coming home was the right decision after all. **–RICHARD STONE**

CREDITS: R. STONE

The Ins and Outs of Exosomes

Cells spit out these mysterious vesicles, but what they do and whether they boast medical uses, such as in cancer vaccines, is up in the air

MONTREAL, CANADA—"Alice in Blunderland" is how biochemist Rose Johnstone describes her 1970s investigations into curious, lipid-encased particles burped out by the sheep red blood cells she was studying. Baffled by the material, which resembled "little florets" under a microscope, Johnstone, of McGill University in Montreal, nevertheless pursued them, gradually drawing in a small cohort of scientists. She anointed the vesicles exosomes; unlike similar-looking structures called endosomes, which carry material into cells, these particles seemed to cart stuff away.

Three decades later, exosomes are beginning to surrender their secrets. Scientists now know that they have been conserved across species, suggesting useful, even life-preserving functions. Exosomes secreted by white blood cells, for example, appear to mediate immune responses, activating and perhaps also suppressing the immune system. Indeed, cancer physicians are already trying to exploit exosomes to trigger immune response against a variety of tumors. And other researchers are exploring whether these vesicles assist the spread of HIV and prions.

In one indication of the exosome's coming of age, the first-ever meeting* devoted to these particles was held here last month, organized by Johnstone and sponsored by the Leukemia and Lymphoma Society. About two dozen biologists from eight countries converged in a classroom at McGill University for 2 days of spirited discussion. Although exosomes are no longer dismissed as simple cell fragments, their biological significance remains tantalizing but uncertain. "Many people think exosomes are pieces of cell running around with no specific function," said Sebastian Amigorena of the Curie Institute in Paris. "I want to believe they're doing something."

Unexpected finds

Most cell biologists enter the exosome field after they stumble across the particles in their experiments. That was the case for Johnstone. She and her colleagues first saw what she would later call exosomes while hunting for an elusive amino acid transporter. Examining blood drawn from sheep, they saw that the immature red blood cells were ejecting "tons of stuff" after binding to an antibody, says Johnstone. The red blood cells of chicks, piglets, frogs, rats, and humans all produced these vesicles. Her group ultimately reported in 1983 that exosomes help nascent red blood cells develop by carting away proteins that are no longer needed.

But exosomes lingered in obscurity until 1996. That year, Graça Raposo and Hans Geuze of Utrecht University in the Netherlands and their colleagues reported that other blood cells, called B cells, secrete exosomes that offer up antigens—tiny bits of pathogens—to the T cells of the immune system. Such antigen presentation is a key initial step in launching an immune response. And exosomes were found to sport the crucial major histocompatibility complex molecules that bind to and display antigens, just as dendritic cells of the immune system do. Indeed, the presence of these immune molecules is one of the identifying signatures of an exosome, along with a characteristic lipid membrane.

Raposo later moved to the Curie Institute, where she and her exosomes attracted other scientists interested in the role these vesicles play in T cell activation. One question is whether exosomes need a partner to arouse T cells, and if so, how that dance is choreographed. Clotilde Théry of the Curie Institute believes that exosomes and dendritic cells work in concert. She and her colleague Laurence Zitvogel, of Paris's Gustave Roussy Institute, have found that, like a relay racer handing off a baton, exosomes in a test tube pass certain antigens onto dendritic cells. The dendritic cells then use those antigens to activate T cells. Whether this also happens inside an animal is unknown.

Dendritic cells themselves appear to produce exosomes, as do an ever-lengthening list of other cell types. For instance, cells at the outer edges of the intestine and cancer cells have also been shown to secrete the vesicles.

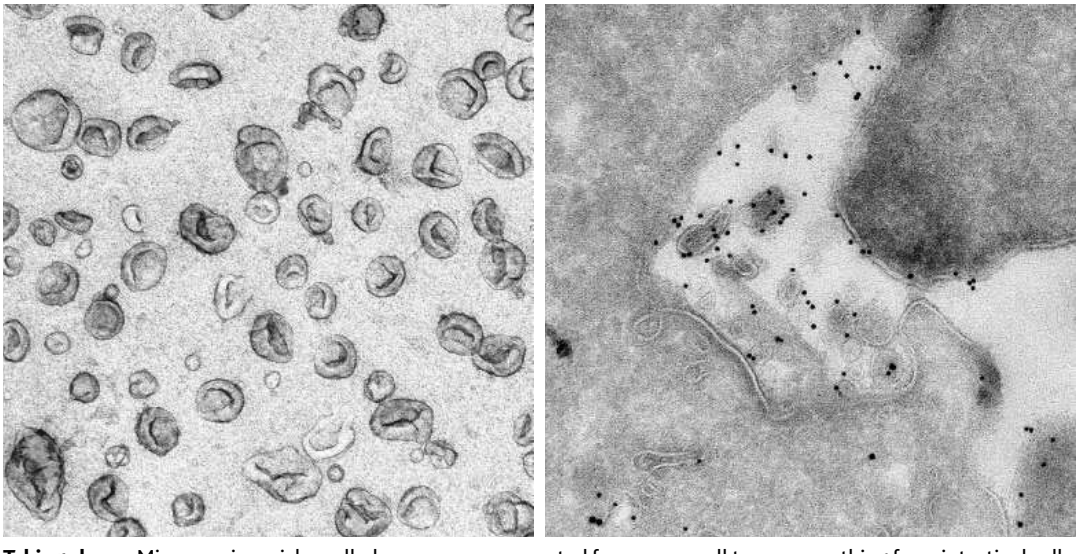

Taking shape. Microscopic vesicles called exosomes are secreted from many cell types, everything from intestinal cells to blood to cancer cells; here, exosomes appear as cup-shaped vesicles (*left*) or are labeled as black dots inside a larger cell structure (*right*). Scientists are only beginning to piece together their functions and importance.

CREDITS: B. FÉVRIER AND G. RAPOSO, *CURRENT OPINION IN CELL BIOLOGY* **16**, 1 (2004), ELSEVIER LTD.

Lassoing a skittish target

Finding that additional cell types make exosomes has only added to confusion over what they do. Further complicating matters is that the particles are maddeningly awkward to work with. "It's difficult to manipulate [and] purify them," says Amigorena.

Aled Clayton of Cardiff University in Wales, U.K., who has followed up on reports that cancer cells secrete exosomes, can attest to that. He theorizes that these exosomes might suppress the immune system rather than activate it, letting the cancer flourish. But despite examining exosomes ejected by various cancer cells, including breast cancer and mesothelioma, he can't

* Exosomes: Biological Significance, Montreal, Canada, 20–21 May.

produce sufficient data to back up the conjecture. After months of painstaking work with the particles, "we've failed miserably at generating any immune responses from exosomes," he confessed at the meeting.

While most exosome researchers have focused on the vesicles' apparent ability to switch on the immune system, Clayton and others continue to probe whether the vesicles play an opposing role in immune suppression. Last month, in the *Journal of Immunology*, molecular biologist Paul Robbins of the University of Pittsburgh, Pennsylvania, reported that exosomes he stumbled across while studying gene therapy for arthritis could heal the autoimmune disease. Trying to understand why delivering gene therapy to one arthritic joint in a mouse helps nearby joints too, Robbins and his colleagues noticed small vesicles traveling from treated joints to untreated joints. "I thought it was cell debris," says Robbins. But when he and his team culled these vesicles from dendritic cells and reinjected them, they found that a single injection into an arthritic animal eliminated the disease. "Our exosomes are very suppressive," says Robbins.

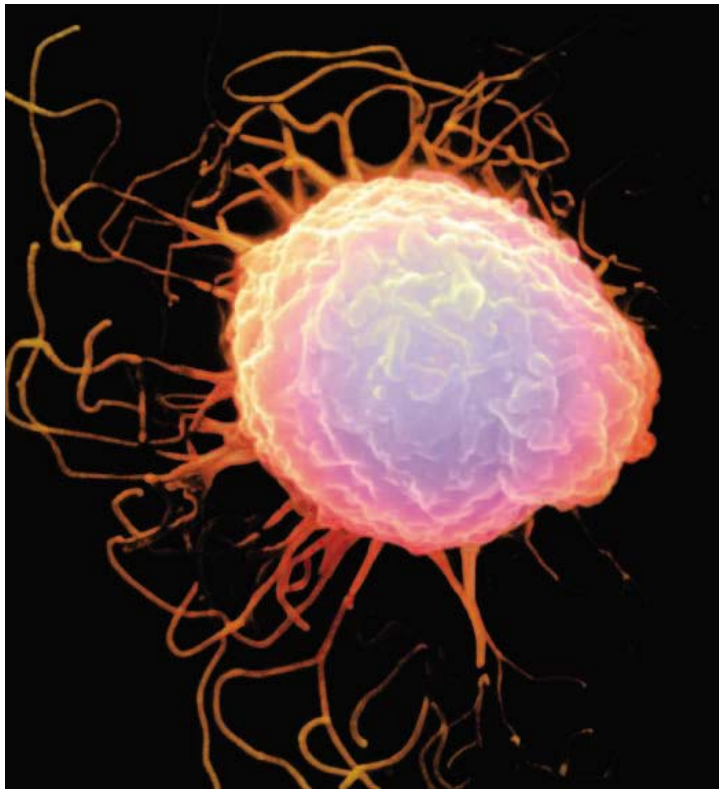

Switching on. Experiments suggest that exosomes can help activate T cells like this one, but debate continues over how they do so.

Supporting that premise, Helen O'Neill of Australian National University in Canberra told the Montreal gathering of studies showing that exosomes appear to reflect the behavior of the cells that release them; immature dendritic cells and their exosomes, which Robbins used, tend to suppress immunity, whereas mature ones and their exosomes stimulate it. Work by Amigorena, Théry, and others published in March in *Blood* did not find this distinction, however.

These finer questions were sometimes overshadowed by more fundamental ones. Do all the vesicles being classed as exosomes really fall into that category? In other words, is everyone studying the same thing? Meeting participants reached no consensus on whether the definition of an exosome should be based on the vesicle's chemical makeup, on how it was formed, or on its purpose. Cell biologist Stephen Gould of Johns Hopkins University in Baltimore, Maryland, argued for a broad characterization. "The more narrow you make the definition, the less interesting this field will be to everyone else," he said.

Tackling cancer

Such fuzziness hasn't stopped oncologists from incorporating exosomes into so-called cancer vaccines, which seek to trigger immune response against tumors. One strategy involves filtering exosomes produced by dendritic cells from a patient's blood. The theory is that these exosomes, produced by dendritic cells that can activate the immune system, sport tumor antigens and can induce a strong immune attack on an individual's cancer if redelivered in sufficient volume.

A Menlo Park, California, company called Anosys, co-founded by Jean-Bernard Le Pecq, funded a small trial in lung cancer and another in melanoma before folding this spring. The exosomes failed to help most of the melanoma patients, Zitvogel, who ran the trial, reported in Montreal. But those with lung cancer fared relatively well, Le Pecq noted, with a handful surviving several years—unusually long for people with the aggressive cancer. One unexpected complication was that not enough exosomes for an individualized vaccine could be extracted from the blood of every volunteer.

Meanwhile, oncologist Malcolm Adams of Cardiff University is working with Zitvogel to launch an ovarian cancer trial of an exosome-based vaccine. Their strategy is slightly different from that used in the lung cancer and melanoma trials: Here, exosomes will be harvested from tumor cells in abdominal fluid. Such cells and their exosomes should bear antigens specific to the individual's cancer. And if the exosomes are administered along with a substance that stimulates the immune system, the vesicles may train the immune system to recognize cancer cells as foreign and attack the cells, suggest Adams and Zitvogel.

Some exosome biologists are investigating whether the particles play a nefarious role in infectious diseases, such as spreading viruses from cell to cell. In 2003, Gould and his colleagues published a provocative theory about HIV dubbed the "Trojan exosome hypothesis." They proposed that retroviruses, such as HIV, hide as exosomes secreted from an infected cell.

In Gould's theory, the HIV exosomes are released from an infected cell and drift toward one that's not infected. That cell takes them up, internalizing the deadly virus. The theory doesn't discount that HIV can directly infect cells, but it suggests that exosomes offer an alternative way for the virus to spread. In Montreal, Gould reported that exosomes bud from domains in the plasma membrane of T cells, which HIV infects. Bolstering his theory, he's also found that HIV Gag, a protein the virus needs to exit a cell, congregates in exosomes.

But HIV researcher Michael Marsh of University College London questions parts of the Trojan exosome hypothesis. Although Marsh believes that HIV and other retroviruses might assemble in the same endosomal cell compartments that spit out exosomes, he says he's never seen the exosome budding from the cell surface that Gould reports.

In addition to HIV, exosomes may act as infectious pawns for prions, misshapen proteins suspected in several neurodegenerative conditions such as "mad cow disease." Raposo has recently published data indicating that exosomes act as vehicles for prion transport between cells. She noted that prions appear to accumulate in endosomes as they near the point of spilling their exosome cargo. Exosomes "probably have something to do with transmission of the infectious agent," she says. In the case of ingested beef causing mad cow disease in people, this could mean ferrying prions from the gut to the central nervous system.

Raposo's prion work—which, she says, elucidates "the dark side" of exosomes—hints at the breadth of potential roles for these vesicles in health and disease. But like so much exosome work, it remains dogged by uncertainties and questions.

–JENNIFER COUZIN

CREDIT: STEM JEMS/PHOTO RESEARCHERS INC.

Random Samples

Edited by Constance Holden

Panoramic Mosaic

A 2000-year-old mosaic uncovered at the ruins of the ancient Roman city of Leptis Magna on the coast of Libya is wowing archaeologists and art historians. The gory depiction of a nearby amphitheater includes a highly detailed profile of a gladiator with his vanquished foe and a spectacular chariot race crash.

Tousled gladiator may have been German.

The 9-meter-long mosaic, described this week in the British archaeological journal *Minerva*, was discovered in 2002 by a team led by Marliese Wendowski, an archaeologist at the University of Hamburg, Germany. "From the start, we knew we had something special because it was so large," says Wendowski. The team members kept the find a secret while they excavated it and transferred it to the nearby Leptis Magna Museum.

"What's extraordinary is how depth was created with foreshortening," a very painterly technique, says *Minerva* editor Mark Merrony. The artist "must have been working from a drawing," he adds.

The mosaic is offering fresh clues for historians. "This was likely an eyewitness account commissioned by a very rich local patron," says Merrony, and it shows how interconnected the Roman empire was at the time. Men are shown wrestling with bears and deer, the first evidence that European animals were imported to Africa for sport. But that's not all. "Judging by his face and hair, I think the gladiator was a German barbarian," says archaeologist Helmut Ziegert, also at the University of Hamburg. That might explain why no name was inscribed, an honor typically bestowed on respected gladiators.

Chimera on a Bike?

A high-profile sports blood-doping case has taken a bizarre twist, with the accused cyclist arguing that testing positive for two distinct types of blood indicates he is a chimera.

Last September, Olympian Tyler Hamilton, 34, of Boulder, Colorado, was accused of taking a blood transfusion to boost his performance after a newly developed test showed he had two different types of red blood cells. Hamilton denied the charge, and with the help of geneticist David Housman of the Massachusetts Institute of Technology in Cambridge, he has been arguing that he might be a chimera: an organism with a mix of genetically distinct cells.

Human chimeras are not all that rare, Housman told a board arbitrating the case in March. Mothers and fetuses often exchange blood-producing stem cells, and fetuses can also get foreign cells from sharing the womb with a "vanishing twin," he said. But the arbitrators didn't bite, voting 2 to 1 to uphold a 2-year suspension and stating that blood doping was "the only reasonable conclusion." Encouraged by the split decision, however, Hamilton is again appealing, this time to a sport arbitration court in Switzerland. Although other blood samples showed that his minority cell population decreased over several months, Housman says that is consistent with chimerism.

Mother-fetus chimerism is unlikely to produce foreign cells at the levels found in Hamilton's blood—about 2%—says geneticist Wendy Robinson of the University of British Columbia in Vancouver, Canada. But Housman predicts that more athletes who are actually chimeras will show up as suspected blood dopers. And, wrote Hamilton this month in his online journal, "If we've accomplished nothing else in this case, we have put a spotlight on the vanishing twin phenomenon."

Early Tree

Paleontologists this week got their best look yet at one of the world's first trees, a palmlike growth that flourished in a tropical environment in the middle Devonian Period, about 380 million years ago.

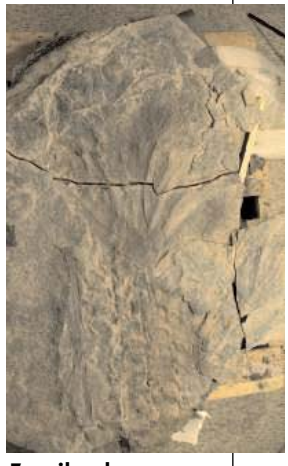

Fossil palm.

Only fragments were previously known of the tree, called *Pseudosporochnus*. But last summer, staff from the New York State Museum in Albany came across a 3-meter-long specimen in a gravel quarry near Conesville, New York—the first time the foliage has been found attached to the trunk. It is well preserved with a crown made up of frondlike branches. Although no roots are in evidence, "it gives us the first clear impression of what this tree looked like," says William Stein of the State University at Binghamton, New York, who is studying the fossil. "What really strikes me is how modern it is," says Stein, noting its leaflike branches. (Modern leaves had not yet evolved.) The fossil was described at the North American Paleontology Conference in Halifax, Nova Scotia, by New York state paleontologist Ed Landing.

CREDITS (TOP TO BOTTOM): HELMUT ZIEGERT/UNIVERSITY OF HAMBURG; WILLIAM STEIN; GUSTAU NACARINO/REUTERS

Edited by Amitabh Avasthi

JOBS

Forward into the past. In more ways than one, molecular evolutionist Alan Cooper is going back to his roots. Leading the new Australian Centre for Ancient DNA at the University of Adelaide will be a homecoming of sorts for the New Zealander, former head of the Ancient Biomolecules Centre at the University of Oxford, U.K. The new post also gives him a better shot at obtaining intact DNA from the puny human species *Homo floresiensis*, who lived in neighboring Indonesia about 18,000 years ago. "It's going to be bloody difficult with that heat," he says. "However, the importance of the material is huge, and we'll throw every trick in the book at it."

The $1.2 million center, set to open in December, will be better than the Oxford lab and rivaled by few in the world, Cooper says. One project already in the works involves handling the ancient DNA portion of the Genographic Project, an international effort to reconstruct past human migrations.

A couple months after Cooper announced his plans to leave Oxford, the university began an investigation into possible misconduct involving one of his grant applications. Cooper says the investigation ended in March with no action taken. Oxford officials would not comment on the outcome, and there's no word on Cooper's successor.

Grand challenge. Chip Groat resigned last week as director of the U.S. Geological Survey (USGS) to lead a new energy and environmental policy institute at the University of Texas, Austin.

Groat, 65, is credited with burnishing the reputation of USGS since taking over in 1998. "He brought more attention to the value of the USGS," says Linda Rowan of the American Geological Institute in Alexandria, Virginia, a move that also protected the survey's budget.

Groat had previously held academic positions in Texas and Louisiana that focused on energy resources and the environment. The new institute, he says, "is a chance to get really involved with science and policy matters on a grand scale."

Pat Leahy, the survey's associate director for geology, has been named acting director.

AWARDS

Kyoto Prizes. Two U.S. scientists have won Kyoto prizes this year for lifetime achievements in advanced technology and basic sciences.

The annual prizes, worth $460,000 each, were created in 1985 by Japanese philanthropist and Kyocera Corp. founder Kazuo Inamori. The technology prize goes to electronics engineer George Heilmeier (top, right), 69, now chair emeritus of Telecordia Tech Inc., who pioneered the use of liquid crystals to create flat-panel displays.

In the basic sciences category, Princeton University ecologist Simon Levin was honored for applying math to model the diversity of complex ecosystems. Levin (middle, right), 64, helped show that the biosphere is a collection of continually adapting systems. A third prize, in the arts and philosophy category, went to Nikolaus Harnoncourt, the former conductor of the Vienna and Berlin Philharmonic orchestras.

Tapping Into New Talent

Mark Lewney, a U.K. patent examiner, knows how to make science sing. This month, Lewney (below) won a U.K. science communication talent contest modeled after *American Idol* in which more than 300 contestants riffed on scientific topics to a panel of academics and journalists. During one of the rounds of FameLab, Lewney explained "why spaceships on the telly are rubbish" (for one, they wouldn't make any noise in space), and described Orion, an interplanetary ship driven by atomic bombs that was proposed in the 1950s.

For his final performance, Lewney took up an electric guitar to explain how the harmonics of its strings create distinctive distorted sounds. "Ignoring the judges' advice about how to be a calm, authoritative TV presenter, I plugged my electric guitar into my amp and turned it up loud," Lewney says. Science writer Simon Singh, one of the judges, found the Orion presentation especially impressive: "He used only a frying pan as a prop and still got the audience excited."

Lewney earned nearly $3700 and a few television spots as well. Runners-up David Booth, an evolutionary biologist from Belfast, and Matt Wilkinson, a zoologist from Cambridge, each won about $1400.

Got any tips for this page? E-mail people@aaas.org

CREDITS (CLOCKWISE FROM TOP LEFT): XULONG LAI; THE INAMORI FOUNDATION; IAN JONES/*THE DAILY TELEGRAPH*; USGS

Problems with Co-Funding in Canada

THE CANADIAN FEDERAL GOVERNMENT HAS prudently invested substantial new resources in research operations and infrastructure, thereby bringing the level of research support in Canada on par with that of most other G8 countries and enabling a world-class research enterprise. Much of this renewed commitment to research, however, is in the form of "co-funded" programs. In Canada, co-funding schemes typically require an equal or greater match of funds from an independent partner, either local, provincial, or foreign governments; private foundations; or industry. In principle, co-funding should leverage funds from other sources and hasten the transition of fundamental research to commercial application. In practice, co-funding can exact a debilitating toll on the research community.

Inevitably, co-funding steers resource allocation, as dictated by the partner entity, which may be to the detriment of some of the best science. In particular, co-funding is often biased against fundamental research that is far from commercialization and so at odds with the short-term goals of industrial partners. The vicissitudes of most co-funding sources also severely compromise the sustainability of long-term research platforms. Co-funding is more easily obtained by well-connected investigators able to draw on resources and contacts inaccessible to many of their colleagues, thereby greatly restricting the pool of eligible science. Moreover, the mega-scale mandate of many co-funding initiatives virtually eliminates the individual researcher or small teams in favor of larger, sometimes artificial, consortiums. Perhaps most troubling from a scientific perspective, the criteria for eligible co-funding are inherently subjective.

A recent example illustrates the latter point. Genome Canada, the primary Canadian funding agency for genome-scale projects, has winnowed its latest round of team applications solely on the basis of the perceived financial suitability of the co-funding source. To this end, each application required up to 10 times more pages of budgetary justification than the scientific proposal itself. Of ~120 initial proposals, ~30 were culled at an early stage without review at all. Of the 93 full proposals allowed to go forward, almost one-third were eliminated by a panel of accountants based on ambiguous financial criteria and without any consideration of scientific merit, with many of the remainder placed in a financially suspect category.

The conclusions to be drawn are obvious: In general, grants are best awarded solely on the basis of scientific peer review, and funded in full without matches, strings, or contingencies that depend on outside agents. By eschewing scientific excellence as the primary consideration, co-funded programs imperil scientific credibility and fail to engage the breadth and depth of national scientific expertise. We encourage governments, scientific administrators, and scientists in Canada and other countries not to succumb to the superficial allure of co-funding but rather to evaluate and fully fund research on its own merits. The manifold benefits to society will inevitably follow, as was long the case before the advent of co-funding programs.

> "By eschewing scientific excellence as the primary consideration, co-funded programs imperil scientific credibility..."
>
> –TYERS ET AL.

MIKE TYERS,[1] ERIC BROWN,[2] DAVID W. ANDREWS,[2] JOHN J. M. BERGERON,[3] CHARLES BOONE,[4] RODERICK BREMNER,[5] HOWARD A. BUSSEY,[3] JAMES C. CROSS,[6] JULIAN E. DAVIES,[7] MICHEL DESJARDINS,[8] JOHN E. DICK,[9] DANIEL J. DUMONT,[10] DANIEL DUROCHER,[1] MICHAEL J. ELLISON,[11] G. BRIAN GOLDING,[2] MICHAEL W. GRAY,[12] LEA A. HARRINGTON,[13] PHILIP A. HIETER,[7] GERALD JOHNSTON,[12] DAVID J. KELVIN,[9] BRIAN E. MCCARRY,[2] STEPHEN W. MICHNICK,[8] FRANCIS OUELLETTE,[7] RON E. PEARLMAN,[14] LINDA J. Z. PENN,[13] JERRY PELLETIER,[3] RICHARD A. RACHUBINSKI,[11] PAUL S. RENNIE,[15] DANIELA ROTIN,[16] ROBERT ROTTAPEL,[13] IVAN SADOWSKI,[7] FRANK SICHERI,[1] LOU SIMINOVITCH,[1] NAHUM SONENBERG,[3] K. W. MICHAEL SIU,[14] MICHEL L. TREMBLAY,[3] NEIL WINEGARDEN,[13] RICHARD W. WOZNIAK,[11] GERARD D. WRIGHT,[2] JAMES R. WOODGETT[13]

[1]Samuel Lunenfeld Research Institute, Toronto, Ontario, Canada. [2]McMaster University, Hamilton, Ontario, Canada. [3]McGill University, Montreal, Quebec, Canada. [4]University of Toronto, Toronto, Ontario, Canada. [5]Toronto Western Hospital Research Institute, Toronto, Ontario, Canada. [6]University of Calgary, Calgary, Alberta, Canada. [7]University of British Columbia, Vancouver, British Columbia, Canada. [8]Université de Montréal, Montréal, Quebec, Canada. [9]Toronto General Research Institute, Toronto, Ontario, Canada. [10]Sunnybrook and Women's College Health Sciences Centre, Toronto, Ontario, Canada. [11]University of Alberta, Edmonton, Canada. [12]Dalhousie University, Halifax, Nova Scotia, Canada. [13]Ontario Cancer Institute, Toronto, Ontario, Canada. [14]York University, Toronto, Ontario, Canada. [15]The Prostate Centre at Vancouver General Hospital, Vancouver, British Columbia, Canada. [16]Hospital for Sick Children, Toronto, Ontario, Canada. Complete affiliations are available as Supporting Online Material at www.sciencemag.org/cgi/content/full/308/5730/1867b/DC1.

Issues in Biosecurity and Biosafety

A 2004 REPORT, *BIOTECHNOLOGY RESEARCH in an Age of Terrorism*, recommended that Institutional Biosafety Committees (IBCs) review research for biosecurity and "dual use" potential, to prevent nefarious applications such as bioterrorism or biowarfare (*1*). To discuss this recommendation, we convened a group of IBC chairs, scientists, and administrative staff from our six universities on 11 May (*2*). We hope that the fruits of our deliberation will be considered by the National Scientific Advisory Board on Biosecurity (NSABB), which will meet for the first time on 30 June.

NSABB's first task is to formulate criteria for "dual use," starting from the seven "experiments of concern" in the 2004 report. Yet the much deeper problem is what to do once concerns are identified. There appears to be little consensus.

Some believe that secrecy is the best policy to stop proliferation. Others believe open science is the best long-term policy; misuse is a risk, but secrecy hinders advances toward drugs, vaccines, and detection methods. There is some agreement between these frameworks, however: Most agree that security measures and the location of dangerous materials should remain secret and that most research results should be published. But experiments reconstituting synthetic polio and the Australian experience with interleukin-4 in mousepox (*3*, *4*) exposed areas of conflict. Many scientists believe publication was appropriate, but it is far from clear that the case for "open science" has been made successfully with the general public, law enforcement officials, or elected officials.

Last year, as the Policy, Ethics, and Law Core of the Southeast Regional Center of Excellence for Biodefense and Emerging

Infections, we reviewed a few experiments that might inadvertently enhance pathogen virulence, similar to protocols IBCs may face. We found little to guide us. Journal editors made a statement committing to vigilance (*5*), but many questions remain for investigators and their institutions: Should they destroy stocks of pathogens? Swear postdocs and graduate students to secrecy? Notify NIH? What should be told to local public health officials? A "new" agent must be registered, but what does this mean?

Adding review of biosecurity (preventing proliferation of bioweapons) to the existing biosafety (mitigating biohazard) mandate for IBCs is a big change. IBCs have gotten little attention and few resources over the past two decades. A 2003 survey found only 21% of IBCs reported that their members had training in biosafety review; 64% had less than one full-time equivalent staff member (*6*). Last year's "Sunshine Project" report on IBCs, although strident and sarcastic, further documented this dearth of attention (*7*). We are concerned that IBCs today might face a situation similar to resource-starved Institutional Review Boards (IRBs) in the late 1990s. IRBs received attention only after human research was conspicuously shut down at major research institutions.

NIH recently gave welcome guidance to IBCs (*8*). The big new task of biosecurity review is nonetheless fraught with ambiguity. Federal guidance to IBCs now comes from NIH's Recombinant DNA Advisory Committee (RAC), focused on biosafety; NSABB will address biosecurity. Sorting out the respective roles of IBCs, RAC, and NSABB will clearly be a challenge. NSABB will not review individual protocols; instead, it will respond to requests for guidance. Protocol review will thus be left to IBCs, at least initially. Are institutions prepared to shoulder this burden?

The stakes are high: Biodefense is a prominent and hotly contested field that has grown immensely in the past 3 years. It is tugged in many different directions, as previous correspondence in these pages testifies (*9*–*11*). Biosecurity review is yet another battleground. IBCs will need resources, training, and guidance to ensure that resources devoted to research on biodefense and emerging infections are used effectively, and that public trust and accountability are preserved.

ROBERT M. COOK-DEEGAN,[1*†] RUTH BERKELMAN,[2†] E. MEGAN DAVIDSON,[1] STUART FINDER,[3†] ELIZABETH HEITMAN,[3†] MAUREEN C. KELLEY,[4†] NANCY M. P. KING,[5†] RAY MOSELEY,[6†] JAMES C. THOMAS,[5†] SAMUEL J. TILDEN,[4†] NIKKI M. VANGSNES[1]

[1]Duke University, Durham, NC 27708, USA. [2]Emory University, Atlanta, GA 30322, USA. [3]Vanderbilt University, Nashville, TN 37235, USA. [4]University of Alabama at Birmingham, Birmingham, AL 35294, USA. [5]University of North Carolina, Chapel Hill, Chapel Hill, NC 27599, USA. [6]University of Florida, Gainesville, FL 32611, USA.

*To whom correspondence should be addressed. E-mail: bob.cd@duke.edu

†Members of the coordinating committee for the Policy Ethics and Law core of the Southeast Regional Center of Excellence for Biodefense and Emerging Infections.

> "Adding review of biosecurity (preventing proliferation of bioweapons) to the existing biosafety (mitigating biohazard) mandate for [Institutional Biosafety Committees] is a big change."
>
> –COOK-DEEGAN ET AL.

References

1. National Research Council, *Biotechnology in an Age of Terrorism* (National Academies Press, Washington, DC, 2004).
2. 11 May 2005 meeting at the Center for the Study of Medical Ethics and Humanities, Duke University, convened by the Policy, Ethics, and Law Core of the Southeast Regional Center of Excellence for Biodefense and Emerging Infections: Universities of Alabama (Birmingham), Florida, and North Carolina; and Duke, Emory, and Vanderbilt Universities.
3. J. Cello, A. V. Paul, E. Wimmer, *Science* **297**, 1016 (2002).
4. R. J. Jackson *et al.*, *J. Virol.* **75**, 1205 (2001).
5. Journal Editors and Authors Group, *Proc. Natl. Acad. Sci. U.S.A.* **100**, 1464 (2003) (posted online 15 Feb. 2003).
6. R. W. Hackney, "Survey of Institutional Biosafety Committees" (University of North Carolina, Chapel Hill, Feb. 2003).
7. Sunshine Project, *Mandate for Failure: The State of IBCs in an Age of Biological Weapons Research* (Sunshine Project, Austin, TX, 4 Oct. 2004).
8. A. D. Patterson, Office of Biotechnology Activities, National Institutes of Health, "Letter to All Institutions Receiving NIH Funding: Recombinant DNA Research and Institutional Biosafety Committees," 6 Dec. 2004.
9. M. Enserink, J. Kaiser, *Science* **307**, 1396 (2005).
10. S. Altman *et al.*, *Science* **307**, 1409 (2005).
11. A. S. Fauci, E. A. Zerhouni, *Science* **308**, 49 (2005).

Problems in Patenting Human Genes

I READ WITH INTEREST THE POLICY FORUM "Patents on human genes: an analysis of scope and claims" (J. Paradise *et al.*, 11 Mar., p. 1566). There is no doubt that patents have been issued with claims that may be exaggerated in scope and would ultimately be held invalid if attempts were made to enforce them. There are a number of instances where

this has occurred, most recently with respect to the claims covering methods to inhibit Cox-2, although there is no universal agreement on the merits in this case (*1*).

That said, the quantitative conclusions drawn by the authors are open to question. Their apparent criteria for concluding that claims are "problematic" themselves appear problematic. For example, the authors complain that applicants take advantage of the redundancy of the genetic code by "claiming the sequence of a protein within a patent and then also asserting rights over all the DNA sequence variants that encode for that protein." This is standard and recognized practice, since the various encoding nucleotide sequences are directly deducible from the protein sequence. The Federal Circuit itself has recognized this recently (*2*).

More confidence might be had in the conclusions drawn by this article were the criteria for its conclusions more closely aligned with the interpretations of the statutory requirements as interpreted by the courts and as generally recognized in the practice.

KATE H. MURASHIGE

Rancho Santa Fe, CA, USA.

References

1. *University of Rochester v. G. D. Searle & Co.*, 358 F3d 916, 69 USPQ2d 1886 (Fed. Circ. 2004), Cert. denied.
2. *In re Wallach*, 378 F3d 1330, 71 USPQ2d 1939 (Fed. Cir. 2004).

THE ANALYSIS OF HUMAN GENE PATENTS BY J. Paradise *et al.* ("Patents on human genes: an analysis of scope and claims," Policy Forum, 11 Mar., p. 1566) offers the reader little confidence for the conclusions drawn, as it opens with two errors. With gene patents, the invention is the chemical compound, not "the information," as the authors purport. This misstatement is followed by another when they say, "Consequently, disclosure of that information does not allow others to build on it." Others can build on the patented compound, as they can with other patented chemical inventions. A study that only considers the issued patent for context will miss the salient points upon which the examiner relied in issuing the patent.

Additionally, Paradise *et al.* do not cite specific patents, so it is impossible to determine if the U.S. Patent and Trademark Office (USPTO) complied with all appropriate statutes, rules, or guidelines in the handling of particular patent applications. However, any study about a patent's validity would be incomplete if it did not review the file history associated with the patent.

The study used patents issued before 1999 (*1*). Since 1999, the USPTO has provided examiners with revised guidelines to ensure compliance with the utility (*2*) and written description (*3*) requirements of the law.

At the USPTO, we work hard to ensure the public's interest is considered and protected. The Office can only fulfill its obligation to serve the public interest if patent applicants fulfill their obligation to inform the USPTO of all information material to patentability (*4*). Patents are the result of a mutual, shared responsibility. The USPTO is the executive branch's policy lead on recommendations on matters of intellectual property. As such, I welcome the input of the scientific community on the direction and goals of the Office.

JOSEPH J. ROLLA

Deputy Commissioner for Patent Examination Policy, U.S. Patent and Trademark Office, MDE, 10th Floor, 600 Dulany Street, Alexandria, VA 22313, USA.

References

1. "Owning the Body and the Soul," *Economist*, 12 March 2005, p. 77.
2. "Revised Interim Utility Examination Guidelines," 64 FR 71440, Dec. 21, 1999; guidelines currently in effect found at 66 FR 1092, Jan. 5, 2001.
3. "Revised Interim Guidelines for Examination of Patent Applications Under the 35 U.S.C. 112, ¶ 1, 'Written Description' Requirement" 64 FR 71427, Dec. 21, 1999; guidelines currently in effect found at 66 FR 1099, Jan 5, 2001.
4. 37 C.F.R. 1.56 Duty to disclose information material to patentability.

Response

OUR STUDY DID PRECISELY WHAT MURASHIGE is calling for. We applied the statutory requirements of 35 U.S.C. § 100 *et. al.* to gene patents. This contrasts with what practicing attorneys routinely do, which is to claim aggressively for their clients, even though some claims might later be invalidated in litigation.

Rolla assumes that we have overestimated utility problems by including patents granted before the USPTO in 1999 issued new utility guidelines. However, because we limited our analysis to gene patents related to specific diseases, the patents we analyzed were not of the offensive expressed sequence tag variety, which the guidelines addressed. The pre-1999 patents we analyzed had a potential use in diagnosing diseases, and the policy change did not affect their patentability.

Rolla criticizes us for not analyzing the file history of the patents we examined. The Federal Circuit, however, has noted that an analysis of the specification [the portion of the patent where the invention is described (*1*)], and not the file history, is usually "dispositive" of any claim construction issues (*2*). That is what the investigators meticulously did in this study. The file history is not relevant in assessing the adequacy of the patent's disclosure and the utility of the invention.

The juxtaposition of Rolla's claim that "the invention is the chemical compound, not 'the information'" and Murashige's "recognized practice" of using a protein sequence to claim exclusive rights to undis-

covered, hypothesized DNA sequences, underscores our point that inventions in this area relate to data, not compounds. Moreover, traditional composition of matter patents cover a chemical composition with a particular function, such as a drug, which can be designed around. A genetic sequence—the alphabet of ATCGs—is strictly information that has no function until it is linked to an intervention such as a method of diagnosis. Yet allowing a patent on that information allows the holder to prevent others from using the basic sequence, even in research (*3*), and one cannot design around a human nucleotide sequence if one wants to study, diagnose, or treat the genetic disease at issue.

Murashige cites *In re Wallach* (*4*), where the court said in dicta, which is not binding precedent, that it "may" (not necessarily, would) in a future case find that knowing the protein sequence alone would allow the patent applicant to claim all DNA sequences coding for that protein. Such a comment conflicts with the holding in *In re Deuel* that knowledge of a protein sequence does not necessarily put the inventor in possession of the DNA sequence, because of the redundancy of the genetic code (*5*).

We were careful to state that our findings represent our team's application of the statutory guidelines and do not necessarily predict what a court would do. In the United States, unlike in Europe, there is no formal mechanism for third-party intervention in the decision to grant a patent, so studies such as ours may be the only way for the larger community to weigh in on the legal appropriateness of gene patent claims.

JORDAN PARADISE, LORI B. ANDREWS, TIMOTHY HOLBROOK

Illinois Institute of Technology, Chicago-Kent College of Law, 565 W. Adams, Chicago, IL 60661, USA.

References

1. 35 U.S.C. § 112.
2. *Vitronics Corp. v. Conceptronic, Inc.*, 90 F.3d 1576, 1582 (Fed. Cir. 1996).
3. See, e.g., K. Blanton, *Boston Globe*, 24 Feb. 2002, p. 10.
4. 378 F.3d 1330, 1333 (Fed. Cir. 2004).
5. 51 F.3d 1552, 1558 (Fed. Cir. 1995).

CORRECTIONS AND CLARIFICATIONS

News of the Week: "With domestic program at issue, House votes to hold up funding for ITER" by E. Kintisch (3 June, p.1395). The amendment by Rep. Sherwood Boehlert (R-NY) to delay any spending on ITER until March 2006 was offered in support of the position of the Department of Energy that funding for some domestic fusion energy experiments may need to be cut to finance ITER. "Unless we can get agreement that the U.S. participation in ITER will require changes to the domestic program, then the U.S. should not sign on to ITER," Boehlert says. His position contrasts with the views of many fusion scientists and with the House Appropriations Committee, which recently declared that supporting ITER at the expense of domestic fusion research is "unwise" and "shortsighted." Boehlert's amendment was attached to a 2006 spending bill for the Department of Energy that passed the House 24 May.

Reports: "ATM activation by DNA double-strand breaks through the Mre11-Rad50-Nbs1 complex" by J.-H. Lee and T. T. Paull (22 Apr., p. 551). The Biomolecular Interaction Network Database (BIND) accession codes given in reference 21 are incorrect. The correct codes are 216040 to 216045.

Reports: "Atomic-scale visualization of inertial dynamics" by A. M. Lindenberg *et al.* (15 Apr., p. 392). Reference 28 was incorrect. It should be A. L. Cavalieri *et al.*, *Phys. Rev. Lett.* **94**, 114801 (2005).

TECHNICAL COMMENT ABSTRACTS

Comment on "*S*-Nitrosylation of Parkin Regulates Ubiquitination and Compromises Parkin's Protective Function"

Stuart A. Lipton, Tomohiro Nakamura, Dongdong Yao, Zhong-Qing Shi, Takashi Uehara, Zezong Gu

Chung *et al.* (Reports, 28 May 2004, p.1328) reported that *S*-nitrosylation of parkin inhibits its ubiquitin E3 ligase activity and neuroprotective function. Concomitantly, we found that *S*-nitrosylation first increases E3 ligase activity. This initial increase may contribute to the formation of Lewy bodies, ubiquitinated inclusions of misfolded proteins which are a hallmark of sporadic Parkinson's disease.

Full text at
www.sciencemag.org/cgi/content/full/308/5730/1870b

RESPONSE TO COMMENT ON "*S*-Nitrosylation of Parkin Regulates Ubiquitination and Compromises Parkin's Protective Function"

Kenny K. K. Chung, Valina L. Dawson, Ted M. Dawson

Further experiments carried out in our laboratory confirm the finding that *S*-nitrosylation of parkin enhances its E3 ligase activity at earlier time points, but inhibits its ligase activity at later time points. We suspect that this biphasic response plays a more important role in regulating the physiologic E3 ligase activity of parkin and the ubiquitination of its substrates.

Full text at
www.sciencemag.org/cgi/content/full/308/5730/1870c

Letters to the Editor

Letters (~300 words) discuss material published in *Science* in the previous 6 months or issues of general interest. They can be submitted through the Web (www.submit2science.org) or by regular mail (1200 New York Ave., NW, Washington, DC 20005, USA). Letters are not acknowledged upon receipt, nor are authors generally consulted before publication. Whether published in full or in part, letters are subject to editing for clarity and space.

MATHEMATICS

Probing Performance Gaps

Debra Lewis

A meaningful analysis of the role of mathematical ability in gender-correlated career trends requires a reliable measure of that ability. The two most widely used assessments, course grades and standardized test scores, give very different perspectives on the perceived gender gap in mathematics—females receive better course grades, while males receive higher scores on gateway standardized math tests such as the Scholastic Aptitude Test–Mathematics (SAT-M) and Graduate Record Examination–Quantitative (GRE-Q). A 1992 study of approximately 67,000 students from 51 U.S. universities found that the correlations between SAT-M scores and grades in freshman mathematics courses were dramatically different for men and women: the average difference between mean scores for female and male calculus students who received the same grade was double the difference between mean scores of males who received adjacent grades, with the mean score of men who received Ds and Fs equal to that of women who received Bs (*1*).

In *Gender Differences in Mathematics*, editors Ann Gallagher (a researcher at the Law School Admission Council) and James Kaufman (director of the Learning Research Institute at the California State University at San Bernardino) offer a collection of self-contained chapters investigating this perceived gender gap in mathematics achievement, particularly the mismatch between course grades and scores on standardized tests. The authors offer persuasive evidence that we know far less than we should about the assessment of mathematical ability and that the measurements we currently use require recalibration. The most intriguing chapters explore the consequences of students' awareness that they are being evaluated and of their apprehensions about the impact of the evaluations on their opportunities and self-image. Not only do different assessments measure different skills and talents, but expectations regarding those assessments can substantially alter performance.

The reviewer is on leave from the Mathematics Department, University of California, Santa Cruz, and is at the Institute for Mathematics and Its Applications, University of Minnesota, 400 Lind Hall, 207 Church Street SE, Minneapolis, MN 55455–0436, USA. E-mail: lewis@ima.umn.edu

Gender Differences in Mathematics
An Integrative Psychological Approach
Ann M. Gallagher and James C. Kaufman, Eds.
Cambridge University Press, Cambridge, 2005. 367 pp. $70, £40. ISBN 0-521-82605-5. Paper, $25.99, £16.99. ISBN 0-521-53344-9.

Most of us know from painful personal experience that "social context can prime particular aspects of one's self-identity, which, in turn, may hinder or *facilitate* intellectual performance." Simply "having to contend with the risk of being personally reduced to a negative stereotype can elicit an extra psychological burden." Several of the authors hypothesize that this phenomenon, known as stereotype threat, is a key factor in gender-correlated performance differences on tests such as the SAT. Studies of stereotype threat suggest that the triumphant underdog is largely a comforting fantasy; eternally ball-dropping, kite-mangling Charlie Brown is a more realistic portrait of the human psyche battling negative expectations. Stereotypes may also increase performance gaps by giving a psychological advantage to members of "successful" groups: under "stereotype lift," the performance of nonstigmatized groups improves when members are aware of negative stereotypes targeted at others (*2*). However, performance can be impaired even among members of groups perceived as dominant in a given domain by appropriately framing that domain and referencing the pertinent stereotypes: the performance of white males on a test of golf skills deteriorated when the stereotype of black athletic prowess was evoked.

What's being measured? These sixth-grade students are taking the math portion of the Texas Assessment of Academic Skills test.

The authors do not claim that the math problems on the SAT, GRE, and similar exams are gender-biased. Rather, the crucial assertion is that the stereotype of inferior female mathematics ability is so pervasive in American culture that simply reminding a woman of her gender can significantly degrade her performance on these tests; the stereotype need not be explicitly referenced. In their chapter, Paul Davies and Steven Spencer cite the finding (*3*) that "women who indicated their gender before the test scored significantly lower on the [Advanced Placement]–Calculus exam than women who indicated their gender following the test." That study led to the estimate that "simply having students indicating their gender following the AP-Calculus exam would result in as many as 2837 additional women per year starting college with advanced credit for calculus." Another study found that the mathematics performance of Asian American females was enhanced by priming them with their ethnicity and degraded by priming them with their gender (*4*).

Research indicating that women use more conservative test-taking strategies than men has been cited in support of the "A for effort" hypothesis that females' good grades should be attributed to "diligence and good study habits," whereas males' superior test scores are due to "cognitive advantage." Given the high value set on innovation and intellectual risk-taking in mathematical research (the diligence and good work habits of the experimentalist are anathema to many mathematicians), the allegation that women are by-the-book grinds is damning. However, changes in intellectual performance in response to stressors have been documented in both genders and many species. A threat response—associated with increased cortisol levels—is correlated with learning impairment and increased reliance on tried-and-true problem-solving strategies, while a challenge response—associated with moderately increased adrenaline levels—is correlated with enhanced problem-solving abilities. In one experiment (*5*), "women who were told the math problems were developed for the SAT were less able to formulate effective problem-solving strategies" than those not given any information about the source of the problems. If the stereotype threat hypothesis is valid, comparative studies of problem-solving strategies must be carefully designed to avoid unintentional biasing of results.

The writing and contents in *Gender Differences in Mathematics* are of uneven quality. Whereas most chapters are clearly written and provocative (in the best sense of the word), some are disappointingly predictable, simplistic, or dogmatic. Others provide frustratingly little information about cited studies, which makes it difficult to compare results in a meaningful manner. Those who seek information such as sample size and source, date of study, and appropriate interpretation of terms like "advanced" or "difficult" mathematics will often need to consult the original papers.

The popular perception of a gender gap in mathematical ability is unlikely to be the sole culprit in the underrepresentation of women in the mathematical sciences. The crucial question isn't "who can do math?" but "who wants to?" The emphasis on tests and skills in discussions of mathematics and gender is, unfortunately, all too representative of much of mathematics education. The emphasis on assessment often overshadows the appeal and power of mathematics; for many gifted students the most enjoyable aspect of math is getting good grades and test scores. The essential math skills—conjuring new worlds, exploring and cataloging their features, recognizing the crucial similarities and differences between these imagined worlds and our actual one, and communicating the resulting insights—are far more fun to practice than those captured by any standardized test. The key to attracting more women (and men) to math may be increased exposure to its pleasures and rewards.

References

1. H. Wainer, L. Steinberg, *Harvard Educ. Rev.* **62**, 323 (1992).
2. G. M. Walton, G. L. Cohen, *J. Exp. Soc. Psychol.* **39**, 456 (2003).
3. L. J. Stricker, *Inquiring About Examinees' Ethnicity and Sex: Effects on AP Calculus AB Examination Performance* (College Board Report no. 98-1, ETS RR No. 98-5, College Entrance Examination Board, New York, 1998).
4. M. Shih, T. L. Pittinsky, N. Ambady, *Psychol. Sci.* **10**, 80 (1999).
5. D. M. Quinn, S. J. Spencer, *J. Soc. Issues* **57**, 55 (2001).

10.1126/science.1112247

MATHEMATICS

Landmarks on the Road to Modern Analysis

Judith V. Grabiner

"The calculus was the first achievement of modern mathematics, and it is difficult to overestimate its importance," wrote John von Neumann. Suppose you agree with his statement. Wouldn't you like to see what Isaac Newton and Gottfried Wilhelm Leibniz actually did in inventing calculus, watch Augustin-Louis Cauchy rigorize the calculus and the theory of infinite series, witness Georg Friedrich Bernhard Riemann work out the theory of the Riemann integral, and view the landmarks in the creation of Weierstrassian rigor? Or you might wish to follow Joseph Liouville's construction of the first number known to be transcendental, appreciate Georg Cantor's first proof that there are more real numbers than rational ones, and understand exactly what Henri Lebesgue did in generalizing the theory of integration and demonstrating the precise conditions under which a function is integrable. One might think that learning all this material would require access to a major library; the ability to read Latin, German, and French; and a comprehension of everything presented in a graduate-level course in real analysis. Not any longer, thanks to William Dunham's remarkable *The Calculus Gallery: Masterpieces from Newton to Lebesgue*.

Through the analogy to an art museum expressed in the book's title, Dunham (a professor of mathematics at Muhlenberg College) makes it clear that he is not claiming to present all the major works of the mathematicians he covers. But he does think he has collected the key masterpieces and that viewing them together gives a good picture of how modern analysis came to be. Moreover, his text and excellent diagrams explain the mathematics clearly. Anyone familiar with calculus and infinite series can, with a bit of effort, enjoy the beauty and profundity of these important mathematical discoveries.

The Calculus Gallery
Masterpieces from Newton to Lebesgue
by William Dunham

Princeton University Press, Princeton, NJ, 2005. 252 pp. $29.95, £18.95. ISBN 0-691-09565-5.

Everyone will have favorites among the results, derivations, and proofs that Dunham describes. The ones listed in my first paragraph are, of course, of interest. But there is much more, ranging from the curious to the profound. Among the curiosities he provides is Jakob Bernoulli's proof of a general theorem about the sums of infinite series composed of fractions whose numerators are the cubes of 1, 2, 3, … and whose denominators are in geometric progression; one corollary is that $1/2 + 8/4 + 27/8 + 64/16 + \ldots k^3/2^k + \ldots = 26$. In the same tradition but much more significant are what Dunham calls the "spectacular sums" discovered by Leonhard Euler, who ingeniously derived product-sum relations to produce large classes of surprising results like $1 - 1/27 + 1/125 - 1/343 + 1/729 \ldots = \pi^3/32$. Dunham also explains and gives the motivation for Euler's introduction of the gamma function. Moving to the mathematical depth typical of the 19th century, we find Cauchy's proof of the fundamental theorem of calculus, Riemann's characterization of integrable functions, and the later improvements to the concepts used in those proofs. For instance, we learn how Karl Weierstrass constructed a continuous nondifferentiable function, what distinguishes pointwise and uniform convergence and what Weierstrass said about that distinction, and how Vito Volterra gave a function whose derivative, though bounded everywhere, cannot be integrated. The book ends with Lebesgue's theory of the integral, including his proof of the integrability of everywhere discontinuous functions.

The book is not—and Dunham would agree that it is not—a history of the calculus. Even given the book's expository goal, I wish that Dunham had consulted additional sources instead of relying so heavily on a small number of scholarly works to identify the key discoveries and to provide their historical context. He cites the articles on Weierstrass, Volterra, and René Baire in the *Dictionary of Scientific Biography* without including the names of their knowledgeable authors (Kurt-R. Biermann, E. Volterra, and Pierre Costabel). And all Dunham's mathematicians seem to be moving toward the same goal; the diversity of their work within pure mathematics, let alone applied mathematics, is not really represented—an aspect I found especially lacking in the section on Newton.

Nevertheless, for what Dunham has set out to do, *The Calculus Gallery* is a wonderful book. The style is inviting; the explanations are clear and accessible. Teachers of calculus wanting a sense of where the key ideas came from will find developments from the 17th century through the early 20th century beautifully laid out. Mathematicians, scientists, and historians alike can learn much that is interesting, much that is mathematically significant, and a good deal that is both. Dunham provides a high-level popularization of sophisticated mathematics. His book helps us understand both how the calculus came to be and many of the leading ideas of classical analysis.

10.1126/science.1111597

The reviewer is at the Mathematics Department, Pitzer College, Claremont, CA 91711, USA. E-mail: jgrabine@pitzer.edu

VOTING TECHNOLOGY

Election Auditing Is an End-to-End Procedure

Ted Selker

After the 2004 U.S. presidential election, allegations of voting machine irregularities appeared on blog sites and in the press. However, the available evidence suggests that electronic voting machines outperformed all other methods used in November's election (*1*, *2*). Data indicate that the residual vote rate (i.e., the number of uncounted votes resulting from an unintentional or intentional nonvote for the presidential race) dropped from 1.91% in 2000 to 1.07% in 2004, with the most dramatic improvements occurring in states that invested heavily in new election technology, as well as improved training and procedures (*3*). Nevertheless, we may never be able to remove lingering doubts because—in spite of the enormous sums of money, energy, and brainpower that have been expended to improve the election process since 2000 and in spite of the significant strides forward that have been made—we have been sloppy in our procedures and in our record-keeping.

These concerns have fueled movements to pass legislation in many states and in the U.S. Congress that would require a paper recording of every vote (*4*). However, early experiments indicate that the Voter-Verifiable Paper Audit Trail (VVPAT), designed to do this for direct recording electronic (DRE) voting machines adds complexity to the tasks that voters, poll workers, and officials perform—increasing confusion and even possibilities for error (*5*). While observing Nevada's September deployment of machines, I witnessed errors by poll workers (see figure, this page) who placed paper-trail printers in unsecured spots; opened the printers without supervision (they should be handled like ballot boxes); and even, in a muddled attempt to reload the paper in a jammed printer, cut out portions of the paper-trail record. Nevada's Secretary of State reported that these state-of-the-art paper-trail printing units added $500 to the cost of each DRE (*6*). Problems observed during earlier tests of Avante's paper-trail system in Sacramento, CA, and Wilton, CT, were even worse (*7*). I have seen or known of every type of similar mishandling of every type of ballot and equipment in use. Such mistakes illustrate that machines work only as well as the people who operate them. Any audit trail system is only valuable to the extent that voters, poll workers, and officials successfully operate it.

People tend to be suspicious of new machines (*8*, *9*). Such fears intensify when relying on unfamiliar technology to determine results of a heated and close election. The public's inherent distrust of voting has been reinforced by lost votes in 2000 and continued confusion. Those forging future elections must not only make a system that works, but also prove to Americans that it does so. Voter verification should be only one part of supervising a complex process (*10*–*12*).

To maximize security during the design phase, the architecture of voting technology can be broken into modules that are designed by separate teams, so that no one person would have knowledge of the entire program (*13*). However, sophisticated code design cannot replace thorough testing.

Proving program correctness is theoretically unsolvable (*14*, *15*). Testing large circuits or programs is accomplished by testing them in pieces and for all possible input scenarios (*16*). New methodologies for improving code quality, such as extreme programming in which small teams work intensively on component modules, institutionalize good practices of incremental testing (*17*). In addition, this technique inherently reduces the ability of any one person to have access to the entire code.

Systems must be tested as a whole for all possible input. In the case of voting machines, so-called logic and accuracy tests are designed to do this. Code programming must be examined as comprehensively as possible to confirm that "malware" has not been fraudulently imbedded.

Maryland and California are among states that have instituted a policy of "parallel monitoring" (*18*), in which a random selection of voting machines is taken out of service on Election Day and test-voted at the same time as the actual polling machines. This method can provide assurance that the test machines are identical to those being used and makes it impossible for a malevolent coder to distinguish between the two groups in advance.

If parallel testing or certification audits show problems, we might rerun an election, as recently happened in the Ukraine. Even better would be to avoid such a costly necessity by demonstrating before an election that voting machines do not have malware and then securing them. Kennesaw State Election Center has successfully caught problems with advance testing of equipment in Georgia, which showed the most dramatic improvement of its residual vote rate of any state in 2004 (*19*). Current Federal Election Commission (FEC) guidelines require voting machines to include internal clocks, which can be forwarded and then tested for software designed to attack on Election Day. One problem with this approach is that the clocks can be programmed to behave differently during an election than at other times; the Nedap Powervote currently used in the Netherlands does not rely on an internal clock (*20*).

The ability of voters and poll workers to operate voting technology successfully must be as thoughtfully conceived and extensively tested as its security. In 2000, more than 1.3 million votes were lost

A paper-trail printer being opened without supervision during the 7 September 2004 election.

The author is codirector of the CalTech/MIT Voting Technology Project and is at Massachusetts Institute of Technology, Cambridge, MA 02139, USA. E-mail: selker@media.mit.edu

because of ballot design problems such as the infamous butterfly layout (*21*). The biggest improvements in error rates in 2004 occurred in states, such as Georgia, that invested heavily in training and voter education, as well as in machines (*3*). In spite of widespread expectations that the massive increase in unfamiliar voting systems would result in millions of trouble-shooting calls, the Election Incident Reporting System recorded under 2500 complaints relating to voting machines nationwide (*22*). These results are encouraging; nevertheless, forensic data and experiments with current equipment estimate that a significant number of voters accidentally make selections other than what they intend to (*20*, *23*). Therefore, system developers must seek new ways to simplify the voting process.

Improving voter accuracy is an achievable goal. For example, a new electronic ballot design, known as the Low-Error Voting Interface (LEVI) has been shown in tests to reduce errors by half (*24*). Among its innovative features, a contemporaneous review sidebar at the edge of the page displays status for each race, which visibly changes as the voter successfully enters a selection. The concept of voter verification offers a similar opportunity to let voters review and correct their work.

An ideal system would improve voting accuracy even as it creates a back-up record for auditing purposes. Moreover, a true verification audit trail should confirm that a vote has been received into the final counting lot, not just into the local precinct machine. By means of special architectures with redundancy and cryptographic controls to guard against manipulation or unwarranted control, the precinct machine could instantaneously transfer a voter's selections to the central counting office, which would return a report confirming receipt (*13*). Voters might also be able to reconfirm, by computer, that their ballots are part of the final count. To avoid the possibility of reports being used in vote-selling schemes, ballot selections would not be displayed.

David Chaum and VoteHere promote work with cryptographic records that could allow voters to keep a receipt from which the voter's selections could later be reassembled to prove that the record had not been altered, without printing the actual completed ballot (*25*). Another verification method, Voter-Verified Audio Audit Transcript Trail (VVAATT), uses a voting machine's existing audio output, earphones, and an inexpensive tape recorder that is locked in a box, to create an audit transcript (*26*). The machine speaks the name of each candidate that a voter selects, and the recorder tapes the entire sequence for each ballot. A primary advantage is that audio prompts help voters recognize unintended selections as they proceed, so that they can immediately correct mistakes (*27*). In addition, if a recount is necessary, the taped transcript can be tallied by hand and/or by machine.

When a voter realizes that the vote cast is not what was intended, there is a natural human reaction to blame the machine rather than to accept responsibility for pressing the wrong button (*27*). A policy of videotaping voters from behind could be used to allow voters to check any claim of machine malfunction. To preserve secrecy, the videotape should overwrite itself. VoteGuard is a screen capture verification system that does not require a camera (*28*).

Regardless of the method, polling-place setup and procedure constitute two of the weakest links in our ability to audit elections. I have witnessed poll workers take ballots out of ballot boxes without supervision; erase and change records; give voters incorrect ballots (electronic and physical); send voters to nonfunctioning booths; misinstruct voters on how to use the voting machine; check over completed ballots; hang over people voting in booths; and transport records and voting materials to the counting place without a corroborating witness (*5*).

Principles for assuring that voting materials are handled in secure ways are commonly overlooked or ignored. Fortunately, these problems should be the easiest to fix. However, such changes require thoughtful collaboration between technology developers and election officials.

There must also be adequate training for poll workers for good habits to become ingrained, such as always working in pairs to corroborate how ballots and equipment have been handled. Mutual oversight has been crucial all election process improvements.

Simple changes like banning the use of pencils that can be easily erased for polling-place recordkeeping may do as much to improve election auditing as advanced voting technology. To secure an election properly, we must look for all of the possible points of failure, check for problems at each of them, and document what has been done at every step. Throughout the process, a team of publicly accountable bipartisan and nonpartisan observers should be required to check over and sign off on every phase—from the development and testing of machines to the counting of votes and storage of records. Let us revisit the entire process before we pass expensive and counterproductive legislation.

References and Notes

1. D. Kimball, "Summary tables on voting technology and residual vote rates"; available at www.umsl.edu/~kimballd/rtables.pdf
2. C. Stewart III, Addendum to voting machines and the underestimate of the Bush vote, December 2004; available at www.vote.caltech.edu/ media/documents/Addendum_Voting_Machines_Bush_Vote.pdf
3. C. Stewart III, Residual vote in the 2004 election, February 2005; available at www.vote.caltech.edu/media/documents/vtp_wp21v2.3.pdf
4. R. Kibrik, www.verifiedvoting.org/article.php?list=type&type=13
5. T. Selker, *User Experience* **4**, 1 (Spring 2005).
6. D. Heller, presentation at the conference "A Report to the Nation on America's Election Process," Washington, DC, 7 December 2004 (supported by Century Foundation and Common Cause).
7. C. B. McCormack, Presentation to the U.S. Election Assistance Committee (EAC), Hearing on Use, Security, and Reliability of Electronic Voting Machines, 5 May 2004; available at www.electiontech.org/downloads/EACtestimony505.pdf
8. A. H. Teich, *Technology and the Future* (Wadsworth, Belmont, CA, 2003).
9. R. Mecuri, *IEEE Spectrum* **39**, 10 (November 2002).
10. E. Fischer, "Election reform and electronic voting systems (DREs): Analysis of security issues; CRS report for Congress" (RL32139, Congressional Research Services, Library of Congress, Washington, DC, 4 November 2003).
11. R. G. Saltman, "Accuracy, integrity, and security in computerized vote-tallying" (Spec. Publ. 500-158, U.S. National Bureau of Standards, Washington, DC, 1989).
12. IEEE Voting Equipment Standards Project 1583 http://grouper.ieee.org/groups/scc38/1583/
13. S. D. Liburd, thesis, Massachusetts Institute of Technology (2004).
14. K. Thompson, *Commun. ACM* **27** (8), 761 (August 1984).
15. P. Popov, L. Strigini, *IEEE Trans. Software Eng.* **29**, 4 (2003).
16. B. Berard *et al.*, *Systems and Software Verification: Model-Checking Techniques and Tools* (Springer-Verlag, New York, 2001).
17. S. W. Ambler, R. Jeffries, *Agile Modeling: Effective Practices for eXtreme Programming and the Unified Process* (Wiley, New York, 2002).
18. California Parallel Monitoring Program, "Report of findings for November 2, 2004" (Secretary of State of California, Sacramento, 2004); available at www.ss.ca.gov/elections/november2004_pmp_report.pdf).
19. B.J. Williams, M. S. King, *Commun. ACM* **47** (10), 39 (October 2004); available at http://theory.lcs.mit.edu/~rivest/voting/reports/cacm/2004-10 CACM p39 Williams King - Implementing Voting Systems - The Georgia Method.pdf
20. R. Sinnott *et al.*, in "First report—December 2004" (Irish Commission on Electronic Voting, Dublin, 2004) Appendix 2C, pp. 153–191; available at www.cev.ie/htm/report/first_report/pdf/Appendix%202C.pdf
21. R. M. Alvarez *et al.*, "Voting: What was, what will be, (Caltech/MIT Voting Technology Project (VTP), California Institute of Technology, Pasadena, CA, and MIT, Cambridge, MA, July 2001; www.vote.caltech.edu/reports/2001report.
22. Election Incident Reporting System, 2004 reported machine problems, 2005; available at https://voteprotect.org/index.php?display=EIRMapNation&tab=ALL&cat=02&start_time=&start_date=&end_time=&end_date=&search=
23. S. M. Sled, "Vertical proximity effects in recall" (VTP Working Pap. 6r, Caltech and MIT, October 2004); available at www.vote.caltech.edu/Reports/vtp_WP6r.pdf.
24. T. Selker, Presentation at Caltech/MIT Voting Technology Project Symposium, Cambridge, MA, 2 October 2004; available at www.vote.caltech.edu/events/2004/voting-tech
25. Voting technology: Innovations for today and tomorrow, Caltech/MIT Voting Technology Project Symposium, Cambridge, MA, 1 and 2 October 2004; available at www.vote.caltech.edu/events/2004/voting-tech
26. T. Selker, *Sci. Am.* **291**, 4 (September 2004).
27. S. Cohen, T. Selker, "An active approach to verification (VTP Working Pap. 28, Caltech and MIT, May 2005), available at www.vote.caltech.edu/media/documents/wps/vtp_wp28.pdf
28. See www.voteguard.com/

29. I thank Carolin Young for numerous discussions and editing improvements.

10.1126/science.1109901

BIOMEDICINE

The Anti-Aging Sweepstakes: Catalase Runs for the ROSes

Richard A. Miller

Organism envy is the unavoidable fate of all who study the physiological genetics of aging in mice. If only our favorite rodents had the grace to die in a few weeks or months, like worms and flies, or better yet to do so after a round or two of hermaphroditic self-fertilization! Clinging desperately to the consoling mantra that mice are more or less just like people, we hold our breath waiting for a discovery in this diminutive mammal worth bragging about. Ergo the exhalations of relief attending the report of Schriner *et al*. (*1*), on page 1909 of this issue, that overexpression of human catalase in the mitochondria of mice extends median and maximal life span by about 20%. Catalase prevents the formation of reactive oxygen species (ROS) that can damage cellular constituents. Although 20% may not seem like much compared to the 50% life-span extension seen in dwarf mice with hormone-altering mutations (*2*), it is roughly 5 times that predicted from complete abolition of human cancer or heart attack (*3*), and thus no small potatoes.

Enhanced online at www.sciencemag.org/cgi/content/full/308/5730/1875

The central mystery for biological gerontology is variable-rate synchrony: If everything must go to pot all at once as organisms approach emeritus status, why does it take 2 years to do so in mice, 10 years in dogs, 20 years in horses, 70 years in people, and longer still in whales and some seabirds? What process, or set of synchronous processes, sets the tempo of aging, and how does aging lead to its unwelcome symptoms? Schriner *et al*. view their new data as support for the notion that oxidative damage is the key villain and, moreover, that mitochondria are a major source of toxic oxygen radicals. There are still a few gaps in their story—most laboratory-bred mice die of tumors rather than of the cardiomyopathy on which Schriner *et al*. focus (what are these mice dying of, then?)—but the report is the first strong evidence that mouse aging can be delayed by antioxidant prophylaxis.

Is it safe to conclude that oxygen molecules are the true culprits in causing aging? Can we now turn our attention to the secondary questions of how they cause physiological decline in the superannuated? There are still some grounds for skepticism here. The search for antioxidant drugs that slow aging and extend life span in mammals has produced much frustration and a lamentable absence of authentic anti-aging pills. Mice heterozygous for the mitochondrial form of superoxide dismutase, an enzyme that destroys a highly reactive derivative of oxygen called superoxide, show high levels of DNA oxidation in multiple organs. In spite of their abnormally oxidized DNA, these animals show no decline in lifespan and no acceleration in certain hallmarks of aging: cataracts, immune dysfunction, and protein modifications (*4*). Thus, mice can live reasonably long and healthy lives despite unusually high levels of oxidative damage. Furthermore, skin-derived fibroblast cells from three different kinds of long-lived dwarf mice are resistant to multiple forms of stress, including oxidants, ultraviolet light, heat, the heavy metal cadmium, and a DNA alkylating agent (*5*). Mutations that extend worm longevity also typically lead to, and perhaps act through, increased resistance to multiple forms of stress (*6*). Thus, it seems plausible that many age-retarding mutations may work by inducing cellular signaling pathways, still poorly defined, that augment defenses against a multitude of insults, including the oxidative ones.

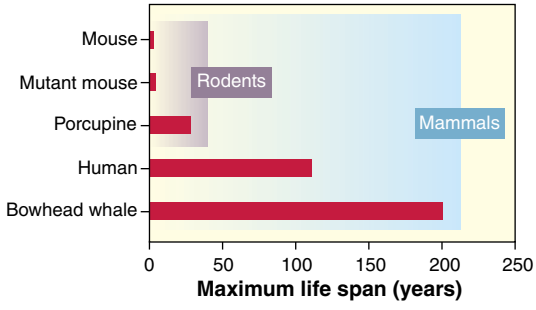

Maximum life-span estimates in various populations. Mutations (or calorie restriction) increase maximal survival in mice by ~50% at most. In contrast, porcupine longevity is greater by about 500%. The value for whales is speculative, based on a small sample number. This juxtaposition suggests that further progress in understanding the pathways that control aging rates in mammals may benefit from greater emphasis on interspecies comparisons.

The Schriner *et al*. paper increases to nine the number of mouse genes whose mutation extends maximal longevity. It is also the second gene whose overexpression in mice has this effect. Five of these loci modulate signals mediated by insulin-like growth factor–I (IGF-I), with lower levels of IGF-I associated with longer life span and slower aging. In dogs, too, genetic polymorphisms that diminish body size by altering IGF-I levels increase life span (*7*). It remains to be seen whether mammalian longevity induced by any of these genetic effects, or by diets low in calories or nutrients, are accompanied by changes in cellular resistance to oxidants, nonoxidant injuries, or both.

So far, the best one can accomplish by combinations of genetic and dietary intervention is to increase median and maximal life span of a given mammalian species by about 80% (*8*). Natural selection, however, routinely engenders new species that outlast their progenitor species by a factor of 10 or more. Among the rodents, species-specific maximal longevities range from 2 to 4 years in shrews, mice, and rats, to at least 27.3 years in naked mole rats, porcupines, and perhaps beavers (see the figure). How does nature do this? Does she rely solely on antioxidant mechanisms or on pathways that control multiple forms of cellular stress resistance? The recent demonstration (*9*) that the replicative potential of mouse cells in culture can be increased to levels seen in human cells by reducing environmental oxygen suggests that resistance to oxidative damage may contribute to the remarkable longevity of our own species. Similarly, resistance of cultured fibroblasts to oxidative stress correlates with maximal life span across a range of mammalian species (*10*). Thus, oxidation defenses have become the heavy favorite among players wishing to bet on a single horse in the anti-aging sweepstakes. But attractive dark horses still lurk within the pack of remaining hypotheses. Perhaps the winning bet will prove to be a trifecta: oxidative damage, protein malformation, and DNA breakage (order to be determined).

The author is in the Department of Pathology and Geriatrics Center, University of Michigan School of Medicine, and Ann Arbor DVA Medical Center, Ann Arbor, MI 48109–0940, USA. E-mail: millerr@umich.edu

Research in basic biogerontology may lead to a pill that slows aging and, as a pleasant side effect, delays all age-related diseases. Deceleration of aging and associated late-life illnesses is now readily achievable in mice, and thus is a conceivable goal for preventive medicine. The value of studies like that of Schriner *et al.* is not that they serve as blueprints for genetic surgeons—gene therapy for aging is still as distant a dream as other sci-fi perennials—but as pointers toward the currently less sexy discipline of comparative physiology. It is time to exploit the modest but growing collection of anti-aging mutations, together with the large and potent collection of slow-aging organisms donated to us by 100 million years of natural selection, to map out the common pathways by which aging can best be modulated.

References

1. S. E. Schriner *et al.*, *Science* **308**, 1909 (2005); published online 5 May 2005 (10.1126/science.1106653).
2. H. M. Brown-Borg, K. E. Borg, C. J. Meliska, A. Bartke, *Nature* **384**, 33 (1996).
3. S. J. Olshansky, B. A. Carnes, C. Cassel, *Science* **250**, 634 (1990).
4. H. Van Remmen *et al.*, *Physiol. Genomics* **16**, 29 (2003).
5. A. B. Salmon *et al.*, *Am. J. Physiol. Endocrinol. Metab.*, inpress.
6. G. J. Lithgow, G. A. Walker, *Mech. Ageing Dev.* **123**, 765 (2002).
7. R. A. Miller, S. N. Austad, in *Handbook of the Biology of Aging*, E. J. Masoro, S. N. Austad, Eds. (Academic Press, New York, in press).
8. A. Bartke *et al.*, *Nature* **414**, 412 (2001).
9. S. Parrinello *et al.*, *Nat. Cell Biol.* **5**, 741 (2003).
10. P. Kapahi, M. E. Boulton, T. B. Kirkwood, *Free Radic. Biol. Med.* **26**, 495 (1999).

10.1126/science.1114393

CHEMISTRY

Dioxygen Surprises

Jan Reedijk

The binding of dioxygen (O_2) to enzyme active sites and its activation and use in enzymatic reactions are crucial for almost all terrestrial life. Nature uses metal ions—mostly iron and copper—to perform these tasks. On page 1890 of this issue, Mirica *et al.* (*1*) shed light on the mechanism by which copper enzymes use dioxygen.

The authors have designed a small molecule that mimics the active site of tyrosinase, an enzyme that plays a crucial role in melanin formation. They show that their mimic uses a mechanism very different from that generally accepted for this enzyme. Tyrosinase-catalyzed oxidation reactions are highly selective: Only the CH group next to a phenolic OH group is hydroxylated via electrophilic substitution. The nature of the enzymatic reaction suggests a mechanism in which the O–O bond is cleaved either at the same time as or after the C–O bond is formed. Mirica *et al.* now show that in their model system, the O–O bond breaks first.

The reversible binding of dioxygen to metals has intrigued chemists and biochemists for decades. Over the years, chemists have reported various possible binding modes. In biological systems, proven binding modes are restricted to proteins that transport dioxygen (such as hemoglobin and myoglobin for iron, and hemocyanin for copper). In the case of enzymes using dioxygen, the catalytic intermediates have only been postulated, often on the basis of the known chemistry of small compounds that mimic the enzyme active site. But even for these mimics, the catalytic intermediates are short-lived and cannot be trapped and studied at room temperature. Very low temperatures and a combination of several spectroscopies (such as ultraviolet/visible, Raman, and extended x-ray absorption fine structure) are required to detect the catalytic intermediates. This is what Mirica *et al.* have done for a tyrosinase-like system.

Dioxygen binding modes to metals can be divided into two broad categories: end-on and side-on, and bound to one or two metal atoms (see the first figure). More than a century ago, Alfred Werner described Co(III) species that contained a peroxo bridge. In the 1960s, side-on binding was reported for nonbiological metals such as Ir(III). Myoglobin and hemoglobin contain an end-on Fe–O–O structure.

In 1987, Karlin (*2*) provided evidence for a peroxo bridge in a dicopper species (mode I in the second figure). Such structures were later found by others, usually only at low temperatures, but in a few cases also at higher temperatures (*3*). This type of dioxygen binding is often described as a nucleophilic binding.

In contrast, Kitajima observed side-on binding (mode II in the second figure) in his biomimetic dicopper compounds (*4*). This binding mode also occurs in the dioxygen transport protein oxyhemocyanin (*5*). When the dioxygen is bound as a peroxide in this geometry, it is electrophilic.

Tolman (*6*) showed that given appropriate ligands and solvent, two Cu(III) ions can be held together by single-oxygen bridges—that is, the O–O bond in a mode II structure can be broken (mode III in the second figure). Mode II and mode III structures can be in equilibrium (*7*, *8*), with the O–O bond present or absent, depending on the ligand, solvent, and temperature (*9*).

Currently, the mechanism of phenol hydroxylation by tyrosinase is far from clear. Until now, it was commonly accepted that a side-on mode II intermediate is the active species. Nonetheless, it is an intriguing question whether the hydroxylation of phenols could perhaps be performed by a mode III species.

Obias *et al.* (*10*) have reported that under conditions where both mode II and mode III species are present, a hydroxylation reaction can occur. From the observed equilibrium between species II and III and detailed analysis of the reaction kinetics, the authors concluded that the active species had to be a mode II intermediate. This

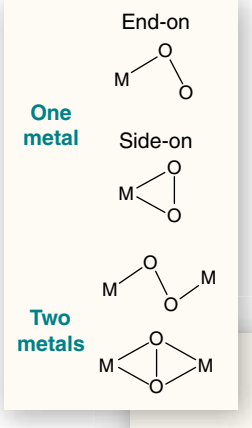

Generic dioxygen binding modes. Dioxygen binds to metals end-on, side-on, or through bridging.

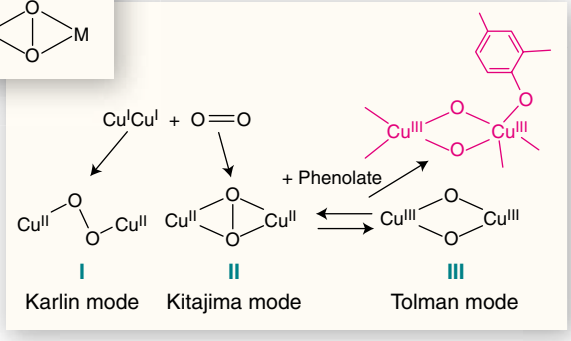

How dioxygen binds to dicopper. There are three known ways in which dioxygen can bind to Cu(I)–Cu(I) species (modes I to III). Mirica *et al.* (*1*) show that the catalytic intermediate of a tyrosinase mimic is a mode III species (red). Copper ligands have been omitted for clarity.

The author is at the Leiden Institute of Chemistry, Leiden University, 2300 RA Leiden, Netherlands. E-mail: reedijk@chem.leidenuniv.nl

proposal has also been followed by other authors (*11*, *12*).

However, Mirica *et al.* demonstrate that upon phenol binding, a mode II species is converted to a mode III species (*1*). The latter subsequently performs the hydroxylation. Their advanced low-temperature experiments, supported by high-level density functional theory calculations, provide the first experimental proof for this species, contrary to earlier assumptions.

The finding of O–O bond breakage upon binding of the substrate (*1*) points to a potentially important mechanism through which enzymes can deal with small molecules. It remains to be shown whether such a reaction occurs in natural enzymes.

References

1. L. M. Mirica *et al.*, *Science* **308**, 1890 (2005).
2. K. D. Karlin, Y. Gultneh, *Prog. Inorganic Chem.* **35**, 219 (1987).
3. J. E. Bol *et al.*, *Angew. Chem. Int. Ed.* **36**, 998 (1997).
4. N. Kitajima, *Adv. Inorg. Chem.* **39**, 1 (1992).
5. K. A. Magnus *et al.*, *Proteins* **19**, 302 (1994).
6. J. A. Halfen *et al.*, *Science* **271**, 1397 (1996).
7. S. Mahapatra *et al.*, *Inorg. Chem.* **36**, 6343 (1997).
8. L. M. Berreau *et al.*, *Angew. Chem. Int. Ed.* **38**, 207 (1999).
9. H. C. Liang *et al.*, *Inorg. Chem.* **43**, 4115 (2004).
10. H. V. Obias *et al.*, *J. Am. Chem. Soc.* **120**, 12960 (1998).
11. C. X. Zhang *et al.*, *J. Am. Chem. Soc.* **125**, 634 (2003).
12. P. Gamez, I. A. Koval, J. Reedijk, *Dalton Trans.* **2004**, 4079 (2004).

10.1126/science.1113708

OCEANS

How Does the Antarctic Ice Sheet Affect Sea Level Rise?

David G. Vaughan

The greatest uncertainty in predictions of future sea level rise lies in the contribution of the Antarctic ice sheet. To the first order, the annual snowfall on the ice sheet is balanced by loss to melting and iceberg calving. However, the equivalent of more than 5 mm of global sea level passes in and out of the ice sheet every year; therefore, even small imbalances between input and output will have a substantial impact on global sea level. Changes in surface elevation are currently the best indication of imbalance in the ice sheet. On page 1898 of this issue, Davis *et al.* (*1*) use altimeter measurements from the European remote sensing (ERS) satellites to compile the longest (11-year) record to date of surface elevation change over Antarctica.

Before the launch of the ERS-1 satellite in 1992, imbalances in the Antarctic ice sheet were hypothesized, but could not be measured over wide areas with the existing technology. A series of studies using data from the ERS satellites (*2*, *3*) is revealing changes over wide areas with ever-increasing precision, demonstrating the value of an infrastructure for measurements of long-term change. Davis *et al.* now demonstrate imbalance in several areas of the ice sheet, but focus on the finding that the East Antarctic ice sheet is thickening (see the figure) (*1*). The thickening is small (1.8 ± 0.3 cm per year) but the area is vast, and its effect is to slow sea level rise by 0.12 ± 0.02 mm per year.

Using output from meteorological forecast models for the same period, Davis *et al.* show that the thickening is probably a result of increased snowfall. It may be premature to predict that the East Antarctic ice sheet will continue to thicken, but the measured change is roughly that expected as a mean response to 20th-century climate change (*4*). If this part of the ice sheet continues to grow—as general circulation model predictions suggest it should (*4*)—then this thickening may become a large negative term in the sea level change equation.

Thickening due to increasing snowfall appears to be the dominant effect in East Antarctica at the present time, but it is not the only change going on in the Antarctic ice sheet (see the figure). A substantial part of West Antarctica is thinning (*5*) in response to acceleration and widening of the glaciers that drain it (*6*). The changes in the glaciers were probably caused by changes in circulation or temperature of the surrounding ocean (*7*). The new maps presented by Davis *et al.* (*1*) show this thinning clearly. They also show that in another part of West Antarctica, the current rates of thinning match those measured by dating the exposure ages of mountains that protrude through the ice sheet [~4 cm per year for the past 10,000 years (*8*)]. This part of the ice sheet may not yet have ended the retreat begun at the end of the last glacial period.

The ERS satellites do not successfully track steep ice surfaces. Therefore, the new maps do not show the thinning of the ice sheet observed in coastal areas of the Antarctic Peninsula as a result of recent regional climate warming (*9*) and glacier acceleration (*10*). Furthermore, the satellite data do not extend south of 81.6°S, precluding measurements of the thickening upstream of the Kamb Ice Stream. This ice stream slowed down around 130 years ago; today, almost all new snowfall remains in its basin, piling up year by year (*11*).

We may aspire to determine the overall contribution of the Antarctic ice sheet to changing sea level as a single number with a single estimate of uncertainty. But this number will necessarily arise from many different

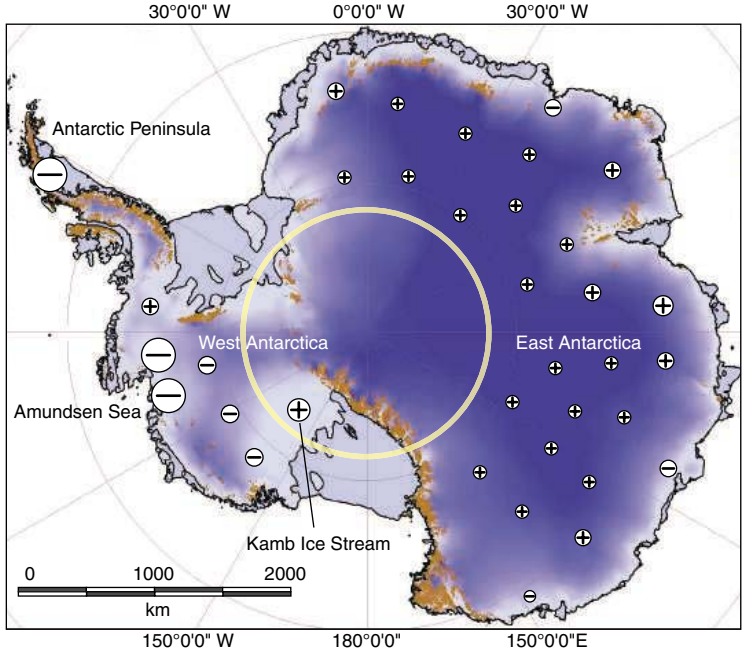

Modes of imbalance. In some parts of Antarctica, such as East Antarctica, the ice sheet is thickening (+ symbols), whereas in others, it is thinning (– symbols). The reasons for these changes differ, making it difficult to predict the future contribution of the Antarctic ice sheet to sea level change.

The author is with the British Antarctic Survey, Natural Environment Research Council, Madingley Road, Cambridge CB3 0ET, UK. E-mail: dgv@bas.ac.uk

modes of imbalance in the ice sheet. Some will have their origin in contemporary climate change, but others will not. Furthermore, the future development of each mode of change may be quite different; the fact that one contribution is greater than another at the moment does not mean that it will continue to be so. For example, if snowfall rates were to revert to their 1991 level, thickening in East Antarctica might cease immediately; on the other hand, if the observed thinning in West Antarctica is accelerating, as one study has suggested (*12*), then that could dominate. Evaluating and understanding each mode of change is the first step toward producing defensible predictions for the whole of Antarctica.

The current thickening in East Antarctica is not sufficient to completely stop sea level rise. It might, in the short term, counteract one of the other contributions, such as the melting of the Greenland ice sheet. But the remaining contributors—melting of nonpolar glaciers, thermal expansion of the oceans, and groundwater changes—will be sufficient to produce sea level rise over the coming decades and centuries, regardless of any thickening that might occur in East Antarctica.

To respond appropriately to the threat of sea level rise, policy-makers urgently need accurate predictions of sea level rise as the sum of all its contributions. Davis *et al.* (*1*) provide the first observation-based estimate of one important contribution, that of the East Antarctic ice sheet. This is a huge step forward, but to reduce our uncertainty, much work is required to determine the underlying cause and likely future of each and every contribution, both positive and negative, in Antarctica and elsewhere.

References

1. C. H. Davis, Y. Li, J. R. McConnell, M. M. Frey, E. Hanna, *Science* **308**, 1898 (2005); published online 19 May 2005 (10.1126/science.1110662).
2. D. J. Wingham, A. J. Ridout, R. Scharroo, R. J. Arthern, C. K. Schum, *Science* **282**, 456 (1998).
3. A. Shepherd, D. J. Wingham, J. A. D. Mansley, H. F. J. Corr, *Science* **291**, 862 (2001).
4. J. A. Church *et al.*, in *Climate Change 2001: The Scientific Basis*, J. T. Houghton *et al.*, Eds. (Cambridge Univ. Press, Cambridge, 2001), pp. 583–638.
5. A. Shepherd, D. J. Wingham, J. A. D. Mansley, *Geophys. Res. Lett.* **29**, 1364 (2002).
6. E. J. Rignot, D. G. Vaughan, M. Schmeltz, T. Dupont, D. R. MacAyeal, *Ann. Glaciol.* **34**, 189 (2002).
7. A. J. Payne, A. Vieli, A. Shepherd, D. J. Wingham, E. Rignot, *Geophys. Res. Lett.* **31**, L23401 (2004).
8. J. O. Stone *et al.*, *Science* **299**, 99 (2003).
9. A. M. Smith, D. G. Vaughan, C. S. M. Doake, A. C. Johnson, *Ann. Glaciol.* **27**, 113 (1998).
10. H. De Angelis, P. Skvarca, *Science* **299**, 1560 (2003).
11. I. Joughin, S. Tulaczyk, *Science* **295**, 476 (2002).
12. R. Thomas *et al.*, *Science* **306**, 255 (2004).

10.1126/science.1114670

IMMUNOLOGY

Close to the Edge: Neutralizing the HIV-1 Envelope

Gary J. Nabel

Human immunodeficiency virus–1 (HIV-1) has infected more than 60 million people worldwide. Nonetheless, there have been few, if any, instances of infected individuals naturally developing protective immunity to the virus. Although cellular immunity (in which HIV-specific immune cells attack and destroy the virus) can help to control HIV infection, the development of a completely effective AIDS vaccine will likely require neutralizing antibodies that react with the diverse strains of this virus. The HIV-1 envelope (Env) glycoprotein contains at least four sites for such antibodies: The first is the binding site for CD4, the T cell protein through which HIV infects these immune cells; the second is a region on Env formed after it binds to CD4, which then interacts with a chemokine receptor in the next step of HIV infection; the third are carbohydrates on the outer face of Env; and the fourth is the region of Env adjacent to the viral membrane, the so-called membrane-proximal region (MPR) (see the first figure). The MPR is particularly attractive as an antibody target because it facilitates viral entry into T cells and is highly conserved among viral strains. Two recent papers provide insights into this antiviral target, at the same time raising several concerns. On page 1906 in this issue, Haynes *et al.* (*1*) report the unexpected result that two well-described antibodies directed against MPR, 2F5 and 4E10, react with self-antigens, including cardiolipin, a phospholipid to which antibodies are formed in lupus and other autoimmune diseases. These antibodies react with their SP41 epitopes 10 to 100 times better than with cardiolipin. A second study, by Trkola *et al.* in *Nature Medicine* (*2*), evaluated the antiviral responses of HIV-infected individuals treated with antibodies 2F5 and 4E10 plus the 2G12 antibody, which targets an unrelated carbohydrate structure. Their data showing lack of response to these antibodies suggest that the MPR region may not be very accessible to 2F5 or 4E10 neutralization in vivo. Together, these studies suggest challenges that must be overcome if the MPR region is used as a target of neutralizing antibodies for HIV vaccines.

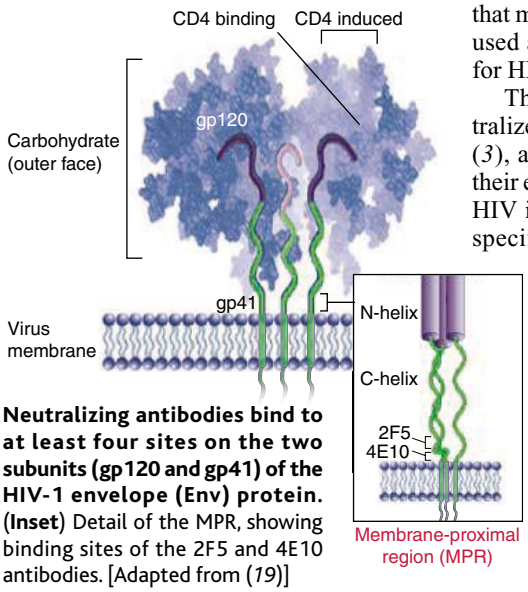

Neutralizing antibodies bind to at least four sites on the two subunits (gp120 and gp41) of the HIV-1 envelope (Env) protein. (**Inset**) Detail of the MPR, showing binding sites of the 2F5 and 4E10 antibodies. [Adapted from (*19*)]

The 2F5 and 4E10 antibodies can neutralize viruses from multiple HIV-1 clades (*3*), and this characteristic has prompted their evaluation for both AIDS vaccines and HIV immunotherapy. Antibodies with this specificity appear infrequently in nature, however; in fact, 2F5 and 4E10 were identified through screening of recombinant antibody libraries. They have also been difficult to detect in serum samples from HIV-1–infected individuals. The results from Haynes *et al.* may explain why. 2F5 and 4E10 interact with autoantigens at affinities similar to those of antibodies associated with autoimmune disease. These findings may account for the low frequency of these antibodies in natural infection, because they would normally be deleted during development of the immune system. Their reactivity with self-antigens also suggests that such antibodies would not be easily elicited by vaccination.

Antibodies to self-antigens have been identified in a variety of diseases, but they do not always cause the underlying autoimmune disease. For example, autoreactive antibodies are causally implicated in myasthenia gravis, pernicious anemia, and Goodpasture's syndrome, where passive

The author is with the Vaccine Research Center (VRC), National Institute of Allergy and Infectious Diseases, National Institutes of Health, Bethesda, MD 20892, USA. E-mail: gnabel@nih.gov

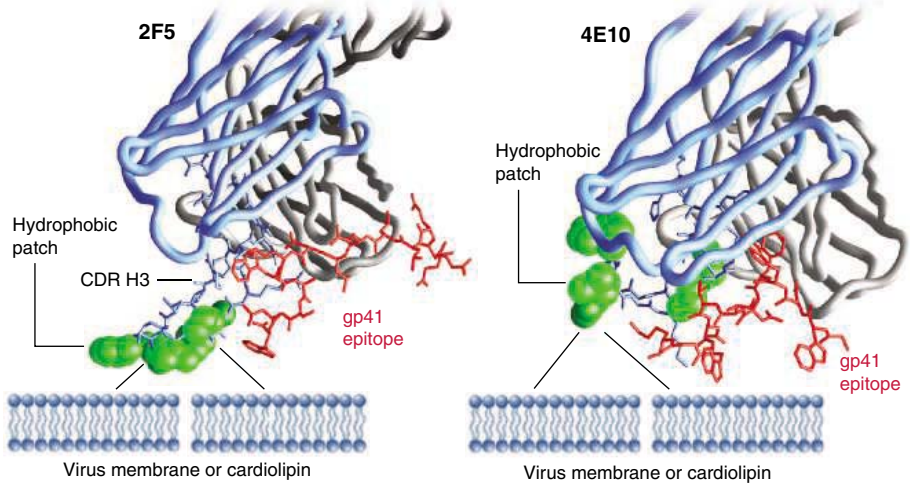

Model of antibody interaction with HIV Env. The proposed interaction of the hydrophobic patch on the CDR loop (green) of antibody 2F5 (**left**) or HE10 (**right**) with the viral membrane or cardiolipin is independent of the peptide binding domain of the gp41 subunit of Env (red). The structures of 2F5 and 4E10 bound to their cognate peptides are from (*4*) and (*6*).

transfer of specific antibodies can reproduce symptoms of the disease. In other autoimmune conditions, such as systemic lupus erythematosus, scleroderma, and rheumatoid arthritis, autoantibodies are a manifestation of an underlying immune response to unrelated antigens of unknown etiology. So it is conceivable that 4E10 and 2F5 may predispose to autoimmunity, although the animal data in favor of this possibility are not compelling. Further, Trkola *et al*. report no adverse events in their studies of humans treated with high, sustained concentrations of both antibodies for several weeks (*2*).

And what of the interaction of these antibodies with the highly lipophilic molecule cardiolipin? A structural study by Ofek and co-workers suggests a possible mechanistic explanation for this finding for 2F5 (*4*). They examined the structure of 2F5 bound to its peptide target and discovered a long complementarity-determining region (CDR) loop on the antibody. A hydrophobic patch of amino acids (Phe, Val, Ile, Leu) at the end of this loop interacts with both the target peptide and adjacent viral membrane (see the second figure, left panel). Mutation of the Phe residue decreases the neutralizing activity of 2F5, and membrane interaction enhances the antibody's reactivity with MPR (*5*). Whether this CDR loop also interacts with cardiolipin, itself a membrane-associated phospholipid, can be addressed by examining whether 2F5 with a mutation in the hydrophobic patch will bind to cardiolipin. Likewise, the crystal structure of 4E10 and its target peptide shows that this peptide adopts a helical conformation in the context of a hydrophobic surface of this immunoglobulin (*6*) (see the second figure, right panel). The 4E10 binding pocket itself is extremely hydrophobic, a property that might promote binding to other hydrophobic antigens.

One would expect strong negative selection against long or hydrophobic, autoreactive CDR regions that interact with lipid surfaces, possibly accounting for the rare occurrence of MPR-specific antibodies during immune cell selection (*7*–*15*). The few individuals with such autoimmune conditions may show relative protection from HIV infection, as suggested anecdotally for patients with systemic lupus (*16*–*18*). Another important consideration is whether specific immunization strategies will be needed to generate such potentially autoreactive antibodies.

If such antibodies can be generated, will they be able to access and neutralize the MPR? Maybe not. In the study by Trkola *et al.* (*2*), patients received passive infusion of monoclonal antibodies 2F5, 4E10, and 2G12, but there was no lasting effect on the virus. In the one instance where the virus was initially controlled but then escaped, mutations arose not to 2F5 or 4E10 epitopes but to the 2G12 epitope, which has more limited reactivity and is outside the MPR. The half-life of 2F5 in vivo was shorter than that of 2G12, but whether this resulted from 2F5 reactivity to self-antigens is not known. Alternatively, these antibodies may not have exerted an antiviral effect because the MPR is not accessible on the virus or is masked during cell-to-cell transfer of virus.

These studies have several implications. First, we knew that neutralizing antibodies to the MPR were detected rarely; now Haynes *et al*. suggest that these antigens may be a challenging target for immunization, both because of their association with the lipid membrane and because they resemble self-antigens and so will tend to be subject to tolerance. Specific vaccination protocols may be needed to elicit such antibodies.

Second, in future studies with therapeutic antibodies, patients will need to be monitored for the development of autoimmune diseases. Although no such diseases have been described in previous nonhuman primate studies or in the study by Trkola *et al*., screening for autoimmunity should be performed in future trials designed to elicit or transfer such autoreactive antibodies. Such theoretical concerns should not, however, preclude empirical research that directly addresses whether these antibodies succumb to tolerance mechanisms.

Finally, the role that 2F5, 4E10, and other MPR antibodies may play in preventive vaccines has not yet been assessed. These antibodies could possibly be effective in circumstances where there is a cell-free virus transmission. The task will not be easy: Passive-transfer studies in nonhuman primates suggest that neutralizing antibodies can protect against infection but that relatively high levels of immunoglobulin are required. Such levels will be difficult to attain with current immunization approaches.

The development of highly effective vaccines and immune therapies for HIV-1 infection remains a pressing need for this devastating infectious disease. Although the highly variable HIV Env protein has devised a myriad of mechanisms to evade the neutralizing antibody response, few such highly conserved structures are as accessible to neutralizing antibodies. It would be premature to abandon this promising therapeutic target for HIV neutralization on the basis of the evidence presented by the new work. Forearmed with the knowledge of both the possibilities and the challenges, investigators can better address these critical questions.

References and Notes

1. B. F. Haynes *et al.*, *Science* **308**, 1906 (2005); published online 28 April 2005 (10.1126/science.1111781).
2. A. Trkola *et al.*, *Nat. Med.* 10.1038/nm1244 (8 May 2005).
3. J. M. Binley *et al.*, *J. Virol.* **78**, 13232 (2004).
4. G. Ofek *et al.*, *J. Virol.* **78**, 10724 (2004).
5. M. B. Zwick *et al.*, *J. Virol.*, **79**, 1252, (2004).
6. R. M. Cardoso *et al.*, *Immunity* **22**, 163 (2005).
7. Y. Louzoun *et al.*, *Bull. Math. Biol.* **65**, 535 (2003).
8. D. Nemazee, *Immunol. Today* **17**, 25 (1996).
9. H. Wardemann *et al.*, *Science* **301**, 1374 (2003).
10. D. Gay *et al.*, *J. Exp. Med.* **177**, 999 (1993).
11. S. L. Tiegs, D. M. Russell, D. Nemazee, *J. Exp. Med.* **177**, 1009 (1993).
12. D. A. Nemazee, K. Burki, *Nature* **337**, 562 (1989).
13. E. Meffre *et al.*, *J. Clin. Invest.* **108**, 879 (2001).
14. F. M. Raaphorst, C. S. Raman, J. Tami, M. Fischbach, I. Sanz, *Int. Immunol.* **9**, 1503 (1997).
15. E. Meffre *et al.*, *Nat. Immunol.* **1**, 207 (2000).
16. R. A. Fox, D. A. Isenberg, *Arthritis Rheum.* **40**, 1168 (1997).
17. R. Palacios, J. Santos, *Int. J. STD AIDS* **15**, 277 (2004).
18. R. T. Canoso, L. I. Zon, J. E. Groopman, *Br. J. Haematol.* **65**, 495 (1987).
19. M. B. Zwick *et al.*, *Nat. Med.* **10**, 133 (2004).
20. I thank P. Kwong and R. Wyatt for discussions and for use of graphic representations of Env and 2F5 structures; J. Mascola, R. Koup, and other VRC scientists for comments; and A. Tislerics, T. Miller, and B. Hartman for preparation of the manuscript.

10.1126/science.1114854

edited by Edward W. Lempinen

SCIENCE AND SOCIETY

In *Vision 2033*, Scientists Mull How to Tame Future Threats

Seen through the lens of popular culture, the future often seems like a time disconnected from the present. The view tends toward strange and dystopic—think *1984* and *2001: A Space Odyssey, Blade Runner,* and *The Matrix.*

But when AAAS convened nearly three dozen top thinkers in science and technology policy to contemplate the year 2033, the perspective was strikingly different. The future, as they saw it, is familiar; many of the perils likely to confront humanity then are already evident today. While there are ominous portents in climate change, mutating viruses and emerging technologies for body and brain enhancement, they agreed that scientists, engineers and policy-makers can limit or prevent future problems—if they begin acting now.

The experts' views of the horizon three decades out come together in *Vision 2033: Linking Science and Policy for Tomorrow's World*, a new book from AAAS. The panel was assembled in May 2004 for a slightly delayed celebration of the 30th anniversary of the AAAS Science and Technology Fellowships, which have brought hundreds of scientists and engineers to Washington, D.C., to learn firsthand about the federal government and apply their expertise to policy. (The event was originally scheduled for September 2003, but was postponed as Hurricane Isabel bore down on the mid-Atlantic coast.)

"As the book demonstrates, our civilization faces a host of complex and difficult problems," said Albert H. Teich, director of Science and Policy Programs at AAAS. "Science and technology can help us solve them and can also create opportunities that beggar today's imagination, but this won't happen automatically. It is up to our leaders as well as our scientists and engineers to shape our policies and our technologies so that technological progress is also human progress."

One of the overarching themes of *Vision 2033* is that technology will become more subtle and more powerful, reaching deeper into daily life.

David Rejeski, director of the Project on Foresight and Governance at the Woodrow Wilson International Center for Scholars, sees "a convergence of bits, atoms, neurons, and genes, or informatics, nanotechnology, neuroscience, and genomics." Already, he said, we're in the midst of the "Next Industrial Revolution."

Three decades from now, panelists said, computer systems may be "self-healing." Scientists will race to use genomics and other cutting-edge technology against fast-mutating microbes. Policy-makers may explore how human technology can be used to support "nature's technology" in slowing or reversing environmental degradation.

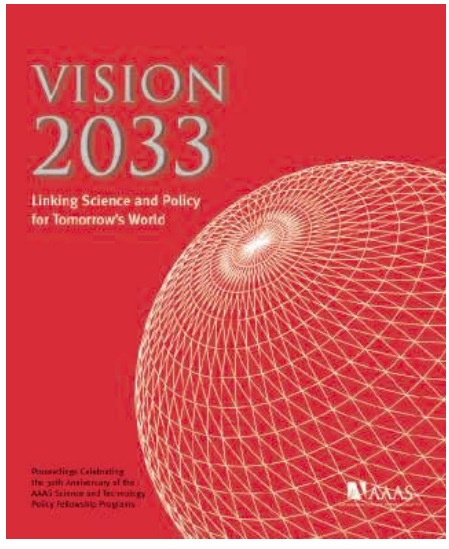

Vision 2033: Linking Science and Policy for Tomorrow's World posits that technology will become more subtle and more powerful, creating new opportunities—and raising new risks—in daily life.

For all of the benefits that might come from the new technology, it also will bring troubling new social and ethical implications, panelists said.

New technology will improve our ability to detect hidden programs to develop weapons of mass destruction, said Victor A. Utgoff, a writer and security expert who formerly served as a staffer on the National Security Council. But that could require "extensive and intensive" surveillance of many nations and millions of people, focusing on everything from financial activity to construction and travel. "This kind of surveillance is pretty scary, to say the least," Utgoff said.

Ismail Serageldin, director of the new Library at Alexandria, Egypt, as well as an author, scholar, and former vice president at the World Bank, held out the development of a "supermouse" as a simple example of the future's promise and dilemmas. Citing a story in *Wired* magazine, Serageldin said that scientists have already used genetic manipulation to make mice smarter, stronger, faster to heal, more efficient in the use and storage of energy, and more long-lived.

Several experts questioned what sorts of discrimination or inequality might develop when such new genetic technologies are

AAAS

Report of the 2005 Council Meeting

The 2005 Meeting of the AAAS Council was held on Sunday, 20 February in the Delaware Ballroom of the Marriott Wardman Park Hotel in Washington, D.C. In addition to President Shirley Ann Jackson's report on the 2004 Board activities and CEO Alan I. Leshner's State of the Association report, the Council received a update on *Science* from Executive Editor Monica M. Bradford; a status report on the R&D funding situation, and briefings on two new centers: the Center for Science, Technology and Security Policy headed by Norman Neureiter and the Center for Advancing Science and Engineering Capacity headed by Daryl Chubin.

Under recommended actions brought forward by the Committee for Council Affairs, the Council approved the reaffiliation of the Entomological Society of America and the Eastern Psychological Association.

available to humans. Who will have access to the new treatments, and who won't? "It's going to be more difficult for people who don't have access to keep up," said Patrick Hines, a recent graduate of the M.D./Ph.D. program at the University of North Carolina.

Meanwhile, some speakers suggested that all of these emerging debates could take place in the context—and tension—of the continuing culture wars. R. Alta Charo, a professor of law and bioethics and the University of Wisconsin and a former member of President Bill Clinton's bioethics committee, warned of a divide between "those who celebrate the transformative power of science and those who fear it."

Some urged scientists to join efforts at public education and dialogue, especially with those who might be hostile to science. Others stressed the need for science and technology to contribute to a new culture of sustainability.

Ronald F. Lehman II, director of Center for Global Security Research at the Lawrence Livermore National Laboratory, offered a more general prescription. "What we need," he said, "is long-term optimism—a vision that we can continue the long march of progress that has been made—but short-term pessimism to really get our adrenaline going and to focus on some of these problems."

To order a copy of *Vision 2033*, visit www.fellowships.aaas.org/30th.

EDUCATION

New from AAAS: Building Strength in Computer Science

Employment in computer- and Internet-related fields is notoriously volatile, but recent developments have raised concerns about the long-term future: The number of undergraduates seeking computer science degrees is down sharply since 2000. The number of women seeking such degrees has plunged. And few minority students are winning advanced degrees in the field.

Now a new study from AAAS has concluded that recruitment of "nontraditional" students into computer science studies and jobs will be critical in keeping the U.S. workforce strong. And yet, the report says, this growing pool of students often is overlooked and underserved by higher education, government, and industry.

Traditional students fit a familiar mold: They start college at 18 or 19, and they leave 4 or 5 years later with a bachelor's degree. Others, however, defy the stereotype: They're older. They may have children. While working full-time, they're seeking new skills or advancement. And many are women and minorities.

"Our workplaces are becoming more technologically dependent, not less so," said report co-author Shirley M. Malcom, AAAS director of Education and Human Resources. "If you accept that for economic and national security reasons we need people with skills in these areas, then how can you be sanguine with the idea that we're not getting the people we need?"

With funding from the National Science Foundation, the authors conducted surveys, visited colleges and universities, and interviewed students, instructors, and employers from 2000 to 2004. Their report is entitled, "Bringing Women and Minorities into the IT Workforce: The Role of Nontraditional Pathways."

Tanya Gunn, today a high-ranking computer technology executive, embodies the trend.

Gunn studied psychology at Howard University for 3 years, but then, driven by a desire for financial independence, she left school and went to work as a secretary at the American Chemical Society in Washington, D.C. She showed a flair for computers; though she won promotions, she knew that she needed more training and a degree to make the most of her potential.

By that time she was married and had two daughters. And so, in the early 1980s, she began taking night classes at the University of Maryland, University College.

She was older, she was black, she was a woman—and in those early years, she wasn't always welcome in the world of computer geeks. "There weren't that many women majoring in computer sciences," Gunn said in an interview. "I kind of struggled because a lot of the guys in the class, including the instructors, really were standoffish. It was like I had the plague, and they didn't know what I was doing there. 'She's a girl—let's don't talk to her. This is a boys' club.' "

But semester by semester, she won respect; in time, fellow students and faculty members came to see her as a leader.

After 17 years of part-time study, Gunn graduated in 2001. Today, after a series of promotions, she is manager of Change and Problem Management at the American Chemical Society, overseeing centralized communication and tracking of IT upgrades to promote better understanding of the changes across the organization.

The new report found such themes common among nontraditional students. Even now, the authors report, traditional 4-year schools often are not structured to meet their needs. Instructors are not always sensitive. And the financial aid system gives advantages to traditional students.

AAAS ANNUAL ELECTION

The slate of candidates for the 2005 election of AAAS officers will be announced in News and Notes in the 29 July issue of *Science*.

One result: For-profit schools such as Strayer University and DeVry Institute of Technology were the top U.S. producers of computer science bachelor's degrees in 2001.

Though the report was begun during the dot-com boom, its findings remain important for the future, the authors say.

Eleanor Babco, executive director of the Commission on Professionals in Science and Technology (CPST), said a recent study by the Higher Education Research Institute at the University of California–Los Angeles showed the percentage of incoming undergraduates who planned to major in computer science declined over 60% between 2000 and 2004.

After 17 years of part-time study, Tanya Gunn graduated in 2001. Today, she is manager of Change and Problem Management at the American Chemical Society,

"Alarmingly," she added, "the proportion of women who thought that they might major in computer science has fallen to levels unseen since the early 1970s…. It is difficult to see how computer sciences can match expected future demand for IT workers without raising women's participation at the undergraduate level."

The report recommends more effort to accommodate nontraditional students at traditional schools; more faculty diversity; more public and private investment in schools that serve nontraditional students; and expanded financial aid to encourage Internet technology students to study part-time in areas of "national need."

"Bringing Women and Minorities into the IT Workforce" was written by Malcom;

Babco; Albert H. Teich, AAAS director of Science and Policy Programs; Jolene Kay Jesse, formerly a senior research associate at AAAS who is now with the U.S. National Science Foundation; Lara Campbell, a senior program associate at AAAS; and Nathan E. Bell, a CPST research associate.

The report is available at www.aaas.org/publications/books_reports/ITW/.

125TH ANNIVERSARY

Celebrating the Past, Exploring the Future

On 3 July 1880, journalist John Michels and inventor Thomas Edison published the first issue of the journal *Science,* with 12 pages of articles on the possibility of electric-powered railroads, the latest observations of the Pleiades, and advice to science teachers on the importance of studying animal brains. One hundred and twenty-five years later, AAAS and *Science* will mark the occasion with a series of events that draw inspiration from the past while looking squarely toward the future.

Already this year, the journal has marked the anniversary with its Global Voices of Science series, featuring an essay each month from one of the leading researchers in the developing world.

During the first 2 weeks of July, the anniversary will be celebrated in Washington, D.C., in London, and in the pages of *Science.* The celebration will feature ambitious exploration of the scientific and technological questions that will preoccupy researchers in the decades ahead—along with a couple of good parties.

The 1 July issue of *Science* will focus on 125 of those as-yet-unsolved mysteries, with a closer look at the 25 biggest questions, all selected with the help of the journal's Board of Reviewing Editors and the Senior Editorial Board. The issue will contain an introduction from *Science* Editor-in-Chief Donald Kennedy and a look at how the unanswered questions confronting scientists and engineers have changed since the journal's debut during the presidency of Rutherford B. Hayes.

"I don't want to give the game away, but they're very interesting questions," said Kennedy. "They range from the cosmos and aspects of its origin and its expansion to mysteries like how the transcription of genes is controlled during their differentiation and development."

On Thursday 7 July, guests at a 3-hour forum organized by AAAS and *Science* will hear presentations on "What We Don't Know in Science."

The special forum will be broken into four 40-minute panels: "The Nature of the Cosmos," moderated by Kennedy; "Memories, Consciousness and Human Life," moderated by Alan I. Leshner, AAAS CEO and executive publisher of *Science*; "Genes, Proteins, and Disease," moderated by Floyd Bloom, who served as editor-in-chief of *Science* from 1995 to 2000; and "Sustainable Development," moderated by Daniel E. Koshland Jr., who served as editor-in-chief from 1985 to 1995.

"Ultimately, great questions like these both define the state of scientific knowledge and drive the engines of scientific discovery," writes author and journalist Tom Siegfried in an introduction to the special issue. "Where ignorance and knowledge converge, where the known confronts the unknown, is where scientific progress is most dramatically made."

The journal *Science* has been keeping readers on the cutting edge since 1880.

"To many of these questions," Kennedy said, "there may be no such thing as a completely final answer. But, certainly, I think most of them will have been subject to considerable resolution in 125 years."

On 14 July, AAAS and *Science* will celebrate the anniversary in London with a cocktail reception in the Earth Galleries at the Natural History Museum. Kennedy and other writers and editors from the journal will be there.

"The journal *Science* continues to provide a highly effective way for scientists of all disciplines to communicate findings that are significant not just for peers in their own fields and countries, but also for leaders in other areas worldwide," said Sir Robert May, president of the Royal Society in the United Kingdom. and formerly Britain's chief scientist. "It is widely recognized as practicing the highest standards of peer review and has a major impact across the full spectrum of scientific disciplines."

For further information on the London event, or to RSVP, e-mail 125th@science-int.co.uk.

COMMUNICATION

Screeners Needed for AAAS Science Journalism Awards

Scientist volunteers are needed to review entries in this year's AAAS Science Journalism Awards program.

Scientists residing in the Washington, D.C., area or who will be in Washington in mid-August to mid-September are invited to help screen print, radio, and television reports for scientific accuracy. The top entries will be passed on to the appropriate judging committees. If you would like to volunteer as a screener, contact Earl Lane (202-326-6431; elane@aaas.org) or Lonnie Shekhtman (202-326-6434; lshekhtm@aaas.org) at the AAAS Office of Public Programs.

More than 300 writers have been honored for their achievements in science reporting since the inception of the awards program in 1945. There will be a new prize category this year, open to journalists worldwide, for excellence in reporting science news for children.

Winners of the awards, which are sponsored by Johnson & Johnson Pharmaceutical Research & Development, L.L.C., will be honored at the AAAS annual meeting in February 2006 in St. Louis. Members of the screening committees will be recognized in literature distributed during the awards ceremony.

Looking for a career that radiates success?

Then talk to someone who knows science.

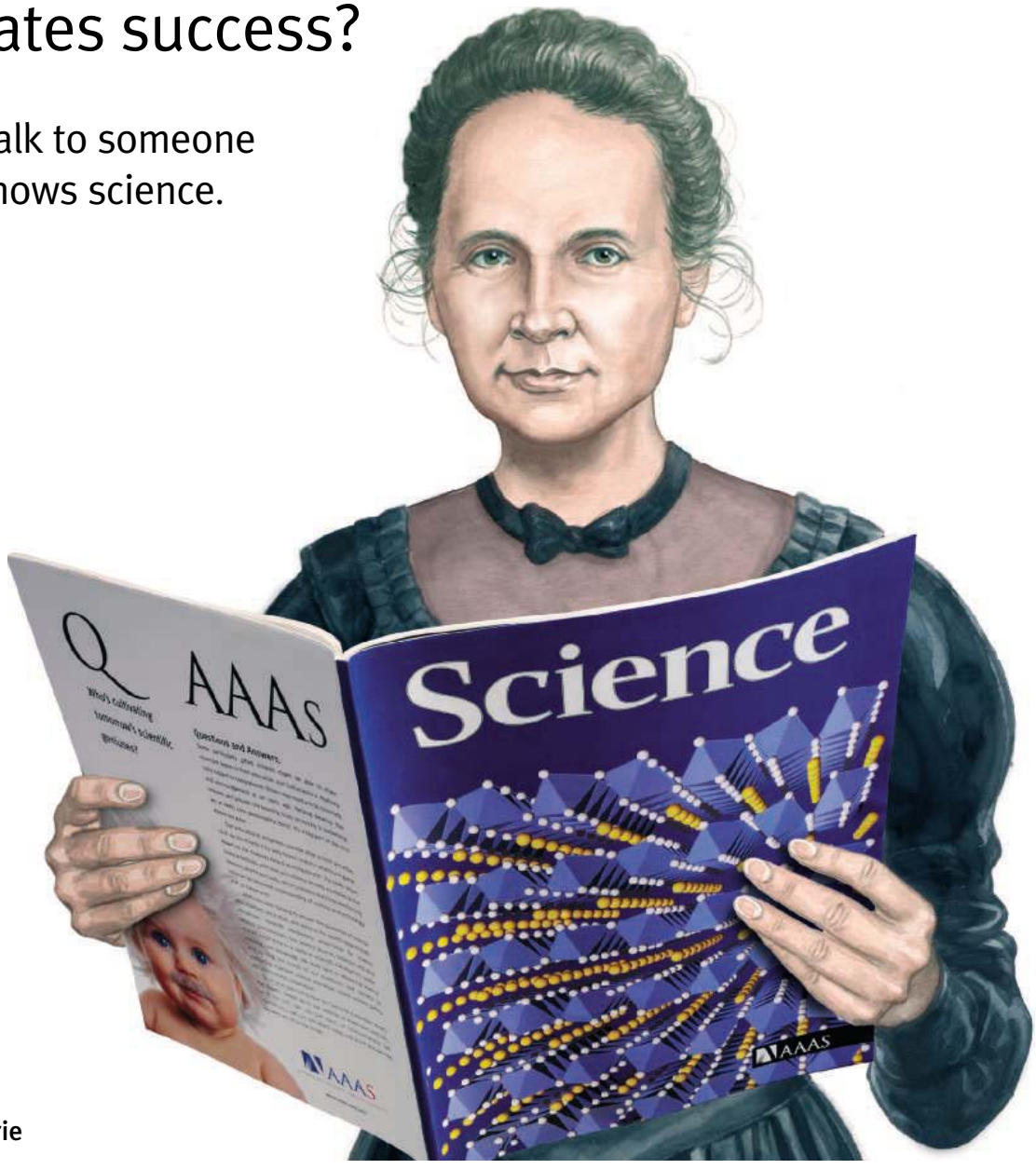

Marie Curie
1867–1934

If you want to shine in the world of science, it's essential you don't leave your career to chance. At ScienceCareers.org we know science. We are committed to helping you find the right job, and to delivering the advice you need. Our knowledge is firmly founded on the expertise of *Science*, the premier scientific journal, and the long experience of AAAS in advancing science around the world. So if you want a glowing career, trust the specialist in science. Visit ScienceCareers.org.

ScienceCareers.org
We know science AAAS

Larger Islands House More Bacterial Taxa

Thomas Bell,[1,3] Duane Ager,[2] Ji-Inn Song,[2,4] Jonathan A. Newman,[3*] Ian P. Thompson,[2] Andrew K. Lilley,[1] Christopher J. van der Gast[2†]

The relationship between species richness and area size is one of the few generalizations in ecology, but recent studies show that the slope of the relationship differs for microbes (*1*, *2*). Here we show that the slope of the taxa-area relationship for natural bacterial communities inhabiting small aquatic islands is comparable to that found for larger organisms. The result implies that analogous processes structure both microbial communities and communities of larger organisms.

Several mechanisms explain how the number of taxa can increase with the size of the area. The number of taxa in a particular area results from the balance between the colonization of new taxa and the extinction of extant taxa. The size of the area influences the rate of colonization and extinction and so indirectly influences biodiversity. Alternatively, if taxa are adapted to a particular habitat, then larger areas likely contain more habitats and therefore more species. Finally, a taxa-area relationship will appear if more effort is devoted to sampling larger areas, because the number of taxa discovered increases with sampling effort (*3*). The relationship between diversity and island or sampling area size is well described by the equation $S = cA^z$, where S is the number of species, c is an empirically derived taxon- and location-specific constant, A is the size of the area, and z is the slope of the line. The value for z is generally consistent across taxa but differs between islands ($z \sim 0.3$) and areas of contiguous habitat ($z \sim 0.1$) (*3*).

Recent work has suggested that, although there appears to be a similar relationship between microbial diversity and area, the slope z for microbial taxa ($z \sim 0.02$ to 0.07) falls well below that observed for taxonomic groups of larger organisms (*1*, *2*, *4*). Many microbial taxa appear to be ubiquitous (*5*), so increasing the area of a survey results in only a marginal increase in the species richness of the sample. However, these studies have investigated the taxa-area relationship only within single contiguous habitats, where it is plausible that constant colonization from adjacent areas rapidly homogenizes the community. The slope of the species-area relationship is expected to be steeper on discrete islands, partly because they present a partial barrier to colonization. We predicted that the slope of species-area relationship for insular bacterial communities would be similar to that found for communities of larger organisms.

The "islands" that we used are water-filled treeholes, a common feature of temperate and tropical forests. Rainwater accumulates in bark-lined pans formed by the buttressing at the base of large European beech trees (*Fagus sylvatica*) to form small but often permanent bodies of water. Each of these islands houses a microecosystem that derives its nutrients and energy from leaf litter. We measured the water volume (island size) and the bacterial genetic diversity (taxon richness) in 29 treehole islands, using denaturing gradient gel electrophoresis (DGGE) (*6*), a standard molecular technique in microbial ecology.

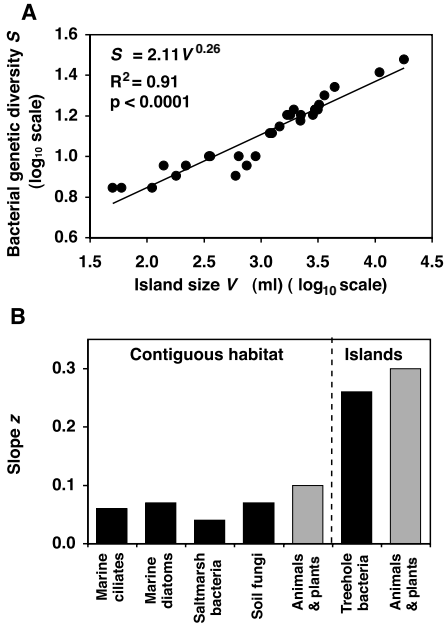

Fig. 1. The species-area relationship for microbial communities. (**A**) Bacterial genetic diversity (the number of DGGE bands, S) in water-filled treeholes increases with increasing island size (volume, V) according to the power law $S = 2.11V^{0.26}$. There is a similar linear relationship (not shown) between island surface area (A, in cm^2) and bacterial genetic diversity ($S = 3.30A^{0.28}$, $R^2 = 0.38$, $P < 0.001$). Treehole volume and surface area are correlated ($r = 0.71$). (**B**) Slope of the species-area relationship for marine benthic ciliates and diatoms, salt marsh bacteria, and fungi inhabiting arid soil compared with slope from the current study. Black bars are microbial studies (*1*, *2*, *7*); gray bars are typical values for studies with larger organisms (*3*).

Bacterial genetic diversity in this system increased with increasing island size according to the familiar species-area power law (Fig. 1A). The slope z of the relationship ($z = 0.26$) is indistinguishable from published values for larger organisms (Fig. 1B). The data show that area size strongly influences the diversity of these microbial communities.

These results have implications for understanding how microbial communities operate and complement recent studies (*1*, *2*) by indicating the conditions under which high microbial z values can occur. In relatively large areas of contiguous habitat, the slope of the species-area relationship appears to be reduced (Fig. 1B). Such communities might never approach equilibrium, because environmental conditions change faster than competitively inferior species become extinct. We suggest that treeholes and similar habitat patches are islands of relative stability where microbial communities can approach equilibrium. Under such conditions, the patterns of abundance and diversity of microbial communities would be similar to those found for larger organisms. It is possible that other mechanisms underlie the difference between our result and those of other microbial studies. Perhaps, for example, the treehole habitat is more heterogeneous, so diversity increases more rapidly with area size. What is evident is that, as for larger organisms, comparatively steep microbial taxa-area relationships are possible.

References and Notes

1. J. L. Green *et al.*, *Nature* **432**, 747 (2004).
2. M. C. Horner-Devine, M. Lage, J. B. Hughes, B. J. M. Bohannan, *Nature* **432**, 750 (2004).
3. M. L. Rosenzweig, *Species Diversity in Space and Time* (Cambridge Univ. Press, Cambridge, 1995).
4. B. J. Finlay, *Science* **296**, 1061 (2002).
5. B. J. Finlay, K. J. Clarke, *Nature* **400**, 828 (1999).
6. Materials and methods are available as supporting material on *Science* Online.
7. A. Azovsky, *Ecography* **25**, 273 (2002).
8. Supported by the NERC Centre for Ecology and Hydrology. T.B. is supported by the Natural Sciences and Engineering Research Council of Canada, the Formation Chercheurs et Aide Recherche and the Clarendon Fund.

Supporting Online Material
www.sciencemag.org/cgi/content/full/308/5730/1884/DC1
Materials and Methods
References and Notes

22 February 2005; accepted 7 April 2005
10.1126/science.1111318

[1]Molecular Microbial Ecology Section, [2]Environmental Biotechnology Section, Natural Environment Research Council (NERC) Centre for Ecology and Hydrology, Mansfield Road, Oxford, OX1 3SR, UK. [3]Department of Zoology, University of Oxford, South Parks Road, Oxford, OX1 3PS, UK. [4]Department of Engineering Science, University of Oxford, Parks Road, Oxford, OX1 3PJ, UK.

*Present address: Department of Environmental Biology, University of Guelph, Guelph, Ontario N1G 2W1, Canada.
†To whom correspondence should be addressed. E-mail: cjvdg@ceh.ac.uk

The Rotational Spectrum and Structure of the HOOO Radical

Kohsuke Suma, Yoshihiro Sumiyoshi, Yasuki Endo*

The adduct of the hydroxyl radical with oxygen has been studied theoretically, in connection with atmospheric reactions, but its stability and structure remained an open question. Pure rotational spectra of the HOOO and DOOO radicals have now been observed in a supersonic jet by using a Fourier-transform microwave spectrometer with a pulsed discharge nozzle. The molecular constants extracted from 12 rotational transitions with fine and hyperfine splittings support a trans planar molecular structure, in contrast to the cis planar structure predicted by most ab initio calculations. The bond linking the HO and O_2 moieties is fairly long (1.688 angstroms) and comparable to the F–O bond in the isoelectronic FOO radical.

In contrast to catenated carbon, our knowledge of molecules containing extended oxygen chains is quite limited; even simple species such as H_2O_3 and H_2O_4 have not yet been well characterized. The HO_3 radical, which contains a chain consisting of three O atoms, can furthermore be regarded as an adduct of OH and O_2, both of which are important open-shell species in the atmosphere. The existence of HO_3 has been considered for the reaction systems

$$H + O_3 \rightarrow OH + O_2 \quad (1)$$

and

$$O + HO_2 \rightarrow OH + O_2 \quad (2)$$

where the HO–O_2 adduct is proposed as a reaction intermediate (*1*). Furthermore, if the reaction

$$OH + O_2 \rightarrow HO_3 \quad (3)$$

is exothermic and has a very small barrier, then a certain amount of HO_3 would exist in Earth's atmosphere, and Eq. 3 would play a crucial role in reactions involving the OH radical (*2*–*4*).

Many theoretical studies along these lines have been reported. Except for a few recent theoretical studies (*1*, *5*), early reports suggest HO_3 to be metastable relative to the OH + O_2 dissociation limit (*6*–*8*). Structure and binding energies vary depending on the computational methods used. Although most studies suggest planar molecular structures, none decisively determines whether the cis planar or trans planar structure is most stable.

In contrast to the extensive theory, experimental information on this radical is quite limited. Nelander and co-workers reported its detection by infrared absorption in a low-temperature Ar matrix (*9*). Detection of gas-phase HO_3 was reported by Cacace *et al*. using neutralization-reionization/collisionally activated dissociation mass spectrometry (*2*). They observed a species of mass 49, persistent for at least a microsecond, but were unable to provide any structural information. In the present study, we were able to detect HO_3 by Fourier-transform microwave (FTMW) spectroscopy and Fourier-transform microwave/mm-wave double resonance (FTMW/mmW DR) spectroscopy, providing sufficient data to precisely determine its ground-state geometry.

The HO_3 radical was produced by electric discharge in a mixture of H_2O and O_2 diluted in Ar in a pulsed discharge nozzle. Discharged products were then expanded in a supersonic jet into a FTMW spectrometer cavity (*10*). Because the molecular structure of the radical was not well predicted, a wide frequency region, ~17.5 to 23 GHz, corresponding to the 1_{01}–0_{00} rotational transition, was searched. We observed only one group of paramagnetic lines, absent without an electric discharge and centered at 18.7 GHz. We optimized the experimental conditions by monitoring these lines: An O_2-rich sample gas (20% O_2, 0.15% H_2O) diluted in Ar with a moderate discharge voltage (1.5 kV) and a high stagnation pressure (6 atm) gave strong signals (Fig. 1). A similar spectral pattern was observed at 17.7 GHz when a gas mixture containing D_2O was used instead of H_2O under otherwise identical experimental conditions. Signal intensities did not change appreciably if Ar was replaced by Ne. However, no signal was observed with either H_2O or O_2 alone in the noble gas.

Because the spectral coverage of our FTMW spectrometer is limited to frequencies below 40 GHz, only two *a*-type *R*-branch rotational transitions could be observed (K_a = 0 and ΔN = 1, where N is the rotational angular momentum and K_a is its projection on the molecular axis). To extend the measurements to other possible rotational transitions and thereby confirm HO_3 as the spectral carrier, we used a double resonance technique. In this technique, higher frequency mm-wave radiation was also sent into the Fabry-Perot cavity of the FTMW spectrometer (*11*), and induced transitions beyond 40 GHz were observed as a dip in intensity of a lower frequency resonance (Fig. 1). A total of 12 rotational transitions in the frequency region 7 to 80 GHz were observed for both HO_3 and DO_3; the two *b*-type (K_a = 1 ← 0) transitions observed by FTMW spectroscopy were also used to monitor transitions for higher frequency measurements. The rotational energy levels of HO_3 and transitions observed by the two spectroscopic methods are summarized in Fig. 2. All the observed transitions, which consist of 62 fine and hyperfine components for HO_3 (table S1) and 75 for DO_3 (table S2), were subjected to a least-squares analysis, using the Watson's *A*-reduced Hamiltonian, including the fine and hyperfine interaction terms (SOM Text). These fits gave reasonable standard deviations of 6.1 kHz for HO_3 and 8.5 kHz for DO_3; the experimentally determined molecular constants for HO_3 and DO_3 are listed in table S3. The rotational constants extracted from the fits agree with

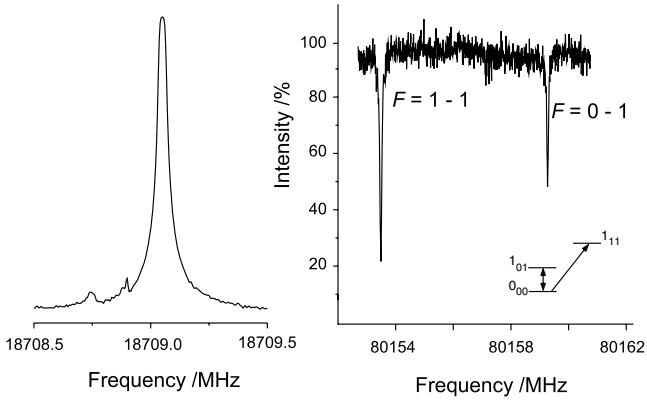

Fig. 1. (**Left**) The rotational transition ($N_{K_aK_c}$ = 1_{01} – 0_{00}, J = 1.5 – 0.5, F = 2 – 1) observed by FTMW spectroscopy. This spectrum was obtained by averaging 200 free induction decay signals, which took 40 s. (**Right**) The double resonance spectrum ($N_{K_aK_c}$ = 1_{11} – 0_{00}, J = 0.5 – 0.5, with hyperfine splitting due to the H atom, F = 1 – 1 and F = 0 – 1), observed as a change in the intensity of this FTMW spectrum (left).

Department of Basic Science, The University of Tokyo, Komaba 3-8-1, Meguro-ku, Tokyo 153-8902, Japan.

*To whom correspondence should be addressed. E-mail: endo@bunshi.c.u-tokyo.ac.jp

those predicted for planar trans-HO_3 by high-level ab initio calculations (Table 1) (*12–14*).

Taken together, the data strongly support our observation of HO_3 and DO_3. The rotational constants of both the H and D species agree with those of the ab initio calculations, and both H_2O and O_2 are required to see the transitions. Moreover, the fine and hyperfine structures are appropriate for a doublet electronic state with a nuclear spin, $I = 1/2$. The planarity of these compounds is confirmed by the small values of their inertial defects, i.e., $\Delta I = 1/C - 1/A - 1/B = 0.0123$ uÅ^2 for HO_3 and $\Delta I = -0.043$ uÅ^2 for DO_3, as expected for planar molecules.

The ab initio calculations give minima for both the cis and the trans geometries; the energy of the trans structure is only 93 cm^{-1} lower than that of the cis structure, and the calculated barrier to convert from the trans to the cis geometry is 322 cm^{-1}. The agreement between theory and experiment, for both isotopomers, is far better for the trans geometry (Table 1). Furthermore, the dipole moment μ_a is predicted to be very small ($\mu_a/\mu_b = 0.13$) for the cis geometry, which is not consistent with the experimental observation that *a*-type and *b*-type transitions are observed with comparable intensities. Despite careful searching, no lines attributable to cis-HO_3 were observed.

The molecular structure (Fig. 3) was determined from the rotational constants *A* and *B* of HO_3 and DO_3, with planar trans geometry assumed, and the bond lengths r_{HO_1} and $r_{O_2O_3}$ were fixed to their ab initio values (the three O atoms are numbered $HO_1O_2O_3$). Most notable is the $r_{O_1O_2}$ bond length of 1.688 Å, which is fairly long in comparison, for example, with the 1.464 Å O–O bond in hydrogen peroxide (*15*). Consistently, this bond is very weak according to the ab initio calculations; the dissociation energy to HO + O_2 is predicted to be only 3.90 kcal/mol. The arrangement of the three O atoms is quite similar in structure to that of the isoelectronic FOO radical, where r(F–O) = 1.65 Å, r(O–O) = 1.20 Å, and ∠FOO = 111° (*16*). The large negative value for one spin-rotation constant, $\varepsilon_{aa} = -1252.6$ MHz, together with the small value for the other, $\varepsilon_{cc} = -3.5$ MHz, indicates that the ground electronic state of HO_3 is $^2A''$, as precedented for the HO_2 (*17*) and FO_2 (*18*) radicals; the unpaired electron occupies a p_Π molecular orbital extending perpendicular to the molecular plane. The ab initio calculations show the unpaired electron to be localized on the terminal O_2; the singly occupied molecular orbital is almost unchanged from the π* orbital of free O_2. This electronic structure is supported by the quite small Fermi coupling constant of the hydrogen nucleus, $a_F = 3.55$ MHz, compared with those of other radical species.

The present experimental results are well accounted for by the fairly large scale multi-reference configuration interaction calculations that we performed. At the same time, previous theoretical calculations have predicted structures with large deviations, presumably because most of the calculations were based on single configuration methods and were therefore unable to properly account for the electron configuration effect. Although the present ab initio calculations provide reasonable explanations for the experimental results, large-amplitude torsional and O_1–O_2 stretching motions should be taken into account to fully understand the properties of the compound.

Because the O_1–O_2 bond dissociation energy is calculated to be 3.90 kcal/mol, and the recombination reaction (Eq. 3) has essentially no activation barrier, a certain amount of HO_3 should exist in Earth's atmosphere. The molecular constants determined in the present study are accurate enough to predict submillimeter wave transitions, which could be used to search for the compound and probe its potential role in atmospheric processes—for example, as a sink of atmospheric OH. The present successful detection of HO_3 has also opened possibilities for the detection of XO_3 (X = halogen, methyl, etc.), H_2O_3, or H_nO_4 (n = 1, 2) using similar experimental setups.

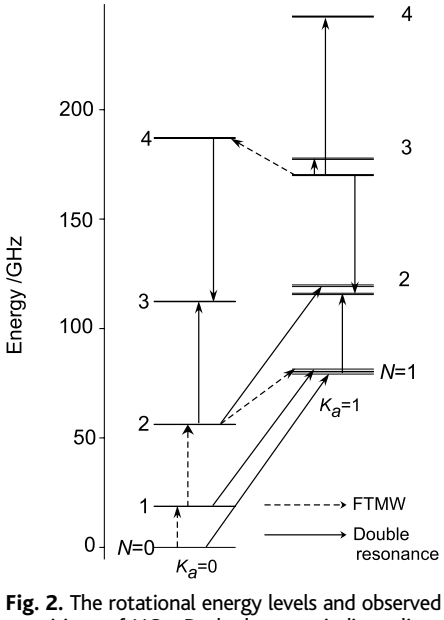

Fig. 2. The rotational energy levels and observed transitions of HO_3. Dashed arrows indicate lines observed by the FTMW spectrometer; solid arrows indicate transitions observed by the double resonance technique, whereby dips are observed in lines monitored by the FTMW spectrometer.

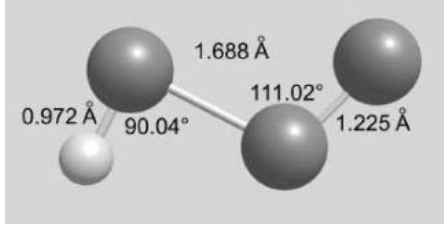

Fig. 3. The molecular structure of the HO_3 radical obtained from the experimental rotational constants. The structural parameters obtained by ab initio calculation are r_{HO_1} = 0.972 Å, $r_{O_1O_2}$ = 1.677 Å, $r_{O_2O_3}$ = 1.225 Å, ∠HO_1O_2 = 95.94°, and ∠$O_1O_2O_3$ = 110.18°.

Table 1. Comparison of the rotational constants of the ab initio cis and trans structures with those determined experimentally (in MHz).

	HOOO			DOOO		
	A	B	C	A	B	C
cis	66824	10986	9435	58304	10778	9096
trans	70676	10103	8839	67765	9502	8333
Exp.	70778	9987	8750	67857	9449	8299

References and Notes

1. D. M. Silveira, P. J. S. B. Caridade, A. J. C. Varandas, *J. Phys. Chem. A* **108**, 8721 (2004).
2. F. Cacace, G. de Petris, F. Pepi, A. Troiani, *Science* **285**, 81 (1999).
3. Y. Ohshima, K. Sato, Y. Sumiyoshi, Y. Endo, *J. Am. Chem. Soc.* **127**, 1108 (2005).
4. C. S. Brauer *et al.*, *Chem. Phys. Lett.* **401**, 420 (2005).
5. O. Setokuchi, M. Sato, S. Matuzawa, *J. Phys. Chem. A* **104**, 3204 (2000).
6. K. B. Mathisen, P. E. M. Siegbahn, *Chem. Phys.* **90**, 225 (1984).
7. M. A. Vincent, I. H. Hillier, *J. Phys. Chem.* **99**, 3109 (1995).
8. A. J. C. Varandas, H. G. Yu, *Mol. Phys.* **91**, 301 (1997).
9. B. Nelander, A. Engdahl, T. Svensson, *Chem. Phys. Lett.* **332**, 403 (2000).
10. M. Iida, Y. Ohshima, Y. Endo, *J. Chem. Phys.* **94**, 6989 (1991).
11. K. Suma, Y. Sumiyoshi, Y. Endo, *J. Chem. Phys.* **121**, 8351 (2004).
12. Calculations used the Molpro 2002.6 suite of programs (*13*) with the multireference single and double excitation configuration interaction method with the Davidson correction (MRCI+Q) using Dunning's correlation-consistent polarized triple split valence basis set with diffuse functions (aug-cc-pVTZ) (*14*). For the MRCI calculations, the preceding complete active space self-consistent field (CASSCF) calculations were performed with 19 electrons seeded in all the 13 valence orbitals. The active space of MRCI is generated by distributing 13 electrons into 10 valence orbitals, excluding three inner valence orbitals corresponding to the 2s orbitals of the three O atoms, while all the single and double excitations from all the 13 valence orbitals are considered.
13. Molpro is a package of ab initio programs designed by H.-J. Werner and P. J. Knowles. The authors are R. D. Amos *et al.*
14. R. A. Kendall, T. H. Dunning Jr., R. J. Harrison, *J. Chem. Phys.* **96**, 6796 (1992).
15. J. Koput, *J. Mol. Spectrosc.* **115**, 438 (1986).
16. C. Yamada, E. Hirota, *J. Chem. Phys.* **80**, 4694 (1984).
17. S. Saito, *J. Mol. Spectrosc.* **65**, 229 (1977).
18. M. Bogey, P. B. Davies, C. Demuynck, J. L. Detombes, T. J. Sears, *Mol. Phys.* **67**, 1033 (1989).

19. We thank J. T. Hougen for critical reading of the manuscript. This work is supported by a Grant-in-Aid for priority research entitled "Radical Chain Reactions" (Grant No. 13127101). K.S. appreciates the support of the Research Fellowships of the Japan Society for the Promotion of Science for Young Scientists (JSPS No. 16-10895).

Supporting Online Material

www.sciencemag.org/cgi/content/full/1112233/DC1
SOM Text
Tables S1 to S3

14 March 2005; accepted 26 April 2005
Published online 5 May 2005;
10.1126/science.1112233
Include this information when citing this paper.

Enols Are Common Intermediates in Hydrocarbon Oxidation

Craig A. Taatjes,[1,2]* Nils Hansen,[1] Andrew McIlroy,[1] James A. Miller,[1] Juan P. Senosiain,[1] Stephen J. Klippenstein,[1] Fei Qi,[1,3] Liusi Sheng,[3] Yunwu Zhang,[3] Terrill A. Cool,[4] Juan Wang,[4] Phillip R. Westmoreland,[5] Matthew E. Law,[5] Tina Kasper,[6] Katharina Kohse-Höinghaus[6]

Models for chemical mechanisms of hydrocarbon oxidation rely on spectrometric identification of molecular structures in flames. Carbonyl (keto) compounds are well-established combustion intermediates. However, their less-stable enol tautomers, bearing OH groups adjacent to carbon-carbon double bonds, are not included in standard models. We observed substantial quantities of two-, three-, and four-carbon enols by photoionization mass spectrometry of flames burning representative compounds from modern fuel blends. Concentration profiles demonstrate that enol flame chemistry cannot be accounted for purely by keto-enol tautomerization. Currently accepted hydrocarbon oxidation mechanisms will likely require revision to explain the formation and reactivity of these unexpected compounds.

Hydrocarbon oxidation mechanisms are applied in many areas of science, from understanding and reducing pollutant formation in combustion (*1*), to describing partial oxidation in fuel cells (*2*–*4*), to modeling oxidation in supercritical water (*5*). Hydrocarbon chemistry also has implications for modeling of planetary atmospheres (*6*) and interstellar chemistry (*7*). These mechanisms rely heavily on measurements in flames. The study of flame chemistry reaches back 150 years (*8*), and comprehensive chemical mechanisms have been devised for many fuels (*9*, *10*). It is remarkable that any commonly occurring intermediate should have eluded detection. Nevertheless, the present work demonstrates that an entire class of molecules absent from standard hydrocarbon oxidation models, the enols, occurs in a wide range of hydrocarbon flames.

Erlenmeyer (*11*) postulated in 1880 that enols should exist only as transient chemical intermediates. Ethenol (vinyl alcohol, CH_2=CHOH), the simplest enol, was not directly detected until 1973 (*12*) and not observed in the gas phase until 1976 (*13*). Ethenol is thermodynamically unstable relative to acetaldehyde (CH_3-HC=O) (*14*), and keto-enol tautomerization is a classically facile acid-catalyzed isomerization in water. Uncatalyzed in the gas phase, tautomerization is computed to have sizeable energy barriers. On storage, ethenol tautomerizes to acetaldehyde (*13*, *15*), probably by surface reactions.

Although acetaldehyde is a well-known intermediate in flames, its isomer ethenol was only recently observed in a fuel-rich ethene flame (*16*). Few experimental data are available on gas-phase neutral enol chemistry, and the presence of enols in hydrocarbon oxidation was mainly speculative. Detection was made possible by combining molecular-beam mass spectrometry with photoionization by tunable vacuum ultraviolet light from a third-generation synchrotron source, the Advanced Light Source at Lawrence Berkeley National Laboratory (*16*). The present work, which indicates a rich and previously unsuspected enol chemistry in a wide range of combustion systems, will have a considerable impact on prevailing hydrocarbon oxidation mechanisms.

We undertook a systematic search for enols among 24 different flames of 14 prototypical single fuels representing the major classes of chemicals appearing in modern fuel blends: alkanes, alkenes, alkynes, cyclic hydrocarbons, aromatics, and alcohols. Additionally, low-pressure flames of commercial gasoline were measured. These flames were comprehensively characterized with complete mass spectra taken as a function of distance from the burner at several selected photoionization energies as well as photoionization efficiency spectra taken at several burner positions.

Studies (*17*) were carried out at the Advanced Light Source as described elsewhere (*16*, *18*) and at the National Synchrotron Radiation Laboratory at Hefei, China. Ionization energies of enols are markedly lower than those of their keto tautomers (*19*), making them readily distinguishable on the basis of photoionization threshold. Figure 1 shows photoionization efficiency spectra for m/z = 44 ions (the mass of ethenol or acetaldehyde) sampled from four of these flames, along with the derived fraction (*16*) of ethenol. Other flames fueled by propyne [ϕ (fuel/oxygen

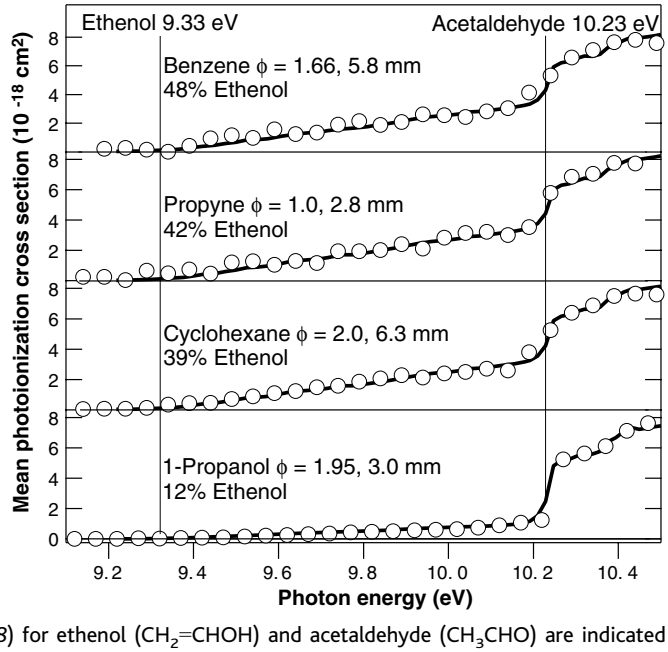

Fig. 1. Photoionization efficiency curves taken for m/z = 44 ions sampled from four representative flames. Photoion signals (circles) taken at the stated distance from the burner have been background-corrected and normalized by the measured photon flux as described previously (*27*). Signals are then scaled to computed mean photoionization cross sections (*16*) (lines) for hypothetical mixtures of ethenol and acetaldehyde that give best fits to the data. The mean cross section is defined as the sum of the photoionization cross sections σ weighted by the mole fractions χ, i.e., $\sigma_{enol}\chi_{enol} + \sigma_{keto}\chi_{keto}$, with $\chi_{enol} + \chi_{keto} = 1$. Ionization energies (*19*, *28*) for ethenol (CH_2=CHOH) and acetaldehyde (CH_3CHO) are indicated by the thin vertical lines.

[1]Combustion Research Facility, Mail Stop 9055, Sandia National Laboratories, Livermore, CA 94551–0969, USA. [2]JILA, National Institute of Standards and Technology and University of Colorado, 440CB, Boulder CO, 80309–0440 USA. [3]National Synchrotron Radiation Laboratory, University of Science and Technology of China, Hefei, Anhui 230026, China. [4]School of Applied and Engineering Physics, Cornell University, Ithaca, NY 14853, USA. [5]Department of Chemical Engineering, University of Massachusetts, Amherst, MA 01003–9303, USA. [6]Physikalische Chemie I, Universität Bielefeld, Universitätsstraße 25, 33615 Bielefeld, Germany.

*To whom correspondence should be addressed. E-mail: cataatj@sandia.gov

ratio relative to a stoichiometric mixture) = 1.8], benzene (ϕ = 1.0), cyclohexane (ϕ = 2.0), 1,3-butadiene (ϕ = 1.46), ethanol (ϕ = 1.97 and ϕ = 1.0), propene (ϕ = 2.3 and ϕ = 1.68), allene (ϕ = 1.8 and ϕ = 1.0), cyclopentene (ϕ = 2.0), and ethene (ϕ = 2.1 to ϕ = 1.2) also show substantial contributions from ethenol, with peak mole fractions in the range of 10^{-3} to 10^{-4}.

Ethenol is below the present detection limit (estimated to be about a mole fraction of 10^{-5}) in ethane, methane, propane, and 2-propanol flames. A small amount of m/z = 44 signal is observed in rich propane and 2-propanol flames at ionization energies below the acetaldehyde threshold of 10.23 eV, but the signal-to-noise ratio is too small to assign a clear ionization threshold. Ethenol is observed over a range of stoichiometries reflecting the chemistry of real combustion devices.

Furthermore, the present experiments demonstrate that larger enols occur in hydrocarbon flames. The m/z = 58 fractions sampled from a stoichiometric (ϕ = 1.0) cyclohexane flame and a rich (ϕ = 1.44) ethanol flame show a signal with an ionization threshold near 8.7 eV, which is assigned to ionization of either propen-1-ol or propen-2-ol (*19*). This observation supports inclusion of larger enols in flame models, from which they are now generally absent. Enol chemistry is also evident in flames of commercial fuels. Figure 2 shows contributions from propenols and butenols in low-pressure flames of commercial gasoline; ethenol is also prominent in these flames. Interpretation of data from a mixed fuel–like gasoline, which may contain hundreds of compounds, requires caution, but the reactions responsible for producing and consuming enols continue to contribute substantially in the chemistry of these fuel blends.

The mass spectrometric results suggest that explaining the presence of enols will require considerable alteration to current models of hydrocarbon oxidation. For example, hydrocarbon oxidation mechanisms have until now assumed C_2H_4O molecules observed in flames to be acetaldehyde or oxirane. Oxirane has an ionization energy of 10.56 eV (*19*) and does not contribute to the present spectra. Detailed chemical mechanisms of oxidation must now include reactions to produce the ethenol tautomer as well as reactions to consume ethenol. At elevated temperatures, a contribution from the less-stable enol form would be expected simply from equilibration of the tautomerization. However, the ethenol fractions derived from the measurements (*16*) are 10 to 100 times greater than the thermodynamic equilibrium fractions of ethenol. Further, the data suggest that ethenol kinetics in flames are distinct from those of the acetaldehyde tautomer. The profiles of acetaldehyde and ethenol versus distance from the burner differ markedly in most of the flames in which ethenol is observed. Flame concentrations are the result of the competing effects of many reactions; the differences between the rise in ethenol and acetaldehyde concentrations with increasing height above the burner suggest separate formation mechanisms for the two species or differential removal of ethenol as it diffuses toward the burner (Fig. 3).

Describing the presence of ethenol in flames of ethene may be within reach. The reaction of ethene with OH has been predicted to produce sizeable ethenol yields at high temperatures (*20*, *21*), although experimental confirmation is not yet available. Modeling a rich ethene flame using computed rate constants (*17*, *22*) for OH with ethene and estimated rate coefficients for removal reactions of ethenol gives near-quantitative agreement with the observations; the shapes of both the ethenol and acetaldehyde profiles are faithfully predicted, and the calculated ethenol mole fraction is within a factor of two of the experiment (Fig. 3). Details of the OH + C_2H_4 potential energy surface will be published elsewhere. The reaction of the OH with ethene offers an attractive general explanation for ethenol formation, because OH and ethene are common in all hydrocarbon flames. An analogous reaction is the source of dichloroethenol in flames of trichloroethene (*23*).

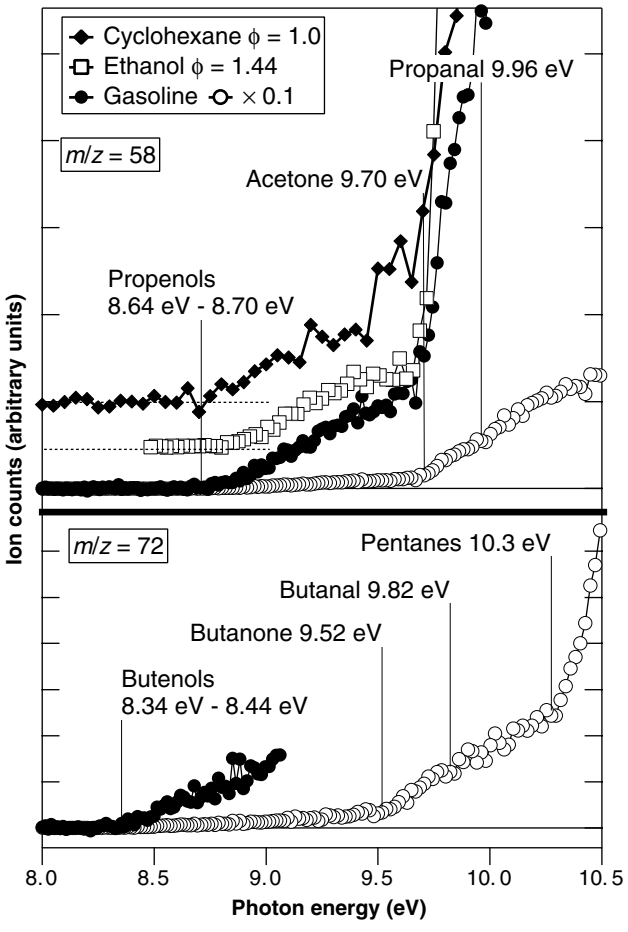

Fig. 2. Propenols and butenols in hydrocarbon flames. (**Top**) Photoionization efficiency spectra taken for m/z = 58, sampled from a cyclohexane flame 2.4 mm from the burner, from an ethanol flame 2.9 mm from the burner, and from a gasoline flame 4.0 mm from the burner. The ethanol and gasoline signals are vertically displaced for clarity. The ion signals were background-corrected and normalized by the measured photon flux (*27*). Ionization energies are indicated for several C_3H_6O species. The threshold near 8.7 eV is attributable to ionization of propenol isomers. (**Bottom**) Photoionization efficiency spectrum taken of m/z = 72, sampled from a gasoline flame 4.0 mm from the burner. Ionization energies are indicated for several mass-72 species. The threshold near 8.4 eV is attributable to photoionization of butenols.

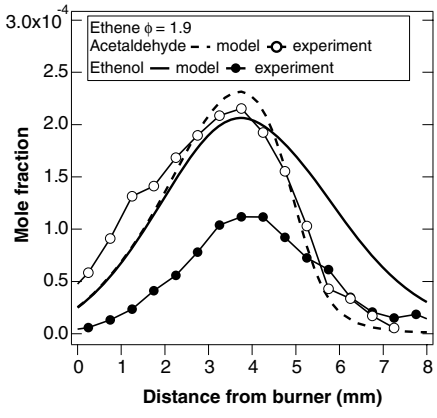

Fig. 3. Mole fractions of ethenol and acetaldehyde as a function of distance from the burner in a ϕ = 1.9 ethene flame. Experimental mole fractions were obtained as described elsewhere (*17*, *18*). The model uses rate constants for ethene plus OH derived from master equation calculations and ab initio characterizations of stationary points on the C_2H_4OH surface (*17*). The experimental profile is shifted by 1.8 mm as an approximate correction for sampling probe effects (*29*).

However, the present evidence points against the reaction of OH with ethene as the sole source of ethenol in other flames. The ratio of ethene to ethenol is by far the highest in the ethene flames and varies by more than a factor of 100 among the flames in which ethenol is observed; increased ethenol is not correlated with higher ethene. Other reactions, such as OH addition to larger unsaturated hydrocarbons or to hydrocarbon radicals, or dehydrogenation of alcohols, may form ethenol. Moreover, ethenol concentrations in rich propane, ethane, and methane flames are below the present detection limits, despite ethene concentrations similar to high-enol flames of fuels such as cyclohexane and cyclopentene.

The chemical fate of the ethenol in hydrocarbon oxidation is demonstrably distinct from that of acetaldehyde. The fraction of ethenol relative to acetaldehyde increases with increasing height above the burner for all the flames in which ethenol has been observed (Fig. 4). This trend parallels the temperature, which rises steeply with increasing height above the burner until the peak flame temperature is reached in the luminous zone. The data therefore suggest that the kinetic process producing ethenol is favored at higher temperature. However, tautomerization is calculated to be the lowest-energy unimolecular reaction pathway for ethenol (*24*). Thus, removal of ethenol is not dominated by tautomerization to acetaldehyde, because ethenol fractions continue to increase until both acetaldehyde and ethenol are consumed in the luminous zone.

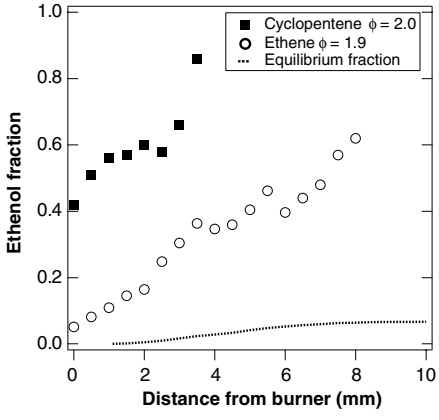

Fig. 4. Fraction of C_2H_4O that exists as ethenol as a function of distance from the burner, measured for the two flames that show the highest peak ethenol fraction [ethenol/(ethenol + acetaldehyde)]: ethene (ϕ = 1.9) and cyclopentene (ϕ = 2.0). Uncertainty limits on the ethenol fraction are about 10%. The luminous zone of the cyclopentene flame is located 3 to 4 mm closer to the burner than that of the ethene flame. The estimated equilibrium fraction (*14*, *19*) of ethenol for the temperature profile of the ethene flame is shown as the dotted line for reference. A similar trend is observed in other flames. The temperature profile of the ϕ = 1.9 ethene flame is given as fig. S1.

Removal of enols in flames most likely proceeds instead by reaction with flame radicals, particularly OH and H. Different products are expected for H abstraction from enols and their keto tautomers. For example, H abstraction from ethenol would produce vinyloxy, whereas from acetaldehyde it would produce the more stable acetyl radical. Radical (e.g., OH, CH_3, or O atom) attack on the carbon-carbon double bond is also possible in enols, and addition of alkyl radicals to ethenol may provide one route to the larger enols.

The detailed consequences of enol chemistry for practical combustion remain unclear at present. However, partial oxidation chemistry, in which the enols play a previously unrecognized part, is critical to many important applications of hydrocarbon oxidation mechanisms. Partial oxidation products are often pollutants. For example, increased acetaldehyde emission is observed when ethanol is added to internal combustion fuels (*25*, *26*). Enol chemistry may play a role in aldehyde production under some oxidation conditions. In addition, the gas-phase chemistry in hydrocarbon/air solid oxide fuel cells is largely partial oxidation. Alkyl addition reactions to enols constitute molecular weight growth pathways for partially oxidized fuel species, and contributions from enols may alter the oxidation of soot precursors.

The present work also has impact for the fundamental chemistry of enols. Modeling of the present results will be slowed by the dearth of experimental measurements of gas-phase neutral enol kinetics. Rate constants and branching fractions for reactions of enols with combustion radicals, most importantly OH and H, remain largely unknown. In the present measurements, the only flames in which ethenol is not observed are those of the simple alkanes (methane, ethane, and propane) and 2-propanol. Higher enol concentrations may occur under other conditions than those used in this work. Removal of ethenol may be more rapid in these flames, for example through reactions with methyl radicals. It is also possible that the formation of enols is reduced in fuels containing more primary C–H bonds; flames of cyclohexane, an alkane without primary hydrogens, are rich in ethenol. Correlations of enols with other open and closed-shell combustion intermediates, in conjunction with kinetics investigations, are necessary to formulate the role of enols in hydrocarbon oxidation models.

References and Notes

1. J. A. Miller, M. J. Pilling, J. Troe, *Proc. Combust. Inst.* **30**, 43 (2005).
2. T. Hibino *et al.*, *Science* **288**, 2031 (2000).
3. S. Park, J. M. Vohs, R. J. Gorte, *Nature* **404**, 265 (2000).
4. A. Naidja, C. R. Krishna, T. Butcher, D. Mahajan, *Prog. Energy Combust. Sci.* **29**, 155 (2003).
5. P. A. Sullivan, J. M. Ploeger, W. H. Green, J. W. Tester, *Phys. Chem. Chem. Phys.* **6**, 4310 (2004).
6. A. Ricca, C. W. Bauschlicher Jr., E. L. O. Bakes, *Icarus* **154**, 516 (2001).
7. R. I. Kaiser, H. Y. Lee, A. M. Mebel, Y. T. Lee, *Astrophys. J.* **548**, 852 (2001).
8. Famously, Michael Faraday's 1859 to 1860 Christmas lecture series on the chemistry of a candle flame, published as *The Chemical History of a Candle*, edited by William Crookes (George Routledge and Sons, New York, 1874, and many other editions).
9. C. K. Westbrook, *Proc. Combust. Inst.* **28**, 1563 (2001).
10. E. Ranzi *et al.*, *Combust. Flame* **99**, 201 (1994).
11. E. Erlenmeyer, *Chem. Ber.* **13**, 305 (1880).
12. B. Blank, H. Fischer, *Helv. Chim. Acta* **56**, 506 (1973).
13. S. Saito, *Chem. Phys. Lett.* **42**, 399 (1976).
14. L. Zhu, C.-J. Chen, J. W. Bozzelli, *J. Phys. Chem. A* **104**, 9197 (2000).
15. W. J. Bouma, D. Poppinger, L. Radom, *J. Am. Chem. Soc.* **99**, 6443 (1977).
16. T. A. Cool *et al.*, *J. Chem. Phys.* **119**, 8356 (2003).
17. Materials and methods are available as supporting material on *Science* Online.
18. T. A. Cool *et al.*, *Proc. Combust. Inst.* **30**, 1681 (2005).
19. P. J. Linstrom, W. G. Mallard, Eds., *NIST Chemistry WebBook, NIST Standard Reference Database Number 69* (National Institute of Standards and Technology, Gaithersburg, MD, 2003).
20. T. Yamada, J. W. Bozzelli, T. Lay, *J. Phys. Chem. A* **103**, 7646 (1999).
21. H. Hippler, B. Viskolcz, *Phys. Chem. Chem. Phys.* **2**, 3591 (2000).
22. J. P. Senosiain, S. J. Klippenstein, J. A. Miller, *J. Phys. Chem. A*, in press.
23. J. H. Werner, T. A. Cool, *Combust. Flame* **120**, 125 (2000).
24. B. J. Smith, M. T. Nguyen, W. J. Bouma, L. Radom, *J. Am. Chem. Soc.* **113**, 6452 (1991).
25. S. G. Poulopoulos, D. P. Samaras, C. J. Philippopoulos, *Atmos. Environ.* **35**, 4399 (2001).
26. B.-Q. He, S.-J. Shuai, J.-X. Wang, H. He, *Atmos. Environ.* **37**, 4965 (2003).
27. C. A. Taatjes *et al.*, *Phys. Chem. Chem. Phys.* **7**, 806 (2005).
28. B. Ruscic, J. Berkowitz, *J. Chem. Phys.* **101**, 10936 (1994).
29. A. T. Hartlieb, B. Atakan, K. Kohse-Höinghaus, *Combust. Flame* **121**, 610 (2000).
30. M. Ahmed, D. S. Peterka, and L. Poisson (Lawrence Berkeley National Laboratory) are gratefully acknowledged for their support in bringing the flame apparatus into operation. This work was supported by the Division of Chemical Sciences, Geosciences, and Biosciences, in the Office of Basic Energy Sciences of the U.S. Department of Energy; the U.S. Army Research Office; the Chinese Academy of Sciences; the National Natural Science Foundation of China; and the Deutsche Forschungsgemeinschaft. Sandia is a multiprogram laboratory operated by Sandia Corporation, a Lockheed Martin Company, for the National Nuclear Security Administration. The Advanced Light Source is supported by the Director, Office of Science, Office of Basic Energy Sciences, Materials Sciences Division, of the U.S. Department of Energy at Lawrence Berkeley National Laboratory. C.A.T. was a JILA visiting fellow from September 2004 to January 2005.

Supporting Online Material

www.sciencemag.org/cgi/content/full/1112532/DC1
Materials and Methods
Fig. S1
References and Notes

21 March 2005; accepted 29 April 2005
Published online 12 May 2005;
10.1126/science.1112532
Include this information when citing this paper.

Tyrosinase Reactivity in a Model Complex: An Alternative Hydroxylation Mechanism

Liviu M. Mirica,[1] Michael Vance,[1] Deanne Jackson Rudd,[1] Britt Hedman,[2]* Keith O. Hodgson,[1,2]* Edward I. Solomon,[1]* T. Daniel P. Stack[1]*

The binuclear copper enzyme tyrosinase activates O_2 to form a μ-η²:η²-peroxodicopper(II) complex, which oxidizes phenols to catechols. Here, a synthetic μ-η²:η²-peroxodicopper(II) complex, with an absorption spectrum similar to that of the enzymatic active oxidant, is reported to rapidly hydroxylate phenolates at –80°C. Upon phenolate addition at extreme temperature in solution (–120°C), a reactive intermediate consistent with a bis-μ-oxodicopper(III)-phenolate complex, with the O–O bond fully cleaved, is observed experimentally. The subsequent hydroxylation step has the hallmarks of an electrophilic aromatic substitution mechanism, similar to tyrosinase. Overall, the evidence for sequential O–O bond cleavage and C–O bond formation in this synthetic complex suggests an alternative intimate mechanism to the concerted or late stage O–O bond scission generally accepted for the phenol hydroxylation reaction performed by tyrosinase.

Tyrosinase is a ubiquitous binuclear copper enzyme, found in fungi, plants, and animals, that catalyzes the hydroxylation of phenols to catechols and the oxidation of catechols to quinones (*1*). The oxygenated form of tyrosinase contains a μ-η²:η²-peroxodicopper(II) species (**P** in Scheme 1), with an intact O–O bond, that hydroxylates phenols through a mechanism consistent with an electrophilic aromatic substitution. Because intermediates beyond the **P** species are unknown, the sequence of intimate steps of bond cleavage and formation remains unclear. Nonetheless, the electrophilic character of the enzymatic reaction suggests a mechanism, generally accepted, in which the O–O bond cleavage occurs either concerted with or after C–O bond formation (*2*, *3*).

The impressive C–H oxidation by tyrosinase has elicited extensive synthetic efforts to create copper complexes that not only react with O_2 to form spectroscopically faithful **P** model complexes (*4*) but also oxidize C–H bonds (*5*). Though many synthetic **P** analogs are known, only a limited number function as hydroxylating agents of externally added phenolate substrates (*6*–*8*). Compared with biological systems (*9*–*11*), the low temperatures and aprotic solvents tolerated by synthetic systems provide potential advantages in detection and characterization of reactive intermediates.

Here, we report the stabilization at –120°C of an intermediate formed in the reaction of a synthetic **P** species with an added phenolate. Spectroscopic characterization indicates a bis-μ-oxodicopper(III)-phenolate complex in which the O–O bond is cleaved and the phenolate is ligated to a copper center. This intermediate decays slowly at –120°C to hydroxylate the aromatic ring through a step that exhibits the hallmarks of an electrophilic aromatic substitution reaction (*7*). The data, in accord with density functional theory (DFT) calculations, strongly support this bis-μ-oxodicopper(III) species as an electrophilic oxidation agent in the hydroxylation reaction. As such, this study provides experimental evidence for an alternative hydroxylation mechanism for the μ-η²:η²-peroxodicopper(II) species in tyrosinase, entailing O–O bond cleavage prior to C–O bond formation (*12*).

The reaction of the copper(I) complex of *N,N′*-di-*tert*-butyl-ethylenediamine (DBED) with O_2 at –80°C in aprotic solvents (tetrahydrofuran, CH_2Cl_2, or acetone) generates a μ-η²:η²-peroxodicopper(II) complex, $\mathbf{P}^{\mathbf{DBED}}$, identified by its characteristic absorption band (350 nm, ε = 36 mM^{-1} cm^{-1}), resonance Raman stretch [υ_{o-o} = 721 cm^{-1}, $\Delta(^{18}O_2)$ = 40 cm^{-1}], and a Cu···Cu distance of 3.45 Å (*8*), similar to other characterized **P** complexes (*4*). $\mathbf{P}^{\mathbf{DBED}}$ reacts rapidly at –80°C with 1 equivalent of sodium 2,4-di-*tert*-butylphenolate, without the appearance of any intermediate species, to yield an ~1:1 mixture of 3,5-di-*tert*-butylcatechol and 3,5-di-*tert*-butyl-1,2-benzoquinone (Scheme 2). The product yield accounts for ~ 90% of the oxidizing equivalents of $\mathbf{P}^{\mathbf{DBED}}$, and one oxygen atom is transferred from $\mathbf{P}^{\mathbf{DBED}}$ to the phenyl ring, as assessed by $^{18}O_2$ substitution (*8*). $\mathbf{P}^{\mathbf{DBED}}$ reacts more slowly with more electron-deficient phenolates (*13*), consistent with an electrophilic aromatic substitution mechanism.

At lower temperature (–120°C) in 2-methyltetrahydrofuran (MeTHF), $\mathbf{P}^{\mathbf{DBED}}$ reacts with sodium 2,4-di-*tert*-butylphenolate to form a transient intermediate **A** that exhibits distinct intense absorption features (Fig. 1). Full formation requires the addition of at least three equivalents of this phenolate at millimolar concentrations. Optical titrations of $\mathbf{P}^{\mathbf{DBED}}$ with sodium 2,4-di-*tert*-butylphenolate support the formation of a 1:1 complex with a binding constant of 16,000 M^{-1} (log K ≈ 4.2) (*14*). Compound **A** decays by a first-order process ($t_{½}$ = 38 min, –120°C), and the resulting solution has an absorption spectrum and hydroxylated product yield nearly identical to those of the reaction performed at –80°C (*15*). The intense charge-transfer band of **A** at 418 nm (ε = 18 mM^{-1} cm^{-1}) is reminiscent of a bis-μ-oxodicopper(III) complex, a species that is now extensively characterized with a wide variety of neutral and anionic ligands (*4*, *16*–*18*). The less intense visible absorption band at 630 nm is assigned to a phenolate-to-Cu charge-

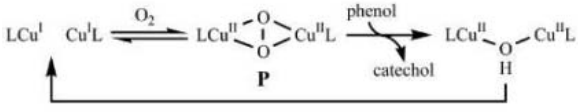

Scheme 1.

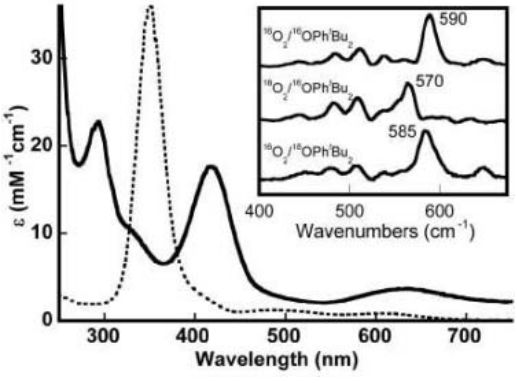

Fig. 1. UV-Vis spectrum of **A** (solid line) and $\mathbf{P}^{\mathbf{DBED}}$ (dashed line) in MeTHF (153 K, [Cu] ≈ 1 mM). Inset: Resonance Raman spectra of **A** (λ_{ex} = 413 nm, MeTHF, 77 K, [Cu] ≈ 1 mM) with $^{16}O_2/^{16}OPh^tBu_2$ (top line), $^{18}O_2/^{16}OPh^tBu_2$ (middle line), or $^{16}O_2/^{18}OPh^tBu_2$ (bottom line).

[1]Department of Chemistry, Stanford University, CA 94305, USA. [2]Stanford Synchrotron Radiation Laboratory, Stanford Linear Accelerator Center, Stanford University, CA 94309, USA.

*To whom correspondence should be addressed. E-mail: stack@stanford.edu (T.D.P.S.); edward.solomon@stanford.edu (E.I.S.); hodgson@ssrl.slac.stanford.edu (K.O.H.); hedman@ssrl.slac.stanford.edu (B.H.)

transfer transition (*19*). Resonance Raman experiments (λ_{ex} = 413 nm) reveal a bis-μ-oxodicopper(III) Cu_2O_2 core stretch at 590 cm^{-1} that shifts by 20 cm^{-1} upon $^{18}O_2$ substitution (*20*, *21*). On addition of ^{18}O-2,4-di-*tert*-butylphenolate, the 590 cm^{-1} stretch shifts by 5 cm^{-1} (Fig. 1, inset). The appreciable coupling of the Cu_2O_2 core and Cu-phenolate vibrations is only possible with a direct interaction of the phenolate ligand with the copper complex in **A**. A Hammett parameter of ρ = –2.2, determined for the decay of a series of **A** complexes with more electron-deficient phenolates at –120°C (Fig. 2), supports an electrophilic aromatic substitution mechanism; the value for tyrosinase is ρ = –2.4 (*22*). Further support for this mechanism is provided by the measured inverse secondary C–H/C–D kinetic isotope effect of 0.83 ± 0.09 on the decay rate of species **A** with 2,4-di-*tert*-butyl-6-H(D)-phenolate at –105°C (*14*).

Solution Cu K-edge x-ray absorption spectroscopy (XAS) on **A** in MeTHF exhibits two very weak pre-edge features at 8979 and 8980.5 eV, the latter of which is characteristic of a Cu(III) center (*23*, *24*). All fits to the extended x-ray absorption fine structure (EXAFS) data required a Cu···Cu contribution at 2.79 Å (*14*), a distance consistent with other structurally characterized bis-μ-oxodicopper(III) complexes (*4*), and each Cu coordination is best fit with four N/O ligands (*25*) at an average distance of 1.89 Å (Fig. 3).

The presented experimental evidence thus supports a bis-μ-oxodicopper(III)-phenolate structure for **A** (Scheme 2). Equatorial phenolate ligation, at the expense of the positioning of one of the amine groups of DBED axially, would be expected to enhance the relative stability of Cu(III) (*4*). It is well documented that the energy difference of the Cu(II) μ-η^2:η^2-peroxodicopper(II) and Cu(III) bis-μ-oxodicopper(III) isomers with sterically demanding neutral ligands such as DBED can be small at low temperatures (*4*, *5*, *26*). This near isoenergetic relation is biased toward the higher oxidation state by the addition of an anionic ligand. The DFT geometry-optimized structure of **A**, which included the entire monocationic complex, supports an electronic preference for the equatorial positioning of the phenolate ligand and predicts Cu···Cu (2.76 Å) and Cu-O/N_{ave} (1.88 Å) distances in good agreement with the EXAFS data (*14*).

On the basis of the present investigation, the hydroxylation of phenolate by $\mathbf{P}^{\mathbf{DBED}}$ through the intermediacy of **A** has the characteristics of an electrophilic aromatic substitution reaction, which is intriguing because such bis-μ-oxodicopper(III) species are generally not considered to be electrophiles (*4*, *26*, *27*). A frontier molecular orbital analysis of the electronic ground state of the DFT-optimized structure of **A** suggests that the equatorial positioning of the phenolate provides an almost ideal geometry for a perpendicular σ-attack of the phenolate-based π highest occupied molecular orbital (HOMO) on the Cu_2O_2-based σ* lowest unoccupied molecular orbital (LUMO) (Fig. 4) (*12*, *28*, *29*). Moreover, the activation energy (10.9 kcal/mol at –120°C) calculated by DFT for the phenolate hydroxylation step of the **A** species agrees well with the experimental activation energy value of ~10.3 kcal/mol (*14*), which supports this pathway as an energetically viable reaction coordinate for hydroxylation.

The associative rearrangement of the anionic ligand into an equatorial position in this model complex parallels anionic ligand-binding behavior observed in tyrosinase (*30*). Although this study uses a phenolate substrate rather than a phenol, an endogenous base in the active site of tyrosinase certainly could deprotonate the incoming phenol. A displaced histidine ligand from a copper center could serve this function, in addition to providing better access of the nascent phenolate to the copper center (*31*). Whether such substrate binding could lead to O–O bond cleavage in the oxygenated **P** form of tyrosinase is unknown. Nevertheless, it is clear that the electrophilic reactivity observed for tyrosinase does not exclude the intermediacy of a bis-μ-oxodicopper(III) species. The potential role of such species in biological oxidation reactions remains an intriguing issue.

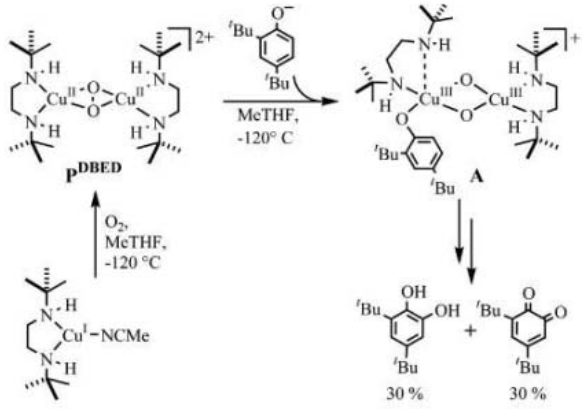

Scheme 2.

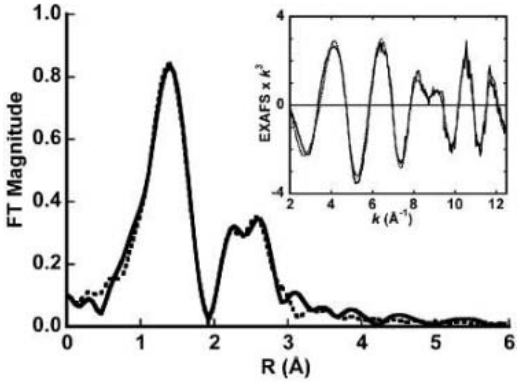

Fig. 3. Non-phase-shift corrected Fourier transform of EXAFS data (solid line) and four-coordinate fit (dashed line) of **A** (MeTHF, 10 K, [Cu] ≈ 1 mM). (**Inset**) The EXAFS data (solid line) and four-coordinate fit (dashed line).

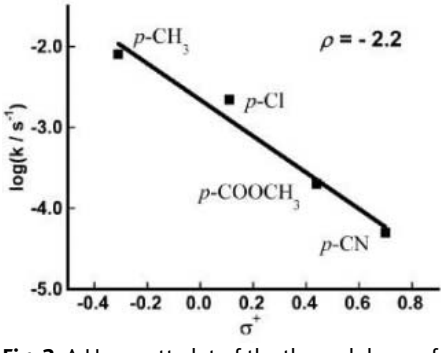

Fig. 2. A Hammett plot of the thermal decay of species **A** at –120°C (ρ = –2.2). The para-substituted phenolates used are indicated on the plot.

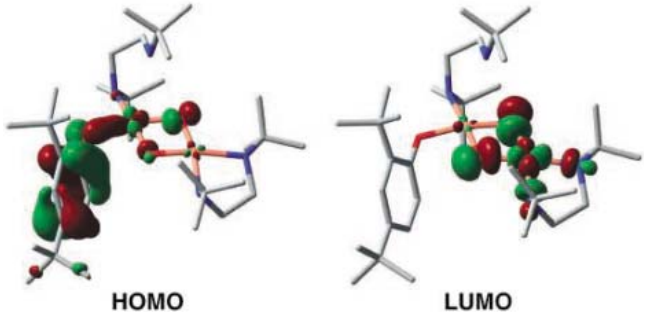

Fig. 4. Spatial representation of HOMO [(**left**) phenolate π orbital] and LUMO [(**right**) Cu_2O_2 core σ* orbital], calculated for the DFT geometry-optimized model of **A**, showing the favorable σ-attack conformation. The orbital contour was set at 0.05 $e^-/Å^3$.

References and Notes

1. E. I. Solomon, U. M. Sundaram, T. E. Machonkin, *Chem. Rev.* **96**, 2563 (1996).
2. H. Decker, R. Dillinger, F. Tuczek, *Angew. Chem. Int. Ed. Engl.* **39**, 1591 (2000).
3. S. Mandal, D. Macikenas, J. D. Protasiewicz, L. M. Sayre, *J. Org. Chem.* **65**, 4804 (2000).
4. L. M. Mirica, X. Ottenwaelder, T. D. P. Stack, *Chem. Rev.* **104**, 1013 (2004).
5. E. A. Lewis, W. B. Tolman, *Chem. Rev.* **104**, 1047 (2004).
6. L. Santagostini *et al.*, *Chem. Eur. J.* **6**, 519 (2000).
7. S. Itoh *et al.*, *J. Am. Chem. Soc.* **123**, 6708 (2001).
8. L. M. Mirica *et al.*, *J. Am. Chem. Soc.* **124**, 9332 (2002).
9. M. Kim *et al.*, *Nat. Struct. Biol.* **9**, 591 (2002).
10. J. C. Price, E. W. Barr, B. Tirupati, J. M. Bollinger, C. Krebs, *Biochemistry* **42**, 7497 (2003).
11. M. T. Green, J. H. Dawson, H. B. Gray, *Science* **304**, 1653 (2004).
12. Note that a synthetic μ-η^2:η^2-peroxodicopper(II) complex has been shown to directly hydroxylate an aromatic ring on a noncoordinating substrate (*32*).
13. A lower yield of the products is observed for electron-deficient substrates.
14. Materials and methods are available as supporting material on *Science* Online.
15. Both catechol and quinone are produced upon acidic workup of the solution mixture, which supports **A** as a reactive species during hydroxylation.
16. J. A. Halfen *et al.*, *Science* **271**, 1397 (1996).
17. S. Mahapatra, V. G. Young, S. Kaderli, A. D. Zuberbühler, W. B. Tolman, *Angew. Chem. Int. Ed. Engl.* **36**, 130 (1997).
18. V. Mahadevan *et al.*, *J. Am. Chem. Soc.* **119**, 11996 (1997).
19. A resonance Raman spectrum resulting from 600-nm excitation shows a C–O stretch at 1280 cm^{-1}, which supports a phenolate to Cu charge-transfer assignment.
20. M. J. Henson, P. Mukherjee, D. E. Root, T. D. P. Stack, E. I. Solomon, *J. Am. Chem. Soc.* **121**, 10332 (1999).
21. No vibrations characteristic for **P** complexes (at ~300 or ~730 cm^{-1}) are observed.
22. S. Yamazaki, S. Itoh, *J. Am. Chem. Soc.* **125**, 13034 (2003).
23. J. L. DuBois *et al.*, *J. Am. Chem. Soc.* **119**, 8578 (1997).
24. J. L. DuBois *et al.*, *J. Am. Chem. Soc.* **122**, 5775 (2000).
25. EXAFS analysis typically cannot distinguish between atoms that differ in Z by 1 (e.g., O and N) (*33*). Given the k range of the EXAFS data (k = 3 to 12.5 $Å^{-1}$), any difference in R less than 0.17 Å between ligands in the first coordination shell (at 1.89 Å) could not be resolved.
26. V. Mahadevan, M. J. Henson, E. I. Solomon, T. D. P. Stack, *J. Am. Chem. Soc.* **122**, 10249 (2000).
27. An electrophilic aromatic substitution mechanism for a bis-μ-oxodicopper(III) complex has been proposed in a case in which a ligand aryl group is hydroxylated (*34*).
28. P. Chen, E. I. Solomon, *J. Inorg. Biochem.* **88**, 368 (2002).
29. E. I. Solomon, P. Chen, M. Metz, S.-K. Lee, A. E. Palmer, *Angew. Chem. Int. Ed. Engl.* **40**, 4570 (2001).
30. D. E. Wilcox *et al.*, *J. Am. Chem. Soc.* **107**, 4015 (1985).
31. P. E. M. Siegbahn, *J. Biol. Inorg. Chem.* **8**, 567 (2003).
32. E. Pidcock, H. V. Obias, C. X. Zhang, K. D. Karlin, E. I. Solomon, *J. Am. Chem. Soc.* **120**, 7841 (1998).
33. R. A. Scott, *Methods Enzymol.* **117**, 414 (1985).
34. P. L. Holland, K. R. Rodgers, W. B. Tolman, *Angew. Chem. Int. Ed. Engl.* **38**, 1139 (1999).

35. We thank R. Pratt for assistance in the synthesis of ^{18}O-di-*t*-butyl-phenolate and J. I. Brauman for insightful discussions. L.M.M. gratefully acknowledges a John Stauffer Stanford Graduate Fellowship. Funding was provided by NIH GM50730 (T.D.P.S), NIH DK31450 (E.I.S.), and NIH RR01209 (K.O.H.). XAS data were measured at the Stanford Synchrotron Radiation Laboratory (SSRL), which is supported by the Department of Energy, Office of Basic Energy Sciences. The SSRL Structural Molecular Biology program is funded by the National Institutes of Health, National Center for Research Resources, Biomedical Technology Program, and the Department of Energy, Office of Biological and Environmental Research.

Supporting Online Material

www.sciencemag.org/cgi/content/full/308/5730/1890/DC1
Materials and Methods
SOM Text
Figs. S1 to S8
Tables S1 to S3
References

10 March 2005; accepted 10 May 2005
10.1126/science.1112081

Sound Velocities of Hot Dense Iron: Birch's Law Revisited

Jung-Fu Lin,[1]* Wolfgang Sturhahn,[2] Jiyong Zhao,[2] Guoyin Shen,[3] Ho-kwang Mao,[1] Russell J. Hemley[1]

Sound velocities of hexagonal close-packed iron (hcp-Fe) were measured at pressures up to 73 gigapascals and at temperatures up to 1700 kelvin with nuclear inelastic x-ray scattering in a laser-heated diamond anvil cell. The compressional-wave velocities (V_P) and shear-wave velocities (V_S) of hcp-Fe decreased significantly with increasing temperature under moderately high pressures. V_P and V_S under high pressures and temperatures thus cannot be fitted to a linear relation, Birch's law, which has been used to extrapolate measured sound velocities to densities of iron in Earth's interior. This result means that there are more light elements in Earth's core than have been inferred from linear extrapolation at room temperature.

The properties of Earth's iron-rich core have been inferred from estimates of iron density at high pressures and temperatures and from measurements of compressional-wave (V_P) and shear-wave (V_S) velocities passing through the core (*1*–*13*). These data have indicated that Earth's core is less dense than pure iron by approximately 10% for the outer core and 3% for the inner core, suggesting the existence of light elements in the core. On the other hand, Birch's law, a linear sound velocity–density relation (*2*, *14*, *15*), has also been used to extrapolate measured sound velocities at high pressures and room temperatures to inner core conditions without considering the temperature effect (*9*, *12*). This linear extrapolation has suggested that the inner core is mainly made of Fe-Ni alloy. The nuclear-resonant inelastic x-ray scattering (NRIXS) technique provides a direct probe of the phonon density of states (DOS) of the resonant isotope (*16*–*18*) using the 14.4125-keV transition of ^{57}Fe. V_P and V_S of hexagonal close-packed (hcp) Fe have been measured up to 153 GPa at 300 K (*10*, *19*). However, the effect of temperature on the sound velocity measurements of Fe in static studies is not well understood. Here we report the static NRIXS study of the sound velocities of hcp-Fe up to 73 GPa and 1700 K in a laser-heated diamond anvil cell (LHDAC), and we discuss the temperature effect on the sound velocities and Birch's law.

We conducted NRIXS experiments in an LHDAC at Sector 3 of the Advanced Photon Source (APS) at Argonne National Laboratory (*20*, *21*). Energy spectra were obtained by tuning the x-ray energy (±70 meV) around the nuclear transition energy of 14.4125 keV and collecting the Fe K-fluorescence (the emission of an x-ray photon via the transition of an atomic electron into an unoccupied 1s state) radiation that was emitted with time delay relative to the incident x-ray pulses. We used a quasiharmonic model to extract the phonon DOS from the NRIXS spectra (Fig. 1) according to the procedure described in (*16*–*18*). With the NRIXS technique, we measured the spectrum of the self-correlation function of the position of the Fe atoms (*17*). In the model, the atomic motions relative to the temperature-dependent averaged position are assumed to be harmonic under the given conditions of pressure, temperature, and other parameters. Thermal effects, such as expansion and change of force constants with atomic distances, were allowed to change but the vibrations were still assumed to occur in a harmonic potential. The average kinetic energy and force constant independently derived from the moments of the measured spectra were consistent with the values evaluated from the quasiharmonic model (*17*), indicating the validity of the model to our high-pressure/temperature data (*22*). The Debye sound velocity (V_D) was derived from parabolic fitting of the low-energy regime of the DOS (*16*–*18*), and the vibrational, elastic, and thermodynamic parameters were obtained by the integration of the DOS. We then calculated the thermal

[1]Geophysical Laboratory, Carnegie Institution of Washington, 5251 Broad Branch Road, N.W., Washington, DC 20015, USA. [2]Advanced Photon Source, Argonne National Laboratory, 9700 South Cass Avenue, Argonne, IL 60439, USA. [3]Consortium for Advanced Radiation Sources, The University of Chicago, Chicago, IL 60637, USA.

*To whom correspondence should be addressed. E-mail: j.lin@gl.ciw.edu

equation-of-state (EOS) parameters of hcp-Fe using the thermal EOS from previous studies (*23*–*25*) and the Birch-Murnaghan EOS (*26*). The adiabatic bulk modulus at zero pressure (K_{0S}) is

$$K_{0S}(T) = K_{0T}(T)(1 + \alpha\gamma T) \quad (1)$$

where K_{0T} is the isothermal bulk modulus at zero pressure (*23*), α is the thermal expansion coefficient (*23*), γ is the Grüneisen parameter (γ = 1.78) (*25*), and T is the temperature. The Birch-Murnaghan EOS is used to calculate the isothermal bulk modulus at high pressures (K_T) and the adiabatic bulk modulus at high pressures (K_S). The K_S, density (ρ), and V_D are used to solve for the aggregate V_P, V_S, and shear modulus G by the following equations (*10*)

$$\frac{K_S}{\rho} = V_P^2 - \frac{4}{3}V_S^2 = V_\Phi{}^2 \quad (2)$$

$$\frac{G}{\rho} = V_S^2 \quad (3)$$

$$\frac{3}{V_D^3} = \frac{1}{V_P^3} + \frac{2}{V_S^3} \quad (4)$$

where V_ϕ is the bulk sound velocity calculated from the thermal EOS parameters of K_S and ρ. The derivation of V_S is relatively insensitive to the differences in the EOS data (*27*). Our results at high pressures and room temperatures are consistent with those of a previous study (*10*). At high temperatures, the bulk sound velocity (V_ϕ) followed Birch's law (V_ϕ is linearly related to the density and mean atomic weight; $dV_\phi/dT = 0$) (*14*), whereas V_P, V_S, and G did not (Fig. 2). At a pressure of ~54 GPa, V_P decreased by ~7%, V_S decreased by ~14%, and G decreased by ~28%, with a temperature increase of 1000 K. The effect of temperature on the sound velocities at constant density is smaller than the effect at constant pressure; i.e., at a density of ~10.25 g cm^{-3}, V_P decreased at a rate of 0.00035 km s^{-1} K^{-1} (dV_P/dT), V_S decreased by 0.00046 km s^{-1} K^{-1} (dV_S/dT), and G decreased by 0.035 GPa K^{-1} (dG/dT). These values are in general agreement with the V_ϕ-density linear relation; if V_ϕ is linearly related to the density without temperature effect, then $V_P(dV_P/dT) - 4/3V_S(dV_S/dT) = 0$ (from Eq. 2). X-ray diffraction spectra showed that the samples after laser heating were in the polycrystalline hcp structure at high pressures without significant preferred orientation, suggesting that the strong effect of temperature on the sound velocities cannot be explained simply by the elastic anisotropy in highly textured hcp-Fe, which can account for a few percent of the difference in V_P (*12*). Different thermal pressure conditions varying from no thermal pressure effect to full thermal pressure effect (*28*) have been used to test the systematic errors in the temperature effect on the sound velocities. We found that the uncertainties in the thermal pressure alone were too small to result in a significant temperature effect on the sound velocities, in particular, the temperature effect on V_S.

Extrapolated sound velocities of hcp-Fe at 3000 and 6000 K, obtained by combining our study at moderate pressure and temperature with a previous NRIXS study at high pressures and 300 K and with shock-wave data at high pressure and high temperature, show that the effect of temperature on the sound velocities of Fe is significant at moderate pressures, but weakens under inner core pressures because a highly compressed Fe has a smaller thermal

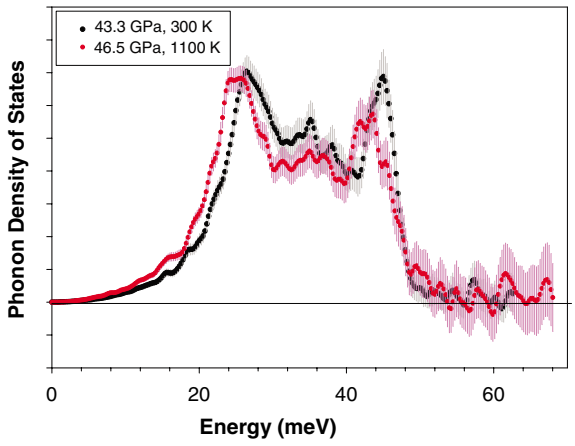

Fig. 1. DOS of hcp-Fe at 43.3 (±2.2) GPa and 300 K (black curve) and 46.5 (±2.8) GPa and 1100 K (±100) (red curve). The spectral features of the DOS are shifted toward lower energies and the initial slope of the low-energy regime increases significantly at high temperature, indicating the softening of the lattice excitation. Debye sound velocities are derived from parabolic fitting of the low-energy regime of the DOS in the range of 3.5 to 14 meV.

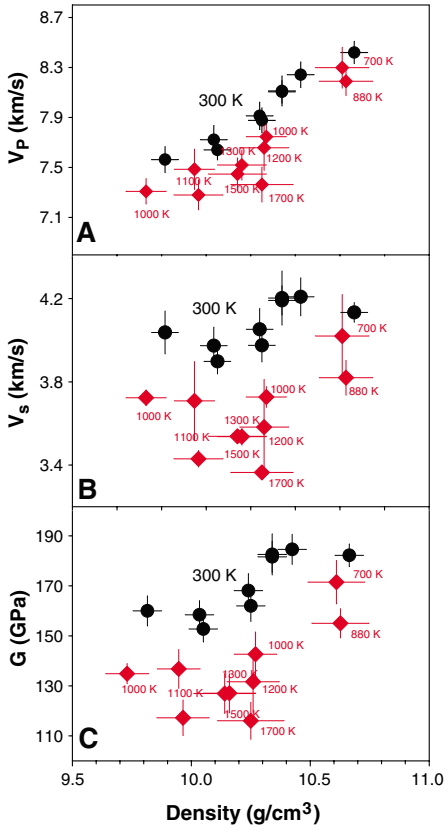

Fig. 2. Experimental results of aggregate V_P (**A**), V_S (**B**), and G (**C**) of hcp-Fe at high pressures and temperatures. Black circles, 300 K; red diamonds, high temperatures. Temperatures are given next to the red diamonds.

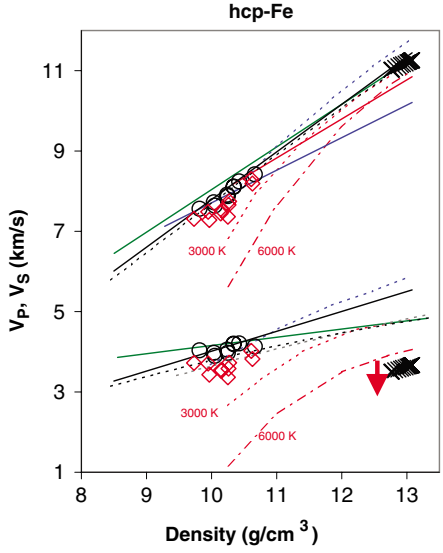

Fig. 3. Comparison of V_P and V_S of hcp-Fe at high pressures and temperatures. Black open circles, this study at 300 K; red open diamonds, this study at high temperatures; X's, Preliminary Earth Reference Model (PREM) (*29*); red solid line, shock wave (*3*); blue dashed line, radial x-ray diffraction at 300 K (*6*); black solid line, NRIXS at 300 K (*10*); black dashed line, x-ray diffraction to 300 GPa and 1200 K (*30*); blue solid line, IXS at 300 K (*9*); green solid line, IXS at 300 K (*12*); gray dashed line, x-ray diffraction study up to 330 GPa and 300 K (*31*); red dashed line (3000 K) and red dash-dotted line (6000 K), extrapolated sound velocities of hcp-Fe at 3000 and 6000 K. At a density of ~10.25 g cm^{-3}, we used the slope of 0.00035 km s^{-1} K^{-1} to extrapolate V_P and 0.00046 km s^{-1} K^{-1} to extrapolate V_S. At higher pressures, we used a previous NRIXS study at high pressures and 300 K (*10*) and shock-wave data at high pressure and high temperature (*3*) to calculate V_P and V_S at 3000 and 6000 K. The red arrow indicates that the extrapolated shear wave of hcp-Fe in the inner core should be further corrected downward, to lower values.

expansion (Fig. 3) (*3*, *9*, *10*, *12*, *29–31*). Because the temperature of the inner core is believed to be close to the melting curve of Fe, the extrapolated V_S of hcp-Fe in the inner core should be corrected to even lower values. The small deviation in V_P between shock-wave data (*3*) and the previous NRIXS study (*10*) at high pressures and room temperature also suggests that the temperature effect on V_P is suppressed under inner core conditions, whereas the large difference in the V_S indicates that temperature has a strong effect on V_S even under core pressures (Fig. 3). Theoretical calculations on the elasticity of hcp-Fe predicted that V_S and G would decrease with increasing temperature at a constant density of 13.04 g cm^{-3} (*11*).

Birch pointed out the likely temperature effect on the sound velocities in his original paper in 1961 (*2*). Our results confirm this idea. It has been shown that the addition of a light element such as Si or S into Fe increases V_P and V_S under high pressures (*32*, *33*). Considering the temperature effect on V_P and V_S of hcp-Fe at inner core pressures and 6000 K (*20*), a few percent of light elements alloyed with Fe are still needed in the inner core to increase V_P to match seismic models (Fig. 3). This results in more light elements in Earth's inner core than has been suggested from the linearly extrapolated V_P of hcp-Fe at high pressures and room temperature (*12*).

References and Notes

1. F. Birch, *J. Geophys. Res.* **57**, 227 (1952).
2. F. Birch, *Geophys. J. R. Astron. Soc.* **4**, 295 (1961).
3. J. M. Brown, R. G. McQueen, *J. Geophys. Res.* **91**, 7485 (1986).
4. J. D. Bass, B. Svendsen, T. J. Ahrens, in *High Pressure Research in Mineral Physics*, M. H. Manghnani, Y. Syono, Eds. (American Geophysical Union, Washington, DC, 1987), pp. 393–423.
5. H. K. Mao, Y. Wu, L. C. Chen, J. F. Shu, *J. Geophys. Res.* **95**, 21737 (1990).
6. H. K. Mao *et al.*, *Nature* **396**, 741 (1999).
7. G. Steinle-Neumnn, L. Stixrude, R. E. Cohen, *Phys. Rev. B* **60**, 791 (1999).
8. D. Alfe, M. J. Gillan, G. D. Price, *Nature* **405**, 172 11 (2000).
9. G. Fiquet, J. Badro, F. Guyot, H. Requardt, M. Krisch, *Science* **291**, 468 (2001).
10. H. K. Mao *et al.*, *Science* **292**, 914 (2001).
11. G. Steinle-Neumann, L. Stixrude, R. E. Cohen, *Nature* **413**, 57 (2001).
12. D. Antonangeli *et al.*, *Earth Planet. Sci. Lett.* **225**, 243 (2004).
13. J. H. Nguyen, N. C. Holmes, *Nature* **306**, 2239 (2004).
14. R. C. Liebermann, A. E. Ringwood, *J. Geophys. Res.* **78**, 6926 (1973).
15. A. J. Campbell, D. L. Heinz, *Science* **257**, 66 (1992).
16. W. Sturhahn *et al.*, *Phys. Rev. Lett.* **74**, 3832 (1995).
17. W. Sturhahn, V. G. Kohn, *Hyperfine Interactions* **123/124**, 367 (1999).
18. M. Hu *et al.*, *Phys. Rev. B* **67**, 094304 (2003).
19. R. Lübbers, H. F. Grünsteudel, A. I. Chumakov, G. Wortmann, *Science* **287**, 1250 (2000).
20. Materials and methods are available as supporting material on *Science* Online.
21. J. F. Lin *et al.*, *Geophys. Res. Lett.* **31**, L14611 (2004).
22. G. Shen *et al.*, *Phys. Chem. Miner.* **31**, 353 (2004).
23. L. S. Dubrovinsky, S. K. Saxena, P. Lazor, *Phys. Chem. Miner.* **25**, 434 (1998).
24. L. S. Dubrovinsky, S. K. Saxena, F. Tutti, S. Rekhi, *Phys. Rev. Lett.* **84**, 1720 (2000).
25. L. S. Dubrovinsky, S. K. Saxena, N. A. Dubrovinskais, S. Rekhi, T. LeBihan, *Am. Mineral.* **85**, 386 (2000).
26. F. Birch, *J. Geophys. Res.* **83**, 1257 (1978).
27. W. Mao *et al.*, *Geophys. Res. Lett.* **31**, L15618 (2004).
28. D. L. Heinz, *Geophys. Res. Lett.* **17**, 1161 (1990).
29. A. M. Dziewonski, D. L. Anderson, *Phys. Earth Planet. Inter.* **25**, 297 (1981).
30. L. S. Dubrovinsky, N. A. Dubrovinskais, T. LeBihan, *Proc. Natl. Acad. Sci. U.S.A.* **98**, 9484 (2001).
31. O. L. Anderson, L. S. Dubrovinsky, S. K. Saxena, T. LeBihan, *Geophys. Res. Lett.* **28**, 399 (2001).
32. J. F. Lin *et al.*, *Geophys. Res. Lett.* **30**, 2112 (2003).
33. J. F. Lin *et al.*, *Earth Planet. Sci. Lett.* **226**, 33 (2004).

34. This work and use of the APS are supported by the U.S. Department of Energy (DOE), Basic Energy Sciences (BES), Office of Science, under contract no. W-31-109-ENG-38, and by the state of Illinois under the Higher Education Cooperation Act. We thank GeoSoilEnviroCARS and APS for the use of the ruby fluorescence system and E. E. Alp, D. Errandonea, S.-K. Lee, V. Struzhkin, M. Hu, D. L. Heinz, G. Steinle-Neumann, R. Cohen, J. Burke, V. Prakapenka, M. Rivers, S. Hardy, T. Duffy, and J. M. Jackson for their help and discussions. Work at Carnegie was supported by DOE/BES, DOE/National Nuclear Security Administration (Carnegie/DOE Alliance Center), NSF, and the W. M. Keck Foundation.

Supporting Online Material

www.sciencemag.org/cgi/content/full/308/5730/1892/DC1
Materials and Methods
Fig. S1
Table S1
References

2 March 2005; accepted 17 May 2005
10.1126/science.1111724

Deep-Sea Temperature and Circulation Changes at the Paleocene-Eocene Thermal Maximum

Aradhna Tripati* and Henry Elderfield

A rapid increase in greenhouse gas levels is thought to have fueled global warming at the Paleocene-Eocene Thermal Maximum (PETM). Foraminiferal magnesium/calcium ratios indicate that bottom waters warmed by 4° to 5°C, similar to tropical and subtropical surface ocean waters, implying no amplification of warming in high-latitude regions of deep-water formation under ice-free conditions. Intermediate waters warmed before the carbon isotope excursion, in association with downwelling in the North Pacific and reduced Southern Ocean convection, supporting changing circulation as the trigger for methane hydrate release. A switch to deep convection in the North Pacific at the PETM onset could have amplified and sustained warming.

PETM was a short-lived global warming event about 55 million years ago (Ma) that may provide insights into the environmental consequences of rising greenhouse gas levels (*1*, *2*). A reduction in the carbonate content of deep-sea sediments (*2*) and a large negative excursion in marine and terrestrial carbon isotope ($\delta^{13}C$) records (*1–3*) are associated with the PETM and indicate the addition of ^{13}C-depleted carbon to the oceans and atmosphere. A possible source of this carbon was the dissociation of ~1000 to 2100 gigatons (Gt) of methane hydrate in ocean sediments (*4*), most or all of which would have oxidized, raising atmospheric CO_2 by 70 to 160 parts per million by volume (ppmv) (*5*, *6*). Benthic foraminiferal taxa exhibit increased extinction rates during the PETM, probably because of deep-sea oxygen deficiency and a decrease in seawater carbonate ion concentration (*2*).

The climatic response to rising greenhouse gas levels in the past has been debated because of equivocal ocean temperature reconstructions based on foraminiferal oxygen isotope ratios ($\delta^{18}O_C$), which are a function of both temperature and seawater $\delta^{18}O$ ($\delta^{18}O_W$). To circumvent this ambiguity, the Mg/Ca temperature proxy has been applied to planktonic foraminifera, and it documented a 4 to 5°C warming of sea-surface temperatures (SST) across the PETM in the subtropical (*7*) and tropical ocean (*7*, *8*).

We investigated the evolution of deep-sea temperatures, high-latitude SST, and circulation patterns using foraminiferal Mg/Ca and stable isotope ratios (*9*, *10*) in order to examine the causes and consequences of the $\delta^{13}C$ excursion and the PETM. We used Mg/Ca ratios of benthic foraminifera to develop estimates of bottom water temperatures (T_B) for deep sites in the subtropical South Atlantic (Site 527) and tropical North Pacific (Site 1209) oceans, and for a site at intermediate depths in the equatorial Pacific Ocean (Site 865) (table S1). These temperatures should reflect surface conditions in high-latitude regions of deep-water formation. We integrated these data with SST records (*7*, *8*) to study the spatial pattern of warming and changes in the

Department of Earth Sciences, University of Cambridge, Downing Street, CB2 3EQ, UK.

*To whom correspondence should be addressed. E-mail: atri02@esc.cam.ac.uk

thermal structure of the tropical oceans. We also constructed the first benthic stable isotope record for the deep Pacific through the PETM for comparison with published records from South Atlantic Sites 527 (*2*) and 690 (Atlantic sector, Southern Ocean) (*1*), in order to investigate basinal gradients in T_B, $\delta^{18}O_W$ and $\delta^{13}C$.

Late Paleocene T_B (Fig. 1) at Atlantic Site 527 were 12 to 13°C (~3400 m in paleodepth), similar to previous early Cenozoic estimates (*11*). Pacific temperatures were warmer, with T_B at deep Site 1209 of ~14°C (~2400 m in paleodepth), and >16°C at intermediate Site 865 (~1300 m in paleodepth). The record of T_B for Pacific Site 865 indicates 2 to 3°C warming at intermediate depths between 55.60 and 55.50 Ma, before the $\delta^{13}C$ excursion. Coincident with the $\delta^{13}C$ excursion is an abrupt increase in benthic foraminiferal Mg/Ca ratios, indicating warming of 3°C at the intermediate site and of 4°C at the two deep sites. Estimated peak T_B are 21°C and 17°C, respectively, similar to recent estimates based on dinoflagellates (*12*) of Arctic Ocean surface temperatures for the PETM. At all sites, T_B decreased within 50,000 years after the $\delta^{13}C$ excursion and reached Late Paleocene background values after 150,000 to 200,000 years, ~50,000 years after $\delta^{13}C$ values recover.

Basinal $\delta^{13}C$ gradients (*13*–*15*) and modeling (*16*) show deep waters would have formed in the high latitudes during the late Paleocene and early Eocene. Tropical and subtropical SST from Mg/Ca ratios show warming of 4 to 5°C (*7*, *8*), implying that the zonal pattern of surface ocean warming was relatively uniform during the PETM. This paleoclimatic response is consistent with minimal sea ice and continental ice during the Late Paleocene, as melting would have accelerated high-latitude warming through ice-albedo feedbacks. The pole-to-equator temperature gradient (presuming convection occurred in the high latitudes) shows no discernable change associated with the carbon release, with a gradient of 19.0 ± 1°C before the carbon isotope excursion and 19.5 ± 1°C during the PETM. Thus, in the absence of extensive continental ice sheets and sea ice, rising greenhouse gas levels resulted in ocean warming at all latitudes, with no detectable amplification of warming in the high-latitude regions of deep-water formation.

$\delta^{18}O_W$ covaries with salinity and is estimated by subtracting the temperature component from benthic $\delta^{18}O_C$ (Fig. 2A) (*1*). From the late Paleocene to the PETM peak, the calculated $\delta^{18}O_W$ decrease at South Atlantic Site 527 is 0.1 to 0.3 per mil (‰), indicating that deep waters freshened in association with warming. At Southern Ocean Site 690, the $\delta^{18}O_W$ decrease is 0.4 to 0.6‰, giving a larger amount of freshening. Global warming is thought to have enhanced precipitation in the high latitudes of the Southern Hemisphere because of greater vapor transport from the subtropics (*16*), and there is also evidence for higher subtropical surface water salinities at the PETM (*7*). In contrast, at Site 1209, $\delta^{18}O_W$ increased by 0.3 to 0.5‰, indicative of more saline deep waters in the North Pacific during the PETM.

Hydrographic sections (Fig. 3) derived by combining estimates of T_B for different depths with mixed-layer and thermocline temperatures for the tropical Pacific (fig. S1) show that the entire water column warmed by 4 to 5°C and that the earliest Eocene thermal structure was similar to that of the Latest Paleocene. Combining this with $\delta^{18}O_C$ indicates that the tropical Pacific vertical salinity gradient must have evolved substantially, with an increase in deep-water salinity and a freshening of overlying waters during the PETM reflect-

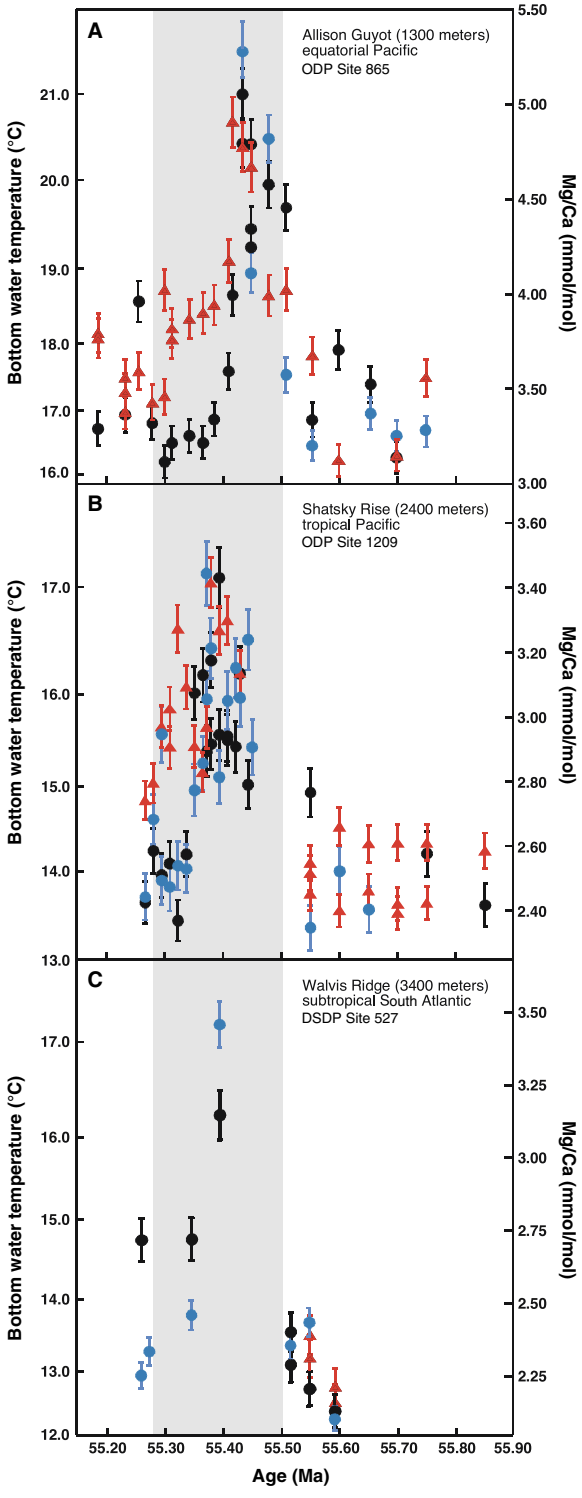

Fig. 1. High-resolution benthic foraminiferal Mg/Ca records across the PETM and corresponding temperature scale (black circles, *Oridorsalis umbonatus*; blue circles, *Nuttallides truempyi*; red triangles, *Cibicidoides* spp.). (**A**) Allison Guyot, ODP site 865 (equatorial Pacific Ocean, 1300 m in depth). (**B**) Shatsky Rise, ODP site 1209 (tropical North Pacific Ocean, 2400 m in depth). (**C**) Walvis Ridge, Deep-Sea Drilling Program (DSDP) site 527 (subtropical South Atlantic Ocean, 3400 m in depth). Mg/Ca ratios are normalized to *O. umbonatus* (*30*). The PETM interval (55.50 to 55.28 Ma) is highlighted (gray bar). In order to place results on a common age scale, we used reported datum levels for the carbon isotope base, peak, and recovery and also used the reported first occurrence of *Discoaster multiradiatus* and *Fasculithes tympaniform* (table S3). Planktic foraminiferal $\delta^{13}C$ data are shown in fig. S3. Absolute chronologies for the PETM are subject to revision.

ing a sensitive hydrologic cycle and/or changing ocean circulation.

The Latest Paleocene intermediate water warming would likely have destabilized large regions of sedimentary methane hydrates, added ^{13}C-depleted carbon to the oceans and the atmosphere, and initiated the PETM (*4*, *16*). To assess whether changing ocean circulation could have triggered intermediate water warming, we inferred deep-water source regions by constraining aging, temperature, and salinity gradients between the South Atlantic, Southern Ocean, and North Pacific during four time intervals. As waters sink and flow through the ocean, they accumulate respired ^{12}C-rich CO_2 and nutrients from the remineralization of raining organic matter, so that young, recently ventilated, deep waters will have higher $\delta^{13}C$ than deep waters that are further from source regions.

1) Late Paleocene (>55.60 Ma): Benthic $\delta^{13}C$ values for Pacific Site 1209 are ~0.5‰ lower than at the Atlantic (Figs. 2B and 4) and Southern Ocean sites (fig. S2), implying that South Atlantic waters were ventilated more recently than those in the North Pacific. Differences in surface water productivity between regions can also affect $\delta^{13}C$ gradients between sites, and the Southern Ocean site may have experienced relatively large changes in productivity across the PETM (*17*). However, the other sites would have been located within subtropical gyres (*16*), characterized by relatively low-productivity surface waters. Comparison of $\delta^{18}O_C$ and T_B shows that bottom waters at the Pacific site were ~1°C warmer and similar in salinity to bottom waters at the Atlantic and Southern Ocean sites (Fig. 4 and fig. S2) and therefore were less dense. Thus, the data are consistent with deep ocean overturning being driven by convection in the Southern Ocean (*13*–*15*, *18*).

2) Latest Paleocene (55.60 to 55.50 Ma): The $\delta^{13}C$ differences between the three sites decrease, converging by the onset of the $\delta^{13}C$ excursion, suggesting that deep water was aging in the South Atlantic and becoming younger in the North Pacific. Waters at the Pacific site became more saline, whereas at the Atlantic site they became slightly fresher and warmer by 1°C (Fig. 4 and table S2). The decrease in planktonic foraminiferal $\delta^{18}O_C$ at Site 690 (*19*) indicates Southern Ocean surface waters also became fresher and/or warmer. These findings suggest that deep-water formation in the Southern Ocean decreased with the gradual development of a second circulation cell in the North Pacific, coincident with intermediate water warming in the Pacific.

3) PETM (~55.45 Ma): Samples from the peak of the PETM indicate a distribution in deep-water $\delta^{13}C$ very different from previous distributions. Although the whole-ocean shift in $\delta^{13}C$ records the injection of ^{13}C-depleted carbon, the differences in $\delta^{13}C$ imply that bottom waters at the Pacific site were younger than at the Atlantic and Southern Ocean sites. Deep waters would have been ^{13}C-poor because of weak rates of overturning in the Southern Ocean and slow

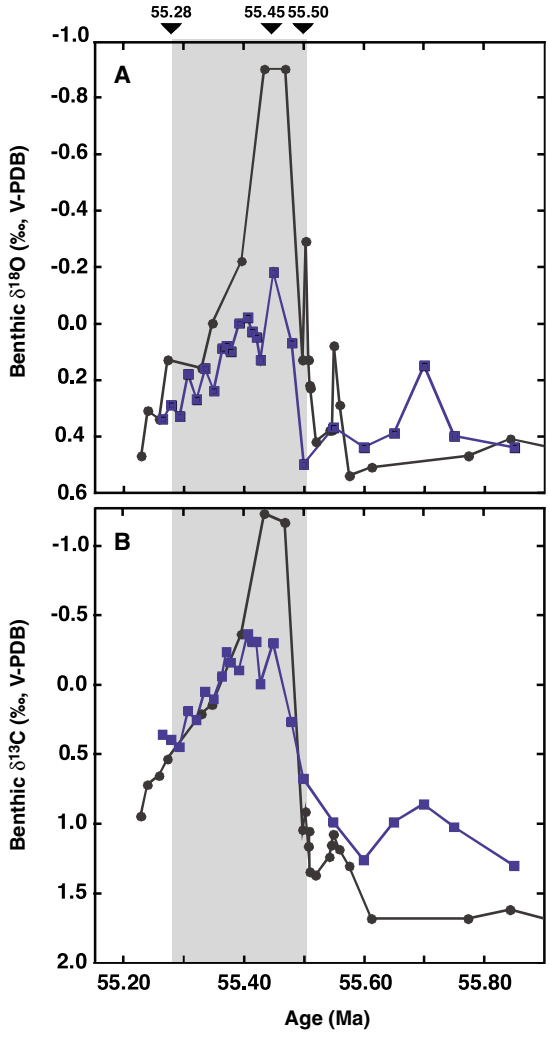

Fig. 2. (**A**) Benthic foraminiferal $\delta^{18}O$ for deep sites in the North Pacific (blue line, ODP Site 1209, Shatsky Rise) and South Atlantic (dark gray line, DSDP Site 527, Walvis Ridge). Black triangles point to datum levels. Not shown are two additional datum levels (56.20 and 55.00 Ma) that were used to constrain the age models for both sites. The PETM interval is shaded. (**B**) Benthic foraminiferal $\delta^{13}C$ for deep sites in the North Pacific and South Atlantic. V-PDB, Vienna Peedee Belemnite.

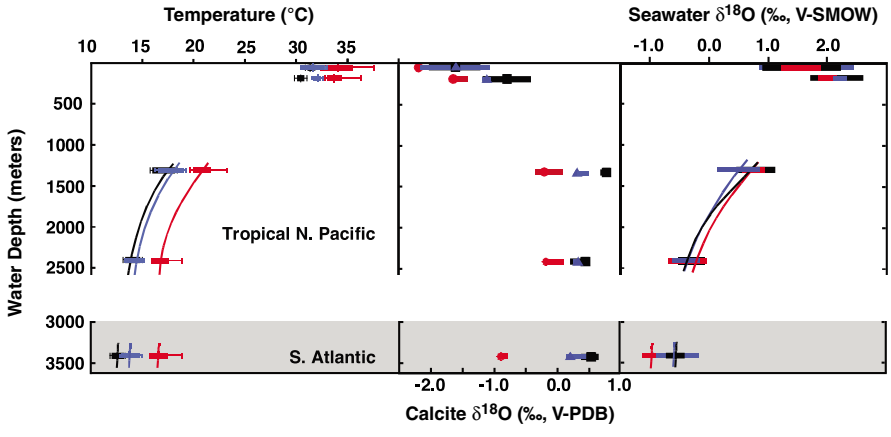

Fig. 3. Vertical profiles of temperature, foraminiferal $\delta^{18}O$, and seawater $\delta^{18}O$ for the tropical Pacific for different time slices during the Late Paleocene (black), PETM (red), and Earliest Eocene (blue). Mixed-layer temperatures and thermocline temperatures are estimated with planktonic foraminiferal Mg/Ca values at ODP Sites 1209 and 865 (fig. S1) (*7*, *8*) and with benthic foraminiferal Mg/Ca–based T_B for sites at different water depths (Fig. 1). Means (symbols), the range of estimates (thick lines), and error bars (thin lines) are shown for each interval. Data for the South Atlantic (DSDP Site 527) are shown in the shaded panel for comparison. V-SMOW, Vienna Standard Mean Ocean Water.

ventilation rates in South Atlantic basins. Elevated Southern Ocean productivity accompanying the PETM (*17*) may have also enhanced the $\delta^{13}C$ contrast with the deep Pacific. Bottom waters at the Pacific site were similar in temperature to those of the Atlantic and Southern Ocean sites, but more salty. These results indicate that the PETM was associated with a unique mode of ocean circulation, with a saline and warm North Pacific deep-water mass that was younger and more dense than South Atlantic and Southern Ocean waters, consistent with convection in the North Pacific and decreased deep-water formation in the Southern Ocean. Data also indicate a switch from mostly thermally stratified to a salinity-stratified, isothermal deep ocean (Fig. 3).

4) Earliest Eocene (<55.25 Ma): The basinal $\delta^{13}C$ gradient was eliminated by 55.40 Ma, consistent with increased South Atlantic ventilation rates. $\delta^{13}C$ values begin to diverge by 55.28 Ma, coincident with the $\delta^{13}C$ recovery, with the highest ratios at the Atlantic and Southern Ocean sites and the lowest at the Pacific site. Bottom waters at the Pacific site were slightly warmer and fresher than at the Atlantic and Southern Ocean sites. As such, an inferred decline in North Pacific overturning rates and increased deep-water formation in the Southern Ocean are associated with the $\delta^{13}C$ recovery.

These reconstructions support ocean modeling experiments representing Late Paleocene thermohaline circulation that predict convection in the Southern Hemisphere between Antarctica and Australia (*16*). Deep waters formed along the Antarctic margin would have filled the deep Pacific and Indian Ocean basins and mixed with intermediate waters in the Atlantic sector of the Southern Ocean to fill the deep South Atlantic basins. Magmatic activity and high heat flow associated with activity of the Iceland Plume is thought to have resulted in enhanced volcanic emissions of CO_2 and the emergence of a North Atlantic land bridge during the Latest Paleocene (*20*). These developments are modeled to have affected ocean circulation by driving an increase in North Pacific surface water salinities and a freshening of Southern Ocean surface waters. Rising CO_2 levels would be expected to have increased high-latitude precipitation, causing a decrease in Southern Ocean surface water salinities. The formation of the land bridge would have restricted the flow of water from the Nordic Seas to the North Atlantic Ocean (*20*) and forced North Pacific surface water salinities to gradually rise, because of enhanced transport of saline thermocline waters from the subtropical North Atlantic into the North Pacific Basin through the Central American Seaway (*16*).

Downwelling in the North Pacific and deepened subtropical subduction during the Latest Paleocene would likely have caused warming of intermediate (Fig. 1) and thermocline (*7*) waters. This process could have destabilized regions of sedimentary methane hydrates and driven the $\delta^{13}C$ excursion (*4*, *16*). The greatest amount of subduction-induced warming and carbon release is modeled to have occurred in Atlantic basins, consistent with the observation that Atlantic carbonate dissolution is much more pronounced than in the Pacific (*16*). Methane hydrate dissociation would have fueled initial PETM warming and hydrologic cycle changes, which in turn would have strengthened overturning rates in the North Pacific, weakened deep-water production in the Southern Ocean, and reduced ventilation rates in the South Atlantic. A threshold response to increasing surface water salinities near the Alaskan Margin

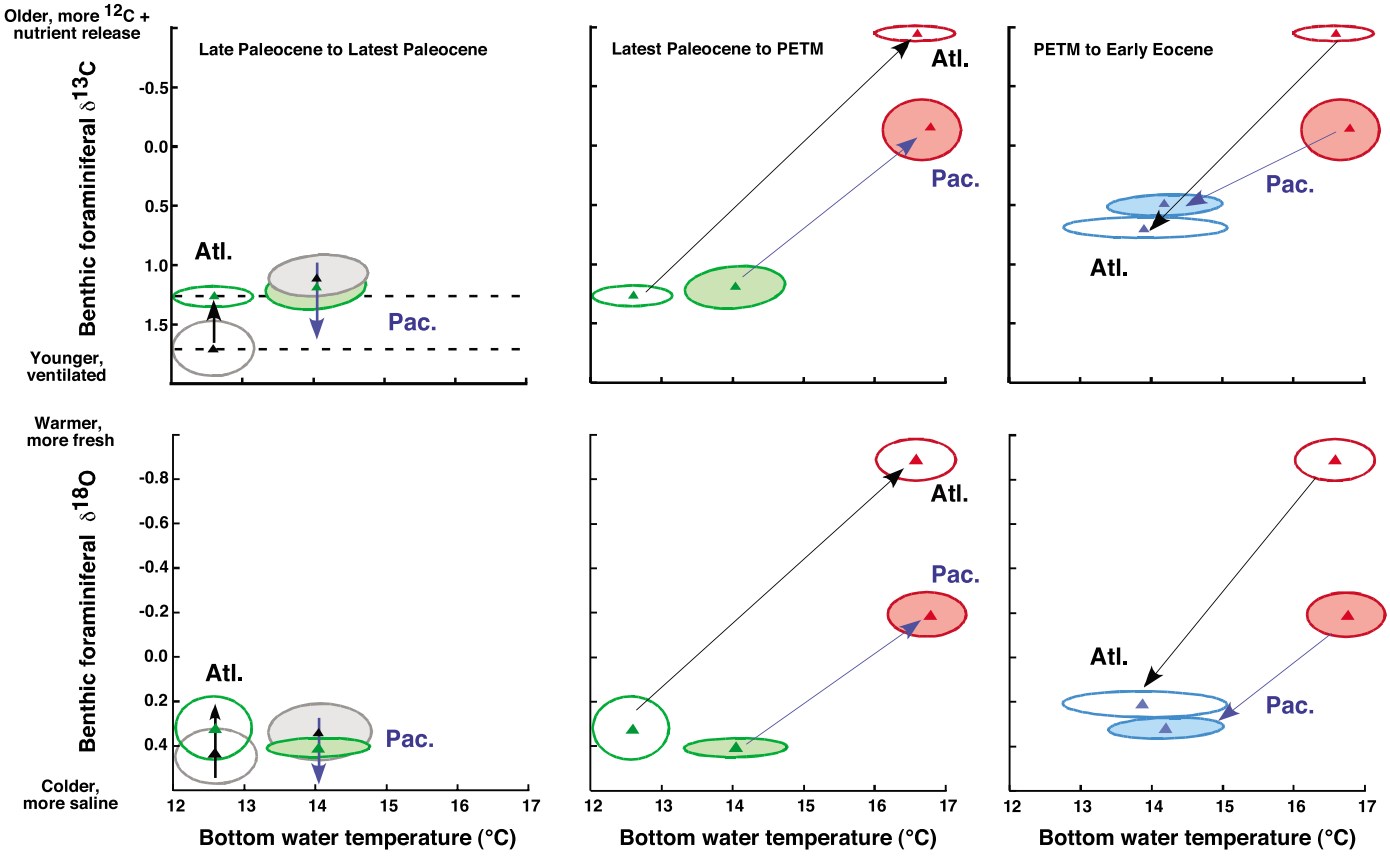

Fig. 4. Cross-plot for T_B versus benthic foraminiferal (top) $\delta^{13}C$ and (bottom) $\delta^{18}O$ across the PETM, illustrating the evolution of deep-water gradients between the North Pacific (Pac., shaded ellipses, Shatsky Rise site) and South Atlantic (Atl., open elipses, Walvis Ridge site). Range (ellipses) and average values (triangles) are shown for specific time slices (gray, Late Paleocene; green, Latest Paleocene; red, PETM; and blue, Earliest Eocene). Dashed lines in the top left panel indicate Atlantic mean $\delta^{13}C$ values. Table S2 shows the change in slope of $\Delta\delta^{18}O/\Delta T_B$ before the PETM (between the Late Paleocene and the Latest Paleocene), indicating a change in the salinity contrast between the South Atlantic and North Pacific.

and salt contrast between the North Pacific and Southern Ocean would have been the sudden onset of deep convection in the North Pacific. Bottom waters formed would have filled deep Pacific basins and flowed through the Indonesian passage into the eastern Indian Ocean basin, and the locus of deep-water formation along Antarctica would have shoaled (*16*).

How would methane hydrate dissociation and an abrupt change in ocean circulation have affected climate? The injection of 2000 Gt of CH_4 into the oceans over ~10,000 years (the amount necessary to drive the $\delta^{13}C$ excursion) would have been insufficient to raise atmospheric CO_2 concentrations enough to drive whole-ocean warming of 4 to 5°C. The radiative forcing associated with a 70- to 160-ppmv increase in CO_2 would have caused only ~1°C warming (*21*), and therefore the clathrate hypothesis necessitates still unresolved climatic feedbacks to amplify and sustain PETM warmth.

The abrupt switch to convection in the North Pacific is modeled to have warmed the deep ocean by up to 3 to 5°C (Fig. 1) (*16*) and could have driven the PETM by maintaining high levels of atmospheric CO_2 and water vapor. Circulation-induced ocean warming could have driven additional increases in atmospheric CO_2 by destabilizing methane hydrates in deep ocean sediments (*16*). The solubility of CO_2 in seawater would also have decreased because of temperature and salinity changes, promoting higher atmospheric CO_2. Tropical ocean warming would have also promoted a more vigorous hydrologic cycle, higher evaporation rates, and saturation vapor pressures, resulting in increased levels of atmospheric water vapor (*22*), consistent with proxy data for surface water salinity (*7*, *8*) and humidity (*23*, *24*) across the PETM. The added radiative absorption from water vapor would have heightened the sensitivity of surface temperatures to rising atmospheric CO_2 and CH_4 concentrations, providing a strong positive feedback to warming (*25*, *26*). The eventual sequestration of carbon through the biologic pump (*17*), terrestrial productivity (*27*), and weathering (*28*) would have resulted in global cooling over ~100,000 to 200,000 years. Associated temperature and hydrologic cycle changes would have driven a return to deep sinking in the Southern Hemisphere and shutdown of convection in the North Pacific (*16*).

References and Notes

1. J. P. Kennett, L. D. Stott, *Nature* **353**, 225 (1991).
2. E. Thomas, N. J. Shackleton, in *Correlation of the Early Paleogene in Northwest Europe*, R. W. O. Knox, R. M. Corfield, R. E. Dunay, Eds. (Geological Society Special Publication 101, London, 1996), pp. 401–441.
3. P. L. Koch, J. C. Zachos, P. D. Gingerich, *Nature* **358**, 319 (1992).
4. G. R. Dickens, J. R. O'Neil, D. C. Rea, R. M. Owen, *Paleoceanography* **10**, 965 (1995).
5. G. R. Dickens, M. M. Castillo, J. C. G. Walker, *Geology* **25**, 259 (1997).
6. G. A. Schmidt, D. T. Shindell, *Paleoceanography* **18**, 10.1029/2002PA000757 (2003).
7. A. Tripati, H. Elderfield, *Geochem. Geophys. Geosyst.* **5**, 10.1029/2003GC000631 (2004).
8. J. Zachos *et al.*, *Science* **302**, 1551 (2003).
9. We analyzed *Oridorsalis umbonatus, Nuttallides truempyi*, and *Cibicidoides* spp. benthic taxa that have previously been used to reconstruct low-resolution T_B records for the Cenozoic and high-resolution records across the Eocene-Oligocene boundary (*11*). Seawater Mg/Ca can be considered constant over the duration of the PETM, because of the relatively long oceanic residence times of Ca (~10^6 years) and Mg (10^7 years) (*29*). The magnitude of warming calculated is therefore independent of seawater Mg/Ca ratio used. Absolute temperatures were calculated with current estimates for taxon-specific pre-exponential constants (*30*) and reconstructions of seawater Mg/Ca for 55 Ma (3.1 mmol/mol) (*31*).
10. Materials and methods are available as supporting material on *Science* Online.
11. C. Lear, H. Elderfield, P. Wilson, *Science* **287**, 269 (2000).
12. Shipboard Scientific Party, "Arctic Coring Expedition (ACEX): Paleoceanographic and tectonic evolution of the central Arctic Ocean" (Integrated Ocean Drilling Program Preliminary Report 302, ECORD, 2005), available at www.ecord.org/exp/acex/302PR.html.
13. D. K. Pak, K. G. Miller, *Paleoceanography* **7**, 405 (1992).
14. R. Corfield, J. Cartlidge, *Terra Nova* **4**, 443 (1992).
15. K. Miller, R. Fairbanks, G. Mountain, *Paleoceanography* **2**, 1 (1987).
16. K. L. Bice, J. Marotzke, *Paleoceanography* **17**, 9 (2002).
17. H. Stoll, S. Bains, *Paleoceanography* **18**, 10.1029/2002PA000875 (2003).
18. D. J. Thomas, T. J. Bralower, C. E. Jones, *Earth Planet. Sci. Lett.* **209**, 309 (2003).
19. D. J. Thomas, J. C. Zachos, T. J. Bralower, E. Thomas, S. Bohaty, *Geology* **30**, 1067 (2002).
20. R. W. Knox, in *Late Paleocene-Early Eocene Climatic and Biotic Events in the Marine and Terrestrial Record*, M. P. Aubry, S. G. Lucas, W. A. Berggren, Eds. (Columbia Univ. Press, New York, 1998), pp. 91–102.
21. H. Rennsen, C. J. Beefs, T. Fichefet, H. Goosse, D. Kroon, *Paleoceanography* **19**, 10.1029/2003PA000968 (2004).
22. A. Inamdar, V. Ramanathan, *J. Geophys. Res.* **103**, 32177 (1998).
23. C. Robert, J. P. Kennett, *Geology* **22**, 211 (1994).
24. G. J. Bowen, D. J. Beerling, P. L. Koch, J. C. Zachos, T. Quattlebaum, *Nature* **432**, 495 (2004).
25. S. Manabe, R. T. Wetherald, *J. Atmos. Sci.* **24**, 241 (1967).
26. D. Rind *et al.*, *Nature* **349**, 500 (1991).
27. D. J. Beerling, *Palaeogeogr. Palaeoclimatol. Palaeoecol.* **161**, 395 (2000).
28. G. Ravizza, R. N. Norris, J. Blusztajn, M. P. Aubry, *Paleoceanography* **16**, 155 (2001).
29. W. S. Broecker, T. H. Peng, *Tracers in the Sea* (Eldigio, Palisades, NY, 1982).
30. C. Lear, Y. Rosenthal, N. Slowey, *Geochim. Cosmochim. Acta* **66**, 3375 (2002).
31. B. Wilkinson, T. Algeo, *Am. J. Sci.* **289**, 1158 (1989).

32. We thank W. Broecker for discussions; K. Bice, M. Bickle, S. Crowhurst, and A. Piotrowski for thoughtful reviews; R. Eagle for his support and advice; P. Rumford, B. Horan, and Gulf Coast Ocean Drilling Program Repository staff for provision of samples; and L. Booth, P. Ferretti, and M. Greaves for their invaluable technical help. This research used samples and data provided by the Ocean Drilling Program (ODP). Supported by the Comer Foundation.

Supporting Online Material

www.sciencemag.org/cgi/content/full/308/5730/1894/DC1
Materials and Methods
Figs. S1 to S3
Tables S1 to S3
References and Notes

27 December 2004; accepted 20 May 2005
10.1126/science.1109202

Snowfall-Driven Growth in East Antarctic Ice Sheet Mitigates Recent Sea-Level Rise

Curt H. Davis,[1]* Yonghong Li,[1] Joseph R. McConnell,[2] Markus M. Frey,[3] Edward Hanna[4]

Satellite radar altimetry measurements indicate that the East Antarctic ice-sheet interior north of 81.6°S increased in mass by 45 ± 7 billion metric tons per year from 1992 to 2003. Comparisons with contemporaneous meteorological model snowfall estimates suggest that the gain in mass was associated with increased precipitation. A gain of this magnitude is enough to slow sea-level rise by 0.12 ± 0.02 millimeters per year.

Recent studies report substantial contributions from the Greenland (*1*, *2*) and Antarctic (*3*, *4*) ice sheets to present-day sea-level rise of ~1.8 mm/year (*5*). Rapid increases in near-coastal Greenland ice-sheet thinning (*2*) and West Antarctic glacial discharge (*4*) strengthen concern about accelerated sea-level rise caused by ice-sheet change. In contrast, the latest Intergovernmental Panel on Climate Change (IPCC) assessment predicts that overall, the Antarctic ice sheet will absorb mass during the 21st century due to increased precipitation in a warming global climate (*6*). Thus, increased precipitation over Antarctica could mitigate some of the mass loss from other terrestrial ice sources and their contributions to global sea-level rise. Here, we analyze elevation change of the Antarctic ice-sheet interior from 1992 to 2003 using nearly continuous satellite radar altimeter measurements. Because temporal variations in snowfall have been linked previously to decadal elevation change in Greenland's interior (*7*), we compare the observed elevation change to newly released meteorological model estimates of contemporaneous snowfall.

After correction for isostatic uplift, ice-sheet elevation-change measurements from continuous and/or repeat altimeter surveys are a direct measure of net mass change. We measured elevation change (*dH*) over 8.5 million km^2 of the grounded Antarctic ice-sheet interior (~70% of total ice-sheet area) using ~347 million *dH* measurements derived from European Remote-Sensing Satellite–1 (ERS-1) and ERS-2 ice-mode satellite radar altimeter data (coverage extends to 81.6°S). These data were processed and analyzed in a manner consistent with the procedures and methods described in (*8*–*10*). We generated time series (Fig. 1) of monthly *dH* averages from 1992 to 2003 for ~1500 1° × 2° (latitude × longitude) regions, 22 major drainage basins, Berkner Island, West and East Antarctica, and the entire region of coverage (ROC) (*11*).

The *dH* time series were fit with an autoregressive (AR) model superimposed upon a longer-term trend (Fig. 1). We used the AR model to characterize seasonal and interannual variations in the elevation-change time series (*8*). The long-term trend was modeled as a polynomial that was estimated from a smoothed version of the time series generated by an iterative local average filter (*10*). We estimated the average rate of elevation change (*dH/dt*) during the 11-year period by a least-squares fit to the long-term polynomial trend and then corrected for isostatic uplift (*12*). The 11-year elevation-change results (Fig. 2) show that the vast majority of regions in East Antarctica are thickening, especially in the interior, whereas regions in West Antarctica exhibit both strong thickening and thinning trends. At the basin scale, *dH/dt* values range from 0 to +6 cm/year for East Antarctica, whereas there is substantial spatial variability in West Antarctica, with *dH/dt* values ranging from –10 to +19 cm/year (table S1). The coarse spatial coverage of satellite radar altimetry compromises its utility as a tool to map elevation changes in steeply sloped coastal regions, so these results only address the average elevation change of the Antarctic ice-sheet interior within the ROC.

The dominant characteristic in East Antarctica is the large and spatially coherent area of slight thickening throughout the interior. Also noteworthy is the area with moderate thickening south and east of the Amery ice shelf in basin B-C, which changes to strong thickening in the near-coastal area of basin C-C′ east of the Amery ice shelf. Overall, the East Antarctic ice-sheet interior within the ROC is thickening at a rate of 1.8 ± 0.3 cm/year. In contrast, the West Antarctic ice sheet exhibits bimodal behavior. There is modest to strong thinning in the basins of Marie Byrd Land (E″-H). Strong thinning in basin G-H is associated with even more rapid thinning in the coastal outlets of the Pine Island and Thwaites glaciers (*4*, *9*, *13*), possibly caused by increased basal melting due to ocean thermal forcing (*14*). Conversely, basins adjacent to the Antarctic Peninsula and Ronne ice

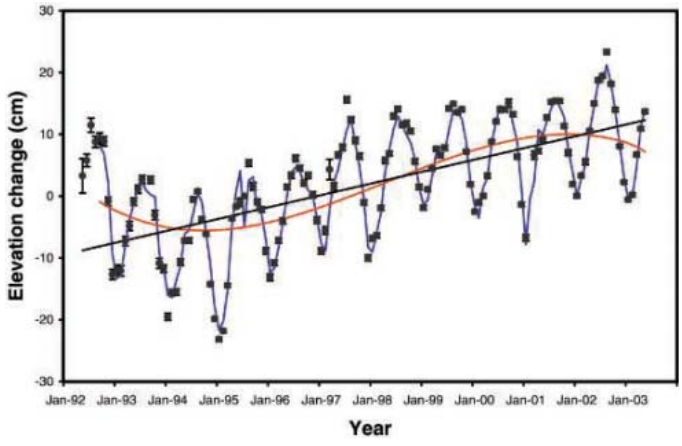

Fig. 1. Elevation-change (black circles) time series from 1992 to 2003 for ~7.1 × 10^6 km^2 of the East Antarctic ice-sheet interior. The seasonal and interannual cycle (blue line) and long-term trend (red line) are modeled as described in the text. The average rate of change (black line) for the entire time period is 1.8 cm/year after adjustment for isostatic uplift. A steady increase in elevation since about 1995 is apparent. The average rate of change from 1995 to 2003 is 2.2 cm/year after adjustment for isostatic uplift.

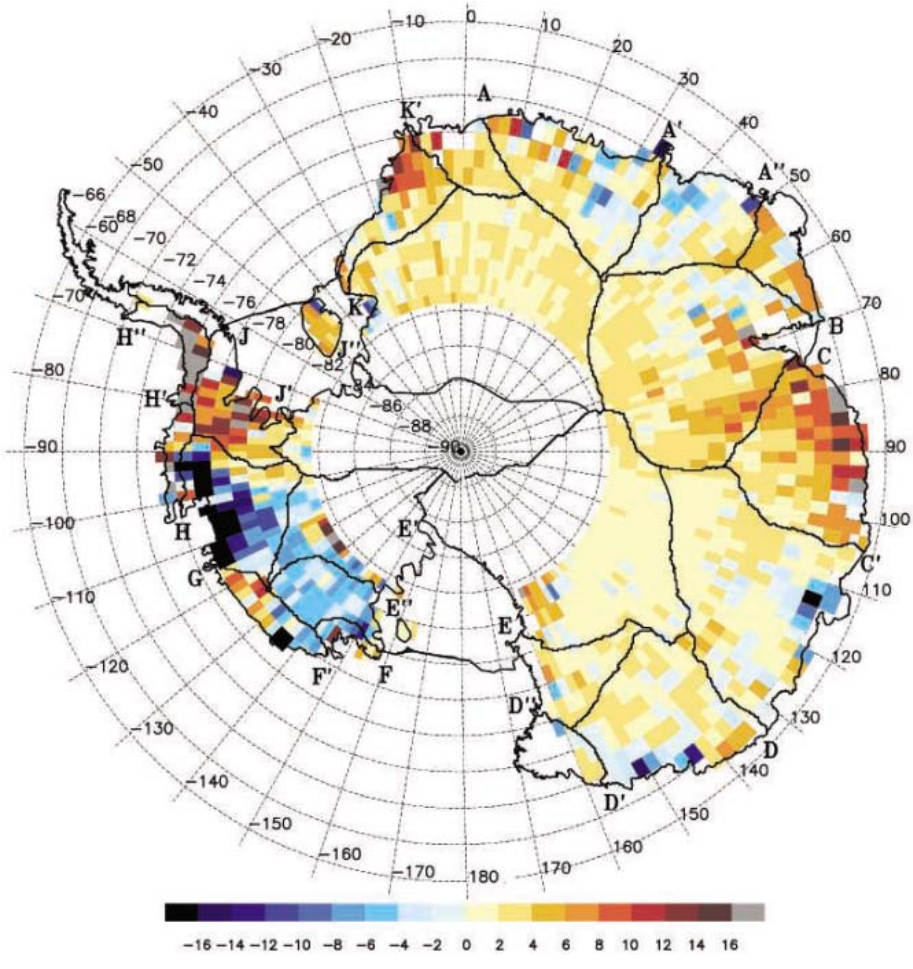

Fig. 2. Elevation-change rate (cm/year) from 1992 to 2003 for 8.5 × 10^6 km^2 of the grounded Antarctic ice-sheet interior. Results are shown in 1° × 2° (latitude × longitude) regions, and boundaries of major drainage basins discussed in the text are superimposed.

[1]Department of Electrical and Computer Engineering, University of Missouri–Columbia, Columbia, MO 65211, USA. [2]Desert Research Institute, University and Community College System of Nevada, Reno, NV 89512, USA. [3]Department of Hydrology and Water Resources, University of Arizona, Tucson, AZ 85721, USA. [4]Department of Geography, University of Sheffield, Sheffield S10 2TN, UK.

*To whom correspondence should be addressed. E-mail: davisch@missouri.edu

shelf (basins H-H′, H′-H″, J-J′) show strong thickening of between 8 and 19 cm/year. However, these regions represent only ~30% of the area of the West Antarctic ice sheet within the ROC, so the overall trend is slight thinning in the interior of 0.9 ± 0.3 cm/year.

Elevation-change results for West Antarctica, East Antarctica, and the ROC are significantly more positive than previously reported for the time period from 1992 to 1996 (*15*). In East Antarctica, this is due primarily to a steady increase in elevation that began in 1995 (Fig. 1). In West Antarctica, this is due to both an increase in spatial coverage for these results (basins H-H′, H′-H″, and J-J′) and a near-zero rate of overall elevation change since 1997, as compared to a more negative overall trend in the preceding years. For the ROC, the 5:1 ratio in East versus West Antarctic area coverage causes slight thickening overall at the rate of 1.4 ± 0.3 cm/year.

Interpretation of elevation-change measurements requires precise knowledge of contemporaneous changes in snowfall because temporal snowfall variations can cause interannual-to-decadal or longer fluctuations in ice-sheet elevation (*7*). Because we have no direct precipitation measurements exactly spanning the time period of the altimetry measurements, we used newly released 1980 to 2001 ERA-40 reanalysis from the European Centre for Medium-Range Weather Forecasts (ECMWF) together with 2002 to 2003 ECMWF operational analyses to evaluate overall temporal trends in snowfall (Fig. 3) during the altimetry measurement period (*11*).

In East Antarctica, the modeled spatial patterns of average snowfall change broadly match the *dH/dt* results derived from radar altimetry, suggesting that much of the 1992 to 2003 elevation change may be linked to changes in snow accumulation. These include many of the dominant elevation-change features observed during the 1992 to 2003 period (Fig. 2). Specifically, the modeled snowfall trend matches the large and coherent area of slight thickening throughout the interior, slight to moderate thinning in the coastal areas of southeastern Queen Maud Land (basin A′-A″) and King George V Land (basin D-D′), moderate thickening for northern Coats Land (basin K-K′), and strong thickening for King Wilhelm II Land (basin C-C′). For East Antarctica, the linear correlation between observed 1992 to 2003 elevation-change trends and modeled snowfall trends is 0.41 ($P \leq 0.01$) at the 1° × 2° region scale and 0.85 ($P \leq 0.01$) at the basin scale (*11*).

Agreement between the spatial patterns is much lower for West Antarctica where changes due to ice dynamics can be substantial (*3*). Comparisons suggest, however, that some of the observed bimodal *dH/dt* behavior may be due to recent snowfall changes. Specifically, the strong thickening observed in basins H′-H″ and J-J′ corresponds to regions with positive snowfall trends. In addition, modest thickening is observed in both trends over Berkner Island. Although there is some general thinning apparent in both maps for the interior areas of E′-E″, E″-F, and G-H, there are strong differences in the coastal areas of F-G, G-H, and H-H′. Consequently, the linear correlation between observed *dH/dt* and modeled snow-precipitation trends is 0.11 for individual 1° × 2° regions and 0.25 for basin trends. Neither is significant at the 90% confidence interval.

Elevation-change rates estimated from model-derived snowfall trends are much smaller than the observed *dH/dt* values, even though the spatial patterns are similar in East Antarctica. To investigate this difference, we compared spatial and temporal variability in snowfall from the ERA-40 and ECMWF models to point observations from ice-core measurements and regional estimates of snow accumulation from remote sensing. Similar prior comparisons in Greenland show that ERA-40 reanalysis closely simulates the relative temporal variability in snow accumulation observed in ice cores (*16*). As with other meteorological models of Greenland precipitation, however, ERA-40 reanalysis predicts too little snowfall in the interior of the ice sheet (*17*, *18*).

Although snowfall rates for much of the Antarctic interior are too low to allow annual-layer preservation in glaciochemical signals, annual snow accumulation can be measured in ice cores from much of West Antarctica. We used 20 ice-core records to evaluate meteorological model estimates of snow accumulation (*11*) in West Antarctica located within or very near basins G-H and E′-E″ (Fig. 3). Linear correlations between the standardized ensembles of model-simulated and observed annual snowfall at the core sites are 0.55 ($P \leq 0.01$) and 0.68 ($P \leq 0.01$) during the period 1980 to 2001 and 0.62 ($P \leq 0.10$) and 0.91 ($P \leq 0.01$) during the period 1992 to 2001 for basins G-H and E-E″, respectively.

Mean annual snowfall rates estimated from the model, however, were only 83% of observed rates for the core sites in basin G-H and 66% for the more interior sites in basin E′-E″. At the South Pole and very arid sites on the polar plateau where annual glaciochemical layers are not preserved, mean snow accumulation from the reanalysis is only 20 to 60% of

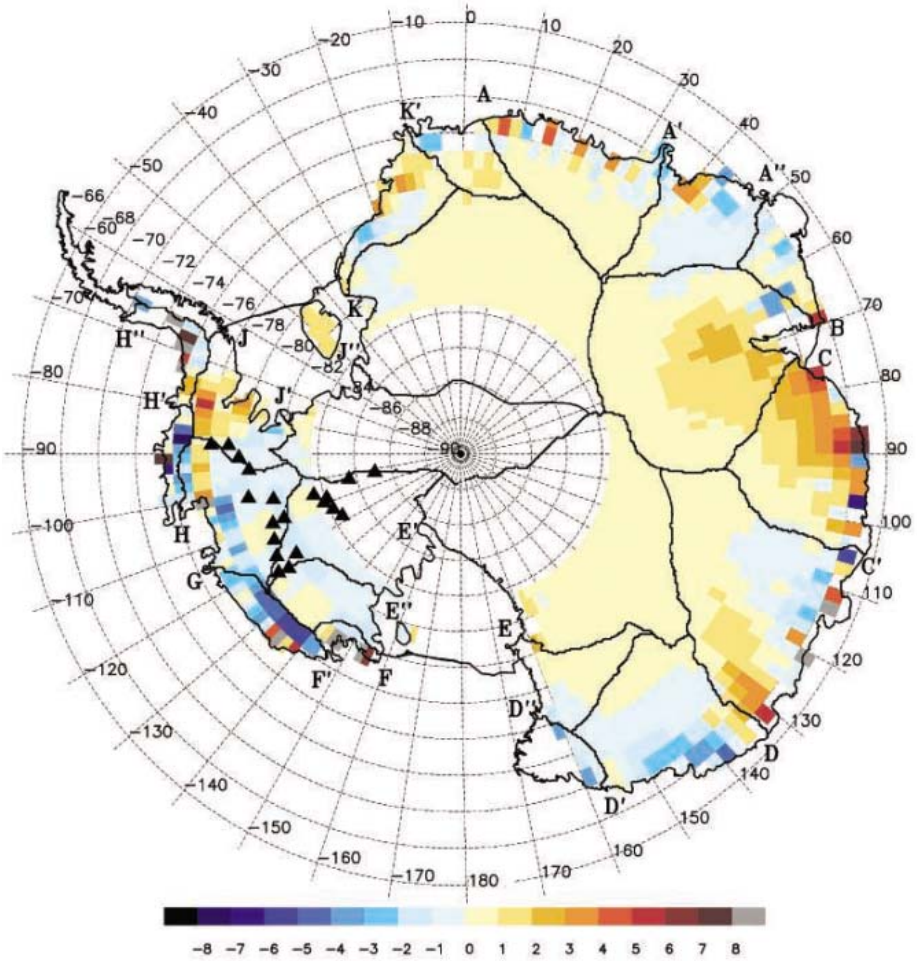

Fig. 3. Precipitation change (cm of snow per year) from 1992 to 2003 corresponding to elevation-change area coverage in Fig. 2. Ice-core locations (black triangles) discussed in the text are also shown.

observed rates. Comparisons at regional to continental scales also show that mean snow accumulation from meteorological models is very low over most of the interior of the Antarctic continent. For example, basin-averaged, model-simulated, mean-annual snow accumulation compared with regional accumulation estimates compiled from in situ and passive microwave measurements (*19*) ranged from 25 to 50% for primarily interior basins (e.g., J″-K and B-C).

It is clear, therefore, that the ERA-40 reanalysis and ECMWF operational analyses used here capture much of the relative temporal variability in accumulation while underestimating the total amount, resulting in underestimation of the magnitude of modeled temporal trends in snowfall rate. Although some of the difference between observed elevation change and modeled snowfall-rate trends likely results from changes in snow densification in response to changing snow accumulation rate and temperature (*20*), most of the difference probably results from underestimation of the magnitude of annual-to-decadal changes in snowfall by the meteorological models.

Placing these results in perspective, a sea-level change of 1 mm/year corresponds to 360 billion metric tons of water per year (*21*). Using a near-surface snow density of 350 kg/m^3, an average elevation change of 1.8 ± 0.3 cm/year over an area of 7.1 million km^2 for the East Antarctic interior (table S1) corresponds to a mass gain of 45 ± 7 billion metric tons of water per year and a corresponding sea-level drop of 0.12 ± 0.02 mm/year. We believe that this is a conservative estimate. The spatially uniform and positive *dH/dt* values for the East Antarctic interior (Fig. 2) suggest that much of the area south of the East Antarctic ROC may also be thickening. These results are consistent with ice-core evidence, though sparse, for increasing accumulation in East Antarctica during the decades preceding our observational time period (*22*–*26*). Thus, we cannot rule out a longer-term mass imbalance due to increased precipitation, as predicted by earlier studies [e.g., (*27*, *28*)] and the most recent IPCC assessment (*6*).

The vast size of the East Antarctic ice sheet means that even a small imbalance has a large effect on sea-level change. For example, a 1.8 cm/year average *dH/dt* over the entire East Antarctic ice sheet (~10 million km^2) would correspond to a sea-level drop of 0.18 mm/year (assuming a recent change and snow density of 350 kg/m^3), nearly as large as the most recent estimate of 0.20 mm/year (*2*) for the Greenland ice sheet's contribution to sea-level rise, and larger than the most recent estimate for the West Antarctic ice sheet's contribution of 0.16 mm/year (*3*).

Our results show that the East Antarctic ice-sheet interior increased in overall thickness within the ROC from 1992 to 2003 and that this increase is probably the result of increased snowfall. Both of these observations are consistent with the latest IPCC prediction for Antarctica's likely response to a warming global climate (*6*). However, the IPCC prediction does not consider possible dynamic changes in coastal areas of the ice sheet. Moreover, these results have only sparse coverage of the coastal areas where recent dynamic changes may be occurring (*4*). Thus, the overall contribution of the Antarctic ice sheet to global sea-level change will depend on the balance between mass changes on the interior and those in coastal areas.

References and Notes

1. W. Krabill *et al.*, *Science* **289**, 428 (2000).
2. W. Krabill *et al.*, *Geophys. Res. Lett.* **31**, L24402 (2004).
3. E. Rignot, R. Thomas, *Science* **297**, 1502 (2002).
4. R. Thomas *et al.*, *Science* **306**, 255 (2004).
5. Intergovernmental Panel on Climate Change, *IPCC Third Assessment Report, Climate Change 2001: The Scientific Basis* (Cambridge Univ. Press, Cambridge, 2001).
6. J. A. Church *et al.*, in *Climate Change 2001: The Scientific Basis* (Cambridge Univ. Press, Cambridge, 2001), pp. 639–694.
7. J. R. McConnell *et al.*, *Nature* **406**, 877 (2000).
8. A. C. Ferguson, C. H. Davis, J. E. Cavanaugh, *IEEE Trans. Geosci. Remote Sens.* **42**, 2426 (2004).
9. C. H. Davis, A. C. Ferguson, *IEEE Trans. Geosci. Remote Sens.* **42**, 2437 (2004).
10. Y. Li, C. H. Davis, Proceedings of the 2005 International Geoscience and Remote Sensing Symposium, Seoul, South Korea (Institute of Electrical and Electronics Engineers, Piscataway, NJ), in press.
11. Materials and methods are available as supporting material on *Science* Online.
12. E. R. Ivins, X. Wu, C. A. Raymond, C. F. Yoder, T. S. James, *Int. Assoc. Geodesy Symp.* **123**, 361 (2001).
13. A. Shepherd, D. J. Wingham, J. A. D. Mansley, H. F. J. Corr, *Science* **291**, 862 (2001).
14. E. Rignot, S. Jacobs, *Science* **296**, 2020 (2002).
15. D. J. Wingham, A. J. Ridout, R. Scharroo, R. J. Arthern, C. K. Shum, *Science* **282**, 456 (1998).
16. E. Hanna, J. R. McConnell, S. Das, J. Cappelen, A. Stephens, *J. Clim.*, in press.
17. J. R. McConnell *et al.*, *J. Geophys. Res.* **40**, 605 (1998).
18. Q. S. Chen *et al.*, *J. Clim.* **10**, 839 (1997).
19. D. G. Vaughan, J. L. Bamber, M. Giovinetto, J. Russell, A. P. R. Cooper, *J. Clim.* **12**, 933 (1999).
20. R. J. Arthern, D. J. Wingham, *Clim. Change* **40**, 605 (1998).
21. S. S. Jacobs, *Nature* **360**, 29 (1992).
22. V. I. Morgan, I. D. Goodwin, D. M. Etheridge, C. W. Wookey, *Nature* **354**, 58 (1991).
23. E. Mosley-Thompson *et al.*, *Ann. Glaciol.* **21**, 131 (1995).
24. E. Mosley-Thompson, J. F. Paskievitch, A. J. Gow, L. G. Thompson, *J. Geophys. Res.* **104**, 3877 (1999).
25. J. Wen *et al.*, *Polar Meteorol. Glaciol.* **15**, 43 (2001).
26. I. Goodwin, M. de Angelis, M. Pook, N. W. Young, *J. Geophys. Res.* **108**, 4673 (2003).
27. J. Oerlemans, *J. Clim.* **2**, 1 (1982).
28. P. Huybrechts, J. Oerlemans, *Clim. Dyn.* **5**, 93 (1990).

29. ERA-40 and ECMWF operational analysis data were provided by A. Stephens (British Atmospheric Data Centre). This work was supported by NASA's Cryospheric Processes Program (C.H.D., Y.L., and J.R.M.) and the NSF Antarctic Glaciology Program (J.R.M. and M.M.F.). We thank the U.S. ITASE field team, R. Kreidberg for help with the manuscript, and two anonymous reviewers for comments that improved this manuscript.

Supporting Online Material

www.sciencemag.org/cgi/content/full/1110662/DC1
Materials and Methods
Figs. S1 to S4
Table S1
References and Notes

3 February 2005; accepted 5 May 2005
Published online 19 May 2005;
10.1126/science.1110662
Include this information when citing this paper.

Cleaning the Air and Improving Health with Hydrogen Fuel-Cell Vehicles

M. Z. Jacobson,[1]* W. G. Colella,[1] D. M. Golden[2]

Converting all U.S. onroad vehicles to hydrogen fuel-cell vehicles (HFCVs) may improve air quality, health, and climate significantly, whether the hydrogen is produced by steam reforming of natural gas, wind electrolysis, or coal gasification. Most benefits would result from eliminating current vehicle exhaust. Wind and natural gas HFCVs offer the greatest potential health benefits and could save 3700 to 6400 U.S. lives annually. Wind HFCVs should benefit climate most. An all-HFCV fleet would hardly affect tropospheric water vapor concentrations. Conversion to coal HFCVs may improve health but would damage climate more than fossil/electric hybrids. The real cost of hydrogen from wind electrolysis may be below that of U.S. gasoline.

Switching from a fossil-fuel economy to a hydrogen economy would be subject to technological hurdles, the difficulty of creating a new energy infrastructure, and considerable conversion costs (*1*) but could provide health, environmental, climate, and economic benefits and reduce reliance on diminishing oil supplies. Although studies have modeled the effects of hydrogen leakage or reduced emission on global tropospheric and stratospheric chemistry (*2*–*4*), no study has examined the effect on urban pollution or health of establishing a hydrogen economy. Furthermore, no study has examined the likely effects of this switch on aerosol particles (which have a large impact on climate and are the deadliest components

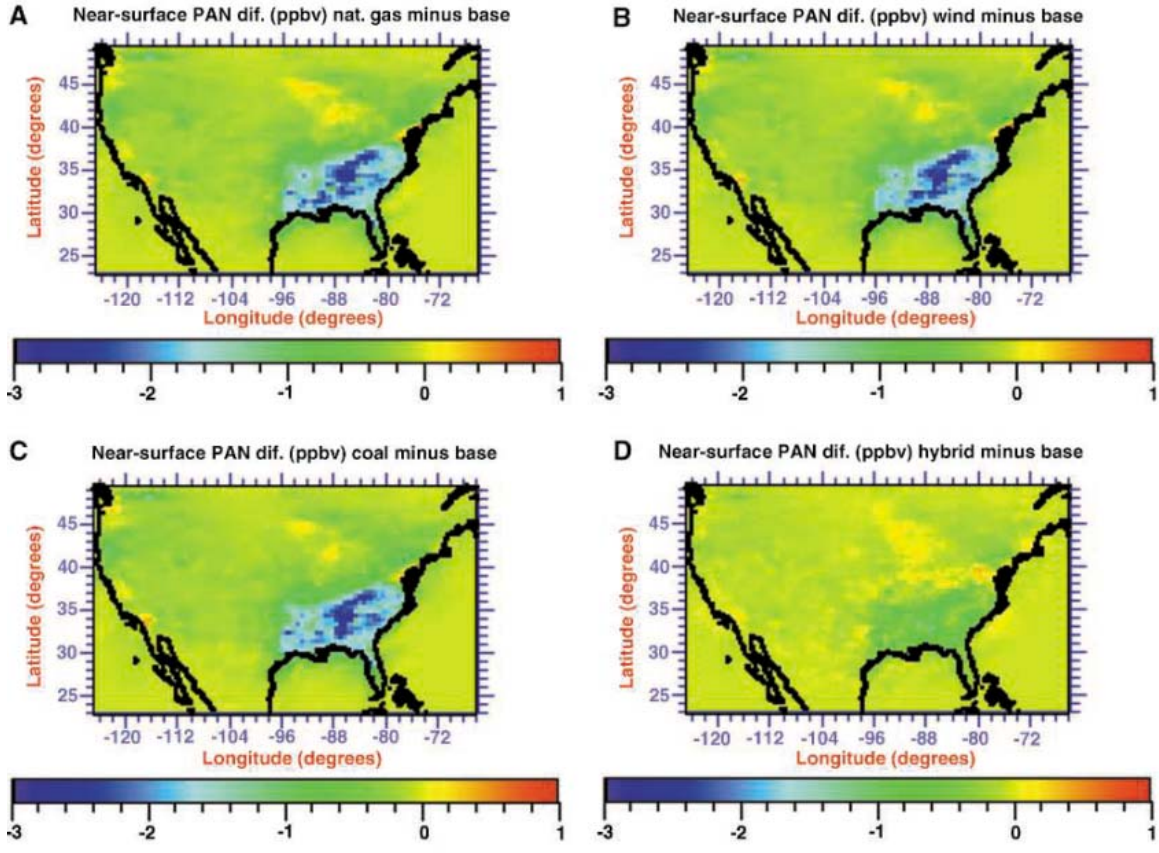

Fig. 1. Modeled differences, averaged over all day and night hours of the month of August 1999, of near-surface PAN. Each panel represents the difference between the (**A**) natural gas, (**B**) wind, (**C**) coal, and (**D**) hybrid cases and the baseline case, respectively. The maximum overall monthly-averaged reduction anywhere in the HFCV cases was 3 ppbv out of a baseline case maximum of 9 ppbv (Fig. S1h). The maximum difference in the hybrid case was 1.2 ppbv.

of air pollution), of generating hydrogen by any method aside from renewable energy, or of examining emission changes upstream of vehicles. Here we examine the possible effects on ambient gas and particle concentrations and on estimated health and climate costs of different methods of replacing all U.S. fossil-fuel onroad vehicles (FFOVs) with hydrogen fuel-cell vehicles (HFCVs).

For the study, we used GATOR-GCMOM, a parallel, global-through-urban nested gas, aerosol, transport, radiation, general circulation, mesoscale, and ocean computer model (*5*–*7*), together with the U.S. National Emission Inventory (NEI) (*8*), both described in (*9*). Emission inventories for HFCV and hybrid sensitivity experiments (summarized in table S1) were prepared for this study in (*10*) after a life-cycle assessment (LCA) that accounted for energy inputs, efficiencies, and pollution outputs during all stages of hydrogen and fossil-fuel production, distribution, storage, and end use. Model data comparisons with the baseline inventory are also given in (*10*).

Five global/regional nested simulations were run: one baseline scenario assuming August 1999 emissions, one where all FFOVs were instantly converted to fossil-fuel/electric hybrid vehicles, and three where FFOVs were switched to HFCVs in which the hydrogen was produced by (i) steam reforming of natural gas, (ii) wind electrolysis, or (iii) coal gasification. Although an instantaneous conversion of all FFOVs to hybrids or HFCVs will not occur, we assumed that it would in order to provide net (not time-dependent) differences in air pollution between current and future vehicle fleets. Because hybrids may represent advanced FFOVs, a comparison of HFCVs with FFOVs and hybrids may give a full range of HFCV benefits and disadvantages relative to current and more efficient FFOVs.

For each case, we modified onroad, power plant, and other NEI emissions. In the HFCV cases, FFOV emissions (including hydrogen and water) were removed, refinery volatile organic emission was reduced by half (the fraction of petroleum used for onroad vehicles), and leaked hydrogen and chemically produced water vapor were added. Also, emission [nitrogen oxides (NO_x), volatile organic carbon (VOC), CO, and CO_2] and leaks (CH_4) from steam reforming and emission (NO_x, CO, CO_2, and SO_2) from coal gasification were added. Carbon sequestration was not included. Emissions produced by power use for compressing hydrogen in all HFCV cases and for gasifying coal in the coal case were added proportionally to the power plant emission mix in the inventory without changing the number of power plants or their control technologies. Energy required for the endothermic steam reforming of natural gas was also included. Emissions from exploration, mining, storage, processing, and transport of fuels and infrastructure were assumed to be similar among cases.

The assumed hydrogen leakage rate was 10%, a probably unrealistic upper bound (*3*). A more realistic value may be 3%. The upper bound was used to ensure that the conclusions here, which were found to show net benefits of HFCVs, are conservative.

The fleet-averaged energy efficiency increase upon conversion of FFOVs to hybrid vehicles was taken as 45% (*11*), corresponding to a 31% emission decrease (1/1.45). Although some new FFOV vehicles will emit less, the fleet-averaged emission, which we are interested in, may not decrease so much, because not all new vehicles will be low emitters, and emission increases with vehicle age. HFCVs will emit only hydrogen and water at any age.

Figure 1 shows August-averaged (day and night) modeled differences in emission of peroxyacetyl nitrate (PAN), a potent eye irritant that also discolors plant leaves, between each case and the baseline case. Switching from current FFOVs reduced PAN in all cases in most locations, predominantly in the southeastern United States. The improvement was greater in the HFCV cases [up to 3 parts per billion by volume (ppbv) out of a baseline maximum of 9 ppbv] than in the hybrid case (up to 1.2 ppbv). Little difference occurred among the HFCV cases, because the emission increase in each

[1]Department of Civil and Environmental Engineering, Stanford University, Stanford, CA 94305–4020, USA. [2]Department of Mechanical Engineering, Stanford University, Stanford, CA 94305–3032, USA.

*To whom correspondence should be addressed. E-mail: jacobson@stanford.edu

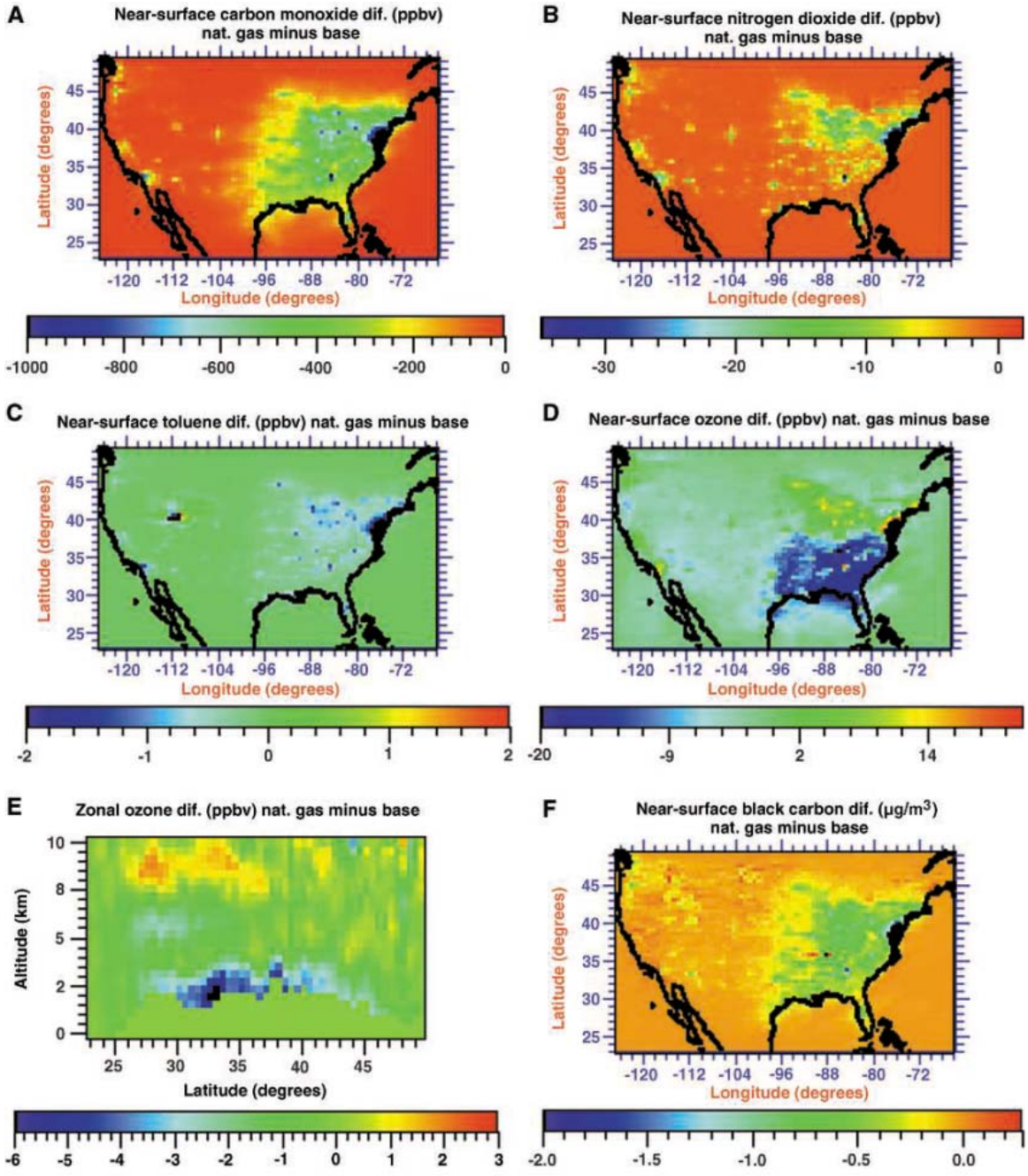

Fig. 2. Same as Fig. 1, but for (**A**) near-surface carbon monoxide (maximum reduction 1000 ppbv out of a baseline maximum of 1900 ppbv), (**B**) near-surface nitrogen dioxide (35 ppbv out of 63 ppbv), (**C**) near-surface toluene (2 ppbv out of 15 ppbv), (**D**) near-surface ozone (20 ppbv out of 103 ppbv), (**E**) zonally averaged (between –125 and –65.75 W) ozone (6 ppbv out of 46 ppbv), and (**F**) near-surface particulate black carbon (2 out of 12 μg/m^3). (E) shows zonally averaged orography as well, where ozone values are zero. Figure S1 shows the baseline cases and other difference cases.

HFCV case was smaller than the emission reduction from eliminating FFOVs. PAN declined most in the southeast, where reducing NO_x had a big impact. PAN increased slightly in the northeast and Los Angeles, possibly because although NO_x and organics decreased there, the decrease in NO and CH_3O_2, which destroy CH_3CO_3, increased CH_3CO_3, which then reacted with NO_2 to increase PAN.

Figure 2 shows August changes in several pollutants from the natural gas HFCV case. Changes were similar among other HFCV cases, as shown in (*9*), which also shows figures for other pollutants. Switching to HFCV reduced CO (Fig. 2A) over most of the United States by up to 1000 ppbv out of a baseline maximum of 1900 ppbv and reduced NO_2 (Fig. 2C) by up to 35 out of 63 ppbv. Toluene (Fig. 2B), a reactive ozone precursor, decreased over most of the United States by up to 2 out of 15 ppbv. Near-surface ozone decreased over most of the United States by up to 20 out of 103 ppbv. Ozone increased in regions of high NO_x and low biogenic hydrocarbon emission, such as in Los Angeles and along the northeast corridor, because reducing NO_x in those places reduced ozone titration by $NO + O_3 \rightarrow NO_2 + O_2$ and increased OH (fig. S1j) Fig. 2E, though, shows that zonally averaged near-surface ozone decreased over all latitudes by up to 6 ppbv.

HFCVs reduced near-surface particulate black carbon (BC) (Fig. 2F) by up to 2 out of 12 μg/m^3. Because particles are the most unhealthful components of air pollution, their reduction represents a benefit of switching to HFCVs (Table 1). Reducing BC, which enhances global warming, may also slightly reduce climate costs; reducing cooling particle components may unmask some global warming, slightly increasing such costs (Table 1).

The main differences among the three HFCV cases were their effects on greenhouse gases. Fig. S1o shows that hydrogen production from natural gas, under the assumption of a 1% natural gas leakage rate (*10*), increased methane by up to 40 ppbv during August out of a background of 1700 ppbv in 1999. Producing hydrogen from wind or coal decreased methane by up to 20 ppbv relative to FFOVs. The hybrid case resulted in

Table 1. Estimated health, climate, and total cost reductions (positive values) or increases (negative values) per year in 2004 dollars for each of the four cases discussed. The table does not reflect capital costs. Three significant digits are shown to illustrate small differences in some cases. The first species in the first column is the emitted pollutant. For health-effect agents, the species after the hyphen, if any, is an ambient pollutant causing a health hazard; otherwise, the emitted species also causes the health hazard. For climate agents, only emitted species are shown. Costs per year for a pollutant in a case were obtained by multiplying the cost per unit mass emission of the pollutant (second column of Table 1) by the change in mass emission per year of the pollutant for the case (table S1). VOC is assumed to be the same as total NMOC (nonmethane organic carbon) in table S1. Costs per unit mass emission were obtained for all species except for CO_2 and CH_4 from (*16, 17*), adjusted from 1991 to 2004 dollars with the gross domestic product (GDP) deflator ratio (1.2721). CO_2 costs per unit mass emission were obtained from (*18*), adjusted from 1995 Euros to 2004 dollars assuming $1.25 per Euro in 1995 and the GDP deflator ratio from 1995 to 2004 (1.1634). CH_4 costs per unit mass emission were estimated as those of CO_2 multiplied by 23, the 100-year global warming potential (GWP) of CH_4. The BC+OM (sum of emitted sub–2.5-μm fossil-fuel particulate black carbon plus organic carbon) climate cost per unit mass was estimated as that of CO_2 multiplied by the 100-year temperature change per unit mass emission of BC+OM relative to that of CO_2, calculated here as 95 to 191 [section 5 of (*9*), using data from (*27*)]. $PM_{2.5}$-cooling components (PM, particulate matter) include emitted sub–2.5-μm sulfate, plus nitrate, plus 40% of SO_x, plus 10% of NO_x, plus 5% of VOC. Its climate cost per unit mass is estimated as that of CO_2 multiplied by the 100-year climate response ratio of SO_x, calculated here as 19 to 39 [calculated from section 5 of (*9*), using data from (*27, 28*)]. Costs per displaced gallon of current fuel (last row of Table 1) were obtained by dividing the total cost of each case (second-to-last row) by the total gasoline plus diesel fuel used for onroad vehicles in the United States in 1999 (1.57×10^{11} gallons) (*10*). For consistency, this quantity was the same as that displaced to generate hydrogen for the cases herein.

Species	$/kg of emission in 2004	Hybrid (billion $/year)	Natural gas (billion $/year)	Wind (billion $/year)	Coal (billion $/year)
SO_x-sulfate PM	8.78–83.3	0.76–7.23	–3.25–(–30.8)	–3.25–(–30.8)	–8.51–(–80.8)
NO_x-nitrate PM	1.30–21.1	3.05–49.5	9.43–153	9.45–153	9.24–150
NO_x-NO_2	0.19–0.93	0.45–2.18	1.39–6.75	1.39–6.76	1.36–6.61
VOC-organic PM	0.13–1.46	0.19–2.23	0.70–8.01	0.70–8.01	0.70–8.01
$PM_{2.5}$	13.3–202.5	0.69–10.6	1.98–30.3	1.98–30.3	1.89–28.9
$PM_{2.5\text{-}10}$	8.52–22.4	0.12–0.32	0.30–0.79	0.30–0.79	0.24–0.64
VOC+NO_x-O_3	0.13–1.46	0.49–5.67	1.62–18.7	1.62–18.7	1.60–18.4
NH_3-ammonia PM	1.30–21.1	0.10–1.56	0.31–5.01	0.31–5.01	0.31–5.01
CO	0.0127–0.11	0.24–2.20	0.79–7.07	0.79–7.07	0.74–6.67
Subtotal health		6.10–81.5	13.2–197	13.3–199	7.56–143
CO_2	0.026–0.067	8.27–21.1	20.8–53.2	32.6–83.2	1.62–4.15
CH_4	0.60–1.54	0.14–0.38	–0.79–(–2.03)	0.49–1.24	0.48–1.24
BC+OM	2.49–12.8	0.11–0.56	0.34–1.74	0.34–1.74	0.34–1.72
Cooling $PM_{2.5}$	0.51–2.62	–0.18–(–0.91)	–0.44–(–2.23)	–0.44–(–2.24)	–0.31–(–1.57)
Subtotal climate		8.35–21.2	19.9–50.7	33.0–84.0	2.14–5.54
Total		14.5–103	33.1–248	46.2–283	9.70–149
Total $/gallon		0.09–0.65	0.21–1.58	0.29–1.80	0.06–0.95

a lesser reduction in methane than did the coal or wind case. Because of its long lifetime (8 to 10 years) and the long-term effect by NO_x and OH on it, ambient methane would change further over a longer simulation.

Table S1 shows that the coal HFCV case resulted in the lowest reduction of CO_2 emission, followed by the hybrid case. The wind HFCV case resulted in the greatest CO_2 emission reduction.

HFCVs increased H_2 by up to 1000 ppbv above the global background of 530 ppbv (*12*) in some locations during August (fig. S1q). The U.S.-averaged increase in the natural gas case was 100 ppbv. The increase in hydrogen had little effect on short-term smog, because hydrogen's chemical lifetime is about 4.5 to 10 years, too long to affect smog except in the background. The overall H_2 lifetime is 2 to 3 years because of its microbial loss in soil (*12–14*). The hybrid case reduced H_2, a fossil-fuel combustion product.

Switching to HFCVs caused virtually no change in water vapor emission. Complete combustion of gasoline, represented by $C_nH_{1.87n}$ (*15*), produces 925 mol of H_2O per 1000 mol of CO_2. With 1371 metric tons of CO_2/year emitted in 1999 from primarily gasoline FFOVs in 1999 (*10*), the U.S. FFOV water vapor emission rate was about 519 tons of H_2O/year. A fuel cell emits 1 mol of H_2O per mol of H_2; thus, an equivalent 1999 fleet of HFCVs that uses 56.8 tons/year of H_2 (*10*) emits about 508 tons of H_2O/year. Additional power to compress hydrogen increased the total HFCV water vapor emission to only 2% above that of current FFOVs. Because HFCVs and FFOVs will be co-located, HFCVs should have virtually no impact on urban-scale water vapor emission. Switching to hybrids reduced water vapor emission. Water vapor emission from U.S. HFCVs, hybrids, and FFOVs paled in comparison with that from natural sources globally, which is 5×10^8 tons of H_2O/year.

Table 1 estimates changes in yearly health and climate costs from switching to HFCVs or hybrids, calculated from the yearly emission change from each case (table S1) and health and climate cost estimates per yearly emission change (Table 1). Neither infrastructure costs due to converting to hydrogen nor our calculated monthly ambient pollutant differences (Figs. 1 and 2) were used in the health/climate cost calculation. The health costs per unit of emission, however, were obtained from studies (*16*, *17*) that first modeled changes in ambient concentrations of U.S. vehicle-derived pollution per unit of emission and then applied estimated health costs per unit change in ambient concentration. Although costs per pollutant in Table 1 accounted for seasonality and location of emission (*16*, *17*), they are conservative because particle health impact estimates and rural exposure to pollutants due to urban sprawl are now higher than at the time of the studies. Health cost uncertainties include exposures and health effects per unit of exposure. Climate costs per unit of emission were estimated from (*18*). Uncertainties include future effects of pollutants on climate and feedbacks effects of climate change on health, environment, coastlines, etc.

Table 1 shows that all four future cases reduced costs as compared with current FFOVs. Benefits from wind HFCVs slightly exceeded those from natural gas HFCVs, primarily because of the climate benefit of wind. Health and climate benefits from wind and natural gas exceeded those from coal and hybrids. Coal HFCVs reduced health problems (Table 2) but worsened climate costs (Table 1) relative to hybrids.

Previous studies (*19*, *20*) suggested that HFCVs may reduce emission and energy efficiency only modestly over hybrids. However, we find that wind HFCVs may save 2300 to 4000 lives/year and $32 billion to $180 billion/year in the United States relative to hybrids (Tables 1 and 2), and that wind or natural gas HFCVs may save 3700 to 6400 lives/year and reduce asthma by 1 million to 3 million cases/year relative to current FFOVs.

Table 2. Avoided health and mortality cases due to each of the four cases discussed. The table was obtained by scaling the number of cases per year in 1990 for each ambient pollutant from [table 2 of (*16*)] by the ratio of the change in emission of the pollutant's precursor(s) for each 1999 case (*10*) to the total U.S. anthropogenic emission of the precursor(s) from 1999 (*29*). The precursors were as follows: CO for ambient CO; NO_x for ambient NO_2; VOC + NO_x for ambient O_3; $PM_{2.5}$ + 0.1 $PM_{10\text{-}2.5}$ + 0.4 SO_x + 0.1 NO_x + 0.05 VOC for ambient PM [predominantly from (*16*)]. The "% mortality reduction" is the change in mortality from reducing primary and secondary PM by implementing HFCV, divided by the total number of deaths from all primary and secondary anthropogenic PM {80,000 or 137,000 deaths per year for the low or high cases, respectively [table 2 of (*16*)]}. This table does not account for global-warming health effects, which is why the wind and natural gas cases differ only in digits not shown. ARD2, any other symptom; RRAD, respiratory restricted activity days.

Ambient pollutant	Health effect	Hybrid (cases/year)	Natural gas (cases/year)	Wind (cases/year)	Coal (cases/year)
CO	Headache	2.34–2.78 × 10^7	7.52–8.94 × 10^7	7.52–8.94 × 10^7	7.09–8.43 × 10^7
	Hospitalization	1,100–3160	3,530–10,200	3,530–10,200	3,330–9,570
	Mortality	70–206	220–660	220–660	208–620
NO_2	Sore throat	2.7–8.3 × 10^7	8.34–8.46 × 10^7	8.35–8.47 × 10^7	8.2–8.3 × 10^7
	Excess phlegm	1.24–1.26 × 10^7	3.82–3.88 × 10^7	3.83–3.89 × 10^7	3.74–3.80 × 10^7
	Eye irritation	1.11–1.13 × 10^7	3.44–3.49 × 10^7	3.45–3.50 × 10^7	3.37–3.42 × 10^7
O_3	Asthma attacks	2.74–8.62 × 10^5	1.03–3.25 × 10^6	1.04–3.25 × 10^6	1.02–3.21 × 10^6
	Eye irritation	2.54–2.80 × 10^6	9.59–10.6 × 10^6	9.59–10.6 × 10^6	9.48–10.5 × 10^6
	Lower respiratory illness	3.65–6.09 × 10^6	1.38–2.30 × 10^7	1.38–2.30 × 10^7	1.36–2.27 × 10^7
	Upper respiratory illness	1.11–1.85 × 10^6	4.19–6.99 × 10^6	4.19–6.99 × 10^6	4.14–6.91 × 10^6
	ARD2	0–2.07 × 10^7	0–7.82 × 10^7	0–7.82 × 10^7	0–7.73 × 10^7
PM	Asthma attacks	5.19–5.48 × 10^4	1.39–1.47 × 10^5	1.39–1.47 × 10^5	1.03–1.08 × 10^5
	RRAD	1.53–2.07 × 10^6	4.11–5.57 × 10^6	4.11–5.57 × 10^6	3.03–4.10 × 10^6
	Chronic illness	673–1610	1,800–4,300	1,800–4,300	1,330–3,180
	Mortality	1,380–2,370	3,710–6,350	3,710–6,350	2,730–4,680
	% mortality reduction	1.7	4.6	4.6	3.4

Because wind HFCVs resulted in the greatest health-plus-climate benefit among all cases, examining the cost to the U.S. economy of producing hydrogen from wind is warranted. This analysis does not consider political issues, such as zoning and larger subsidies for conventional electricity sources, affecting wind's competitiveness.

The unsubsidized near-term (<10 years) cost of producing hydrogen from wind is estimated as follows (table S2) [direct electricity from modern wind turbines in the presence of annual winds at speeds of >6.9 m/s, present over >20% of the United States (*21*)]: cost, \$0.03 to \$0.05 per kilowatt-hour (kWh) (*22*, *23*); transmission cost, \$3.45 × 10^{-6} to \$1.38 × 10^{-5} per kWh/km (*22*); transmission distances, 20 to 1500 km; internal combustion engine efficiency, 0.16 (*10*); HFCV efficiency, 0.43 to 0.46 (*10*); electrolyzer cost, \$400 to \$1000/kW (*11*); interest rate, 6 to 8%; electrolyzer energy requirement, 53.4 kWh/kg of H_2 (*24*); fraction of time wind is available to electrolyzer, 0.5 to 0.95 (*9*); compressor cost, \$0.7 to \$1.34/kg of H_2 (*25*, *26*); and storage cost, \$0.31/kg of H_2 (*26*). The total is \$3.0 to \$7.4/kg of H_2, or \$1.12 to \$3.20/gallon of displaced gasoline/diesel, which compares with the actual costs of U.S. gasoline and diesel in mid-March 2005 of \$2.06 and \$2.19, respectively. Adding the reduction in health and mortality costs from wind HFCVs of \$0.29 to \$1.80/gallon (Table 1), which is the externality cost of gasoline, gives a direct cost plus externality cost of U.S. gasoline/diesel of \$2.35 to \$3.99/gallon, which exceeds the mean cost of hydrogen from wind (\$2.16/gallon) even if retail hydrogen is marked up.

This model sensitivity experiment concludes that switching from the 1999 FFOV fleet to an HFCV or hybrid fleet may reduce air pollution, health, and climate problems and costs. Although the three HFCV cases all reduced health costs (because most improvements in air quality resulted from eliminating FFOV exhaust), wind and natural gas HFCVs reduced such costs the most and reduced ozone by up to 20 ppbv. Wind HFCVs reduced climate costs the most, making it the most beneficial environmental technology. Natural gas HFCVs increased CH_4 but reduced CO_2, making them second. Hybrids reduced climate costs but increased health costs relative to coal HFCVs, suggesting a rough tie for third. Both HFCVs and hybrids reduced health and climate costs relative to FFOVs. HFCVs had little impact on water vapor emission. Some uncertainties are the health and climate (to a greater extent) costs per unit of emission, how emission changes outside the United States over the next few decades might affect U.S. background pollution, and how climate change may affect biogenic emission.

References and Notes

1. R. F. Service, *Science* **305**, 958 (2004).
2. T. K. Tromp, R.-L. Shia, M. Allen, J. M. Eiler, Y. L. Yung, *Science* **300**, 1740 (2003).
3. M. G. Schultz, T. Diehl, G. P. Brasseur, W. Zittel, *Science* **302**, 624 (2003).
4. N. J. Warwick, S. Bekki, E. G. Nisbet, J. A. Pyle, *Geophys. Res. Lett.* **31**, L05107 (2004).
5. M. Z. Jacobson, *J. Geophys. Res.* **106**, 5403 (2001).
6. M. Z. Jacobson, *J. Geophys. Res.* **106**, 5385 (2001).
7. M. Z. Jacobson, J. H. Seinfeld, G. R. Carmichael, D. G. Streets, *Geophys. Res. Lett.* **31**, L02116 (2004).
8. U.S. Environmental Protection Agency (EPA), Clearinghouse for Inventories and Emission Factors (2003) (www.epa.gov/ttn/chief/).
9. Supporting materials are available on *Science* Online.
10. W. C. Colella, M. Z. Jacobson, D. M. Golden, *J. Power Sources*, in press.
11. National Academy of Sciences, *The Hydrogen Economy: Opportunities, Costs, Barriers, and R&D Needs* (National Academies Press, Washington, DC, 2004).
12. P. C. Novelli *et al.*, *J. Geophys. Res.* **104**, 30427 (1999).
13. T. Rahn *et al.*, *Nature* **424**, 918 (2003).
14. R. G. Derwent, W. J. Collins, C. E. Johnson, D. S. Stevenson, *Clim. Change* **49**, 463 (2001).
15. J. B. Heywood, *Internal Combustion Engine Fundamentals* (McGraw-Hill, New York, 1988).
16. D. R. McCubbin, M. A. Delucchi, *J. Transp. Econ. Policy* **33**, 253 (1999).
17. M. A. Delucchi, *J. Transp. Econ. Policy* **34**, 135 (2000).
18. ExternE—Externalities of Energy, Vol. 7: Methodology 1998 (1998) (www.externe.info/reports.html).
19. J. A. Turner, *Science* **305**, 972 (2004).
20. N. Demirdoven, J. Deutch, *Science* **305**, 974 (2004).
21. C. L. Archer, M. Z. Jacobson, *J. Geophys. Res.* **108**, 4289 (2003).
22. M. Z. Jacobson, G. M. Masters, *Science* **293**, 1438 (2001) and E-Letter response (www.sciencemag.org/cgi/eletters/294/5544/1000).
23. M. Bolinger, R. Wiser, "Summary of Power Authority Letters of Intent for Renewable Energy" (memorandum, Lawrence Berkeley National Laboratory, 30 October 2001).
24. National Renewable Energy Laboratory (NREL), *Technology Brief: Analysis of Current-Day Commercial Electrolyzers* (NREL report FS-560-36705, NREL, Golden, CO, September 2004).
25. D. B. Myers, G. D. Ariff, R. C. Kuhn, B. D. James, Hydrogen from renewable energy sources: Pathway to 10 quads for transportation uses in 2030 to 2050, FY 2003 Progress Report (2003) (www.eere.energy.gov/hydrogenandfuelcells/pdfs/iia11_myers.pdf).
26. K. Lee, *Economic Feasibility of Producing Hydrogen Using Excess Electricity from Wind Turbines on the Big Island of Hawaii* (World Renewable Energy Congress VIII, Denver, CO, 3 September 2004), www.sentech.org/Lee,%20K_Economic%20Feasibility%20Hawaii.pdf.
27. M. Z. Jacobson, *J. Geophys. Res.* **109**, D21201 (2004).
28. M. Z. Jacobson, *J. Geophys. Res.* **107** (D19), 4410 (2002).
29. U.S. Environmental Protection Agency, Clearinghouse for Inventories and Emission Factors (www.epa.gov/ttn/chief).

30. Supported by the Global Climate and Energy Project at Stanford University and by NASA. We thank J. Koomey and M. Delucchi for helpful comments.

Supporting Online Material

www.sciencemag.org/cgi/content/full/308/5730/1901/DC1
SOM Text
Fig. S1
Tables S1 and S2
References

27 December 2004; accepted 18 May 2005
10.1126/science.1109157

Cardiolipin Polyspecific Autoreactivity in Two Broadly Neutralizing HIV-1 Antibodies

Barton F. Haynes,[1]* Judith Fleming,[1] E. William St. Clair,[1] Herman Katinger,[2] Gabriela Stiegler,[2] Renate Kunert,[2] James Robinson,[3] Richard M. Scearce,[1] Kelly Plonk,[1] Herman F. Staats,[1] Thomas L. Ortel,[1] Hua-Xin Liao,[1] S. Munir Alam[1]

The design of a human immunodeficiency virus–1 (HIV-1) immunogen that can induce broadly reactive neutralizing antibodies is a major goal of HIV-1 vaccine development. Although rare human monoclonal antibodies (mAbs) exist that broadly neutralize HIV-1, HIV-1 envelope immunogens do not induce these antibody specificities. Here we demonstrate that the two most broadly reactive HIV-1 envelope gp41 human mAbs, 2F5 and 4E10, are polyspecific autoantibodies reactive with the phospholipid cardiolipin. Thus, current HIV-1 vaccines may not induce these types of antibodies because of autoantigen mimicry of the conserved membrane-proximal epitopes of the virus. These results may have important implications for generating effective neutralizing antibody responses by using HIV-1 vaccines.

A major obstacle to generating a successful human immunodeficiency virus–1 (HIV-1) vaccine is the inability to induce broadly reactive neutralizing antibodies after immunization with HIV-1 envelope proteins (Env) (*1*). HIV-1 infection and vaccination induce multiple types of antibodies, including antibodies to envelope variable loops, the CD4 binding site, and the chemokine receptor binding site. However, these antibodies do not control HIV-1 and are readily escaped by the virus (*1*). The human monoclonal antibodies (mAbs) 2F5 and 4E10 represent rare antibodies with broadly neutralizing activity made from B cells of HIV-1–infected humans, which react with conserved membrane-proximal amino acids in HIV-1 gp41 (*2*–*4*). Both antibodies have relatively long hydrophobic CDR3 regions (*3*, *4*). A major conundrum has been that HIV-1 envelopes that express membrane-proximal epitopes fail to induce equivalent antibodies in animal models or humans (*5*–*8*). Long hydrophobic CDR3 regions are generally typical of polyreactive autoantibodies (*9*), and HIV-1–infected patient B lymphocytes are driven to make polyclonal antibodies with reactivity to the endogenous phospholipid, cardiolipin (*10*). In light of these observations, we assayed 2F5 and 4E10 mAbs, along with other mAbs to HIV-1, for cardiolipin and other autoantigen reactivities.

The mAbs 2F5 and 4E10, two additional rare broadly reactive neutralizing mAbs (2G12 and IgG1b12) (*11*–*13*), and 31 common human mAbs to HIV-1 Env were tested for reactivity with cardiolipin (*14*) (Table 1). Both 2F5 and 4E10 reacted with cardiolipin, whereas all 33 of the other human mAbs did not react. mAb 2F5 also reacted with histones and the centromere B autoantigen, whereas mAb 4E10 reacted with the systemic lupus erythematosus (SLE) auto-

[1]Duke University School of Medicine, Durham, NC 27710, USA. [2]Institute of Applied Microbiology, University of Agriculture, Vienna, Austria. [3]Tulane University School of Medicine, New Orleans, LA 70112, USA.

*To whom correspondence should be addressed. E-mail: hayne002@mc.duke.edu

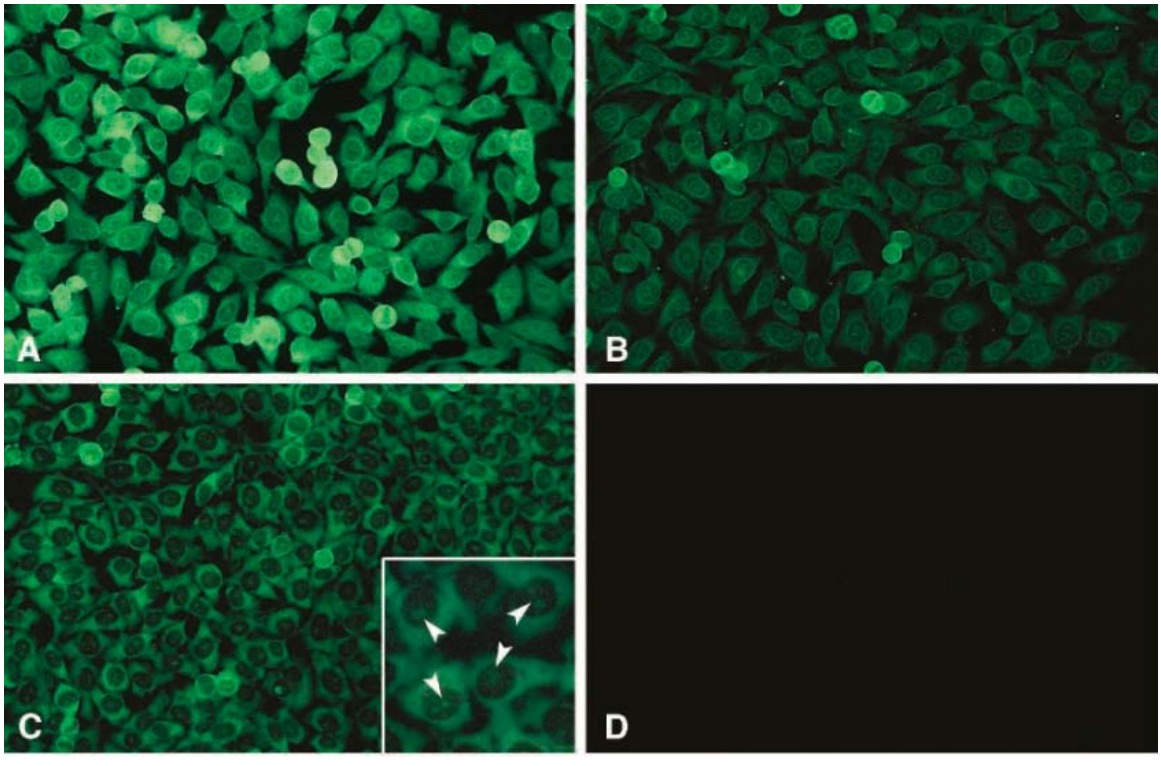

Fig. 1. Reactivity of 2F5, 4E10, and IgG1b12 mAbs with human HEp-2 epithelial cells. (**A**) mAb 2F5 reacting with HEp-2 cells in a diffuse cytoplasmic and nuclear pattern. (**B**) mAb 4E10 reacting with HEp-2 cells in a pattern similar to 2F5. (**C**) mAb IgG1b12 reacting with HEp-2 cells in a diffuse cytoplasmic pattern, with nucleoli reactive in the nucleus. (Inset) Higher magnification of cells showing the nucleolar reactivity of IgG1b12 (arrows). (**D**) Negative reactivity of mAb 1.9F on HEp-2 cells. Antibody amounts per slide assayed in [(A) to (D)] were 3.75 μg per slide (150 μg/ml) of mAb. mAb 2F5 was positive on HEp-2 cells at 0.125 μg per slide (5 μg/ml). mAb 4E10 was positive on HEp-2 at 0.125 μg per slide (5 μg/ml), and IgG1b12 was positive at 1.25 μg per slide (50 μg/ml). All panels are shown at magnification ×200; the inset in (C) is ×400. Images shown are from an experiment representative of three performed.

antigen SS-A/Ro (Table 1). We also tested all human mAbs against the human epithelial HEp-2 cell line that is used in clinical antinuclear antibody assays (*15*). Both 2F5 and 4E10 also reacted with HEp-2 human epithelial cells in a diffuse cytoplasmic and nuclear pattern (*14*) (Fig. 1, A and B), further revealing polyspecific autoreactivity of both antibodies.

Of the two other rare neutralizing mAbs, one mAb, 2G12 (*11*, *13*), was not autoreactive, whereas another mAb against the CD4 binding site, immunoglobulin G 1b12 (IgG1b12) (*12*), reacted with ribonucleoprotein, double-stranded DNA (dsDNA), centromere B, and histones, as well as with HEp-2 cells in a cytoplasmic and nucleolar pattern (Table 1 and Fig. 1). Of the 31 more common mAbs to HIV-1 studied, only two mAbs with specificity for binding near the CD4 binding site (A32 and 1.4G) and two mAbs to a non-neutralizing gp41 epitope (2.2B and KU32) showed any evidence of autoantigen reactivity (Table 1).

To determine whether 2F5 and 4E10 were similar to anticardiolipin antibodies found in SLE or the antiphospholipid antibody syndrome (APS) (*16*–*20*), both mAbs were tested for lupus anticoagulant activity (*18*) and for the ability to bind to prothrombin (*19*), β2 glycoprotein-1 (*17*), phosphatidylserine (PS) (*16*), phosphatidylcholine (PC) (*16*), phosphatidylethanolamine (PE), and sphingomyelin (SM) (*14*). Whereas 2F5 was negative for all of these reactivities, 4E10 had lupus anticoagulant reactivity (*14*); reacted strongly with PS, PC, and PE; reacted weakly with SM (Fig. 2A) and prothrombin (*14*); and did not react with β2 glycoprotein-1 (*14*).

The specificity of mAb binding was demonstrated by the inhibition of 2F5 binding to cardiolipin by a 2F5 anti-idiotype mAb, as well as by gp41 peptides, and by the inhibition of 4E10 binding to cardiolipin by gp140 envelope protein (Fig. 2, B to E) (*21*). A murine mAb to 2F5 idiotype, 3H6, which blocks 2F5 neutralization of HIV-1 (*21*), inhibited binding of mAb 2F5 to cardiolipin by 70% (Fig. 2B). The amino acid sequence to which mAb 2F5 binds on HIV-1 gp41 includes amino acids 662 to 668 (Glu-Leu-Asp-Lys-Trp-Ala) (*3*, *22*). Two synthetic peptides containing this sequence, but not a scrambled peptide, also blocked the binding of 2F5 to cardiolipin by 70% with an inhibitory concentration 50% (IC_{50}) of 0.9 and 2.1 μM (Fig. 2E). mAb 4E10 bound to cardiolipin with a half-maximal molar concentration (effective concentration 50%, EC_{50}) of 80 nM (Fig. 2C), and recombinant oligomeric HIV-1 envelope inhibited the binding of mAb 4E10 to cardio-

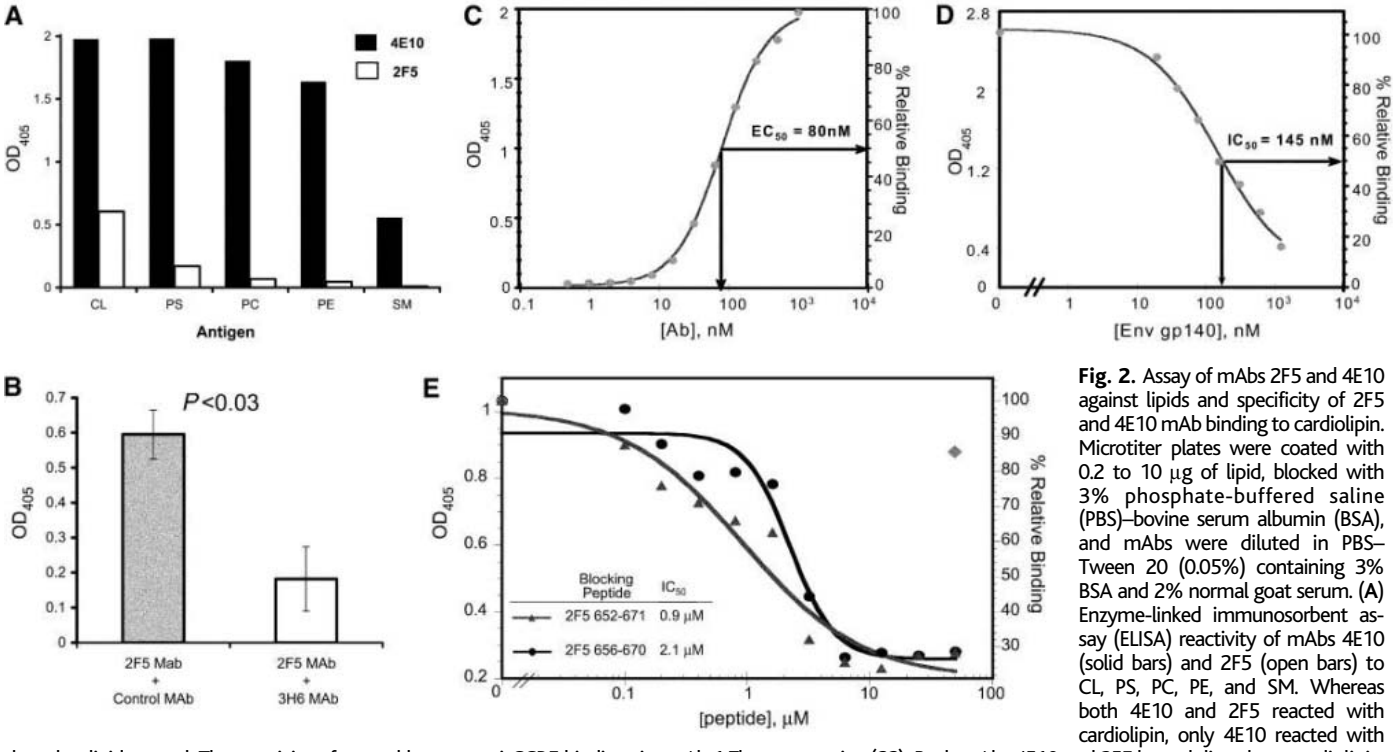

Fig. 2. Assay of mAbs 2F5 and 4E10 against lipids and specificity of 2F5 and 4E10 mAb binding to cardiolipin. Microtiter plates were coated with 0.2 to 10 μg of lipid, blocked with 3% phosphate-buffered saline (PBS)–bovine serum albumin (BSA), and mAbs were diluted in PBS–Tween 20 (0.05%) containing 3% BSA and 2% normal goat serum. (**A**) Enzyme-linked immunosorbent assay (ELISA) reactivity of mAbs 4E10 (solid bars) and 2F5 (open bars) to CL, PS, PC, PE, and SM. Whereas both 4E10 and 2F5 reacted with cardiolipin, only 4E10 reacted with the other lipids tested. The reactivity of control human anti-CCR5 binding site mAb 1.7b was negative (*33*). Both mAbs 4E10 and 2F5 bound directly to cardiolipin, because cardiolipin binding in ELISA did not require the presence of bovine serum as a source of β2 glycoprotein-1; as an additional negative control, the reactivity of mAbs against empty methanol-coated plates was negative for 2F5 and was seen only at concentrations of 4E10≥2.5 μg per milliliter (*33*). (**B**) To show specificity of binding of mAb 2F5 to cardiolipin, we used 150 μg of 2F5 per milliliter and 500 μg of murine mAb to 2F5 idiotype 3H6 per milliliter, which blocks the neutralization of HIV-1 by mAb 2F5 (*8*). The 2F5 anti-idiotype significantly blocked the binding of mAb 2F5 to cardiolipin by a mean of 70% in three separate experiments ($P < 0.03$). In separate ELISAs, mAb 2F5 bound to cardiolipin with EC_{50} responses that ranged from 0.66 to 2.2 μM (*33*). (**C**) The dose response curve of 4E10 mAb binding to cardiolipin. The EC_{50} response of 4E10 binding (80 nM) was calculated from a four-parametric sigmoidal-curve fitting analysis. Binding data were acquired from an ELISA of 4E10 mAb binding (0.5 to 1000 nM) to cardiolipin coated on an ELISA plate (1.35 μg per well). (**D**) Soluble HIV-1 Env gp140 oligomers (CON-S) expressing the 4E10 epitope inhibit binding of 4E10 mAb to cardiolipin. The IC_{50} of inhibition of 4E10 binding to cardiolipin was calculated to be 145 nM. The inhibition assay was carried out with varying concentrations of gp140 (19.25 to 1230 nM) mixed with 10 μg of 4E10 mAb per milliliter, which were then added to wells containing 1.35 μg of cardiolipin. mAb 3H6 (1 mg/ml) (but not control mAb) also blocked the binding of mAb 2F5 to Sjögren's syndrome antigen A (SSA)/Ro, centromere B, and histones (*33*) as well as blocked to background the binding of MAB 2F5 to HEp-2 cells in indirect immunofluorescence assay (*33*). (**E**) The nominal epitope of the HIV-1 Env gp41 inhibits the binding of mAb 2F5 to cardiolipin. In this experiment, two gp41 2F5 epitope peptides, 2F5 amino acids 652 to 671 (QQEKNEQELLELDKWASLWN), and 2F5 amino acids 656 to 670 (NEQELLELKDWASLW-biotinylated) were used at concentrations ranging from 0 to 50 μM to block the binding of mAb 2F5 to cardiolipin (10 μg per well) (*34*). First, the apparent binding affinity of mAb 2F5 to each peptide was determined and found to be 0.34 nM for 2F5 652–671, and 0.47 nM for 2F5 656–670. (E) demonstrates that both nominal 2F5 epitope peptides inhibited 2F5 mAb binding to cardiolipin, with IC_{50} of 2F5 652 to 671 equal to 0.9 μM, and IC_{50} of 2F5 656 to 670 equal to 2.1 μM. In contrast, a scrambled version of 2F5 656 to 670 did not significantly inhibit mAb 2F5 binding at all concentrations (0 to 50 μM) tested. This is represented by the single diamond at the 50 μM concentration of scrambled 2F5 656 to 670 peptide. All data in [(A) to (E)] are representative of at least two experiments performed.

lipin with an IC_{50} of 145 nM. Thus, the Fab regions of 4E10 and 2F5 mAbs that are involved in binding to gp140 and neutralizing HIV-1 are also involved in binding to cardiolipin. However, the apparent affinity of each with cardiolipin was distinct, with mAb 4E10 nanomolar, whereas the apparent affinity of mAb 2F5 was micromolar.

Antibodies to cardiolipin can be found in patients with disordered immunoregulation caused by autoimmune disease or infection (*10*, *23–25*). Antibodies to cardiolipin are induced by syphilis, leprosy, leishmaniasis, Epstein-Barr virus, and HIV-1 (*10*, *23–25*). Unlike antibodies to cardiolipin found in SLE, "infectious" antibodies to cardiolipin, such as those found in HIV-1 infection, are rarely pathogenic and are transient (*23–25*). Consistent with this, mAbs 2F5, 2G12, and 4E10 have been administered to HIV-1–infected patients with no observed side effects (*2*).

Neutralizing antibodies against 2F5 and 4E10 epitopes are rarely made in HIV-1–infected humans (*5*, *6*) or in the setting of immunization (*7*, *8*). The observation that human mAbs against these epitopes are polyspecific autoantibodies may explain why these antibodies are rarely made in humans. Autoreactive B cell clones with long CDR3 lengths are normally deleted from the repertoire or made tolerant to self antigens, thereby preventing antibody production (*9*). Thus, it is conceivable that HIV-1 may have evolved to escape membrane-proximal antibody responses by having conserved neutralizing epitopes as mimics of autoantibody epitopes. Similarly, these data also raise the hypothesis that current HIV-1 vaccines do not routinely induce robust membrane-proximal antienvelope neutralizing antibodies, because antibodies targeting these epitopes are derived from autoreactive B cell clones that are normally deleted or made tolerant upon antigenic stimulation by HIV-1 Env.

Finally, these observations may also explain the rare occurrence of HIV-1 in SLE patients who may be unable to delete these self-reactive clones (*26*, *27*). If broadly neutralizing antibodies to HIV-1 are made in the context of disordered B cell immunoregulation in autoimmune disease, then autoimmune patients may be fully or partially protected on this basis (*27*, *28*). Polyspecific autoantibodies made by innate B1 and marginal zone B cells are the first line of defense against infections (*29*, *30*). The study of the regulation of polyspecific autoantibody production and the B cells from which they are derived may provide insights into how to induce broadly neutralizing antibodies in the setting of HIV-1 vaccination.

Table 1. Reactivity of HIV-1 Env human mAbs with autoantigens and human cells. All mAbs were negative in assays for reactivity with ribonucleoprotein, La (SSB), Sm, Scl-70, and Jo-1, except for Ku32 mAb, which reacted with Sm, and IgG1b12, which reacted with ribonucleoprotein. Ro (SSA), dsDNA centromere B, histone, and cardiolipin antibody values are in relative units based on a standard curve. –, negative.

mAb type and antibody name	Cardiolipin	HEp-2 cell reactivity	Ro (SSA)	dsDNA	Centromere B	Histones
Membrane-proximal external region (2F5)	47	+Cytoplasmic nuclear	290	–	1776	1011
Membrane-proximal external region (4E10)	15,434	+Cytoplasmic nuclear	221	–	–	–
CD4 binding site (IgG1b12)	–	+Cytoplasmic nucleolar	–	513	479	185
CD4 binding site (F1, 5E, 25G)	–	–	–	–	–	–
Adjacent CD4 binding site (A32)	–	–	–	–	1131	–
Adjacent CD4 binding site (1.4G)	–	–	–	768	1422	539
Adjacent CD4 binding site (1.4C, 4.6H, 4.11C)	–	–	–	–	–	–
Third variable loop (CO11, F2A3, F3.9F, LA21, 447-52D)	–	–	–	–	–	–
gp41 immunodeficient region (7B2, KU32)	–	–	–	–	–	–
gp41 immunodeficient region (2.2B)	–	+Intermediate filament	–	–	314	–
C1-C4 gp120 (8.2A, 2.3B)	–	–	–	–	–	–
C1-C4 gp120 (EH21, C11)	–	–	–	–	–	–
Glycan-dependent (2G12)	–	–	–	–	–	–
CCR5 binding site (1.7B, 2.1C, LF17, E51, 1.9F, LA15, 4.8E, LA28, 1.9E, E047, 2.5E, ED10)	–	–	–	–	–	–
Positive control serum	34	+Homogeneous nuclear	1365	228	624	281
Negative control	<16	–	<120	<120	<120	<120

References and Notes

1. D. R. Burton *et al.*, *Nat. Immunol.* **5**, 233 (2004).
2. G. Stiegler, H. Katinger, *J. Antimicrobiol. Chemother.* **51**, 757 (2003).
3. G. Ofek *et al.*, *J. Virol.* **19**, 10724 (2004).
4. R. M. F. Cardoso *et al.*, *Immunity* **22**, 163 (2005).
5. D. Opalka *et al.*, *J. Immunol. Methods* **287**, 49 (2004).
6. Shaw and colleagues (*31*) transplanted the HIV-1 4E10 and 2F5 epitopes into the HIV-2 Env scaffold, thereby rendering these chimeric viruses susceptible to neutralization by 4E10 and 2F5 (IC_{50} < 0.1 μg/ml). Using this extremely sensitive and specific assay, they were unable to detect either 4E10- or 2F5-like neutralizing antibodies in any one of 175 HIV-1–infected individuals representing the same 10 HIV-1 subtypes or circulating recombinant forms.
7. G. B. McGaughey *et al.*, *Biochemistry* **42**, 3214 (2003).
8. Haynes and colleagues (*32*) have immunized guinea pigs and rabbits with constrained HIV-1 Env immunogens that have 2F5 and 4E10 epitopes stably expressed and have found that neither animal model responded to immunization with HIV-1 Envs with broadly reactive neutralizing antibodies or with antibodies against the 2F5 or 4E10 epitopes.
9. E. Meffre *et al.*, *J. Clin. Invest.* **108**, 879 (2001).
10. C. Petrovas *et al.*, *J. Autoimmun.* **13**, 347 (1999).
11. D. A. Calarese *et al.*, *Science* **300**, 2065 (2003).
12. J. A. Kessler *et al.*, *AIDS Res. Hum. Retroviruses* **13**, 575 (1997).
13. C. N. Scanlan *et al.*, *Adv. Exp. Med. Biol.* **535**, 205 (2003).
14. Materials and methods are available as supporting material on *Science* Online.
15. M. Fenger *et al.*, *Clin. Chem.* **50**, 2141 (2004).
16. E. L. Radway-Bright, C. T. Ravirajam, D. A. Isenberg, *Rheumatology* **39**, 427 (2000).
17. J. Delgado-Alves *et al.*, *Arthritis Rheum.* **46**, 2686 (2002).
18. E. M. Bevers, M. Galli, T. Barbui, P. Comfurius, R. F. Zwaal, *Thromb. Haemostasis* **66**, 629 (1991).
19. J. Guerin *et al.*, *Br. J. Haematol.* **102**, 896 (1998).
20. M. Zhu *et al.*, *Br. J. Haematol.* **105**, 102 (1999).
21. R. Kunert *et al.*, *AIDS* **16**, 667 (2002).
22. G. Barbato *et al.*, *J. Mol. Biol.* **330**, 1101 (2003).
23. L. Weiss *et al.*, *Clin. Immunol. Immunopathol.* **77**, 69 (1995).
24. N. Abuaf *et al.*, *Thromb. Haemostasis* **77**, 856 (1997).
25. S. Loizou *et al.*, *Ann. Rheum. Dis.* **62**, 1106 (2003).
26. R. A. Fox, D. A. Isenberg, *Arthritic Rheum.* **40**, 1168 (1997).
27. R. Palacios, J. Santos, *Int. J. STD AIDS* **15**, 277 (2004).
28. A. Douvas, Y. Takehana, G. Ehresmann, T. Chernyovskiy, E. S. Daar, *AIDS Res. Human Retrovirol.* **12**, 1509 (1996).
29. J. P. Bouvet, G. Dighiero, *Infect. Immun.* **66**, 1 (1998).
30. F. Martin, A. M. Oliver, J. F. Kearney, *Immunity* **14**, 617 (2001).
31. G. Shaw *et al.*, personal communication.
32. B. F. Haynes *et al.*, unpublished observations.
33. B. F. Haynes *et al.*, data not shown.
34. Single-letter abbreviations for the amino acid residues are as follows: A, Ala; C, Cys; D, Asp; E, Glu; F, Phe; G, Gly; H, His; I, Ile; K, Lys; L, Leu; M, Met; N, Asn; P, Pro; Q, Gln; R, Arg; S, Ser; T, Thr; V, Val; W, Trp; and Y, Tyr.

35. Supported by the Duke Center for Translational Research NIH grant AI51445 and by NIH grant PO-1 AI52816. The authors thank D. Howell for fluorescent microscopy; D. Burton and the AIDS Reagent Repository for mAbs IgG1b12 and 447-52D, respectively; G. Kelsoe and T. Kepler for insightful discussions; and D. Lewis and K. Klemp for coagulation assays.

Supporting Online Material

www.sciencemag.org/cgi/content/full/1111781/DC1
Materials and Methods
Fig. S1
Table S1
References

3 March 2005; accepted 19 April 2005
Published online 28 April 2005;
10.1126/science.1111781
Include this information when citing this paper.

Extension of Murine Life Span by Overexpression of Catalase Targeted to Mitochondria

Samuel E. Schriner,[1,5] Nancy J. Linford,[2] George M. Martin,[1,2] Piper Treuting,[3] Charles E. Ogburn,[2] Mary Emond,[4] Pinar E. Coskun,[5] Warren Ladiges,[3] Norman Wolf,[2] Holly Van Remmen,[6] Douglas C. Wallace,[5] Peter S. Rabinovitch[2]*

To determine the role of reactive oxygen species in mammalian longevity, we generated transgenic mice that overexpress human catalase localized to the peroxisome, the nucleus, or mitochondria (MCAT). Median and maximum life spans were maximally increased (averages of 5 months and 5.5 months, respectively) in MCAT animals. Cardiac pathology and cataract development were delayed, oxidative damage was reduced, H_2O_2 production and H_2O_2-induced aconitase inactivation were attenuated, and the development of mitochondrial deletions was reduced. These results support the free radical theory of aging and reinforce the importance of mitochondria as a source of these radicals.

A causative role for reactive oxygen species (ROS) in aging processes, referred to as the free radical theory of aging (*1*), proposes that ROS in biological systems attack molecules and cause the functional decline of organ systems that eventually leads to death. Accumulation of this damage over time is thought to result in pathologies associated with aging, including arteriosclerosis, neoplasia, and cataracts (*2*). ROS are generated, in large part, from single electrons escaping the mitochondrial respiratory chain and reducing molecular oxygen to form the superoxide anion ($O_2^{\cdot-}$). Superoxide dismutase (SOD) converts $O_2^{\cdot-}$ into hydrogen peroxide (H_2O_2) that then produces a highly reactive hydroxyl radical (·OH) in the presence of reduced metal atoms unless H_2O_2 is removed by the action of glutathione peroxidase or catalase.

The hypothesis that longevity can be enhanced by increasing antioxidant defenses has been controversial because of contradictory findings in invertebrate models of aging. These include whether or not the overexpression of SOD or catalase enhances the life span of the fruit fly *Drosophila melanogaster* (*3–6*) and whether synthetic antioxidants extend the life span of the nematode *Caenorhabditis elegans* (*7–10*). Although there is an increasing number of long-lived mutant mouse models, most of them do not directly test the free radical theory of aging. Overexpression of the antioxidant protein thioredoxin was reported to increase mean and maximum life span in a short-lived strain, although the identities of the specific agents that limited life span were not determined (*11*).

To determine the role of H_2O_2 in limiting mammalian life span, we targeted human catalase, normally localized in the peroxisome (PCAT), to the nucleus (NCAT) and mitochondria (MCAT). Catalase activities in MCAT animals were elevated in heart and skeletal muscle of both founder lines (Fig. 1, A and B) and in brain (Fig. 1C) of the 4033 founder line. Furthermore, catalase activity in the cardiac mitochondrial fraction of MCAT animals was 50 times higher than that in their wild-type littermates (Fig. 1D). Quantitative reverse transcription polymerase chain reaction (RT-PCR) confirmed transgene expression in these tissues (fig. S1) (*12*). Endogenous catalase expression was similar between MCAT and wild-type animals, with the highest expression in liver, kidney, and lung (fig. S1). Confocal immunolocalization revealed that about 10 to 50% of cells in the MCAT heart expressed detectable levels of human catalase, co-localized with a mitochondrial marker in heart and fibroblast cultures from MCAT transgenic animals (Fig. 2). Human catalase was not detected in heart or fibroblasts from wild-type littermates. PCAT and NCAT gene products localized to peroxisomes and nuclei, respectively, as previously described (*13*).

To determine whether the expression of PCAT, NCAT, or MCAT could modulate life span, we maintained transgenic animals and wild-type littermates until death. PCAT animals showed a slight extension of median life span of 3 months (10%) and 3.5 months (13%) in the two founder lines compared with controls (Fig. 3A); this was significant only for the 2088 line ($P = 0.02$). Differences in maximal life span were not statistically significant. NCAT mice showed only 1-month (4%) and 3-month (11%) increases in median life span in the two founders; neither was significant (Fig. 3B). Targeting catalase to the mitochondria, however, afforded 4.5-month (17%, $P < 0.0001$) and 5.5-month (21%, $P = 0.0002$) increases in median life spans of founders 4403 and 4033, respectively (Fig. 3C). There was a similar extension of maximal life span: The 10% longest-lived MCAT animals showed a 4.5-month longer median life span than wild-type littermates (both founders combined, $P = 0.001$). Increased life span was evident in both males ($P < 0.0001$) and females ($P = 0.0003$) without any statistically significant sex differences (fig. S2). The MCAT longevity data fit a Gompertz distribution (exponential increase in mortality rate with age) with parallel log mortality rates for MCAT and wild-type littermates (fig. S3), a result often interpreted as a delay in onset of aging. None of the transgenic lines showed a difference in weight or food consumption when compared to littermate controls (table S1), and there were no gross physical abnormalities.

Young (9 to 11 months) and older (20 to 25 months) MCAT and wild-type littermates were examined by histopathology. Little ab-

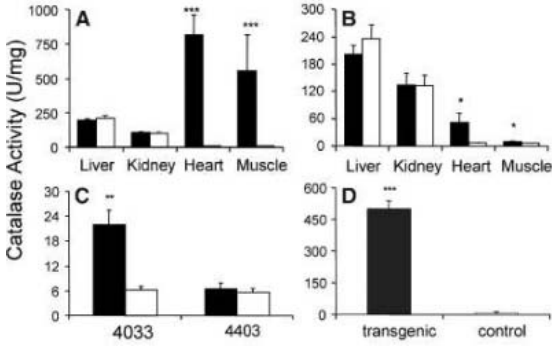

Fig. 1. Catalase activity in MCAT animals. Catalase activities (*12*) (mean ± SEM) in control (open) and transgenic (solid) liver, kidney, heart, and skeletal muscle whole tissue of two founder lines of MCAT mice, (**A**) founder 4033 and (**B**) founder 4403. Note differing ordinate scales. (**C**) Catalase activity in wild-type (WT) control and transgenic whole brain of these two lines ($n = 4$ animals per group). (**D**) Catalase activities in the crude mitochondrial fraction (*12*) of 4033 transgenic and WT control heart ($n = 3$ per group). Asterisk indicates $P < 0.05$; double asterisks, $P < 0.003$; and triple asterisks, $P < 0.001$.

[1]Department of Genome Sciences, [2]Department of Pathology, [3]Department of Comparative Medicine, [4]Department of Biostatistics, University of Washington, Seattle, WA 91895, USA. [5]Center for Molecular and Mitochondrial Medicine and Genetics, Department of Biological Chemistry and Department of Ecology and Evolutionary Biology, University of California, Irvine, Irvine, CA 92697, USA. [6]Department of Cellular and Structural Biology, University of Texas Health Sciences Center at San Antonio, San Antonio, TX 78229, USA.

*To whom correspondence should be addressed. E-mail: petersr@u.washington.edu

normality was seen in either group at 9 to 11 months of age. In older animals, there was a trend toward reduced splenomegally and splenic lymphoid neoplasia in MCAT (1 of 21) compared with wild-type (4 of 24) mice, but this effect was not statistically significant. Cardiac pathology (subendocardial interstitial fibrosis, hyaline cytoplasmic change, vacuolization of cytoplasm, variable myocyte fiber size, hypercellularity, collapse of sarcomeres, mineralization, and arteriolosclerosis) was the most consistent difference between 20- to 25-month MCAT and wild-type mice. These changes are also commonly observed in elderly human hearts, often in association with congestive heart failure (*14*); the latter has also been associated with functional abnormalities of mitochondria (*15*). The severity of pathology was graded on a score of 0 to 4 for a cross-sectional cohort of 21 MCAT and 20 wild-type mice age 20 to 25 months from both founder lines. The severity of arteriosclerosis was 1.29 on average for MCAT and 1.85 for wild-type ($P = 0.04$). The severity of cardiomyopathy was 1.19 for MCAT and 2.00 for wild-type ($P = 0.004$; $P = 0.002$ when combined with arteriosclerosis). This demonstrates the potential of the MCAT protein to protect the heart and suggests that these mice experience a prolonged health span as well as life span. The severity of cataracts, quantitated on a four-point scale by slit-lamp examination, was reduced in 17-month-old founder 4033 MCAT mice compared with age-matched wild-type mice (1.5 ± 0.13 and 1.95 ± 0.13, respectively, $P = 0.003$) but not in founder 4403 compared with wild-type. However, this trend became of borderline significance at 27 months ($P = 0.06$), and by the age of 30 months both groups had similar cataract scores of ~2.5.

The ability of the MCAT protein to enhance protection of mitochondria from ROS was investigated by measuring aconitase activity in isolated heart mitochondria from 5-, 19-, and 30- to 33-month-old animals (Fig. 4, A, B, and C). Aconitase is rapidly inactivated in H_2O_2-treated mitochondria isolated from wild-type hearts of all ages. This inactivation was significantly attenuated in MCAT heart mitochondria at all ages compared to controls, suggesting that these mitochondria eliminate H_2O_2 more effectively and are thereby better protected from oxidative damage. The MCAT protein also decreased mean H_2O_2 production from heart mitochondria 25% compared with wild-type animals (Fig. 4D), a significant difference ($P = 0.004$).

To determine whether MCAT overexpression could reduce oxidative damage to total DNA, we measured 8-hydroxydeoxyguanosine (8-OHdG) in DNA from skeletal muscle and heart. An age-related increase in 8-OHdG in skeletal muscle, but not heart, was observed in control animals, and MCAT mice were protected from this change (Fig. 4E) ($P = 0.03$). Mitochondrial deletions associated with oxidative damage were measured as low molecular weight products by long-extension polymerase chain reaction (LX-PCR). These increased with age in both wild-type heart and skeletal muscle (*16*); however, a statis-

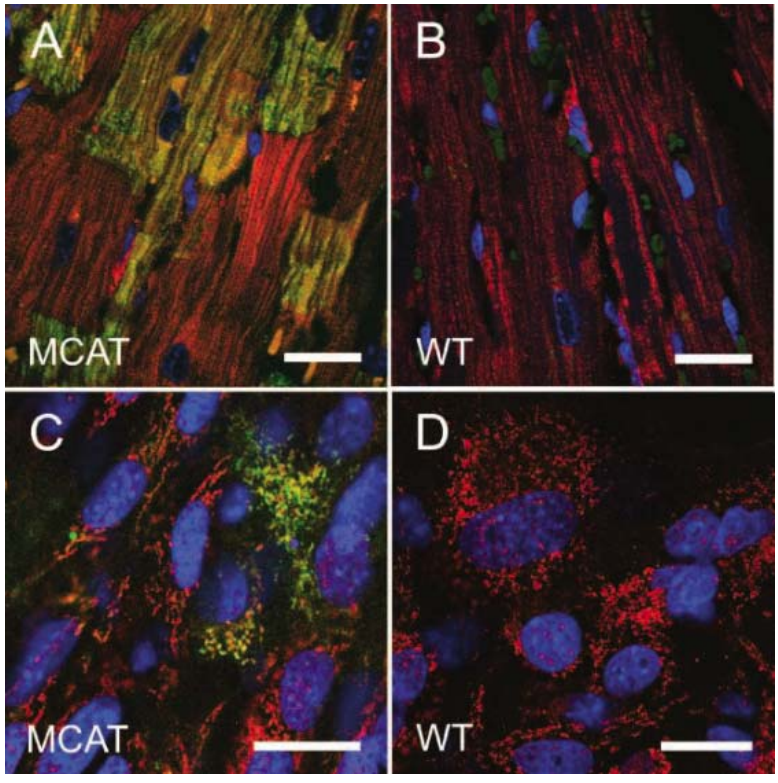

Fig. 2. Mitochondrial localization of human catalase. MCAT (**A**) and WT (**B**) mouse cardiac tissue (9 months old) stained for human catalase (green) and the mitochondrial marker cytochrome c (red) with a 4′,6′-diamidino-2-phenylindole (DAPI) nuclear counterstain (blue). MCAT (**C**) and WT (**D**) mouse embryonic fibroblast cultures stained for human catalase (green) and the mitochondrial marker prohibitin (red) with a sytox green nuclear counterstain (blue). Scale bars indicate 20 μm.

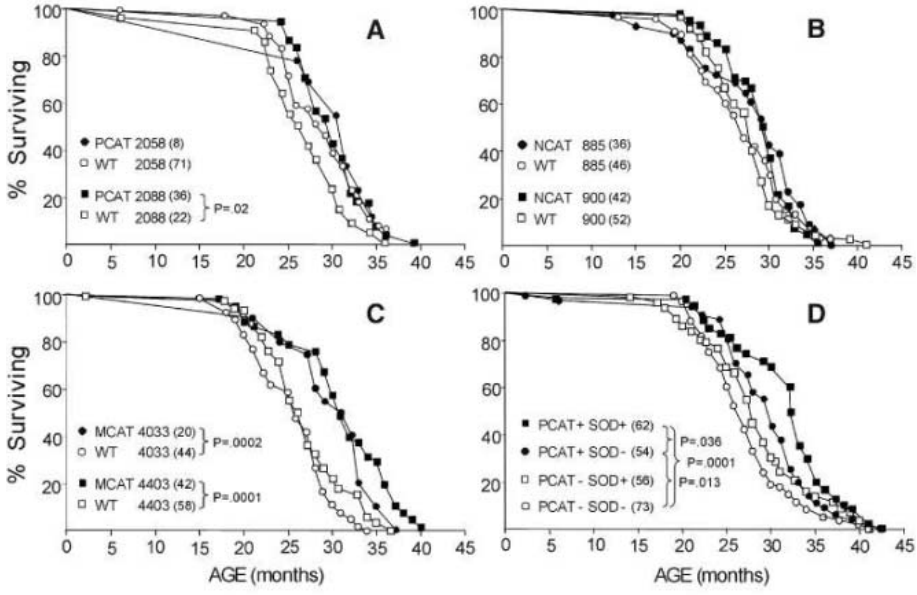

Fig. 3. Life span and catalase overexpression. Survival of transgenic animals and littermate pairs was analyzed for (**A**) PCAT (**B**) NCAT, and (**C**) MCAT, each for two independent founder lines. (**D**) shows the survival of all four genotypes resulting from a cross of hemizygous PCAT mice from line 2088 with hemizygous SOD1-overexpressing mice. The number of mice of each genotype is shown in parentheses. *P* values of significant differences in mean life span between genotypes are indicated.

tically significant decrease in the number of deletion products was noted in 21-month-old MCAT skeletal muscle (Fig. 4F). A decrease was also detected in 30+-month MCAT skeletal muscle and 21-month-old MCAT heart, but neither reached statistical significance.

To examine the possibility that combined enhanced antioxidant defenses might provide further extension of life span in mammals, we bred hemizygous PCAT-overexpressing animals to hemizygous SOD1-overexpressing animals (*17*). The double transgenic mice had an 18.5% extension of median life span compared with wild-type ($P < 0.0001$) and a 7% extension compared with PCAT littermates ($P = 0.036$), but without extension of maximum life span (Fig. 3D). There were no apparent deleterious phenotypic changes in these animals. It seems likely that SOD1 × MCAT or SOD2 × MCAT mice might exhibit an even greater extension of longevity, because both the combination of antioxidant enzymes chosen for enhancement and the subcellular localization appear to have profound effects on the life span extension phenotype.

The life span extension of MCAT mice (Fig. 3) was similar in magnitude to that resulting from knockout of the fat-specific insulin receptor (*18*) but less than that achieved by caloric restriction or dwarfism or that observed in other genetic models of delayed and decelerated aging (*19*). However, the effect of MCAT on life span is accomplished without apparent deleterious side effects and without disabling a major transduction pathway. Although the MCAT longevity phenotype likely results from the direct beneficial effects of reduced oxidative stress in aging, it is also possible that indirect effects, such as a stress response secondary to reduced intracellular H_2O_2-dependent signaling, may also contribute to the longevity phenotype. The mosaic pattern of catalase expression might also play a role in modulating the life span extension. Mosaicism may result from selection against cells expressing high catalase activities during early development because ROS may be an important mitogen (*20*). In addition, silencing of the CAG promoter-enhancer and/or the progressive loss of transgene expression as the founder C3H alleles from the B6 (B6C3F1) hybrid embryos were diluted out through successive B6 back crosses may have reduced or modified MCAT expression (*21*). As a result, the observed MCAT protection against mitochondrial H_2O_2 toxicity, oxidative DNA damage, and mitochondrial DNA deletion accumulation might have been much higher in the aging cohort mice than in the mice that were subsequently tested in biochemical assays. Aging cohort and cardiac pathology studies were performed on mice two to four generations after establishing the transgenic lines. Biochemical tests were done at generation 9 or later, when the genetic background was >99% B6 and the mice had been moved to a new facility, and the life span extension phenotype appears to be diminished. Nonetheless, these results support the conclusion that mitochondrial ROS can be an important limiting factor in determining mammalian longevity and provide impetus for studies of new and combined antioxidant mouse models.

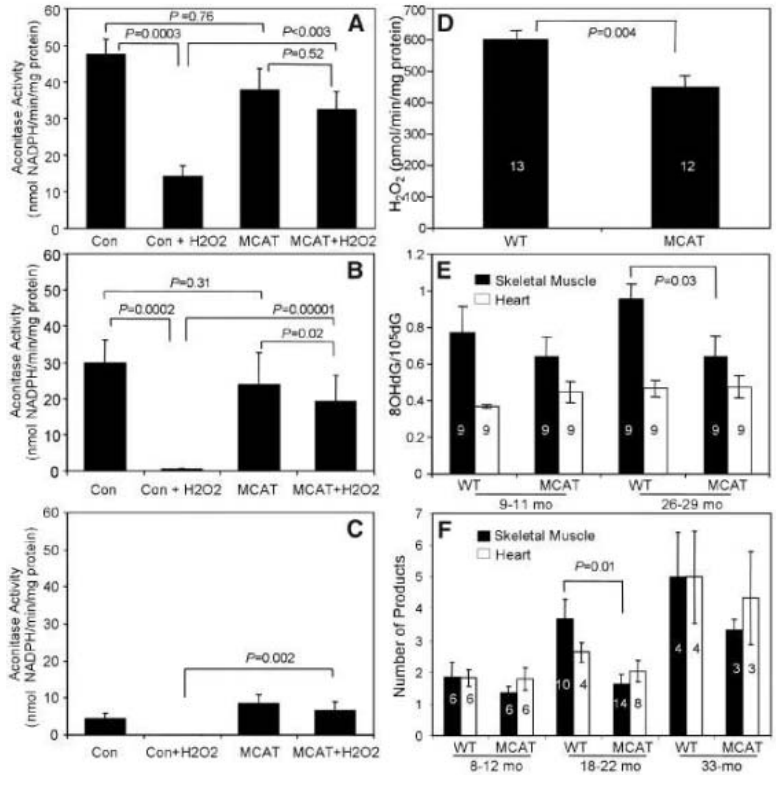

Fig. 4. Aconitase activity, ROS production, and oxidative damage (mean ± SEM). Aconitase activity was measured in cardiac mitochondria from (**A**) 5-month, (**B**) 19-month, and (**C**) 30- to 33-month-old MCAT and WT mice before and after treatment with 50 μM H_2O_2 for 15 minutes at 0°C. $N = 6$ for each group in (A) and (B). In (C), cardiac tissue was pooled from three animals of each genotype and measured in triplicate. When aconitase activity is expressed as a ratio of before versus after H_2O_2 treatment, the differences between WT and MCAT are 3-fold at 5 months ($P < 0.002$), 43-fold at 19 months ($P < 0.0004$), and >50-fold at 30 to 33 months ($P < 0.00005$). (**D**) H_2O_2 production in cardiac mitochondria from 6-month-old mice. (**E**) 8OHdG in skeletal muscle (black) and heart (white) of young and old mice. (**F**) LX-PCR results for genomic DNA derived from skeletal muscle and heart from three age groups. Significant differences between control (WT) and MCAT mice are shown. The numbers within the bars indicate the number of animals examined; in (E), nine animals in three pools of three were examined in each category.

References and Notes

1. D. Harman, *J. Gerontol.* **2**, 298 (1957).
2. T. Finkel, N. J. Holbrook, *Nature* **408**, 239 (2000).
3. J. Sun, D. Folk, T. J. Bradley, J. Tower, *Genetics* **161**, 661 (2002).
4. W. C. Orr, R. S. Sohal, *Science* **263**, 1128 (1994).
5. W. C. Orr, R. J. Mockett, J. J. Benes, R. S. Sohal, *J. Biol. Chem.* **278**, 26418 (2003).
6. R. J. Mockett, A. C. Bayne, L. K. Kwong, W. C. Orr, R. S. Sohal, *Free Radic. Biol. Med.* **34**, 207 (2003).
7. J. N. Sampayo, A. Olsen, G. J. Lithgow, *Aging Cell* **2**, 319 (2003).
8. S. Melov *et al.*, *Science* **289**, 1567 (2000).
9. M. Keaney, D. Gems, *Free Radic. Biol. Med.* **34**, 277 (2003).
10. M. Keaney, F. Matthijssens, M. Sharpe, J. Vanfleteren, D. Gems, *Free Radic. Biol. Med.* **37**, 239 (2004).
11. A. Mitsui *et al.*, *Antioxid. Redox Signal.* **4**, 693 (2002).
12. Materials and methods are available as supporting material on *Science* Online.
13. S. E. Schriner *et al.*, *Free Radic. Biol. Med.* **29**, 664 (2000).
14. T. R. Burns, M. Klima, T. A. Teasdale, K. Kasper, *Mod. Pathol.* **3**, 336 (1990).
15. E. J. Lesnefsky, S. Moghaddas, B. Tandler, J. Kerner, C. L. Hoppel, *J. Mol. Cell. Cardiol.* **33**, 1065 (2001).
16. S. Melov, D. Hinerfeld, L. Esposito, D. C. Wallace, *Nucleic Acids Res.* **25**, 974 (1997).
17. T. T. Huang *et al.*, *J. Gerontol. Ser. A* **55**, B5 (2000).
18. M. Bluher, B. B. Kahn, C. R. Kahn, *Science* **299**, 572 (2003).
19. V. D. Longo, C. E. Finch, *Science* **299**, 1342 (2003).
20. J. A. Petros *et al.*, *Proc. Natl. Acad. Sci. U.S.A.* **102**, 719 (2005).
21. J. Jiang, E. Yamato, J. Miyazaki, *J. Biochem.* (*Tokyo*) **133**, 423 (2003).

22. We thank L. Loeb, B. Preston, and E. Ruiz-Pesini for insightful comments; S. Chen, S. Tsang, S. Knoblaugh, R. Mangalindan, and N. Hudson for technical contributions; and C. Epstein for SOD1-overexpressing animals. Supported by NIH grants AG001751, ES07033, and AG13280.

Supporting Online Material

www.sciencemag.org/cgi/content/full/1106653/DC1
Materials and Methods
Figs. S1 to S3
Table S1
References

22 October 2004; accepted 15 April 2005
Published online 5 May 2005;
10.1126/science.1106653
Include this information when citing this paper.

Climate Change and Distribution Shifts in Marine Fishes

Allison L. Perry,[1]* Paula J. Low,[2]† Jim R. Ellis,[2] John D. Reynolds[1]*

We show that the distributions of both exploited and nonexploited North Sea fishes have responded markedly to recent increases in sea temperature, with nearly two-thirds of species shifting in mean latitude or depth or both over 25 years. For species with northerly or southerly range margins in the North Sea, half have shown boundary shifts with warming, and all but one shifted northward. Species with shifting distributions have faster life cycles and smaller body sizes than nonshifting species. Further temperature rises are likely to have profound impacts on commercial fisheries through continued shifts in distribution and alterations in community interactions.

Climate change is predicted to drive species ranges toward the poles (*1*), potentially resulting in widespread extinctions where dispersal capabilities are limited or suitable habitat is unavailable (*2*). For fishes, climate change may strongly influence distribution and abundance (*3*, *4*) through changes in growth, survival, reproduction, or responses to changes at other trophic levels (*5*, *6*). These changes may have impacts on the nature and value of commercial fisheries. Species-specific responses are likely to vary according to rates of population turnover. Fish species with more rapid turnover of generations may show the most rapid demographic responses to temperature changes, resulting in stronger distributional responses to warming. We tested for large-scale, long-term, climate-related changes in marine fish distributions and examined whether the distributions of species with fast generation times and associated life history characteristics are particularly responsive to temperature changes.

We studied the demersal (bottom-living) fish assemblage in the North Sea. This group is composed of more than 90 species with varied biogeographical origins and distribution patterns. North Sea waters have warmed by an average of 0.6°C between 1962 and 2001, based on four decadal means before 2001, and by 1.05°C from 1977 to 2001 (*7*), which correspond with our fish survey time series. Survey data were used to calculate catch per unit effort to determine centers of abundance (mean latitudes and depths) for all species and boundary latitudes for those species that have either northerly or southerly range limits in the North Sea (*7*). No species range was entirely confined to the North Sea. Measures of distribution were regressed against same-year and time-lagged bottom temperatures, and also a composite measure of temperatures, the North Atlantic Oscillation Index, the Gulf Stream Index, and the ratio of abundances of northern and southern calanoid copepod species (*7*). We also controlled for changes in abundance that may have influenced species distributions (*7*).

Centers of distribution as measured by mean latitudes shifted in relation to warming for 15 of 36 species (Table 1). These trends were shown by both commercially exploited species [such as Atlantic cod (*Gadus morhua*) and the common sole (*Solea solea*)], and by species that are not targeted by fisheries [such as scaldfish (*Arnoglossus laterna*) and snake-blenny (*Lumpenus lampretaeformis*)]. Distances moved ranged from 48 to 403 km (average distance $\bar{x}$ = 172.3 ± 98.8 km, n = 15 species) (Fig. 1) and most of these shifts (13 of 15) were northward (Table 1). The spatial temperature gradient of the North Sea is somewhat unusual; water temperatures become colder with increasing latitude in the southern North Sea but become slightly warmer with increasing latitudes in the north (*8*), where warm North Atlantic Current waters enter the region (*9*). This temperature pattern may explain one of the two exceptional species that moved south, the Norway pout (*Trisopterus esmarkii*). Its distribution was centered in the northern North Sea, and its southern movement brought it into cooler waters. The other exception was the common sole. We speculate that the southward shift in its distribution may have been caused by the fact that the cleanup of the Thames estuary led to its emergence as a major sole nursery ground during the study period (*10*).

Most species that showed climate-related latitudinal changes also shifted in depth, which was unsurprising because North Sea depths are roughly positively correlated with latitude (*8*). A further six species, including plaice (*Pleuronectes platessa*) and cuckoo ray (*Leucoraja*

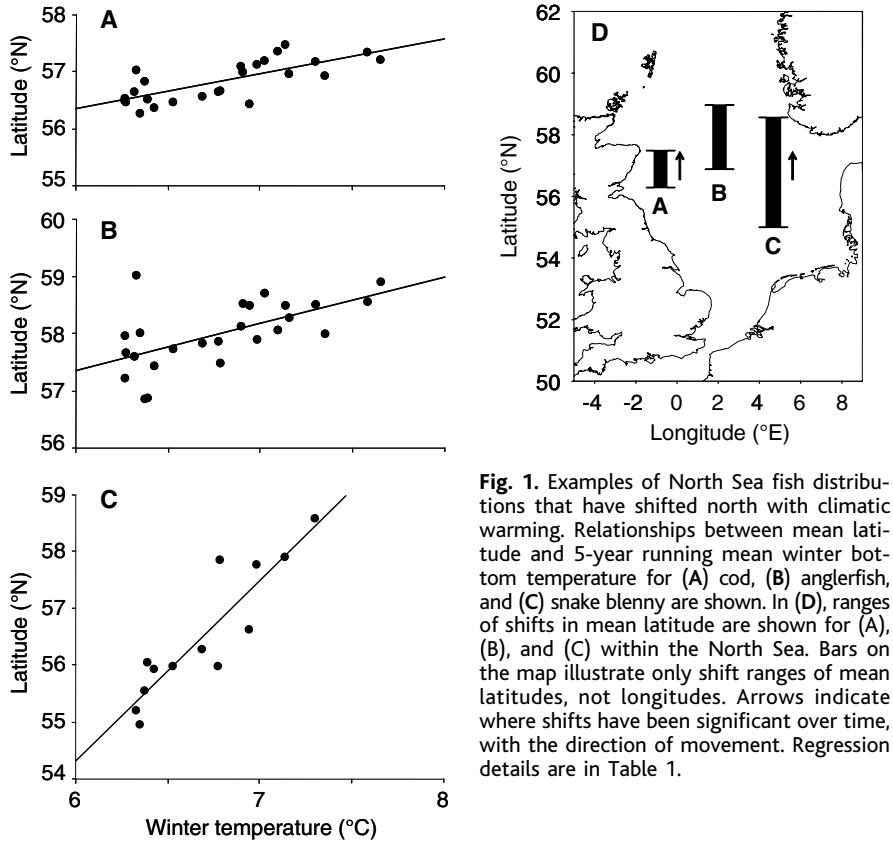

Fig. 1. Examples of North Sea fish distributions that have shifted north with climatic warming. Relationships between mean latitude and 5-year running mean winter bottom temperature for (**A**) cod, (**B**) anglerfish, and (**C**) snake blenny are shown. In (**D**), ranges of shifts in mean latitude are shown for (A), (B), and (C) within the North Sea. Bars on the map illustrate only shift ranges of mean latitudes, not longitudes. Arrows indicate where shifts have been significant over time, with the direction of movement. Regression details are in Table 1.

[1]Centre for Ecology, Evolution and Conservation, School of Biological Sciences, University of East Anglia, Norwich NR4 7TJ, UK. [2]Centre for Environment, Fisheries and Aquaculture Science, Lowestoft Laboratory, Lowestoft NR33 0HT, UK.

*To whom correspondence should be addressed. E-mail: a.perry@uea.ac.uk (A.L.P.); reynolds@uea.ac.uk (J.D.R.).

†Present address: University Marine Biological Station Millport, Isle of Cumbrae KA28 0EF, UK.

naevus), moved deeper with warming but did not change in latitude, suggesting that they may have responded to climatic variation through local movements offshore or into pockets of deeper water. Considering both latitude and depth, nearly two-thirds of species (n = 21 out of 36) have shown distributional responses to climatic warming (table S1).

We tested whether species boundaries have also been displaced by warming, by examining those 20 species from our data set with a southern or a northern range limit in the North Sea. The boundaries of half of these fishes moved significantly with warming (Fig. 2 and table S2). Southern boundaries shifted in 6 of 12 cases, and all shifts were northward. Four of eight northern boundaries also moved with warming. All but one of these species shifted north, despite the fact that their northern range limits lay in the relatively intensively fished southern North Sea (*11*). Shifting species again included both exploited and nonexploited fishes. Boundaries moved over distances ranging from 119 to 816 km ($\bar{x}$ = 304 ± 196 km, n = 10), with the highest value describing the range of movement of the southern boundary of blue whiting (*Micromesistius poutassou*), which is the target of the largest fishery in the Atlantic (*12*). In the case of bib (*Trisopterus luscus*), the northern boundary shifted by 342 km from 1978 to 2001, a trend that is supported by observations that North Sea catches of this species have been increasing (*13*).

To identify shifts that may have been driven by fishing or other nonclimatic influences, we also examined distribution changes over time. Fishing pressure could not be included explicitly in our analyses because reliable fishing effort data on a comparable spatial and temporal scale do not exist for the North Sea. However, during at least the last decade of the 25-year period of analysis, the spatial distribution of effort remained relatively constant (*11*), and total fishing effort may have declined slightly (*14*). Temporal trends in distribution suggested that fishing alone could not explain climate-related shifts; despite the general increase in temperature over the study period, warming-related shifts occurred independently of time for centers of distribution in 8 of 36 species and for range limits in 4 of 20 species (table S3). Such shifts may have reflected year-to-year environmental variability, with northward movement during warm years cancelled by southward movement during cool years. If so, long-term distribution shifts could depend strongly on future climatic variability, in addition to longer-term average conditions.

The examination of temporal trends also allowed for rough comparisons to be drawn with rates of warming-related distribution shifts in other taxa. A recent meta-analysis of climate-change impacts on natural systems estimated the mean annual rate of boundary movement for 99 species of birds, butterflies, and alpine herbs at 0.6 km northward or 0.6 m upward (*1*). From the current study, the mean rate of movement for the six fish species whose boundaries shifted in relation to both climate and time [bib, blue whiting, lesser weever

Table 1. Statistically significant multiple regressions of the effects of three measures of North Sea warming on mean latitudes of 36 demersal fishes from 1977 to 2001. PC1, first principal component from principal components analysis (PCA) of eight environmental variables (PC1 generally describes warming). Winter temp. and summer temp. indicate 5-year running mean bottom temperatures for December to March and June to September, respectively.

Species	Common name	df	Mean latitude (°N)	SD	PC1	r^2	P	Winter temp.	r^2	P	Summer temp.	r^2	P
Agonus cataphractus	Pogge	22	54.67	0.90									
Anarhichus lupus	Atlantic wolffish	21	58.14	0.46									
Argentina spp.	Argentines	24	59.59	0.30									
Arnoglossus laterna	Scaldfish	15	54.17	0.31				0.456	0.43	0.006			
Buglossidium luteum	Solenette	23	54.14	0.28									
Callionymus lyra	Dragonet	23	55.40	0.65	0.265	0.16	0.049	0.937	0.34	0.002			
Echiichthys vipera	Lesser weever	24	53.30	0.13				0.191	0.39	0.001			
Eutrigla gurnardus	Grey gurnard	23	56.13	0.35	0.194	0.30	0.006	0.651	0.61	<0.001	0.402	0.17	0.040
Gadiculus argenteus	Silvery pout	23	59.83	0.41									
Gadus morhua	Atlantic cod	23	56.81	0.34	0.256	0.58	<0.001	0.534	0.38†	<0.001	0.578	0.33†	<0.001
Glyptocephalus cynoglossus	Witch	24	58.22	0.42									
Hippoglossoides platessoides	Long rough dab	24	57.62	0.21				0.304	0.40	0.001			
Lepidorhombus boscii	Fourspot megrim	24	60.51	0.37									
Leucoraja naevus	Cuckoo ray	19	58.06	0.57									
Limanda limanda	Dab	24	55.86	0.13				0.180	0.35†	0.001			
Lophius piscatorius	Anglerfish	23	57.99	0.58	0.254	0.19	0.032	0.818	0.37	0.001			
Lumpenus lampretaeformis	Snake blenny	12	56.52	1.15				3.174	0.81	<0.001			
Melanogrammus aeglefinus	Haddock	24	57.91	0.16									
Merlangius merlangus	Whiting	23	56.57	0.15	0.066	0.19	0.034						
Merluccius merluccius	Hake	24	58.84	0.59									
Micromesistius poutassou	Blue whiting	21	60.13	0.48									
Microstomus kitt	Lemon sole	24	57.06	0.24									
Molva molva	Ling	24	59.26	0.74									
Myxine glutinosa	Hagfish	11	57.51	0.62									
Pleuronectes platessa	Plaice	24	55.52	0.18									
Pollachius virens	Saithe	24	59.44	0.20									
Psetta maxima	Turbot	13	54.73	0.31									
Rhinonemus cimbrius	Four-bearded rockling	22	56.05	0.68	0.419	0.40	0.001	1.147	0.53	<0.001	0.950	0.28	0.008
Scyliorhinus canicula	Small-spotted catshark	20	58.34	0.89									
Sebastes spp.	Redfish	18	59.89	0.49									
Solea solea	Common sole	13	53.68	0.66				–0.941	0.38	0.020	–0.963	0.34	0.028
Squalus acanthias	Spurdog	19	56.29	0.68									
Trigla lucerna	Tub gurnard	19	53.89	0.50									
Trisopterus esmarkii	Norway pout	23	58.59	0.26	–0.190	0.52	<0.001	–0.304	0.25	0.010	–0.429	0.37	0.001
Trisopterus luscus	Bib	9	53.29	0.51				0.489*	0.45	0.035			
Trisopterus minutus	Poor cod	23	55.63	0.66	0.334	0.26	0.012	0.877	0.33	0.003	0.753	0.18	0.035

*A relationship with annual mean summer or winter temperature. †To identify the proportion of variance in distribution accounted for by warming, r^2 and P describe the squared semi-partial correlation coefficient, where abundance was also a significant predictor of distribution.

(*Echiichthys vipera*), Norway pout, scaldfish, and witch (*Glyptocephalus cynoglossus*)] was 2.2 km per year. It is perhaps unsurprising that the rate of shift might be higher for marine fishes than for alpine herbs and butterflies, given that marine fish may generally face fewer constraints on movement. However, if such a difference is indicative of more widespread trends in marine fishes, climate change could pose a greater threat to fish populations that are constrained by their dispersal capabilities or habitat requirements.

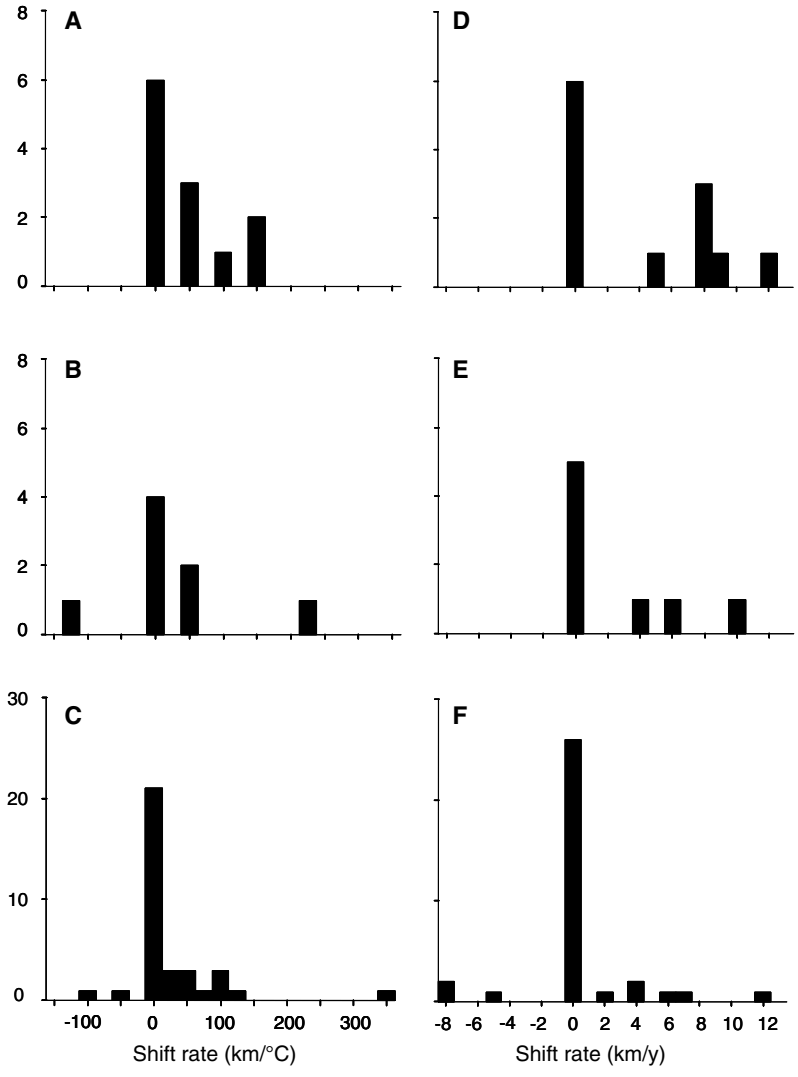

Fig. 2. Frequency distributions of fish species shift rates in relation to warming and time. (**A**) Rates of shift for northerly species' (southern) boundaries with climate. (**B**) Southerly species' (northern) boundaries with climate. (**C**) All species' mean latitudes with climate. (**D**) Northerly species'(southern) boundaries over time. (**E**) Southerly species' (northern) boundaries over time. (**F**) All species' mean latitudes over time. Rates for shifting species are slopes from regressions.

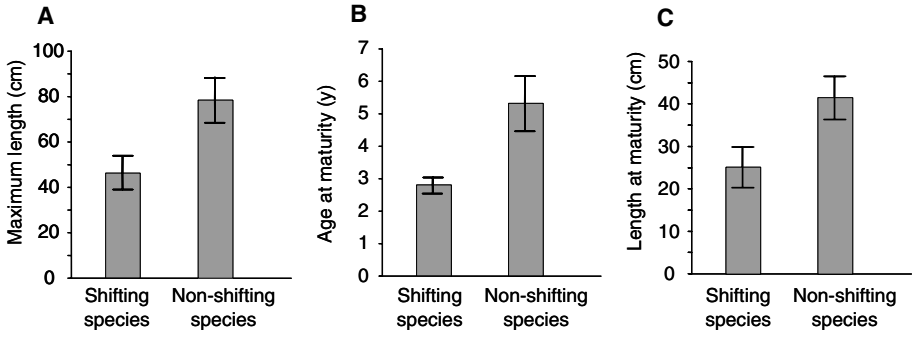

Fig. 3. Differences in life-history traits between shifting (n = 15) and nonshifting (n = 21) species with respect to centers of distribution (mean latitudes). (**A**) Maximum body size [t = –2.41, degrees of freedom (df) = 34, P = 0.02]. (**B**) Age at maturity (t = –2.86, df = 27, P = 0.01). (**C**) Length at maturity (t = –2.29, df = 29, P = 0.03). Means are shown with standard errors.

If the differences in rates of movement among the taxa documented here result from differential rates of population turnover, we would expect species with life history traits associated with fast population growth to have responded most strongly to climate change. To test this prediction, we compared life history traits between shifting and nonshifting species (*7*). As predicted, shifting species tend to have faster life histories than do nonshifting species, with significantly smaller body sizes, faster maturation, and smaller sizes at maturity (Fig. 3). Body growth rates did not differ significantly between shifting and nonshifting species (P = 0.19). These relationships therefore provide a starting point for predicting species' responses to future climate change. These predictions could be refined, through detailed studies of the relative sensitivities of different life history stages, to uncover the specific mechanisms driving the patterns.

Our study shows that climate change is having detectable impacts on marine fish distributions, and observed rates of boundary movement with warming indicate that future distribution shifts could be pronounced. Mean annual surface temperatures in the North Sea are predicted to increase by 0.5 to 1.0°C by 2020, 1.0 to 2.5°C by 2050, and 1.5 to 4.0°C by 2080 (*15*). We used the midpoints of these temperature ranges as the basis for a rough approximation, which suggested that two types of commercial fishes, blue whiting and redfishes (*Sebastes* spp.), may retract completely from the North Sea by 2050, and by 2080, bib may extend its range northward to encompass the entire region. Such changes will clearly also depend on the responses of their predators and prey to increases in bottom temperature and on the availability of suitable habitat.

These findings may have important impacts on fisheries. For example, species with slower life histories are already more vulnerable to overexploitation (*16*–*18*) and may also be less able to compensate for warming through rapid demographic responses. A further concern is that differential rates of shift could result in altered spatial overlap among species, thereby disrupting interactions and also potentially compounding the decoupling effects of climate-driven changes in phenology (*19*). Previous work off the eastern United States has shown that fishes with the most temperature-sensitive distributions included key prey species of nonshifting predators (*20*). Such changes could have unpredictable effects in an ecosystem already under heavy anthropogenic pressure.

References and Notes

1. C. Parmesan, G. Yohe, *Nature* **421**, 37 (2003).
2. C. D. Thomas *et al.*, *Nature* **427**, 145 (2004).
3. C. M. Wood, D. G. McDonald, Eds., *Global Warming: Implications for Freshwater and Marine Fish* (Cambridge Univ. Press, Cambridge, 1997).
4. K. Brander *et al.*, *Int. Counc. Explor. Sea Mar. Sci. Symp.* **219**, 261 (2003).
5. G. Beaugrand, K. M. Brander, J. A. Lindley, S. Souissi, P. C. Reid, *Nature* **426**, 661 (2003).
6. G. Beaugrand, P. C. Reid, F. Ibañez, J. A. Lindley, M. Edwards, *Science* **296**, 1692 (2002).
7. Materials and methods are available as supporting material on *Science* Online.
8. R. J. Knijn, T. W. Boon, H. J. L. Heessen, J. F. G. Hislop, *Atlas of North Sea Fishes* [International Council for the Exploration of the Sea (ICES) Cooperative Research Report 194, ICES, Copenhagen, 1993].
9. A. N. Strahler, A. H. Strahler, *Physical Geography: Science and Systems of the Human Environment* (Wiley, New York, 1997).
10. R. M. Thomas, in *A Rehabilitated Estuarine Ecosystem: The Environment and Ecology of the Thames Estuary*, M. J. Attrill, Ed. (Kluwer, Dordrecht, Netherlands, 1998), pp. 115–139.
11. S. Jennings *et al.*, *Fish. Res.* **40**, 125 (1999).
12. ICES Advisory Committee on Fishery Management (ACFM), *Report of the Northern Pelagic and Blue Whiting Fisheries Working Group* (ICES CM 2004/ACFM:24, ICES, Copenhagen, 2004).
13. S. I. Rogers, J. R. Ellis, *Int. Counc. Explor. Sea J. Mar. Sci.* **57**, 866 (2000).
14. N. Daan, H. Gislason, J. Pope, J. Rice, *Changes in the North Sea Fish Community: Evidence of Indirect Effects of Fishing?* (ICES CM N:10, ICES, Copenhagen, 2003).
15. U.K. Climate Impacts Programme, *UKCIP02 Scenarios Gateway—Maps Gateway*; available at www.ukcip.org.uk/scenarios/marine/marine.html.
16. N. K. Dulvy, Y. Sadovy, J. D. Reynolds, *Fish Fish.* **4**, 25 (2003).
17. S. Jennings, J. D. Reynolds, S. C. Mills, *Proc. R. Soc. London Ser. B* **265**, 333 (1998).
18. J. D. Reynolds, S. Jennings, N. K. Dulvy, in *Conservation of Exploited Species*, J. D. Reynolds, G. M. Mace, K. H. Redford, J. G. Robinson, Eds. (Cambridge Univ. Press, Cambridge, 2001), pp. 145–168.
19. M. Edwards, A. J. Richardson, *Nature* **430**, 881 (2004).
20. S. A. Murawski, *Trans. Am. Fish. Soc.* **122**, 647 (1993).
21. We thank A. Taylor, P. C. Reid, T. Osborn, P. Jones, the ICES Oceanographic Database, and the UK Climate Impacts Programme for providing data; J. Gill, W. Sutherland, and A. Watkinson for commenting on earlier drafts; and M. Attrill, K. Brander, R. Clark, C. Fox, J. Gill, and S. Jennings for valuable discussion. This research was undertaken under the Defra-funded project MF0730, with additional support from a Commonwealth Scholarship to A.L.P. and an NERC grant to J.D.R.

Supporting Online Material

www.sciencemag.org/cgi/content/full/1111322/DC1
Materials and Methods
Tables S1 to S4
References

22 February 2005; accepted 28 April 2005
Published online 12 May 2005;
10.1126/science.1111322
Include this information when citing this paper.

Community Proteomics of a Natural Microbial Biofilm

Rachna J. Ram,[1] Nathan C. VerBerkmoes,[3,4] Michael P. Thelen,[1,6] Gene W. Tyson,[1] Brett J. Baker,[2] Robert C. Blake II,[7] Manesh Shah,[5] Robert L. Hettich,[4] Jillian F. Banfield[1,2]*

Using genomic and mass spectrometry–based proteomic methods, we evaluated gene expression, identified key activities, and examined partitioning of metabolic functions in a natural acid mine drainage (AMD) microbial biofilm community. We detected 2033 proteins from the five most abundant species in the biofilm, including 48% of the predicted proteins from the dominant biofilm organism, *Leptospirillum* group II. Proteins involved in protein refolding and response to oxidative stress appeared to be highly expressed, which suggests that damage to biomolecules is a key challenge for survival. We validated and estimated the relative abundance and cellular localization of 357 unique and 215 conserved novel proteins and determined that one abundant novel protein is a cytochrome central to iron oxidation and AMD formation.

Microbial communities play key roles in the Earth's biogeochemical cycles. Our knowledge of the structure and activities in these communities is limited, because analyses of microbial physiology and genetics have been largely confined to studies of organisms from the few lineages for which cultivation conditions have been determined (*1*). An additional limitation of pure culture–based studies is that potentially critical community and environmental interactions are not sampled. Recent acquisition of genomic data directly from natural samples has begun to reveal the gene content of communities (*2*) and environments (*3*). Here we combined "shotgun" mass spectrometry (MS)–based proteomics (*4–6*) with community genomic analysis to evaluate in situ microbial activity of a low-complexity natural microbial biofilm.

The biofilm samples used in this study and prior work (*2*) were collected from underground sites in the Richmond mine at Iron Mountain, near Redding, California (USA). These pink biofilms grew on the surface of sulfuric acid–rich (pH ~0.8), ~42°C solutions that contain near-molar concentrations of Fe and millimolar concentrations of Zn, Cu, and As (*7*) (Fig. 1). We used oligonucleotide probes (*8*) to demonstrate that *Leptospirillum* group II dominated the sample, but it also contained *Leptospirillum* group III, *Sulfobacillus*, and Archaea related to *Ferroplasma acidarmanus* and "G-plasma" (Fig. 2). This was similar in structure and composition to the community previously used as a source of genomic sequence (*2*).

In general, proteins could be assigned to organisms, because the genes that encode them are on DNA fragments (scaffolds) that have been assigned to different organism types (*2*). From the genomic dataset (*2*), we created a database of 12,148 proteins (Biofilm_db1) that was used to identify two-dimensional (2D) nano–liquid chromatography (nano-LC) (200 to 300 nl/min) tandem mass spectrometry (MS/MS) spectra (*8–13*) from different biofilm fractions. One or more peptides were assigned to ~5994 proteins (Table 1). This corresponds to ~49% of all proteins encoded by the genomes of the five most abundant organisms. We estimated the likelihood of false-positive protein identification using a variety of detection criteria and databases derived from organisms not present in this environment (*8*). Because of these results, for all subsequent analyses, we required matching of two or more peptides per protein for confident detection (*8*). After removal of duplicates, we detected 2003 different proteins (table S1). An additional 30 proteins were found that were encoded by alternative or overlapping open reading frames (*8*).

We detected 48% of the predicted proteins (i.e., 1362 of 2862) from *Leptospirillum* group II (table S2). This percentage exceeded those of most prior proteomic studies of microbial isolates (*10*, *12*, *13*). In part, this may reflect the presence of cells in many different growth stages, as well as microniches within the biofilm (*14*). We also detected 270 *Leptospirillum* group III, 84 *Ferroplasma* type I, 99 *Ferroplasma* type II, and 122 "G-plasma" proteins. In addition, we found 30 proteins on unassigned archaeal scaffolds and 36 on unassigned bacterial scaffolds. The proportion of proteins detected from each organism type was similar to the proportion of cells from each organism type in the biofilm (*8*). Most proteins from low-abundance members were probably in concentrations too low to be detected by the presence of two peptides.

[1]Department of Environmental Science, Policy, and Management, [2]Department of Earth and Planetary Science, University of California at Berkeley, Berkeley, CA 94720, USA. [3]Graduate School of Genome Science and Technology University of Tennessee–Oak Ridge National Laboratory, 1060 Commerce Park, Oak Ridge, TN 37830, USA. [4]Chemical Sciences Division, [5]Life Sciences Division, Oak Ridge National Laboratory, Oak Ridge, TN 37831, USA. [6]Biosciences Directorate, Lawrence Livermore National Laboratory, Livermore, CA 94551, USA. [7]College of Pharmacy, Xavier University, New Orleans, LA, 70125, USA.

*To whom correspondence should be addressed. E-mail: jill@seismo.berkeley.edu

Furthermore, we were unable to identify proteins from organisms such as *Sulfobacillus*, for which there is little genome sequence (*2*).

Using the MS data, we estimated the relative abundance of individual proteins in different biofilm fractions (*15*). Overall, the biofilm was dominated by novel proteins that are the products of genes previously annotated as "hypothetical" (42% of genes in the original genomic dataset). On the basis of the BLASTP algorithm (*16*), these proteins lack significant homology (*17*) to proteins with functional assignments. Of the abundant proteins, 15% were "unique" (not significantly similar to any known protein), and 2% were "conserved" (similar to other predicted proteins, but not significantly similar to characterized proteins). Other functional groups prominent in the group of most abundant biofilm proteins were ribosomal proteins (13%), chaperones (11%), thioredoxins (9%), and proteins involved in radical defense (8%). Ten abundant disulfide isomerases were detected, at least four of which were present in the extracellular fraction. Together these findings suggest that protein stability in pH < 1 solutions is achieved in part by refolding, catalyzed by abundant enzymes that were tolerant of low pH. Peroxiredoxin and some other abundant proteins (e.g., rubrerythrin and catalase) are involved in defense against oxidative stress, which indicates an important challenge in the AMD environment.

On the basis of MS sequence coverage, the extracellular fraction was enriched (*18*) in unique proteins (52%) and contained ~14% conserved novel proteins. These proteins presumably function in AMD solution and may be important for adaptation to the acidic, metal-rich environment. Among extracellular proteins, the three with the highest sequence coverage in this fraction are encoded by hypothetical genes. One showed weak similarity to c-type cytochromes and Fe/Pb permeases (table S2), and originated from *Leptospirillum* group II.

Although 67% of the predicted amino acid sequence of the protein that resembles cytochrome c could be reconstructed from multiple overlapping peptides, there were three gaps (Fig. 3). Further analysis revealed that one gap contains a signal peptide (*19*); the two others contain single amino acid differences in the cytochrome variant found in the biofilm used for proteomic analysis versus the biofilm used to generate the genomic data (*8*). After taking into account these factors, 100% of the protein was recovered by MS. Therefore, combining community genomics with proteomics data allows detection of protein variants and signal sequence cleavage in natural samples.

This extracellular protein also contained a heme-binding consensus sequence, indicating that it may play a role in electron transport. We verified by gel electrophoresis analysis and N-terminal sequencing that this is a heme-containing protein that is abundant in the extracellular fraction (*8*) (fig. S3). Interestingly, the peptide sequence differed from the predicted sequence, because it contained leucine in place of isoleucine at a position encoded by ATC, which suggests atypical codon usage. The proteomic analysis is blind to this substitution because isoleucine and leucine share the same mass. Abundant iron-oxidizing cytochromes with absorption peaks around 579 nm have been detected in *Leptospirillum ferrooxidans* (a member of *Leptospirillum* group I) and *Leptospirillum ferriphilum* (a member of *Leptospirillum* group II) isolates (*20*, *21*) (fig. S4). Amino acid sequences for these cytochromes have not been reported. Because the absorption at 579 nm is unique to

Table 1. Number of proteins detected through triplicate analysis of biofilm fractions using different filtering levels. The LCQ and LTQ datasets were derived from redundant protein counts from global contrast files using two different MS techniques (*8*). Liberal filters require at least one peptide per gene; conservative filters require at least two peptides per gene; ultraconservative filters require at least three peptides per gene. Xcorrs of at least 1.8 (+1), 2.5 (+2), 3.5 (+3) were used in all cases.

Filtering level	LCQ data set	LTQ data set	Combined data sets
Liberal filters	3127	5534	5994
Conservative filters	1160	2077	2146
Ultraconservative filters	837	1419	1435

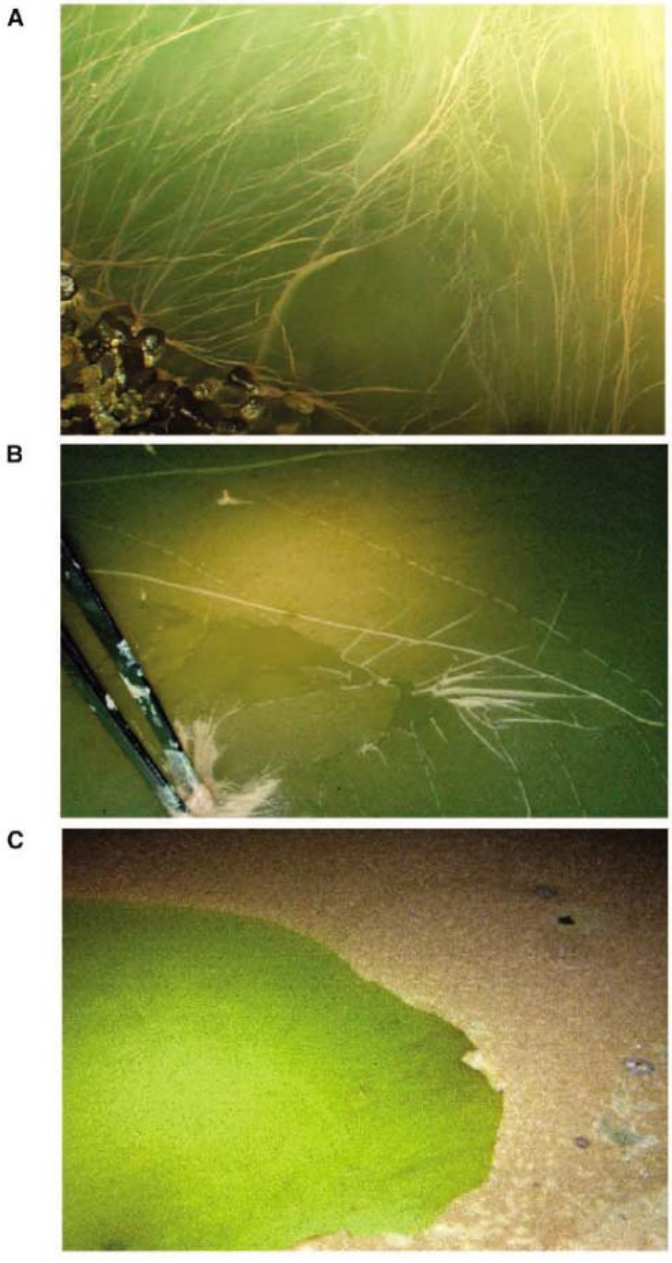

Fig. 1. (**A**) Photograph of the biofilm during collection in January 2004. The biofilm occurs as a continuous sheet over the surface of the AMD pool; wrinkles form because of movement of the solution. [Photograph taken from the AB end location (fig. S1).] (**B**) Close-up photograph during sample collection showing that the biofilm is thin and apparently homogeneous. (**C**) A thicker biofilm in the same location 5 months later, which suggests that the initial biofilm was actively growing when sampled. [Photographs by T. Johnson]

the abundant *Leptospirillum* cytochrome type, we henceforth refer to these proteins as cyt_{579}.

The first 40 amino acids of cyt_{579} purified from the periplasm of *L. ferriphilum* (*8*) matched the predicted sequence of the extracellular cytochrome in *Leptospirillum* group II derived from the biofilm after taking into account loss of the 23 amino acid signal peptide and the substitution of leucine for isoleucine. The cleavage of a leader sequence from the N terminus indicates that the mature protein is exported across the cytoplasmic membrane. The rate constant for the ferrous iron–dependent reduction of cyt_{579} purified from *L. ferriphilum* was greater than or equal to the overall turnover number for the transfer of electrons from ferrous iron to molecular oxygen by whole cells (*8*). Furthermore, the apparent standard reduction potential of cyt_{579} was ~670 mV (*8*). This relatively high potential would be expected for an electron carrier in a transport chain where the electron donor (ferrous ions complexed with sulfate in acidic solution) has a reduction potential of ≥660 mV. Thus, cyt_{579} has both kinetic and thermodynamic properties consistent with a central role in iron oxidation by *Leptospirillum* group II. The high abundance, localization to the extracellular fraction, and enzymatic activity of cyt_{579} imply that it is the primary iron oxidant in the electron transport chain (fig. S5). Eight c-type cytochromes and three other novel proteins with heme-binding motifs were also detected.

As the supply of ferric iron is the rate-limiting step for pyrite oxidation in this environment (*22*), the metabolic activity of iron-oxidizing microorganisms largely determines the rate of AMD formation. *Leptospirillum* group II dominates most biofilms from the Richmond mine and is frequently detected at other mining sites and bioleaching plants (*23*). Thus, cyt_{579} is likely one of the key enzymes that connects the biology and geochemistry of metal-rich acidic environments.

Overall a probable function was assigned to 69% of the detected *Leptospirillum* group II proteins on the basis of sequence similarity (table S2). We assigned all detected *Leptospirillum* group II proteins to functional categories on the basis of clusters of orthologous genes (COGs) (*24*) to evaluate the degree of expression of novel proteins and to estimate how biochemical resources were partitioned to different metabolic activities by this organism. Most commonly detected were unique and conserved novel proteins (Fig. 4). Proteins involved in amino acid metabolism, translation, and energy production and conversion were the next most commonly detected, followed by cell envelope biogenesis, coenzyme metabolism, and protein folding and modification.

Many proteins involved in cobalamin and heme biosynthesis were detected. The reason for a high cobalamin demand by *Leptospirillum* group II is unclear. Additional analysis is needed to determine whether other community members manufacture this vitamin or obtain it from *Leptospirillum* group II. Heme is essential for biosynthesis of cytochromes such as cyt_{579}. A high demand for cyt_{579} is consistent with the relatively low energy yield associated with iron oxidation (*25*). Heme is also likely incorporated into the abundant catalase and peroxidase proteins, which are important for peroxide and radical detoxification. Similarly, the detection of many enzymes involved in protein refolding may reflect the challenge associated with maintaining protein integrity in the hot, acid environment. The apparently abundant thioredoxins may also construct and maintain the conformation of the abundant acid-exposed heme-based proteins localized in the periplasm.

Proteins from COG families involved in secondary metabolite biosynthesis, transport, and catabolism; cell division and chromosome partitioning; and inorganic ion transport and metabolism made up the smallest numbers of detected proteins. In part, this may reflect our inability to assign these metabolic roles to novel environment- and lineage-specific proteins.

Despite the predominance of novel proteins, it is noteworthy that only 38% of the proteins encoded by conserved hypothetical genes and 35% of the proteins encoded by unique hypothetical genes were detected. In contrast, we detected 86% of proteins predicted to be involved in amino acid metabolism and 86% of those involved in translation. This suggests that many hypothetical genes are nonfunctional, encode proteins required at low abundance, or are expressed under conditions different from those at the time of sampling. We compared the fraction of genes in the genome associated with each function with the fraction of proteins in the proteome associated with that function. Amino acid metabolism, translation, nucleotide metabolism, protein refolding and modification were all more highly represented in the proteome than in the genome. In all other categories (except transposases), we observed that representation in the proteome was similar to that in the genome (Fig. 4).

Proteomic data can provide direct insights into how essential functions are carried out and partitioned among members of natural communities. For example, although we detected a RuBisCO (ribulose-1,5-bisphosphate carboxylase-oxygenase)–like protein in *Leptospirillum* group II (*2*) (47% MS sequence

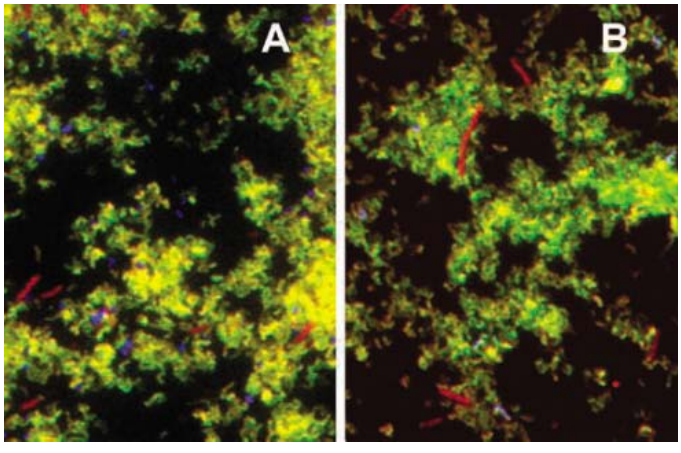

Fig. 2. Fluorescence in situ hybridization analysis (*8*) of the biofilm collected from the same site as Fig. 1 (AB end) in January 2004. In both images, *Leptospirillum* group II is yellow, and other bacteria (*Sulfobacillus* spp.) are red. Archaea are probed in (**A**) and appear blue; *Leptospirillum* group III are probed in (**B**) and appear white.

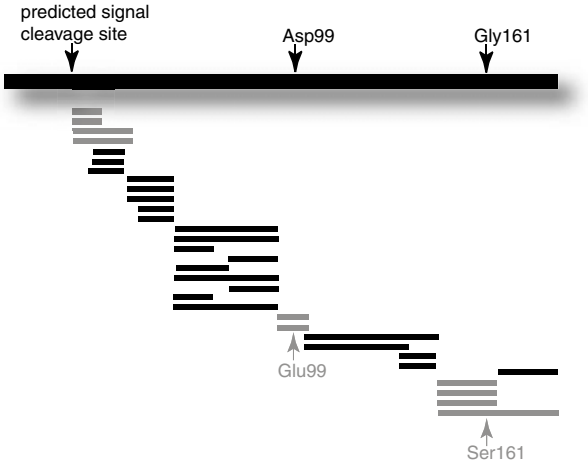

Fig. 3. Recovery of peptides spanning the entire sequence of a natural variant of cyt_{579}. The predicted sequence for cyt_{579}, on the basis of the community genomic data (*2*), is represented by a large black bar. Below, the smaller black bars represent tryptic peptides identified through proteomic analysis. Gray bars represent regions of the mature protein recovered by MS after consideration of two amino acid differences due to strain variation and cleavage of an N-terminal signal peptide.

coverage), further examination suggests that this protein plays another role, possibly in methylthioadenosine recycling (*26*). The high MS detection of *Por* genes and carbon monoxide dehydrogenase with acetyl coenzyme A (acetyl-CoA) synthase in *Leptospirillum* group II may reflect carbon fixation via the acetyl-CoA pathway. NifH, encoded by *Leptospirillum* group III was detected, which is consistent with the inference that this relatively low abundance organism is central to nitrogen fixation in the AMD system (*2*). We also detected proteins involved in nitrogen regulation and ammonia uptake in *Leptospirillum* group II, as would be expected if this organism depends on nitrogen fixed by *Leptospirillum* group III. However, failure to detect other *Leptospirillum* Nif proteins (*27*) suggests a relatively low level of nitrogen fixation at the time of sampling. Both nitrogen fixation and carbon fixation via the acetyl-CoA pathway suggest that some metabolic activities occur in microenvironments protected from molecular oxygen.

Each of the genomes from the biofilm organisms encodes genes that are potentially used to synthesize extracellular polymers. Genes involved in production of cellulose, a likely biofilm constituent (*28*), are expressed by *Leptospirillum* group II; however, many of the polymer production proteins of *Leptospirillum* group II were not detected. Despite the much lower degree of sampling of the *Leptospirillum* group III and *Ferroplasma* type II genomes, we detected proteins from these organisms that may be involved in creating biofilm architecture. Overall the proportion of detected proteins involved in carbohydrate metabolism is considerably greater in *Leptospirillum* group III than in *Leptospirillum* group II (Fig. 4), which implies that *Leptospirillum* group III plays a key role in this biofilm-essential function.

For 15 putative operons composed only of hypothetical genes, we detected all the predicted proteins (table S2). For example, one operon encodes five *Leptospirillum*-specific proteins, and another encoded three *Leptospirillum* group II–specific proteins, all of which were found in the membrane and extracellular fractions (*8*). These operons of lineage-specific proteins may provide functions that are central to adaptation to the AMD environment. Clues to the functions of other novel proteins were inferred from operon structure (Fig. 5). For *Leptospirillum* group II, we detected 280 novel proteins encoded within 212 operons, almost all of which encoded one or more genes with a functional annotation (table S2). For example, one operon that encoded two novel membrane-associated proteins also encoded three proteasome subunits. Two unique proteins were encoded in a four-gene operon with two putative nitrogen regulatory proteins, which suggests roles in nitrogen metabolism. Four other novel proteins, possibly involved in motility, were encoded in an operon of 15 genes that included at least eight flagellar genes.

Both the *Leptospirillum* group II proteome and the community proteome display a bimodal distribution of isoelectric points around ~6 to 6.9 and ~9 to 9.9 (figs. S2 and S6). In contrast, the distribution of isoelectric points for proteins enriched in the extracellular fraction is predominantly in the range ~9 to 10.9 (fig. S6). Thus, separation based on isoelectric points may be useful during purification of acid-stable proteins for functional characterization.

Often the hypothetical proteins not detected were encoded in blocks. In *Leptospirillum* group II, more than 15 genome fragments including at least 273 genes (50% of them novel) have been identified as of probable plasmid origin on the basis of the presence of typical plasmid genes and the absence or low abundance of core metabolic genes and the absence of tRNAs (table S2). On average, products of only 14% of genes encoded on the putative plasmid fragments were detected, in contrast to 51% of genes on chromosome-like fragments. This low incidence of protein detection (table S2) indicates that many laterally acquired genes serve no function, are rarely important, or are expressed only at low levels.

The *Leptospirillum* group II genome encodes more than 100 transposases or transposase fragments, and products of 8 of at least 17 distinct transposase groups were detected. It is noteworthy that the products of transposase genes that are highly duplicated in the *Leptospirillum* group II genome (e.g., genes grouped as T5, table S2) were not detected. However, we did find the products of transposase genes that occur only once or twice in the genome (e.g., T1 and T2 in table S2). One detected transposase is a strain-specific type found in some *Ferroplasma* type I variants.

More than 20 partial or complete integrases or recombinases were encoded in the *Leptospirillum* type II genome, and three distinct integrases or recombinases were found associated with genomic regions inferred to be acquired by lateral transfer. This finding indicates substantial plasmid and/or phage activity in the community at the time of sampling. One detected integrase identical in *Ferroplasma* type I and *Ferroplasma* type II has an unusually low GC content (29%, compared with ~38% in *Ferroplasma* typically) and may be derived from a prophage that recently infected both species.

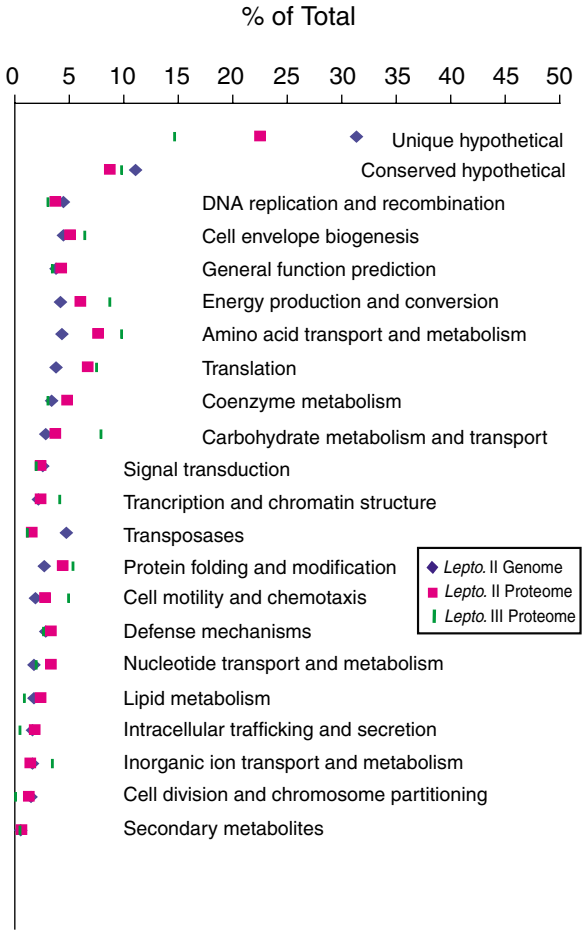

Fig. 4. Functional categories of *Leptospirillum* group II proteins predicted from the genome dataset and *Leptospirillum* groups II and III detected in the proteome. The percentage of total proteins or genes in each category are depicted.

Although it is well documented that microorganisms promote AMD formation (*22*, *23*), little was known about how these organisms function in their natural environments or as consortia. Our "proteogenomic" methods revealed that, in addition to extreme acidity and metal toxicity, reactive oxygen species are a significant challenge in this environment. Moreover, biofilm polymer production and nitrogen fixation appeared to be partitioned among community members, and many novel environment- and/or lineage-specific proteins were expressed that are presumably important. One of these was an abundant acid-stable protein capable of iron oxidation, a process central to AMD generation. However, many novel genes associated with phage- and plasmid-like insertions were only weakly expressed or not expressed.

MS–based de novo sequencing approaches (*29*) and MS^3 analysis (*30*) should reduce the requirement for exact gene sequence data, which would broaden the applicability of genome sequence information for environmental studies. As more environmental genomic sequences become available and MS methods improve, proteogenomics may be applied to other natural communities of environmental, medical, or industrial importance.

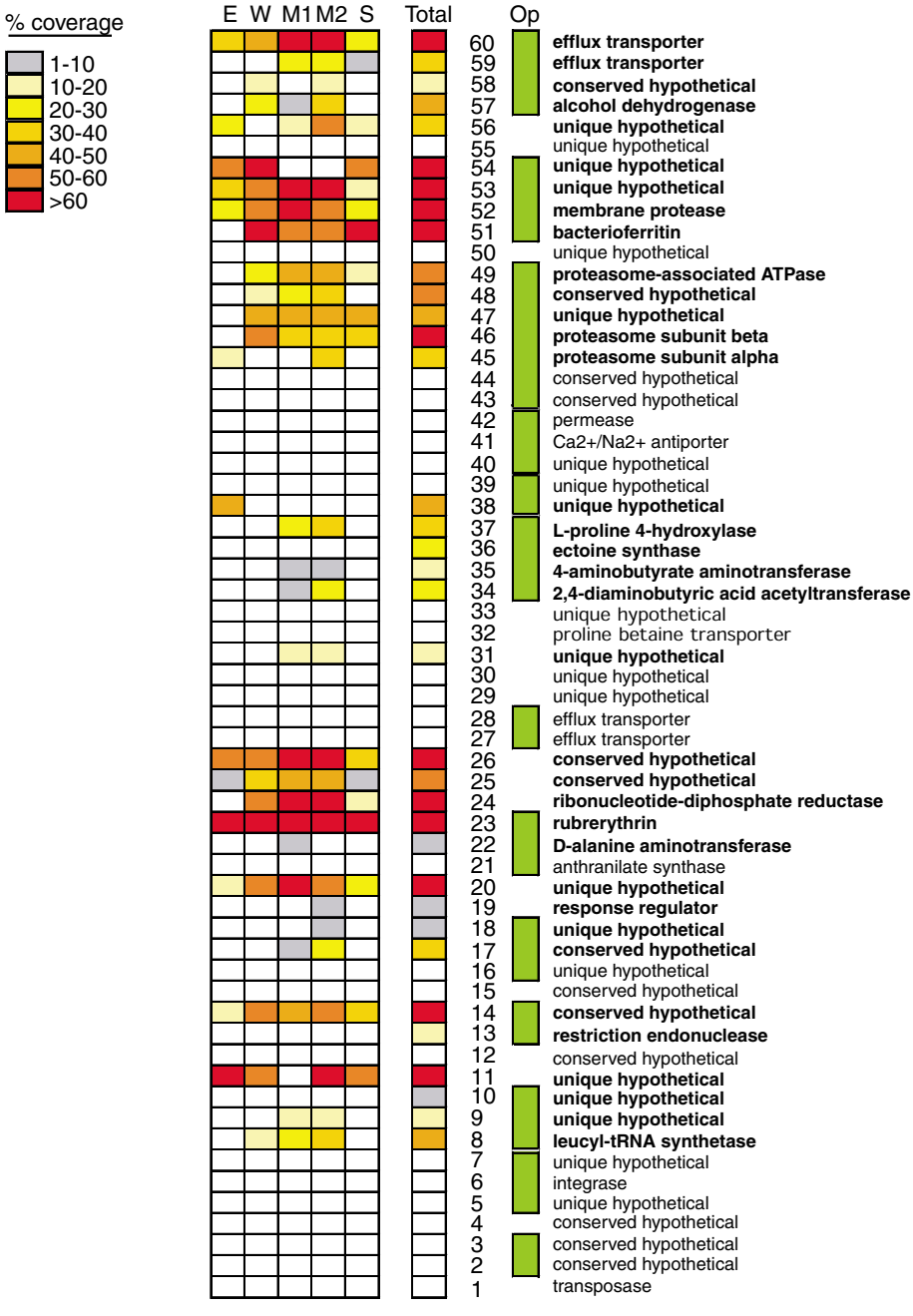

Fig. 5. Characterization of a genome fragment using the proteome dataset. The diagram shows the annotation, putative operon (Op) structure, and gene number on *Leptospirillum* group II scaffold 21. If the protein encoded by a gene was confidently detected (i.e., matching of two or more peptides), its annotation is in bold type. Colored boxes convey the percentage of each protein detected via MS in extracellular (E), whole-cell (W), membrane (M1 and M2), and cytoplasmic (S) fractions, as well as in the combined biofilm fractions (T). Membrane fractions were prepared by using two different protocols (*8*).

References and Notes

1. E. F. Delong, N. R. Pace, *Syst. Biol.* **50**, 470 (2001).
2. G. W. Tyson *et al.*, *Nature* **428**, 37 (2004).
3. J. C. Venter *et al.*, *Science* **304**, 66 (2004).
4. M. S. Lipton *et al.*, *Proc. Natl. Acad. Sci. U.S.A.* **99**, 11049 (2002).
5. J. Peng, J. E. Elias, C. C. Thoreen, L. J. Licklider, S. P. Gygi, *J. Proteome Res.* **2**, 43 (2003).
6. W. Zhu, C. I. Reich, G. J. Olsen, C. S. Giometti, J. R. Yates III, *J. Proteome Res.* **3**, 538 (2004).
7. G. K. Druschel, B. J. Baker, T. H. Gihring, J. F. Banfield, *Geochem. Trans.* **5**, 13 (2004).
8. For details, supplementary online materials are available at *Science* Online.
9. A. S. Essader, B. J. Cargile, J. L. Bundy, J. L. Stephenson Jr., *Proteomics* **5**, 24 (2005).
10. N. C. Verberkmoes *et al.*, *J. Proteome Res.* **1**, 239 (2002).
11. W. H. McDonald *et al.*, *Int. J. Mass Spectrom.* **219**, 245 (2002).
12. M. P. Washburn, D. Wolters, J. R. Yates III, *Nat. Biotechnol.* **19**, 242 (2001).
13. R. W. Corbin *et al.*, *Proc. Natl. Acad. Sci. U.S.A.* **100**, 9232 (2003).
14. P. Watnick, R. Kolter, *J. Bacteriol.* **182**, 2675 (2000).
15. We used spectral count (number of spectra detected per protein), peptide count (number of times any unique peptide is detected from a protein), and sequence coverage (percentage of protein sequence detected) to infer the 10 most abundant proteins in each fraction. All three measures gave generally similar results.
16. S. F. Altschul, W. Gish, W. Miller, E. W. Myers, D. J. Lipman, *J. Mol. Biol.* **215**, 403 (1990).
17. Significant homology required an EXPECT (E) value of $<e^{-10}$ by BLASTP analysis when compared with nonredundant proteins in the National Center for Biotechnology Information (NIH) database.
18. Proteins enriched in the extracellular fraction were defined as having an average MS sequence coverage in this fraction that is >10% and more than twice the average sequence coverage in any other fraction.
19. J. D. Bendtsen, H. Nielsen, G. von Heijne, S. Brunak, *J. Mol. Biol.* **340**, 783 (2004).
20. A. Hart, J. C. Murrell, R. K. Poole, P. R. Norris, *FEMS Microbiol. Lett.* **81**, 89 (1991).
21. R. C. Blake II *et al.*, *FEMS Microbiol. Rev.* **11**, 9 (1993).
22. G. W. Luther *et al.*, *Geochim. Cosmochim. Acta* **51**, 3193 (1987).
23. B. J. Baker, J. F. Banfield, *FEMS Microbiol. Rev.* **44**, 139 (2003).
24. R. L. Tatusov, E. V. Koonin, D. J. Lipman, *Science* **278**, 631 (1997).
25. R. C. Blake II, B. Johnson, *Environmental Microbe-Metal Interactions*, D. R. Lovley, Ed. (ASM Press, Washington, DC, 2000), pp. 53–78.
26. T. E. Hanson, F. R. Tabita, *Proc. Natl. Acad. Sci. U.S.A.* **98**, 4397 (2001).
27. V. Parro, M. Moreno-Paz, *Proc. Natl. Acad. Sci. U.S.A.* **100**, 7883 (2003).
28. R. J. Ram *et al.*, unpublished observations.
29. K. G. Standing, *Curr. Opin. Struct. Biol.* **13**, 595 (2003).
30. J. V. Olsen, M. Mann, *Proc. Natl. Acad. Sci. U.S.A.* **101**, 13417 (2004).
31. http://compbio.ornl.gov/biofilm_amd/

32. We thank T. Arman (owner, Iron Mountain mines), R. Sugarek, D. Dodds, and R. Carver for mine access and on-site assistance. We thank D. Tabb, the Yates Laboratory, the Institute for Systems Biology for software, F. Larimer for computer access, U. Kappler for heme-staining protocols, W. Sand for strain P3A, E. Allen for help with genomic analysis, J. Flanagan

for genomic DNA, and R. Whitaker and G. Fox for their comments on the manuscript. Research was supported by grants from the U.S. Department of Energy (DOE) Microbial Genome Program (J.F.B.), NSF Biocomplexity Program (J.F.B.), NASA Astrobiology Institute (J.F.B.), DOE Energy Biosciences Program (R.C.B.), and DOE Genomes to Life Program (R.H.). DDBJ/EMBL/GenBank accession numbers for the community genomic data are AADL01000000 and AADL00000000. All data, databases, and resulting identifications are available online; see (*31*).

Supporting Online Material
www.sciencemag.org/cgi/content/full/1109070/DC1
Materials and Methods
SOM Text
Figs. S1 to S6
Tables S1 and S2
References and Notes

23 December 2004; accepted 27 April 2005
Published online 5 May 2005;
10.1126/science.1109070
Include this information when citing this paper.

Synapses Form in Skeletal Muscles Lacking Neuregulin Receptors

P. Escher,[1]* E. Lacazette,[1]* M. Courtet,[1] A. Blindenbacher,[1] L. Landmann,[2] G. Bezakova,[3] K. C. Lloyd,[4] U. Mueller,[5] H. R. Brenner[1]†

The formation of the neuromuscular junction (NMJ) is directed by reciprocal interactions between motor neurons and muscle fibers. Neuregulin (NRG) and Agrin from motor nerve terminals are both implicated. Here, we demonstrate that NMJs can form in the absence of the NRG receptors ErbB2 and ErbB4 in mouse muscle. Postsynaptic differentiation is, however, induced by Agrin. We therefore conclude that NRG signaling to muscle is not required for NMJ formation. The effects of NRG signaling to muscle may be mediated indirectly through Schwann cells.

Motor neurons, terminal Schwann cells, and muscle fibers express two neuregulin genes, *nrg-1* and *nrg-2* (*1*–*3*). NRGs activate receptor tyrosine kinases of the ErbB family (*4*) that are expressed in the same cells. Motor neuron–derived NRG1β, originally isolated from brain as acetylcholine receptor (AChR)–inducing activity (ARIA) in cultured myotubes (*1*), is widely accepted to induce *AChR* gene transcription in subsynaptic myonuclei by activating ErbB receptors; the receptors stimulate the same regulatory elements in *AChR* gene promoters as the motor nerve (*5*–*7*). Agrin, another nerve-derived signal for NMJ formation (*8*), activates its receptor MuSK in muscle (*9*) and thus recruits AChRs, muscle-derived NRGs, ErbBs, and other synaptic components to the subsynaptic muscle membrane. Whereas the importance of Agrin in NMJ formation has been demonstrated by genetic means (*10*), the analysis of NRG/ErbB signaling has been less obvious. Mice lacking *nrg1*, *erbB2*, or *erbB4* die during development because of heart malformation, which prevents analysis of their function in synapse development. Transgene rescue experiments or muscle-specific gene ablation have been used to circumvent embryonic lethality. However, because Schwann cells depend on NRG signals from motor neurons for their survival and differentiation (*11*) and signals from Schwann cells regulate motor neuron function (*12*), the effect of NRG on subsynaptic muscle differentiation could not be resolved in the genetically rescued mice. Moreover, whereas ErbB2 is required for muscle spindle development (*13*), neither ErbB2 nor ErbB4 receptors alone are essential for NMJ formation (*14*). However, they may have redundant functions on synapse-specific gene expression (*3*).

To abolish all NRG signaling to muscle, we inactivated both the ErbB2 and ErbB4 receptors selectively in muscle without affecting their expression in Schwann cells. To this end, we crossed mice double-homozygous for loxP-flanked alleles of the *erbB2* (*13*) and *erbB4* (*15*) genes with a mouse line that begins to express Cre recombinase under the control of the human skeletal actin promoter in muscle precursors at embryonic day 9 (E9) (*16*), i.e., before neuromuscular synapse formation at E13.

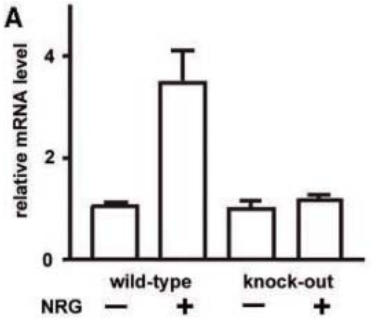

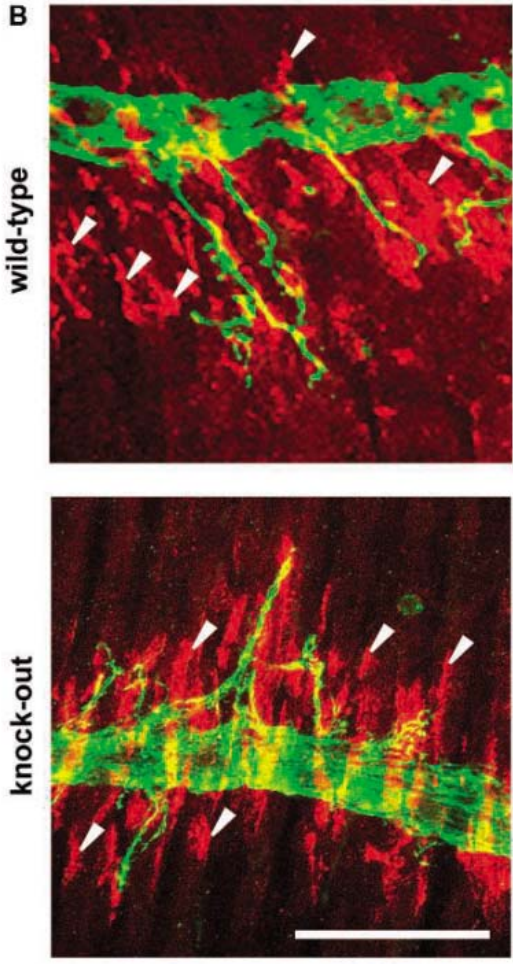

Fig. 1. NRG signaling is blocked in mutant myotubes; fetal neuromuscular junctions in *HSA-Cre;erbB2$^{fl/-}$;erbB4$^{fl/fl}$* mice develop normally. (**A**) Wild-type, but not ErbB-deficient myotubes express AChRε mRNA in response to 5 nM NRG1β (means ± SEM, from three mutant and four wild-type cultures). *P* values in two-tailed *t* tests are <0.01 for wild-type and >0.2 for mutant cultures. (**B**) Wild-type and mutant diaphragm muscles stained for AChR (red), neurofilament, and synaptophysin (green) at E14.5. Arrowheads denote nerve-free AChR clusters. Scale bar, 50 μm.

[1]Institute of Physiology and [2]Institute of Anatomy, Department of Clinical-Biological Sciences, [3]Division of Pharmacology, Biozentrum, University of Basel, 4056 Basel, Switzerland. [4]Center for Comparative Medicine, School of Veterinary Medicine, University of California, Davis, CA 95616, USA. [5]Department of Cell Biology and Institute for Childhood and Neglected Disease, The Scripps Research Institute, La Jolla, CA 92037, USA.

*These authors contributed equally to this work.
†To whom correspondence should be addressed. E-mail: Hans-Rudolf.Brenner@unibas.ch

Mutant mice (*HSA-Cre*$^{+/-}$;*erbB2*$^{fl/-}$;*erbB4*$^{fl/fl}$) were born in the expected Mendelian ratio. They were viable, but their body weight was reduced by about 30% compared with littermates (fig. S1), which suggested a role of ErbBs in muscle growth.

Several lines of evidence indicate that NRG signaling to mutant muscle was effectively inactivated. First, cultured myotubes did not respond to NRG1β (Fig. 1A), and in fetal myotubes at E13, loxP-flanked *erbB* alleles were recombined (fig. S2). Second, only 41% of all nuclei in mouse gastrocnemius muscle are myonuclei (fig. S3B); because Cre expression is selective for myonuclei (fig. S3A), the maximal fraction of recombined *erbB* alleles will be 41%. This is in good agreement with the 40% recombination of the mutant *erbB2* and *erbB4* alleles as determined from Southern blots of DNA from mutant muscle (fig. S3B), which indicates complete recombination in all myonuclei. However, even if recombination occurred in only 80% of myonuclei, combinatorial considerations predict that the probability for a nonrecombined nucleus to be located at the synapse, which would allow ErbB-mediated AChR gene expression, would be too low to explain normal maintenance of synapses in all fibers (see supporting online text). Third, consistent with the complete recombination of loxP-flanked *erbB* alleles in myonuclei observed above, >98% of myonuclei were Cre positive (fig. S3C). Fourth, erbB2 mRNA was reduced to <10% normal amounts, and erbB4 mRNA to below the detection limit (fig. S3D), whereas erbB1 and erbB3 mRNAs were not affected (*17*). The remaining erbB2 mRNA likely originates from Schwann cells (*11*), because ErbB2 protein from nerves rather than muscle fibers accounted for the protein detected in mutant muscle, and ErbB2 could not be detected in nerve-free muscle segments (fig. S3E; ErbB4 protein could not be resolved). Combined, these data strongly suggest that undetected failure of recombination, if present at all, cannot explain ErbB-dependent maintenance of neuromuscular synapses in all fibers.

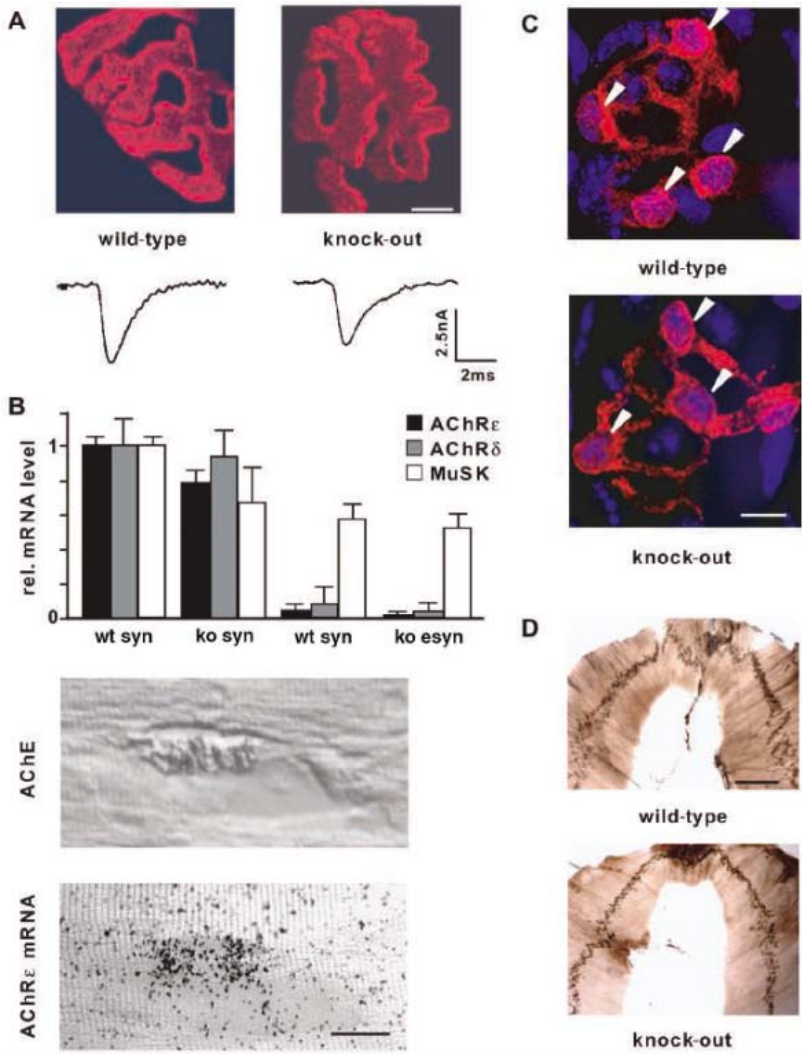

Fig. 2. Neuromuscular junctions in adult muscle of *HSA-Cre;erbB2*$^{fl/-}$;*erbB4*$^{fl/fl}$ mice are marginally affected. (**A**, top) Endplate AChRs and sample MEPCs. Scale bar, 5 μm. The rapid MEPC decay at mutant endplates indicates synaptic AChRε channels. (**B**) Relative levels of AChRε, AChRδ, and MuSK mRNAs in synaptic (syn) and extrasynaptic (esyn) regions of wild-type (wt) and mutant (ko) diaphragm muscles (means ± SEM, n = 6 to 8; the relatively high extrasynaptic expression of MuSK mRNA combined with limited accuracy of synaptic dissection obscures true differences in synaptic versus extrasynaptic mRNA levels). (Bottom) In situ hybridization indicates focal synaptic accumulation of AChRε mRNA. Scale bar, 10 μm. (**C**) Terminal Schwann cells stained with antibody to S-100 (red, arrowheads) are similar in morphology and number in mutant and wild-type muscles (Table 1). Nuclei are blue. Scale bar, 10 μm. (**D**) Acetylcholinesterase staining of endplate bands in diaphragm. Scale bar, 3 mm.

We next compared synapses in wild-type and mutant animals. In wild-type diaphragm, nerve-free AChR clusters developing as part of an intrinsic developmental program can be seen from E13 up to E16.5; they are then consolidated into mature synaptic contacts opposed by nerve terminals (*18*, *19*). Innervated as well as nerve-free AChR clusters were also observed in mutant muscles of the same age (Fig. 1B at E14.5). Another hallmark of developing endplates is a synapse-specific switch in AChR subunit composition from $\alpha_2\beta\gamma\delta$ to $\alpha_2\beta\varepsilon\delta$, beginning in leg muscle during the first postnatal week (*20*). A similar switch occurred in ErbB-deficient muscle (fig. S4). Taken together these experiments suggest that the development of the AChR clusters, the timing of innervation, and the developmental maturation of the endplates were not affected by the lack of NRG/ErbB signaling to muscle.

Whereas initial stages of the formation of postsynaptic structures might be independent of transcriptional regulation by the nerve, the maintenance of postsynaptic function in electrically active muscles is dependent on *AChR* gene expression in subsynaptic myonuclei (*21*). We therefore determined whether NRG signaling is required for synaptic maintenance in adult muscle fibers. Synapses in ErbB-deficient muscles appeared morphologically normal (Fig. 2A). Synaptic AChR levels, as estimated from their fluorescence after staining with Texas red–α-bungarotoxin, and the amplitudes of miniature endplate currents (MEPCs) were reduced by about 10%, and the MEPC rise and decay times were slightly prolonged (Fig. 2A; Table 1). Nevertheless, the short MEPC decay time constant in the mutants indicates that synaptic AChRs contained ε subunits, as observed in wild-type synapses. No obvious defects were observed in the appearance of nerve terminals (*22*), the number and morphology of terminal Schwann cells, and the innervation pattern (Fig. 2, C and D; Table 1), which suggested that reciprocal signals from muscle regulating

presynaptic differentiation were not significantly affected.

In agreement with the minor reduction in the levels of synaptic AChR numbers and MEPC amplitudes, in mutant muscle fibers we observed a minor reduction in the levels of synaptic AChRε, AChRδ, and MuSK mRNA levels (Fig. 2B). Endplate bands of diaphragm analyzed separately from extrasynaptic segments revealed a reduction by 20 to 30% in AChR mRNAs in mutant muscles, but the marked synapse-specific expression of AChR mRNAs was maintained. Thus, the nerve induces close-to-normal *AChR* and *musk* expression in fibers lacking ErbB receptors.

The small changes in synaptic physiology did not affect sustained muscle strength, as indicated by the ability of wild-type and mutant mice to cling upside-down onto a horizontal wire mesh without falling off (inverted screen test). Both groups (n = 8) performed equally up to 120 s when the test was discontinued. Based on the fact that myasthenic mice fall off the wire mesh between 30 and 60 s (*23*), we conclude that the mutant mice studied here had no myasthenic condition.

To analyze whether synapses form de novo in adult ErbB-deficient muscle, we induced the formation of ectopic endplates. The proximal stumps of the transsected fibular nerve were transplanted onto the endplate-free region of mutant soleus muscle. Sectioning the soleus nerve led to the formation of new ectopic endplates in wild-type and ErbB-deficient muscle (Fig. 3, A to C). Exogenous stimulation of the foreign motor axons elicited endplate potentials and action potentials followed by vigorous twitch contractions. Thus, functional ectopic endplates form in mutant adult muscle for which quantitative recombination has been demonstrated (fig. S3).

If NRG signaling to the muscle is not required for synapse formation, the question arises how the neural induction of synapse-specific AChR transcription is mediated. In wild-type electrically active muscles, recombinant neural Agrin can induce ectopic postsynaptic membranes, a process depending on ectopic *AChR* gene transcription (*24*). Neural Agrin induced ectopic membranes also in ErbB-deficient fibers (Fig. 3, D to G), and it activated expression of a luciferase reporter gene driven by an *AChRε* subunit gene promoter-fragment, consistent with *AChRε* subunit gene induction (Fig. 3H). Ectopic AChR densities were on average lower than those in the nerve-induced endplate of the same muscle (Fig. 3F). However, at 3 out of 16 Agrin-induced ectopic sites examined, AChR densities were equal to or larger than those at the original endplates with the lowest AChR density. Thus, overexpressed Agrin alone can account for normal subsynaptic AChR density. The lower mean density could be related to the fact that Agrin is deposited by the nerve more focally than by transfected muscle fibers, and/or that accumulation of AChRs may depend on additional factors of limited abundance in the muscle, as suggested by the wider spread of ectopic Agrin deposits and MuSK aggregates compared with the corresponding AChR aggregates (*25*). Alternatively, physical interactions between the nerve terminal and the muscle fiber (*26*) may be involved.

Our findings demonstrate that the development and maintenance of neuromuscular synapses are only marginally affected in muscles that lack the ErbB2 and ErbB4 receptors. Neural Agrin can induce postsynaptic differentiation, a process requiring the induction of genes for synaptic components such as MuSK, Rapsyn, and AChRε. Taken together, our results indicate that the nerve regulates synapse-specific gene transcription, at least in part by the secretion of Agrin, and that neuromuscular NRG signaling is redundant with that by Agrin (but not vice versa). Finally, NRG is not required to activate the reverse signaling mechanisms from muscle that control differentiation of the presynaptic nerve terminal.

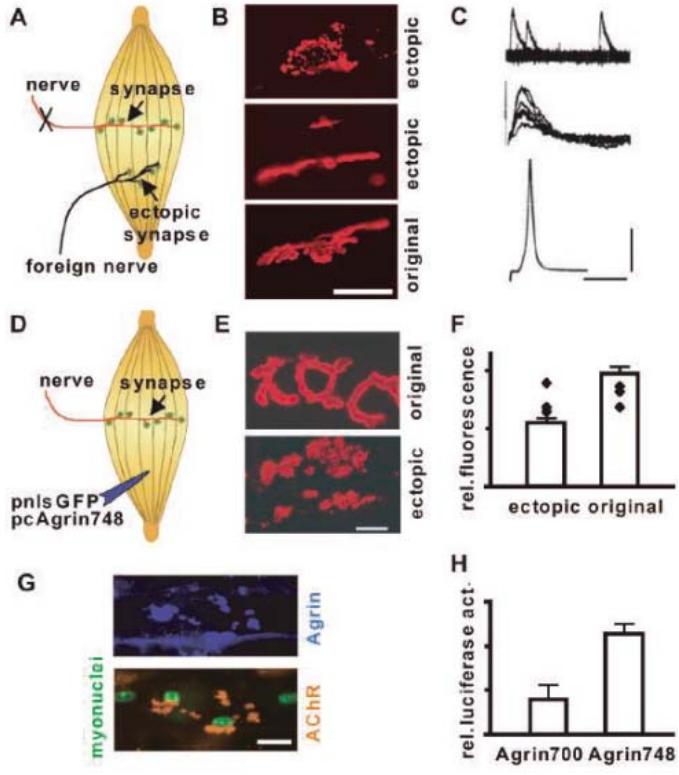

Fig. 3. Formation of ectopic postsynaptic membranes by nerves and by Agrin in adult muscle of *HSA-Cre;erbB2$^{fl/-}$;erbB4$^{fl/fl}$* mice. (**A**) Experimental procedure. (**B**) Ectopic endplates (top and middle) and original endplate (bottom) from same muscle, 40 days after foreign nerve transplantation and 18 days after soleus nerve section. Scale bar, 20 μM. (**C**) Miniature endplate potentials, synaptic potentials, and action potential recorded from ectopic innervation region. Calibration bars: 0.5, 1, 40 mV; 2, 20 ms. (**D** to **H**) Expression plasmids for neural chicken Agrin (pcAgrin748) and green fluorescent protein tagged with nuclear localization signal (pnlsGFP) injected intracellularly into extrasynaptic regions of single fibers induce nerve-free endplate membranes in ErbB-deficient muscles. (D) Experimental procedure. (E) Original endplate and Agrin-induced ectopic AChR cluster from same muscle. Scale bar, 5 μM. (F) Mean AChR densities (± SEM, nine ectopic and six original endplates in two muscles) are lower, but overlapping at Agrin-induced sites (diamonds). (G) Agrin-induced AChR clusters colocalize with Agrin deposits. Scale bar, 20 μM. (H) Injection of expression plasmid for neural Agrin (Agrin748), but not for nonneural Agrin (Agrin700) activates an AChRε subunit gene promoter–luciferase reporter construct (relative luciferase activity, means ± SEM, n = three muscles each).

Table 1. Physiological and morphological parameters of mutant versus wild-type synapses. The rapid MEPC decay time constant in mutant endplates indicates the presence of adult AChRε channels. Endplate band width in left hemidiaphragm. Means ± SEM. *N*, number of synapses examined.

Parameter	Wild type	*N*	Mice (*n*)	*HSA-Cre;erbB2$^{fl/-}$; erbB4$^{fl/fl}$*	*N*	Mice (*n*)	*P*
Relative AChR density (%)	100 ± 2	25	5	92 ± 2	27	5	<0.05
MEPC amplitude (nA)	3.07 ± 0.11	20	3	2.70 ± 0.14	20	3	<0.05
MEPC decay time constant (ms)	1.00 ± 0.05	20	3	1.35 ± 0.07	20	3	<0.02
MEPC rise time (μs)	262 ± 5	20	3	321 ± 9	20	3	<0.01
Endplate band width (μm)	366 ± 38		4	321 ± 33		4	>0.4
Schwann cells/endplate	4.35 ± 0.28	30	2	4.68 ± 0.30	30	2	>0.5

The changes in synaptic physiology in ErbB-deficient muscles are more subtle than those observed in mice heterozygous for a certain NRG1β isoform (*27*). Because Schwann cells depend on NRG-mediated signaling from motor neurons for survival (*12*), the stronger defects in the NRG1β mutants could be explained by impaired Schwann cell function, which in turn may impair the motor neuron's ability to maintain the synaptic muscle membrane.

Given that NRG is not required for synapse-specific gene transcription at the NMJ, the proposed function of NRG in regulating glutamate receptor expression during synapse development in the brain (*28*) warrants further examination.

References and Notes

1. D. L. Falls, K. M. Rosen, G. Corfas, *Cell* **72**, 801 (1993).
2. L. M. Moscoso *et al.*, *Dev. Biol.* **172**, 158 (1995).
3. M. Rimer *et al.*, *Mol. Cell. Neurosci.* **26**, 271 (2004).
4. E. Tzahar *et al.*, *Mol. Cell. Biol.* **16**, 5276 (1996).
5. S. A. Jo, X. Zhu, M. A. Marchionni, *Nature* **373**, 158 (1995).
6. G. C. Chu, L. M. Moscoso, M. X. Sliwkowski, *Neuron* **14**, 329 (1995).
7. L. Schaeffer, N. Duclert, M. Huchet-Dymanus, *EMBO J.* **17**, 3078 (1998).
8. U. J. McMahan, *Cold Spring Harb. Symp. Quant. Biol.* **55**, 407 (1990).
9. T. M. DeChiara *et al.*, *Cell* **85**, 501 (1996).
10. M. Gautam *et al.*, *Cell* **85**, 525 (1996).
11. A. N. Garratt, S. Britsch, C. Birchmeier, *Bioessays* **22**, 987 (2000).
12. S. Britsch *et al.*, *Genes Dev.* **15**, 66 (2001).
13. M. Leu *et al.*, *Development* **130**, 2291 (2003).
14. H. Tidcombe *et al.*, *Proc. Natl. Acad. Sci. U.S.A.* **100**, 8281 (2003).
15. W. Long *et al.*, *Development* **130**, 5257 (2003).
16. M. Schwander *et al.*, *Dev. Cell* **4**, 673 (2003).
17. P. Escher, H. R. Brenner, unpublished observations.
18. X. Yang *et al.*, *Neuron* **30**, 399 (2001).
19. W. Lin *et al.*, *Nature* **410**, 1057 (2001).
20. A. C. Missias, G. C. Chu, B. J. Klocke, *Dev. Biol.* **179**, 223 (1996).
21. V. Witzemann *et al.*, *Proc. Natl. Acad. Sci. U.S.A.* **93**, 13286 (1996).
22. G. Bezakova, H. R. Brenner, unpublished observations.
23. J. Cossins *et al.*, *Hum. Mol. Genet.* **13**, 2947 (2004).
24. S. Hashemolhosseini *et al.*, *Mol. Cell. Neurosci.* **16**, 697 (2000).
25. T. Meier *et al.*, *J. Neurosci.* **17**, 6534 (1997).
26. M. J. Marques, J. A. Conchello, J. W. Lichtman, *J. Neurosci.* **20**, 3663 (2000).
27. A. W. Sandrock *et al.*, *Science* **276**, 599 (1997).
28. M. Ozaki, M. Sasner, R. Yano, *Nature* **390**, 691 (1997).

29. We thank O. Dorchies (Geneva) for help with myoblast purification and M. A. Ruegg, Y. Barde, and B. Bettler (Basel) for critical comments on the manuscript. This work was supported by the Swiss National Science Foundation, the Swiss Foundation for Research on Muscle Diseases, the Novartis Foundation for Medicine and Biology, and NIH.

Supporting Online Material

www.sciencemag.org/cgi/content/full/308/5730/1920/DC1
Materials and Methods
SOM Text
Figs. S1 to S5
References and Notes

3 December 2004; accepted 25 April 2005
10.1126/science.1108258

Dependence of Olfactory Bulb Neurogenesis on Prokineticin 2 Signaling

Kwan L. Ng, Jia-Da Li, Michelle Y. Cheng, Frances M. Leslie, Alex G. Lee, Qun-Yong Zhou*

Neurogenesis persists in the olfactory bulb (OB) of the adult mammalian brain. New interneurons are continually added to the OB from the subventricular zone (SVZ) via the rostral migratory stream (RMS). Here we show that secreted prokineticin 2 (PK2) functions as a chemoattractant for SVZ-derived neuronal progenitors. Within the OB, PK2 may also act as a detachment signal for chain-migrating progenitors arriving from the RMS. PK2 deficiency in mice leads to a marked reduction in OB size, loss of normal OB architecture, and the accumulation of neuronal progenitors in the RMS. These findings define an essential role for G protein–coupled PK2 signaling in postnatal and adult OB neurogenesis.

In mammals, neurogenesis occurs mainly during embryonic to early postnatal stages. However, there are two areas in the adult mammalian brain that generate new neurons throughout life: OB and the dentate gyrus of the hippocampus (*1*, *2*). In rodents as well as primates, granular and periglomerular interneurons of the OB are continuously generated from SVZ of the lateral ventricle and are added throughout adulthood (*3–5*). SVZ progenitor cells migrate tangentially to the ependyma and subependymal layers of the olfactory ventricle (OV) in homotypic cell chains that coalesce to form RMS (*6–8*). Within the OB, the progenitors detach from their homotypic chains as individual cells and switch from tangential to radial migration before differentiating into interneurons of the granule and periglomerular layers (*6*, *7*). Genetic studies in mice have revealed that the polysialylated form of neural cell adhesion molecule (PSA-NCAM) is crucial for the establishment of homotypic chains of the RMS (*8–11*). Reelin and tenascin-R signaling may be involved in the dispersion of chained neuronal progenitors into single cells (*12*, *13*). Slit, a secreted repellent for axons, repels the postnatal SVZ neurons (*14*, *15*). Although a neuronal attractant from the OB has yet to be identified, diffusible attractants for SVZ neuronal progenitors may exist within layers of the OB (*16*). Here we show that prokineticin 2 (PK2) possesses features expected of a chemoattractant for SVZ-derived neuronal progenitors and is indispensable for the establishment of normal OB architecture.

Prokineticins PK1 and PK2 are cysteine-rich secreted proteins that regulate diverse biological processes by the activation of two cognate G protein–coupled receptors (*17–23*). Our analysis indicated that both prokineticin receptors (PKR1 and PKR2) are expressed in the areas active in neurogenesis during adulthood. The mRNAs of both receptors are expressed in the SVZ, the entire RMS, and the ependyma and subependymal layers of the OV, as well as the dentate gyrus of the hippocampus (Fig. 1, A to C, and figs. S1 and S12). The expression of PKR1 has detected in all these areas, although less abundantly than PKR2 (fig. S1) Whereas PK1 mRNA was not detected in any of these brain regions (*24*), PK2 has expressed in the granular and periglomerular layers of the OB (Fig. 1, D and E). The PK2 expression pattern is complementary to that of its receptors, PKR1 and PKR2; PK2 is expressed in the mature granular and periglomerular layers of the OB, whereas its receptors are expressed in the immature ependyma and subependymal layers of the OV. Similar patterns for PK2 and its receptors were observed during neonatal stages, postnatal day (P) 1, and P7 (Fig. 1, F to I; PKR1) (*24*). The expression level of PKR2 was greater during neonatal development, reflecting that the RMS forms a much thicker stream of migrating neuronal progenitors in neonates than in adults (Fig. 1, F, H, and I) (*25*). The complementary expression pattern of ligand (PK2) and receptors (PKR1 and PKR2) suggests that this ligand-receptor(s) pair may be involved

Department of Pharmacology, University of California–Irvine (UCI), Irvine, CA 92697, USA.

*To whom correspondence should be addressed. E-mail: qzhou@uci.edu

in OB neurogenesis. This hypothesis is supported by the similarities that exist between angiogenesis and neurogenesis (*26*, *27*). In particular, prokineticins can stimulate the proliferation, survival, and migration of endothelial cells derived from endocrine organs (*19*, *28*). PK2 and its receptors may serve a similar function for SVZ-derived neuronal progenitors en route to the OB during neonatal and adult stages.

To investigate whether PK2 can function as a chemoattractant for SVZ neuronal progenitors, we used a Transwell assay. Dissociated cells from the RMS and OV regions that highly expressed PKR1 and PKR2 from P7 and adult rats were placed in the upper chamber and allowed to migrate through the membrane filter separating the upper and lower chambers. Cells that migrated to the lower side of the filter were stained with Tuj1, a marker for immature neurons, and counted. When purified recombinant human PK2 (*17*) was added to the lower chamber, the migration of neuronal progenitors was enhanced (fig. S2) [P7 rat data (*24*)]. A prokineticin receptor antagonist (A1MPK1) (*29*) inhibited the PK2-stimulated cell migration (fig. S2). Thus, PK2 can stimulate the motility of neuronal progenitors from the SVZ-OB pathway. To further assess whether the PK2-stimulated cell migration is directional, coculturing experiments with the anterior portion of the SVZ (SVZa) and a stable T293 cell line expressing human PK2 were carried out in collagen gel matrices (*15*). When SVZa explants from P7 rats were cocultured with untransfected T293 cells for 24 hours, cells migrating from each explant were symmetrically distributed around its circumference (Fig. 2A). When SVZa explants were cocultured with T293 cells stably expressing human PK2, cell migration was highly asymmetric, with more cells migrating into the quadrant proximal to the PK2-expressing cells (Fig. 2B). Over time, the entire circumference of the explant showed more outwardly migrating cells, consistent with the increased motility and migration seen with the Transwell assay (fig. S3). The proximal/distal ratio of cells migrating from the SVZa-PK2 coculture was significantly higher than the control (SVZa-PK2, 3.97 ± 0.18, n = 38 explants; control, 1.05 ± 0.05, n = 23 explants; P < 0.0001) (Fig. 2D). Similar results were obtained from explants taken along the RMS (*24*). Immunocytochemistry with Tuj1 antibody confirmed the neuronal nature of the cells migrating out of the SVZa explants (fig. S4). Moreover, the addition of A1MPK1 to the collagen gel matrices in SVZa explants cocultured with PK2 T293 cells resulted in a symmetric distribution of cells (1.03 ± 0.07, n = 6 explants) and fewer migrating cells (Fig. 2, C and D). To further discern the directional nature of the PK2 signal, SVZa explants were cultured in collagen gel for 24 hours, and then control cells or PK2-expressing cell aggregates were placed nearby (*30*). A significant increase in the mean number of migrating neuronal progenitors in quadrants proximal to the PK2-expressing cells was observed (fig. S5). With SVZa-PK2 cocultures in addition to more cells migrating into the proximal quadrant, they also traveled farther away compared to controls (Fig. 2E). We also tested the motility effect of recombinant PK2 in SVZa explants by embedding it in collagen gel matrices. Figure 2F shows that PK2 increased the distance of neuronal migration; the average migration distance of individual cells in the presence of PK2 was 150.6 ± 10.5 μm versus 68.3 ± 5.8 μm in the control cultures (n = 5 explants, P < 0.0001). Taken together, these results indicate that PK2 can function as a chemoattractant for neuronal progenitors that traverse the SVZ/RMS/OB pathway.

A required step in the switch from tangential to radial migration is the detachment of neuronal progenitors from their homotypic chains. We tested whether PK2 facilitates this detachment process with matrigel (*8*). In the absence of PK2, SVZa explants showed a symmetric pattern of cell chains emanating from each explant after 24 to 30 hours in culture (Fig. 2G). These chains were either linear aggregates radiating from the explants or intricate three-dimensional networks. With recombinant PK2 embedded in the matrigel, cell chains were rarely observed and tended to be fragmented, and many cells migrated out of the explants as individuals (Fig. 2H). PK2 treatment caused a fourfold increase in the number of individual cells migrating out of explants (control, 28.9 ± 1.7, n = 40 explants; PK2-treated, 139.4 ± 5.1, n = 40 explants; P < 0.0001) (Fig. 2I). The increase in cell motility seen with PK2 treatment was also obvious with the matri-

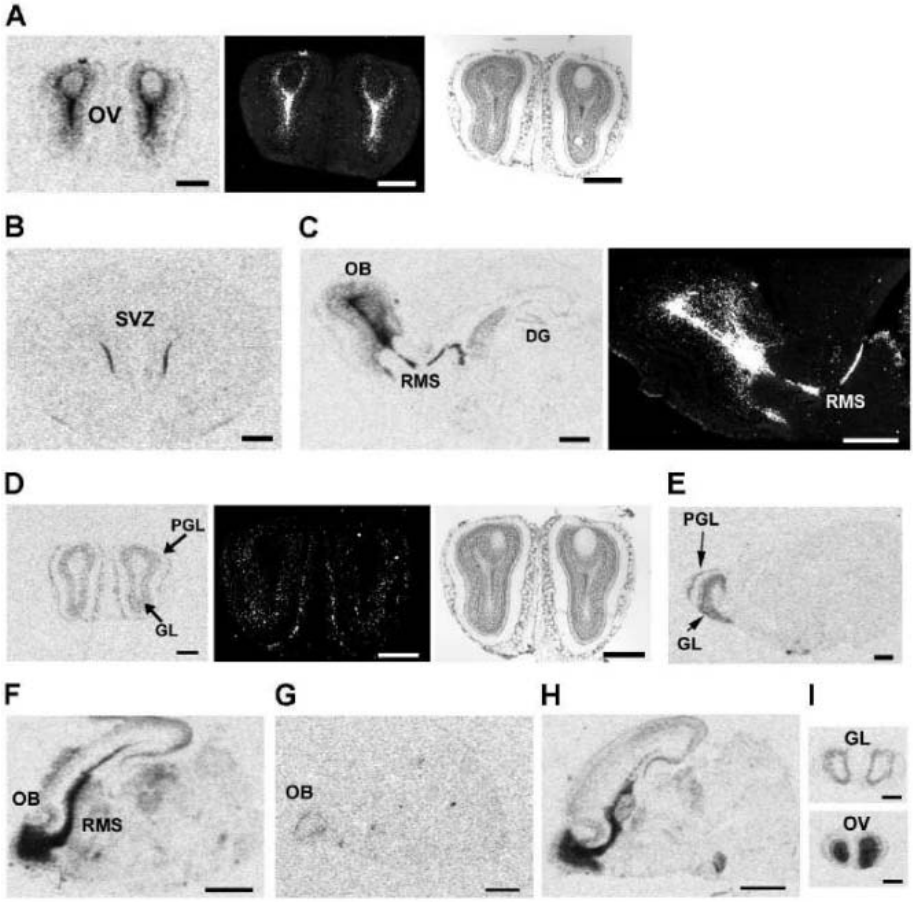

Fig. 1. PK2 and PKR2 mRNA expression. (**A**) Coronal section of adult OB, showing PKR2 (left) in the ependyma and subependymal layers of the OV, a darkfield image (middle), and cresyl violet staining (right). (**B**) PKR2 in the adult SVZ of the lateral ventricle (coronal section). (**C**) Sagittal section of an adult brain (left), depicting PKR2 in the RMS, OB, and the dentate gyrus (DG) of the hippocampus, and a darkfield image (right). (**D**) PK2 (left) in the GL and PL of adult OB, a darkfield image (middle), and cresyl violet staining (right). (**E**) Sagittal section of an adult brain, depicting PK2 in the GL and PGL. (**F**) PKR2 and (**G**) PK2 in sagittal sections of P1 brain. (**H**) Sagittal section of PKR2 in a P7 brain. (**I**) PK2 (top) and PKR2 (bottom) in coronal sections of P7 OB. Scale bar, 1 mm.

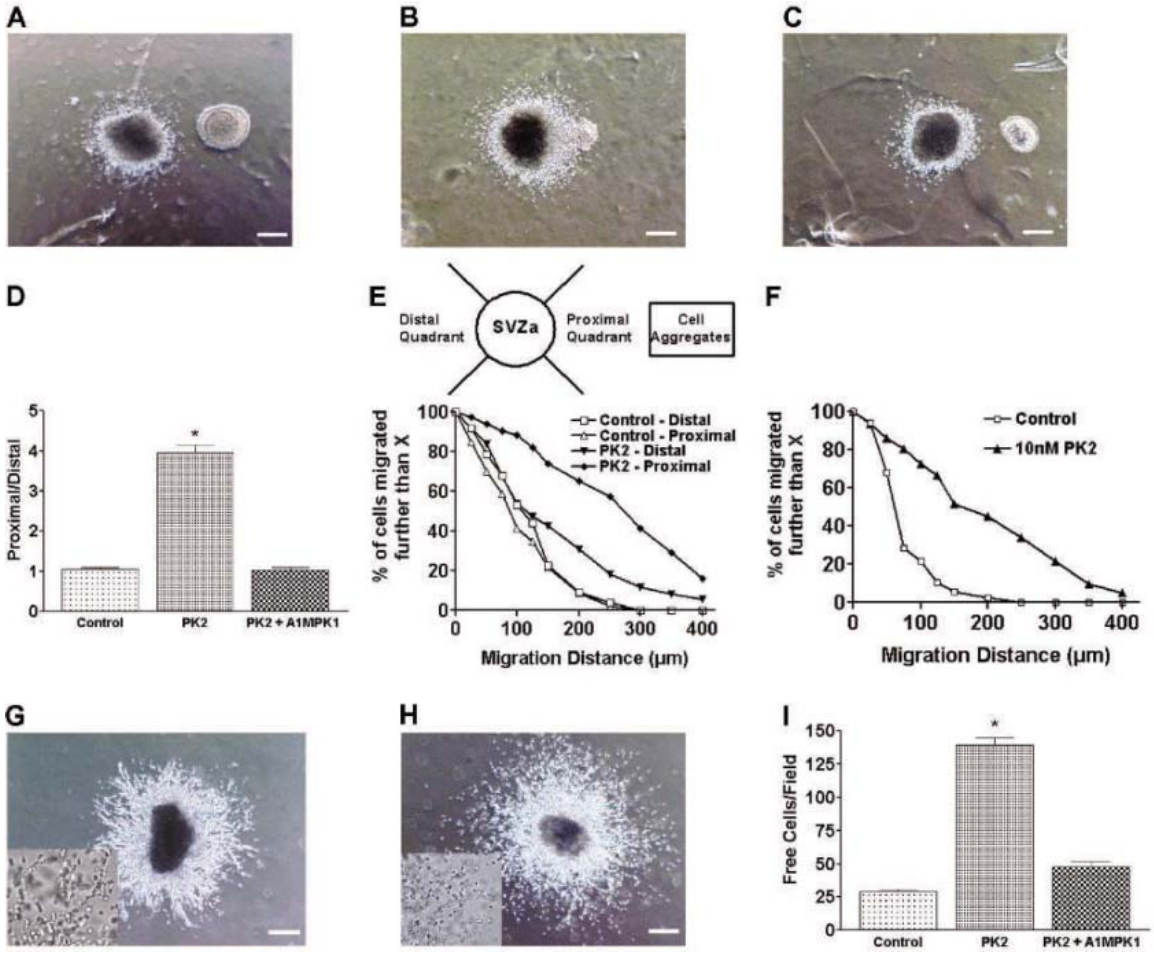

Fig. 2. Effects of PK2 on neuronal migration. (**A** to **C**) Migration of SVZa cells cocultured with (A) T293 cells, (B) the stable PK2 cell line, and (C) the PK2 stable cell line with 100-nM A1MPK1. (**D**) Proximal/distal distribution of SVZa cells in cocultures: control, PK2, or PK2 with 100-nM A1MPK1 (*, $P < 0.0001$). (**E**) Migration distances of SVZa cells with control cells or the PK2 stable cell line. The *x* axis shows the distance of cells from SVZa explants; the *y* axis, the percentage of cells that migrated further than the distance on the *x* axis. Values shown are representative of three independent experiments. (**F**) Increased motility of SVZa cells in collagen embedded with 10-nM PK2 versus control cells at 24 hours. Values shown are representative of five independent experiments. (**G**) Chains of cells migrating from SVZa explant cultured alone in matrigel. (Inset) Higher magnification of (G). (**H**) Dispersal of cells from SVZa explant cultured with 60-nM PK2. (**Inset**) Higher magnification of (H), highlighting changes in cellular organization. (**I**) Quantification of distinguishable individual cells per visual field, in matrigel cultures with either 60-nM PK2 or 60 nM PK2 and 120-nM A1MPK1 (*, $P < 0.0001$). Scale bar, 500 μm.

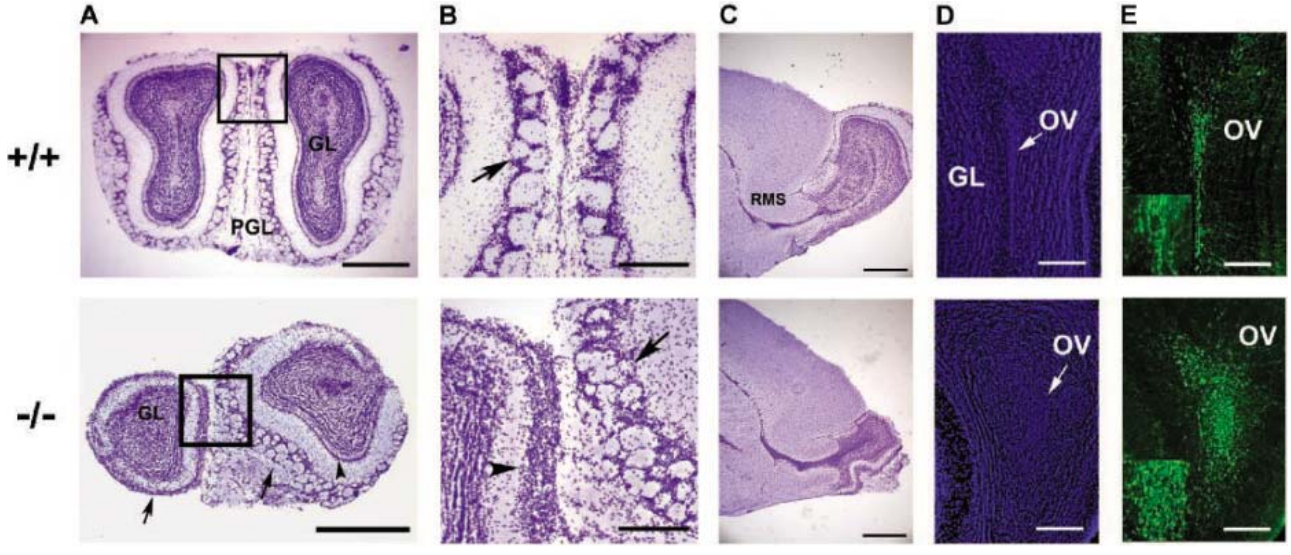

Fig. 3. Analysis of olfactory bulbs from $PK2^{-/-}$ mice. (**A**) Nissl-stained coronal section of WT (top) and $PK2^{-/-}$ OB (bottom). GL and PGL (arrows) are disorganized in $PK2^{-/-}$ OB. The arrowhead shows the mitral cell layer. (**B**) Magnification of the PGL (box) in (A). The top panel shows normal PGL (arrow) in WT OB; the bottom shows, in $PK2^{-/-}$ OB, abnormal glomeruli formation (arrow) and a single uninterrupted PGL (arrowhead). (**C**) Nissl-stained sagittal sections of WT (top) and $PK2^{-/-}$ (bottom) brain. (**D**) 4′, 6-diamidino-Z-phenylindole-stained (blue) coronal sections of WT (top) and $PK2^{-/-}$ OB (bottom). (**E**) Sections in (D) immunostained for PSA-NCAM (green). The top panel shows PSA-NCAM–labeled neuronal progenitors in the OV of WT OB. (Top inset) A higher magnification of the top panel shows normal OV. The bottom panel shows an expanded OV with accumulation of neuronal progenitors in $PK2^{-/-}$ OB. (Bottom inset) A higher magnification of the bottom panel shows tight clusters of PSA-NCAM–labeled neuronal progenitors in the OV. Scale bars, 1 mm in (A) and (C); 250 μm in (B), (D), and (E).

gel cultures (Fig. 2, G and H). Moreover, the separation of individual cells in PK2-treated cultures was reduced with the addition of the antagonist A1MPK1 (Fig. 2I). Thus, PK2 may act as a detachment signal for neuronal progenitors migrating within the chain.

In mutant mice deficient in the PK2 gene ($PK2^{-/-}$ mice) (*31*), the total weight and gross morphology of brains did not differ from those of wild-type (WT) controls, but the size of their OBs was less than half that of the WT controls (rostral to caudal length: 3.68 ± 0.09 mm versus 1.27 ± 0.11 mm, WT versus $PK2^{-/-}$, respectively, $n = 20$ mice, $P < 0.0001$; weight: 7.67 ± 0.33 mg versus 16.67 ± 1.45 mg, $PK2^{-/-}$ versus WT, respectively, $n = 3$ mice, $P < 0.005$) (fig. S6). Although OBs from $PK2^{-/-}$ mice were smaller than those from WT controls in all cases, ~50% of $PK2^{-/-}$ mice displayed asymmetric bulb formation (fig. S6A). Histological examination revealed multiple abnormalities of the OB from $PK2^{-/-}$ mice (Fig. 3, A to C). Whereas the mitral cell layer appeared normal in the OB of $PK2^{-/-}$ mice, the granular cell layer (GL) was abnormally thin (fig. S6B), and the number of granular cells was reduced (*24*). The periglomerular layer (PGL) was either indiscernible or malformed in $PK2^{-/-}$ mice (Fig. 3, A to C). In contrast, the small OBs in NCAM-deficient mice have a normal PGL (*10*). In 16 of the 28 OBs examined in $PK2^{-/-}$ mice, the PGL was not discernable and was replaced by an uninterrupted layer of periglomerular cells (Fig. 3B). In the remaining OBs examined, multiple glomeruli layers were compacted on a single side of the OB (Fig. 3B). The PGL possesses a population of dopaminergic (DA) interneurons born from the SVZ-OB pathway (*32*). Immunostaining for tyrosine hydroxylase (TH), a marker for these interneurons, in the OB of $PK2^{-/-}$ mice that had no discernable PGL was minimal, whereas collectively there was a fourfold reduction in DA interneurons in the PGL compared to that of WT controls (102.7 ± 16.4 TH^+ cells/mm² versus 24.7 ± 20.2 TH^+ cells/mm², WT versus $PK2^{-/-}$, respectively; $n = 3$ mice, $P < 0.05$) (fig. S7).

The smaller OB in $PK2^{-/-}$ mice was accompanied by a significant enlargement of both the OV and the RMS at the entrance of OB (Fig. 3C and fig. S8). Immunostaining for chains of neuronal progenitors with PSA-NCAM demonstrated the accumulation of neuronal progenitors around the OV in $PK2^{-/-}$ mice (Fig. 3, D and E). PSA-NCAM–positive cells clustered tightly around the OV in the $PK2^{-/-}$ mice (Fig. 3, D and E). The accumulation of neuronal progenitors in the rostral portion of the RMS and OV and a layer specific reduction in a subset of interneurons derived from the SVZ suggests that cell migration was initiated but compromised in the OB in $PK2^{-/-}$ mice.

The normal distribution and density of bromodeoxyuridine-labeled ($BrdU^+$) cells in the SVZ and RMS in $PK2^{-/-}$ mice indicates that the smaller OB is not due to reduced cell proliferation (fig. S9). A pulse of BrdU was used to trace the migration of neuronal progenitors through the SVZ-OB pathway however revealed differences between WT and $PK2^{-/-}$ mice (Fig. 4, A and B). Five days after the pulse in $PK2^{-/-}$ mice, $BrdU^+$ cells accumulated abnormally in the RMS outside the OB (Fig. 4E and fig. S10) and in the OV (Fig. 4, A, B, and E) (551.3 ± 56.7 versus 969.1 ± 129.5 $BrdU^+$ cells/mm² in the RMS outside of the OB and 867.6 ± 139.8 versus 1571 ± 142.0 $BrdU^+$ cells/mm² in the OV for WT and $PK2^{-/-}$ mice, respectively; $n = 3$ mice, $P < 0.05$). At 28 days after the pulse in WT mice, most $BrdU^+$ cells were found in the rostral half of the OB integrated into the GL and PGL (Fig. 4, C and D). In $PK2^{-/-}$ mice, $BrdU^+$ cells in the OB were reduced (128.9 ± 9.0 $BrdU^+$ cells/mm² versus 50.2 ± 2.8 $BrdU^+$ cells/mm², WT versus $PK2^{-/-}$, respectively; $n = 3$ mice, $P < 0.001$) (Fig. 4, C, D, and F), and most of these $BrdU^+$ cells were found at the entrance of the OB and in the OV. The distribution of $BrdU^+$ cells suggests that the accumulation of neuronal progenitors in the OV of $PK2^{-/-}$ mice might lead to a higher rate of cell death within the OB. Terminal deoxynucleotidyl transferase mediated–deoxyuridine triphosphate UTP nick-end labeling (TUNEL) analysis indicated increased apoptosis in the OB of $PK2^{-/-}$ mice (6.8 ± 2.2 $TUNEL^+$ cells/mm² versus 27.9 ± 5.9 $TUNEL^+$ cells/mm², WT versus $PK2^{-/-}$, respectively; $n = 3$ mice, $P < 0.05$) (fig. S11). These observations are consistent with the marked buildup

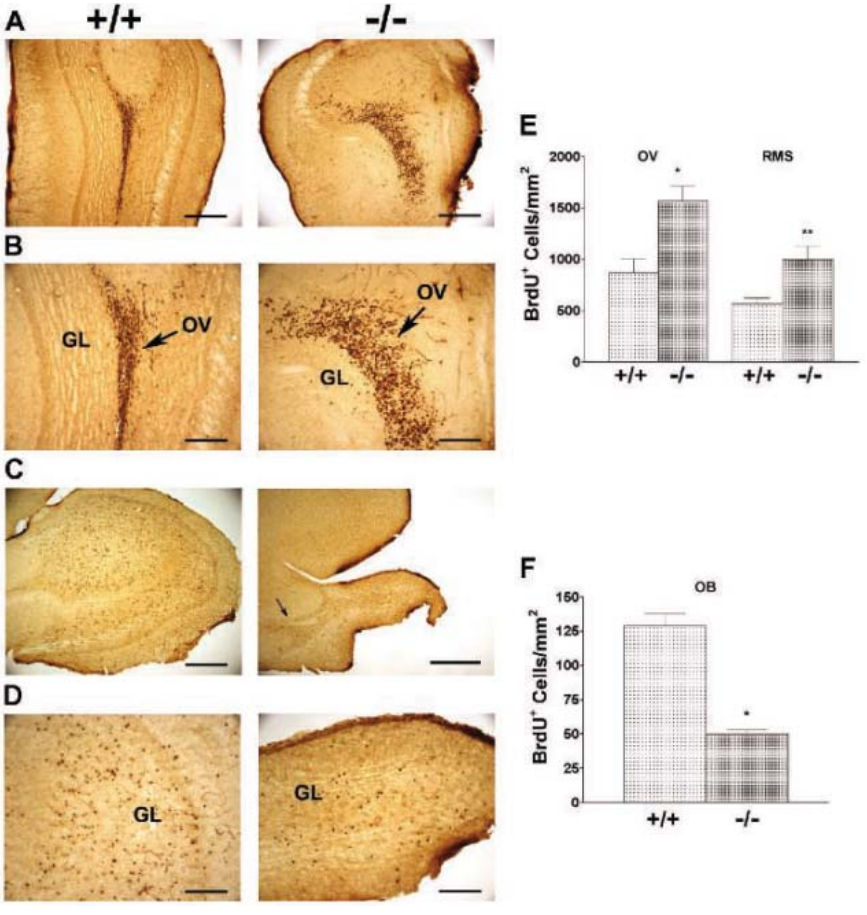

Fig. 4. Migration of neuronal progenitors in $PK2^{-/-}$ mice. (**A**) Coronal section of WT OB 5 days after pulse injection of BrdU, showing (left) diaminobenzidine-stained $BrdU^+$ cells in the OV and (right) increased $BrdU^+$ cells around the OV in $PK2^{-/-}$ OB. (**B**) Higher magnifications of (A), showing a wider OV in $PK2^{-/-}$ OB (right). (**C**) Sagittal section of WT OB 28 days after a pulse of BrdU, showing (left) numerous $BrdU^+$ cells. $PK2^{-/-}$ OB (right) shows a reduction of $BrdU^+$ cells and accumulation near the entrance of the OB (arrow). (**D**) High magnification showing numerous $BrdU^+$ cells in the GL and the PGL in WT OB (left). In $PK2^{-/-}$ OB (right), $BrdU^+$ cells were reduced and around the OV and GL. (**E**) Quantification of $BrdU^+$ cells in the OV and RMS from the 5-day pulse study (* and **, $P < 0.05$). (**F**) Quantification of $BrdU^+$ cells in the OB from the 28-day pulse study (*, $P < 0.001$). Scale bars, 500 μm in (C); 250 μm in (A); 125 μm in (B) and (D).

of PKR2-positive cells in the rostral portion of the RMS and OV of PK2$^{-/-}$ mice (fig. S12), also shown by PSA-NCAM immunostaining (Fig. 3E). Analysis of PKR2 mRNA expression in PK2$^{-/-}$ mice showed an overall decrease in neuronal progenitors migrating away from the OV into the GL and PGL (fig. S12). The compaction of PKR2-positive cells in the OV indicates that, in the absence of PK2 signaling, chained neuronal progenitors are either not detached properly or disoriented about the direction of migration. To evaluate whether PK2 is a genuine chemoattractant for SVZ neuronal progenitors, we performed SVZa explants coculture assay with the GL of the OB, where PK2 is primarily expressed (Fig. 1, D and E). Cell migration was directed toward the GL tissue from WT OB, whereas the corresponding tissue from PK2$^{-/-}$ OB exhibited no chemotaxis activity (proximal/distal ratio: 1.87 ± 0.31 versus 0.99 ± 0.06, WT versus PK2$^{-/-}$, respectively; $n = 6$ explants, $P < 0.05$) (fig. S13). Taken together, these results indicate that the migration of neuronal progenitors mediated by PK2 signaling is essential for the normal development and maintenance of the OB.

Thus, PK2 serves as a chemoattractant for SVZ-derived neuronal progenitors, and the establishment of normal OB architecture requires PK2 signaling. Together with other signals (*12*, *13*, *15*), PK2 appears to guide the migration of neuronal progenitors from the SVZ through the RMS to their final layers in the OB. The similar response of PKR1 and PKR2 to PK2 (*22*) implies that these receptors may mediate a redundant role for OB development. As with endothelin-3 signaling for the migration of enteric neurons (*33*) and orphan receptor GPR56 in the regional development of the cerebral cortex (*34*), our results further indicate that G protein–coupled receptors may be crucial for the establishment of the layered structures in the nervous system.

References and Notes

1. J. Altman, *J. Comp. Neurol.* **137**, 433 (1969).
2. F. H. Gage, *Science* **287**, 1433 (2000).
3. M. S. Kaplan, J. W. Hinds, *Science* **197**, 1092 (1977).
4. S. A. Bayer, *Exp. Brain Res.* **50**, 329 (1983).
5. V. Pencea, K. D. Bingaman, L. J. Freedman, M. B. Luskin, *Exp. Neurol.* **172**, 1 (2001).
6. M. B. Luskin, *Neuron* **11**, 173 (1993).
7. C. Lois, A. Alvarez-Buylla, *Science* **264**, 1145 (1994).
8. H. Wichterle, J. M. Garcia-Verdugo, A. Alvarez-Buylla, *Neuron* **18**, 779 (1997).
9. H. Tomasiewicz *et al.*, *Neuron* **11**, 1163 (1993).
10. H. Cremer *et al.*, *Nature* **367**, 455 (1994).
11. K. Ono, H. Tomasiewicz, T. Magnuson, U. Rutishauser, *Neuron* **13**, 595 (1994).
12. I. Hack, M. Bancila, K. Loulier, P. Carroll, H. Cremer, *Nat. Neurosci.* **5**, 939 (2002).
13. A. Saghatelyan, A. de Chevigny, M. Schachner, P. M. Lledo, *Nat. Neurosci.* **7**, 347 (2004).
14. H. Hu, U. Rutishauser, *Neuron* **16**, 933 (1996).
15. W. Wu *et al.*, *Nature* **400**, 331 (1999).
16. G. Liu, Y. Rao, *J. Neurosci.* **23**, 6651 (2003).
17. M. Li, C. M. Bullock, D. J. Knauer, F. J. Ehlert, Q. Y. Zhou, *Mol. Pharmacol.* **59**, 692 (2001).
18. M. Y. Cheng *et al.*, *Nature* **417**, 405 (2002).
19. J. LeCouter *et al.*, *Proc. Natl. Acad. Sci. U.S.A.* **100**, 2685 (2003).
20. C. Mollay *et al.*, *Eur. J. Pharmacol.* **374**, 189 (1999).
21. L. Negri *et al.*, *Br. J. Pharmacol.* **137**, 1147 (2002).
22. D. C. Lin *et al.*, *J. Biol. Chem.* **277**, 19276 (2002).
23. T. Soga *et al.*, *Biochim. Biophys. Acta* **1579**, 173 (2002).
24. K. L. Ng *et al.*, unpublished data.
25. K. Kishi *et al.*, *Arch. Histol. Cytol.* **53**, 219 (1990).
26. H. Zhang, L. Vutskits, M. S. Pepper, J. Z. Kiss, *J. Cell Biol.* **163**, 1375 (2003).
27. T. D. Palmer, A. R. Willhoite, F. H. Gage, *J. Comp. Neurol.* **425**, 479 (2000).
28. J. LeCouter *et al.*, *Nature* **412**, 877 (2001).
29. C. M. Bullock, J. D. Li, Q. Y. Zhou, *Mol. Pharmacol.* **65**, 582 (2004).
30. M. Ward, C. McCann, M. DeWulf, J. Y. Wu, Y. Rao, *J. Neurosci.* **23**, 5170 (2003).
31. J. D. Li *et al.*, unpublished data.
32. R. Betarbet, T. Zigova, R. A. Bakay, M. B. Luskin, *Int. J. Dev. Neurosci.* **14**, 921 (1996).
33. A. G. Baynash *et al.*, *Cell* **79**, 1277 (1994).
34. X. Piao *et al.*, *Science* **303**, 2033 (2004).

35. We thank H. van Praag, O. Steward, and C. Zhang for discussions; C. Tu and H. Shen for technical assistance; and the laboratories of C. Cotman and F. LaFerla for access to equipment. Supported by a University of California Discovery grant. K.N. is a recipient of a UCI Medical Scientist Training Program training grant.

Supporting Online Material

www.sciencemag.org/cgi/content/full/308/5730/1923/DC1
Materials and Methods
Figs. S1 to S13
References and Notes

10 March 2005; accepted 2 May 2005
10.1126/science.1112103

GDF11 Controls the Timing of Progenitor Cell Competence in Developing Retina

Joon Kim,[1,2] Hsiao-Huei Wu,[1,2]* Arthur D. Lander,[2,3] Karen M. Lyons,[4] Martin M. Matzuk,[5] Anne L. Calof[1,2]†

The orderly generation of cell types in the developing retina is thought to be regulated by changes in the competence of multipotent progenitors. Here, we show that a secreted factor, growth and differentiation factor 11 (GDF11), controls the numbers of retinal ganglion cells (RGCs), as well as amacrine and photoreceptor cells, that form during development. GDF11 does not affect proliferation of progenitors—a major mode of GDF11 action in other tissues—but instead controls duration of expression of *Math5*, a gene that confers competence for RGC genesis, in progenitor cells. Thus, GDF11 governs the temporal windows during which multipotent progenitors retain competence to produce distinct neural progeny.

The vertebrate neural retina comprises seven neural cell types, all derived from one population of multipotent progenitors (*1*, *2*). Retinal cell types do not arise synchronously but are generated in a stereotyped sequence (*3*, *4*). In vitro results imply that retinal progenitors at different stages differ in their competence to produce distinct cell types (*5*–*7*). Such changes in potential are likely dictated by changes in expression of the transcription factors encoded by proneural genes (*8*, *9*), but mechanisms of proneural gene regulation are poorly understood. An important role for cell-cell signaling is suggested by the fact that production of at least two retinal cell types, retinal ganglion cells (RGCs) and amacrine cells, can increase to compensate for losses of mature cells in either population (*10*, *11*). This process has been postulated to be mediated by a feedback signal produced by mature cells (*12*), but the identity of the signal(s) is unknown.

GDF11, a member of the transforming growth factor-β superfamily of secreted signaling molecules, is expressed in several regions of a developing nervous system, including the retina (*13*). In olfactory epithelium (OE), GDF11 negatively regulates neuron number by causing cell-cycle arrest of the progenitor cells that give rise to olfactory receptor neurons (ORNs) (*14*). Here, we demonstrate that GDF11 is also a negative regulator of neuron number in neural retina, but through a completely different mechanism: GDF11 controls

[1]Department of Anatomy and Neurobiology, [2]Developmental Biology Center, [3]Department of Developmental and Cell Biology, University of California, Irvine, CA 92697, USA. [4]Department of Molecular, Cell, and Developmental Biology, University of California, Los Angeles, CA 90095, USA. [5]Department of Molecular and Human Genetics, Baylor College of Medicine, Houston, TX 77030, USA.

*Present address: Department of Biochemistry, Vanderbilt University, Nashville, TN 37232, USA.
†To whom correspondence should be addressed. Email: alcalof@uci.edu

the period during which retinal progenitor cells are competent to produce certain progeny, thus governing the relative numbers of neural cell types that arise.

In mouse retina, *Gdf11* expression begins about embryonic day (E) 12.5, when RGCs begin to differentiate (Fig. 1A). *Gdf11* mRNA is observed throughout the retina, including the neuroblastic layer (NBL), until at least the first postnatal day (P0), although by E15.5, expression is highest in the developing ganglion cell layer (GCL). Expression of *follistatin* (*Fst*), which encodes a secreted GDF11 antagonist (*15*), is first detected at E13.5. From E15.5 on, *Fst* expression is highest in the nascent GCL but also evident in the NBL and presumptive amacrine cells. Putative receptors for GDF11 (*14*, *16*–*18*) are also expressed in appropriate patterns in the neural retina from E12.5 to 13.5 onward (fig. S1).

To investigate the role of *Gdf11* in retinal development, we examined mice homozygous for the null allele $Gdf11^{tm2}$ (*14*). $Gdf11^{tm2/tm2}$ retinas show obvious changes as early as E14.5, when closure of the optic fissure is incomplete (fig. S2). By E17.5, the presumptive GCL of mutant embryos has an abnormally high cell density, and the inner plexiform layer (IPL), well demarcated in wild-type littermates, is not observed (Fig. 1B). Increased cell density in the mutant GCL is accompanied by widening of the cell layer expressing *Brn3b* [$Gdf11^{tm2/tm2}$, 49.5 ± 3.3 μm (SD); wild-type, 38.5 ± 0.4 μm (SD)], which encodes a POU-domain transcription factor specific for differentiated RGCs (*19*, *20*). By P0, the latest time at which the mutant is viable, $Gdf11^{tm2/tm2}$ GCLs contain ~50% more cells than wild types (Fig. 1C). The excess RGCs that form in $Gdf11^{tm2/tm2}$ animals appear to differentiate normally, extending axons through the optic chiasm and tracts, which also appear abnormally thick (Fig. 1D). By neurofilament immunohistochemistry, we estimate a 37% increase in the cross-sectional areas of optic nerves in $Gdf11^{tm2/tm2}$animals (Fig. 1E and fig. S2).

These changes, observed in all mutant mice examined (>32), imply that *Gdf11* is a negative regulator of RGC genesis. In this respect, the changes in $Gdf11^{tm2/tm2}$ retinas recall those in OE, in which $Gdf11^{tm2/tm2}$ mice also have excess differentiated ORNs (*14*). However, unlike the situation in OE (*14*), $Gdf11^{tm2/tm2}$ retinas display no increase in overall thickness, nor are the distribution or number of proliferating cells significantly altered (fig. S3). These observations suggest that the mechanism by which *Gdf11* regulates neurogenesis in the retina differs from that in the OE.

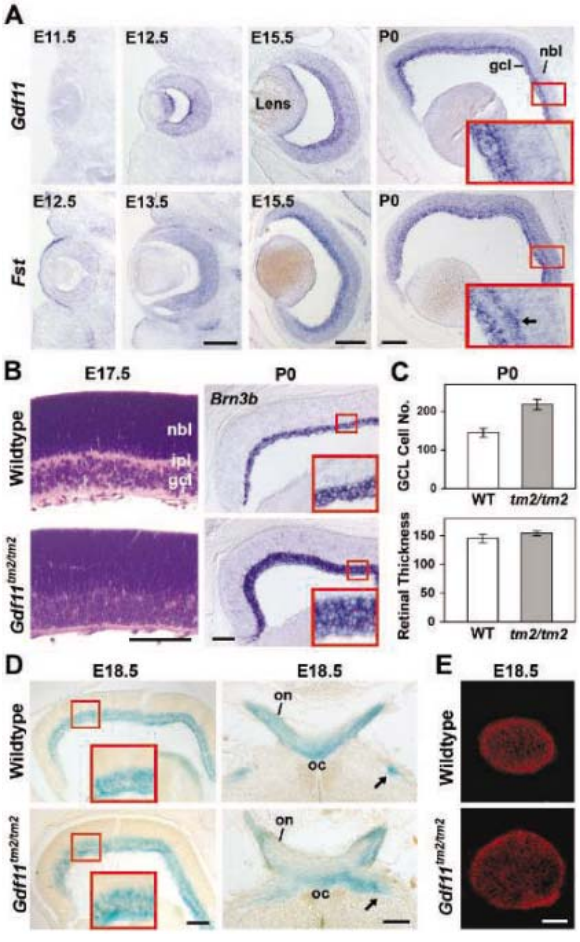

Fig. 1. Retinal abnormalities in *Gdf11* mutants. (**A**) In situ hybridization (ISH) for *Gdf11* and *Fst* in developing mouse retina. nbl, neuroblastic layer; gcl, ganglion cell layer. Arrow in inset indicates *Fst* expression in presumptive amacrine cells. Scale bars, 200 μm. (**B**) Left, hematoxylin-eosin-stained paraffin sections of retina. Right, ISH for *Brn3b*. Insets, higher magnification of $Brn3b^{+}$ gcl . Scale bars, 100 μm. (**C**) Top, increased cell number ($P < 0.01$, Student's *t* test) in $Gdf11^{tm2/tm2}$ retinas. Total cell nuclei in GCL + IPL were counted in 300 μm of central retina in P0 cryosections stained with Hoechst. Bottom, no significant change in central retina thickness. Histograms show mean ± SEM of measurements from 4 to 5 animals of each genotype. (**D**) B-galactosidase (X-gal) staining of sections of $Gdf11^{tm2/tm2}$;*Tattler-1* and $Gdf11^{+/+}$;*Tattler-1* littermate embryos (*33*). Scale bars, 200 μm. on, optic nerve; oc, optic chiasm. Arrows point to optic tract. (**E**) Cross sections of dissected optic nerves stained with antibodies to neurofilament. Scale bar, 50 μm.

Because Fst is known to antagonize GDF11 function in vivo and in vitro (*14*, *15*), we also examined $Fst^{-/-}$ and $Gdf11^{tm2/tm2}$;$Fst^{-/-}$ retinas. $Fst^{-/-}$ retinas showed a 26% reduction in the number of cells in the GCL and a large decrease in thickness of the $Brn3b^{+}$ cell layer (Fig. 2, A and B), which indicates that *Fst* is a positive regulator of RGC development. $Gdf11^{tm2/tm2}$;$Fst^{-/-}$ retinas showed an expanded *Brn3b*+ GCL, comparable to that observed in $Gdf11^{tm2/tm2}$ retinas, consistent with the primary role of Fst as an inhibitor of GDF11 (Fig. 2B). Just as in $Gdf11^{tm2/tm2}$ retinas, the level and pattern of progenitor cell proliferation was unaltered in $Fst^{-/-}$ retinas (fig. S3). The fact that cell proliferation is normal in $Gdf11^{tm2/tm2}$ and $Fst^{-/-}$ retinas suggests that the size of the progenitor pool is not regulated by GDF11. Moreover, expression of several genes involved in early eye specification, patterning, and expansion is also normal in $Gdf11^{tm2/tm2}$ mice (fig. S4).

During development, RGCs are born at the outer margin of the neural retina and migrate inward to the GCL during a defined period (*21*). Detailed examination of $Gdf11^{tm2/tm2}$ and $Gdf11^{tm2/tm2}$;$Fst^{-/-}$ retinas at E17.5 revealed that the NBL of these mutants contains three times as many $Brn3b^{+}$ cells (migrating RGCs) as do wild types (Fig. 2B, insets, and fig. S5). This suggested that, in $Gdf11^{tm2/tm2}$ retinas, RGC production may be prolonged beyond its normal period. To test this, we performed birthdating experiments. The results, shown in Fig. 2C, show an abnormally large number of bromodeoxyuridine-positive ($BrdU^{+}$) cells in the GCL of $Gdf11^{tm2/tm2}$ animals pulsed with BrdU from E15.5 to E17.5. Conversely, $BrdU^{+}$ cells in the GCL of $Fst^{-/-}$ animals pulsed over this same time course were strongly decreased in number, as expected if Fst acts to inhibit GDF11. These differences were not seen when pulse labeling was done at earlier ages (Fig. 2E). Thus, although onset of RGC production appears unaffected by loss of *Gdf11* or *Fst*, its down-regulation is delayed in $Gdf11^{tm2/tm2}$ retinas (and accelerated in $Fst^{-/-}$). A lengthened period of RGC production likely explains why $Gdf11^{tm2/tm2}$ retinas accumulate abnormally large numbers of RGCs.

To determine whether *Gdf11* regulates production of other retinal cell types, we examined rod photoreceptors and amacrine cells, two cell types whose peak periods of differentiation follow that of RGCs. *Crx1*, a marker for early photoreceptors, is normally up-regulated around birth when rod photoreceptor production peaks, and expands to cover much of the NBL (*22*). In $Gdf11^{tm2/tm2}$ retinas, up-regulation and expansion of *Crx1* expression are not observed (Fig. 3A). Amacrine cells may be visualized by expression of syntaxin (*23*), as well as *Pax6* and *Prox1* (*24*, *25*). In the amacrine cell layer of $Gdf11^{tm2/tm2}$ retinas, expression of all three markers was reduced

(Fig. 3A). Altogether, these results suggest that prolonged production of RGCs in *Gdf11*$^{tm2/tm2}$ retinas occurs at the expense of cell types (amacrine cells and photoreceptors) that normally differentiate after RGC production has declined. We observed no obvious increase in amacrine cell or photoreceptor production in *Fst*$^{-/-}$ animals, possibly because excess GDF11 activity in *Fst*$^{-/-}$ retina is mitigated by the reduction in RGC cells, which express the highest levels of *Gdf11* (Fig. 1).

We further tested the idea that GDF11 controls amacrine and photoreceptor cell number, as well as RGC number, by using retinal explant cultures to examine effects of exogenous GDF11 on wild-type retinas (*26*). E13.5 retinal explants grown in GDF11 exhibited a large reduction in *Brn3b*$^{+}$ RGCs, whereas expression of both *Crx1* and syntaxin were increased with GDF11 treatment (Fig. 3B). These findings support the idea that GDF11 is an important regulator of all three retinal cell types.

The finding that RGC genesis is increased, whereas amacrine and rod production are decreased, in *Gdf11* nulls led us to hypothesize that *Gdf11* regulates induction of cell-intrinsic changes by which progenitor cells lose competence to produce RGCs and acquire competence to produce later-born cell types. If GDF11 directly controls progenitor cell competence, *Gdf11* mutants might exhibit changes in expression of factors that determine competence states. *Math5* is among the first such factors expressed during retinal neurogenesis and is required for competence to produce RGCs (*27*–*29*). *Math5* expression is initiated normally in *Gdf11*$^{tm2/tm2}$ retinas, but mutants maintain high levels of expression in the NBL for an abnormally long period. Normally, *Math5* expression is down-regulated in central NBL by E16.5 and is essentially absent by E18.0; in *Gdf11*$^{tm2/tm2}$ retinas, however, *Math5* expression is still evident at these ages (Fig. 4A). Conversely, down-regulation of *Math5* expression occurs prematurely in *Fst*$^{-/-}$ retinas (Fig. 4B) and is accelerated when retinal explants are cultured in GDF11 (Fig. 4C). The prolonged period of *Math5* expression in *Gdf11*$^{tm2/tm2}$ retinas corresponds to the period of prolonged RGC genesis (Fig. 2).

The alteration in the period of *Math5* expression in *Gdf11*$^{tm2/tm2}$ retinas is accompanied by a shift in onset of expression of two other proneural genes, *Mash1* and *NeuroD*, which are involved in the development of bipolar and amacrine cells (*30*, *31*). In *Gdf11*$^{tm2/tm2}$ embryos, expression of both genes is barely detectable at E14.5, when substantial levels are seen in wild types (Fig. 4D). Conversely, *Mash1* expression occurs prematurely in *Fst*$^{-/-}$ retinas, at E13.5, when wild-type littermates express only low levels of *Mash1* (Fig. 4E). By E17.5, both *Mash1*

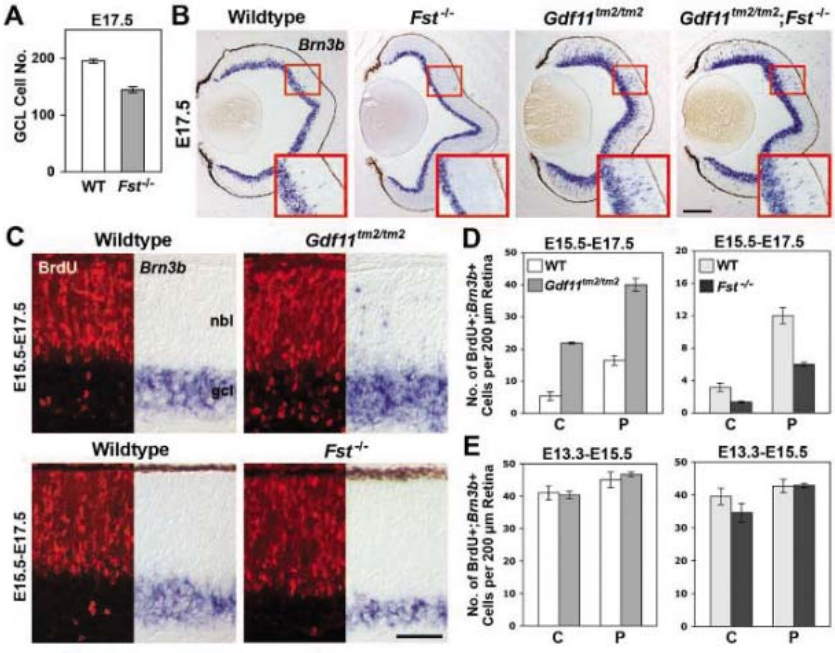

Fig. 2. The period of RGC genesis is altered in *Gdf11*$^{tm2/tm2}$ and *Fst*$^{-/-}$ retinas. (**A**) Total cell nuclei per 300 μm GCL of *Fst*$^{-/-}$ central retina counted after Hoechst staining. (**B**) ISH for *Brn3b* on cryosections of *Fst*$^{-/-}$, *Gdf11*$^{tm2/tm2}$, and *Gdf11*$^{tm2/tm2}$;*Fst*$^{-/-}$ retinas. Insets show superabundance of *Brn3b*$^{+}$ cells in NBL of *Gdf11*$^{tm2/tm2}$ and *Gdf11*$^{tm2/tm2}$;*Fst*$^{-/-}$ retinas. Scale bar, 200 μm. (**C**) Dividing progenitor cells were labeled in vivo by BrdU injection into pregnant dams at E13.5 or E15.5, and retina cryosections (20 μm) were processed 2 days later for *Brn3b* ISH and BrdU immunostaining. Scale bar, 50 μm. (**D**) Quantitative analyses of experiments illustrated in (C). Histograms show mean ± SEM of total *Brn3b*,BrdU double-positive cells in GCL per 200 μm of retina. $N = 2$ to 3 animals of each genotype at each age. $P < 0.05$ (Student's t test, all comparisons). C, central retina; P, peripheral retina (200 μm from peripheral margin). (**E**) Quantitative analysis of RGC birthdating following BrdU injection at E13.5 and analysis at E15.5. No significant differences were observed.

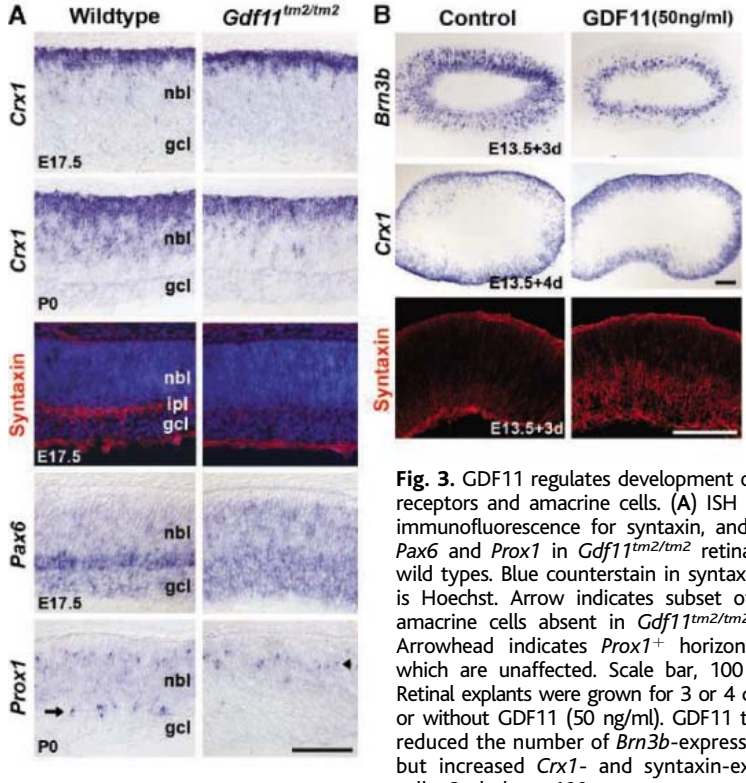

Fig. 3. GDF11 regulates development of photoreceptors and amacrine cells. (**A**) ISH for *Crx1*, immunofluorescence for syntaxin, and ISH for *Pax6* and *Prox1* in *Gdf11*$^{tm2/tm2}$ retinas versus wild types. Blue counterstain in syntaxin panels is Hoechst. Arrow indicates subset of *Prox1*$^{+}$ amacrine cells absent in *Gdf11*$^{tm2/tm2}$ retinas. Arrowhead indicates *Prox1*$^{+}$ horizontal cells, which are unaffected. Scale bar, 100 μm. (**B**) Retinal explants were grown for 3 or 4 days with or without GDF11 (50 ng/ml). GDF11 treatment reduced the number of *Brn3b*-expressing cells, but increased *Crx1*- and syntaxin-expressing cells. Scale bars, 100 μm.

and *NeuroD* expression recover to normal levels in *Gdf11*$^{tm2/tm2}$ retinas (Fig. 4D), which suggests that progenitor cells can acquire competence to produce later-born cell types even though *Math5* expression (and RGC genesis) remain elevated. Altogether, these observations suggest that GDF11 regulates the timing of progenitor competence by controlling the expression of genes crucial for progenitor cell fate determination.

Does GDF11 regulate generation of all retinal cell types, or only some? Because *Gdf11*$^{tm2/tm2}$ animals die at birth (*14*), this question cannot yet be answered with certainty. Expression of Lim1, a horizontal cell-specific transcription factor (*32*), appears to be normal in *Gdf11*$^{tm2/tm2}$ retinas (fig. S6), although changes in expression of a number of other regulatory genes expressed by retinal progenitors are observed (fig. S7). However, the absence of an effect on horizontal cells indicates that GDF11 signaling does not regulate production of all cell types in the retina. Instead, it must govern either a specific subprogram of retinal neurogenesis or act on only a subset of multipotent progenitor cells. This last idea suggests that early retinal progenitors, despite possessing the potential to give rise to all retinal cell types, are nonetheless heterogeneous, at least with respect to their capacity to respond to GDF11.

Our finding that GDF11 governs retinal progenitor cell fate without altering proliferation supports the idea—suggested by retroviral lineage studies—that regulation of cell division and cell-type determination occur independently in the retina (*2*). Moreover, our results highlight the difference in feedback mechanisms employed in different regions of the developing nervous system to effect proper neuron number. In retina, feedback regulation of neural cell number, mediated by GDF11 expressed by the earliest born neurons, is accomplished by altering the fates of multipotent progenitor cells independent of proliferation. In other regions, such as OE, neuronal GDF11 feeds back to regulate progenitor cell proliferation, independent of changes in cell fate (*14*). Finally, these studies demonstrate the diversity of action of GDF11 itself. In OE, GDF11 exerts its anti-neurogenic action by inducing reversible cell-cycle arrest in committed progenitors through increased expression of the cyclin-dependent kinase inhibitor p27^{Kip1} (*14*). In retina, by contrast, GDF11 controls the time course of expression of genes that regulate competence to produce RGCs, but neither p27^{Kip1} levels nor cell proliferation are affected (figs. S3 and S8). Thus, GDF11 acts as a negative feedback regulator of neurogenesis during development by altering either progenitor cell proliferation or progenitor cell fate in different tissues.

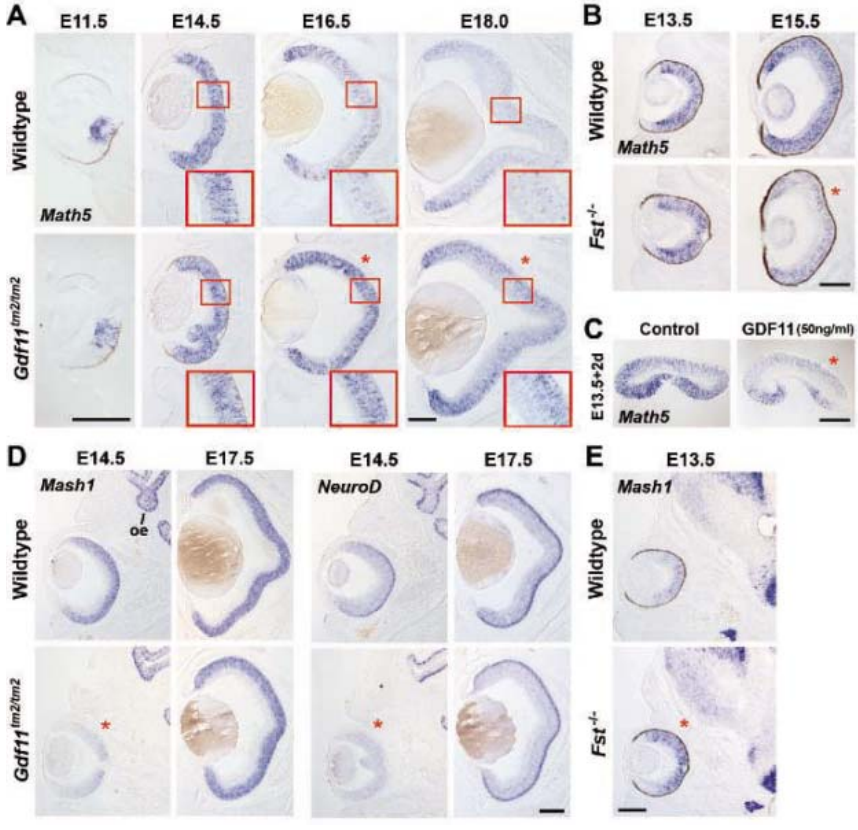

Fig. 4. GDF11 and Fst regulate temporal changes in *Math5* expression. (**A**) ISH for *Math5* in retinas of *Gdf11*$^{tm2/tm2}$ and wild-type littermates. (**B**) ISH for *Math5* expression in *Fst*$^{-/-}$ and wild-type littermate retinas. (**C**) E13.5 retinal explants grown in presence or absence of GDF11 (50 ng/ml) for 2 days (E13.5 + 2 days), then hybridized with probe to *Math5*. (**D**) Expression of *Mash1* and *NeuroD* in retina in *Gdf11*$^{tm2/tm2}$ mice and wild-type littermates. oe, olfactory epithelium. (**E**) Early onset of *Mash1* expression in *Fst*$^{-/-}$ retinas. Asterisks in (A) to (E) indicate reproducible differences from wild-type controls. Scale bars, 200 μm.

References and Notes

1. R. Wetts, S. E. Fraser, *Science* **239**, 1142 (1988).
2. D. L. Turner, E. Y. Snyder, C. L. Cepko, *Neuron* **4**, 833 (1990).
3. R. W. Young, *Anat. Rec.* **212**, 199 (1985).
4. D. H. Rapaport, L. L. Wong, E. D. Wood, D. Yasumura, M. M. LaVail, *J. Comp. Neurol.* **474**, 304 (2004).
5. T. Watanabe, M. C. Raff, *Neuron* **4**, 461 (1990).
6. M. J. Belliveau, C. L. Cepko, *Development* **126**, 555 (1999).
7. D. H. Rapaport, S. L. Patheal, W. A. Harris, *J. Neurobiol.* **49**, 129 (2001).
8. M. L. Vetter, N. L. Brown, *Semin. Cell Dev. Biol.* **12**, 491 (2001).
9. T. Marquardt, P. Gruss, *Trends Neurosci.* **25**, 32 (2002).
10. M. Gonzalez-Hoyuela, J. A. Barbas, A. Rodriguez-Tebar, *Development* **128**, 117 (2001).
11. T. A. Reh, T. Tully, *Dev. Biol.* **114**, 463 (1986).
12. D. K. Waid, S. C. McLoon, *Development* **125**, 1059 (1998).
13. M. Nakashima, T. Toyono, A. Akamine, A. Joyner, *Mech. Dev.* **80**, 185 (1999).
14. H. H. Wu *et al.*, *Neuron* **37**, 197 (2003).
15. L. W. Gamer *et al.*, *Dev. Biol.* **208**, 222 (1999).
16. S. P. Oh *et al.*, *Genes Dev.* **16**, 2749 (2002).
17. S. M. Federman *et al.*, *J. Bone Miner. Res.* **15**, S103 (2000).
18. S. J. Lee, A. C. McPherron, *Proc. Natl. Acad. Sci. U.S.A.* **98**, 9306 (2001).
19. M. Xiang *et al.*, *Neuron* **11**, 689 (1993).
20. L. Gan *et al.*, *Proc. Natl. Acad. Sci. U.S.A.* **93**, 3920 (1996).
21. D. K. Waid, S. C. McLoon, *Neuron* **14**, 117 (1995).
22. S. Chen *et al.*, *Neuron* **19**, 1017 (1997).
23. C. J. Barnstable, R. Hofstein, K. Akagawa, *Brain Res.* **352**, 286 (1985).
24. T. Marquardt *et al.*, *Cell* **105**, 43 (2001).
25. M. A. Dyer, F. J. Livesey, C. L. Cepko, G. Oliver, *Nat. Genet.* **34**, 53 (2003).
26. J. R. Sparrow, D. Hicks, C. J. Barnstable, *Brain Res. Dev. Brain Res.* **51**, 69 (1990).
27. S. Kanekar *et al.*, *Neuron* **19**, 981 (1997).
28. N. L. Brown, S. Patel, J. Brzezinski, T. Glaser, *Development* **128**, 2497 (2001).
29. Z. Yang, K. Ding, L. Pan, M. Deng, L. Gan, *Dev. Biol.* **264**, 240 (2003).
30. J. Hatakeyama, K. Tomita, T. Inoue, R. Kageyama, *Development* **128**, 1313 (2001).
31. E. M. Morrow, T. Furukawa, J. E. Lee, C. L. Cepko, *Development* **126**, 23 (1999).
32. W. Liu, J. H. Wang, M. Xiang, *Dev. Dyn.* **217**, 320 (2000).
33. Materials and methods are available as supporting material on *Science* Online.

34. This work was supported by the March of Dimes Birth Defects Foundation, NIH grants DC03583 and HD38761 to A.L.C. A.D.L. is supported by HD38761, K.M.L. by AR44528, and M.M.M. by HD32067.

Supporting Online Material

www.sciencemag.org/cgi/content/full/308/5730/1927/DC1
Materals and Methods
Figs. S1 to S8
References

25 January 2005; accepted 29 April 2005
10.1126/science.1110175

Elementary Response of Olfactory Receptor Neurons to Odorants

Vikas Bhandawat,* Johannes Reisert, King-Wai Yau*

Signaling by heterotrimeric GTP-binding proteins (G proteins) drives numerous cellular processes. The number of G protein molecules activated by a single membrane receptor is a determinant of signal amplification, although in most cases this parameter remains unknown. In retinal rod photoreceptors, a long-lived photoisomerized rhodopsin molecule activates many G protein molecules (transducins), yielding substantial amplification and a large elementary (single-photon) response, before rhodopsin activity is terminated. Here we report that the elementary response in olfactory transduction is extremely small. A ligand-bound odorant receptor has a low probability of activating even one G protein molecule because the odorant dwell-time is very brief. Thus, signal amplification in olfactory transduction appears fundamentally different from that of phototransduction.

Odorants activate specific receptor proteins (*1*) on the cilia of olfactory receptor neurons (ORNs) and, by way of a G protein (G_{olf}), stimulate an adenylyl cyclase (type III) to synthesize adenosine 3′,5′-cyclic monophosphate (cAMP) (*2*, *3*). cAMP opens a cyclic-nucleotide–gated (CNG) cation channel to produce a membrane depolarization (*2*, *3*). Influx of Ca^{2+} through the CNG channel opens a Ca^{2+}-activated chloride (Cl) channel, leading to Cl^- efflux and further depolarization (*2*, *3*). Simultaneously, the Ca^{2+} influx decreases cAMP synthesis and the effective affinity of CNG channels for cAMP, both effects producing olfactory adaptation (*2*, *3*).

Little is known about signal amplification in olfactory transduction. It has been suggested (*4*) that, in physiological (Ringer) solution, a single odorant-receptor molecule triggers an elementary (or unitary) olfactory response of ~1 pA in membrane current, indicating an amplification similar to that in phototransduction. However, this conclusion has been challenged (*5*, *6*). The supralinear relation (i.e., Hill coefficient >1) reported between odorant concentration and response amplitude (*7*) is also puzzling because it may suggest a nonlinear summation of the elementary responses. At odorant concentrations low enough to give few odorant-binding events, the overall response should arise from spatially segregated, noninteracting transduction domains on the cilia triggered by individual activated membrane receptor molecules (the "units"). Thus, despite intrinsic transduction nonlinearities [multiple cAMP molecules are required to open a CNG channel (*2*, *3*) and multiple Ca^{2+} to open a Ca^{2+}-activated Cl channel (*2*, *3*)], these segregated domains should sum linearly, as is the case for single-photon responses in rod photoreceptors (*8*, *9*).

To characterize the elementary olfactory response, we measured membrane currents from single, dissociated frog ORNs with the suction-pipette method (*10*, *11*). By stimulating an ORN in normal Ringer solution with a brief pulse of the odorant cineole (*12*), we confirmed a supralinear relation between response amplitude and odorant concentration (Hill coefficient n = 1.5 to 6.0; mean ± SD = 3.0 ± 1.6 from nine cells) (Fig. 1, A and C). At low (20 μM) external Ca^{2+} concentration [replaced by equimolar Mg^{2+} to retain divalent block of the CNG channel (*13*)], the response to a weak stimulus increased substantially, presumably owing to removal of Ca^{2+}-dependent adaptation. The foot of the dose-response relation also became linear (Fig. 1, B to D) (14 cells). Likewise, a supralinear relation between response amplitude and odorant duration (at constant concentration) in Ringer solution (Fig. 1E) (n = 2.8 ± 0.8 from six cells) became linear in 20 μM Ca^{2+} solution (Fig. 1F) (14 cells). The simplest interpretation of the linearity is that only one odorant molecule is required for activating a membrane receptor and that, at low event frequencies, the elementary responses indeed sum linearly. The odorant concentrations in Fig. 1, A to F, were high because of the short odorant pulses used. Longer stimulus durations in either Ringer or 20 μM Ca^{2+} solution decreased the half-saturating odorant concentration ($K_{1/2}$) of the dose-response relation (Fig. 1, G and H). The lowest $K_{1/2}$ with a 500-ms cineole stimulus was ~1 μM from more than 340 cineole-responsive cells (*12*); this value would presumably be even lower with longer stimulus durations.

To perform quantal analysis (*14*) for extracting information about the unitary response, we decreased the external Ca^{2+} concentration to 100 nM to further increase the response. Successive weak, identical odorant pulses elicited responses with a constant time course but fluctuating, quantized amplitudes (Fig. 2, A and B). Assuming Poisson statistics, the variance/mean ratio (σ^2/m) of the response ensemble (*8*) (Fig. 2B, inset) gave a unitary response amplitude of 0.9 pA, matching the first nonzero peak in the amplitude histogram. Dividing the mean response (2.9 pA) by 0.9 pA yielded a mean quantal content of 3.2. The predicted amplitude distribution can thus be generated from the Poisson distribution (Fig. 2B) (*12*). This fits well with the experimental histogram, hence validating Poisson statistics. A total of five cells were analyzed, with similar results. The unitary amplitude was quite similar from cell to cell (Fig. 2C) (0.94 ± 0.19 pA; 19 cells, including 14 with only σ^2/m values).

The quantal analysis was repeated with an external Ca^{2+} concentration of 20 μM. The unitary response was smaller (0.42 pA in Fig. 3, A to C) and only extractable from σ^2/m. In cases (e.g., Fig. 3D) where the unitary amplitude was estimated at several mean response amplitudes (by varying odorant concentration or duration) in the same cell, this value was fairly constant, further validating the variance analysis. Again, the unit across cells was quite constant (0.40 ± 0.07 pA, 18 cells) (Fig. 3E), despite randomly selected ORNs [each of which should have a different odorant receptor (*1*, *15*, *16*)] and the use of several odorants (cineole, isoamylacetate, and acetophenone). Thus, the unitary response amplitude appears to be independent of the odorant or the receptor.

As expected, the quantal analysis in normal Ringer solution failed, owing to the nonlinear dose-response relation. Nonetheless, the unitary amplitude can still be estimated. Linear extrapolation from the foot of the dose-response relation in Ringer solution containing 20 μM Ca^{2+} (Fig. 1C) gave a macroscopic current of 132 pA at 300 μM cineole. Dividing this value by a unitary amplitude of 0.4 pA at this Ca^{2+} concentration yields 330 events. In Ringer solution, the same cineole concentration elicited a response of only 5 pA. Thus, the unitary amplitude in Ringer solution would be 5/330 = 0.015 pA (assuming the receptor-odorant interaction to be Ca^{2+} independent). This is an upper estimate because some nonlinear summation of units may already exist at 5 pA. From analysis of five cells, similar calculations gave a mean unit size of 0.026 (± 0.015) pA, a factor of 100 smaller than previously reported (*4*). Why is the foot of the dose-response relation

Department of Neuroscience, Johns Hopkins University School of Medicine, Baltimore, MD 21205, USA.

*To whom correspondence should be addressed. Room 907 Preclinical Teaching Building, Johns Hopkins University School of Medicine, 725 North Wolfe Street, Baltimore, MD 21205, USA. E-mail: vbhanda@mail.jhmi.edu (V.B.); kwyau@mail.jhmi.edu (K.-W.Y.)

linear in low-Ca^{2+} solution but not in Ringer solution? Simply, the unitary response in Ringer solution is so small that, in any detectable macroscopic response, there are already so many binding events that their domains overlap spatially and hence sum supralinearly owing to the intrinsic transduction nonlinearities.

To confirm that the unitary response is independent of the receptor-odorant complex (Figs. 2C and 3E), we examined ORNs that responded to two odorants separately (very rare encounters). In Fig. 4A, a 50-ms pulse of either 1 or 2 mM acetophenone in 20 μM Ca^{2+} solution elicited small, identical responses (suggesting that all receptors were bound). In contrast, a 1 mM cineole pulse half as long (25 ms) produced a response seven times as large as that to acetophenone, possibly before saturating all receptors. Thus, the efficacy of cineole in activating the odorant receptor in this cell was at least 14 times that of acetophenone. Nonetheless, the unitary responses derived from σ^2/m were ~0.5 pA for both odorants and had comparable response kinetics (Fig. 4A). Four other cells gave similar results.

The similar response kinetics elicited by two odorants of widely different efficacies on a cell suggests that the odorant dwell-time [a parameter coupled to the efficacy of the receptor-odorant complex (*12*)] is not a dominant time constant in the response waveform; otherwise, the more effective odorant would have elicited a more prolonged response (*12*). Also, if a single membrane receptor, during the odorant dwell-time, activates a large number of G protein molecules, an odorant with a longer dwell-time should produce a larger unitary response. Thus, a parsimonious interpretation of the constant unitary response is that the receptor-odorant complex has a low probability of activating even one G_{olf} molecule (although this probability will still determine the relative sizes of the macroscopic responses triggered by different receptor-odorant complexes). Consequently, the action of one G_{olf} molecule [formally equivalent to the action of one adenylyl cyclase molecule because one G protein molecule at most activates one adenylyl cyclase molecule (*17*)] should become the dominant unitary event underlying the stochastic response fluctuations. This could explain the constancy of the unitary response because essentially all ORNs use G_{olf} and adenylyl cyclase for transduction. In short, a very low amplification exists between an odorant-binding event and the activation of adenylyl cyclase. Theoretically, an alternative scenario of one receptor activating multiple G_{olf} molecules is also possible, but the probability of G_{olf} activating adenylyl cyclase would have to be proportionately reduced further. We think this scenario is unlikely because of the short dwell-time of odorant on the receptor (see below).

Not only is the relation between response amplitude and odorant duration linear in low-Ca^{2+} solution, but it also has a time intercept near zero (14 cells) (Fig. 1F). This time intercept is a measure of the effective odorant dwell-time, provided the odorant on-rate far exceeds its off-rate (*12*). Accordingly, we stimulated an ORN (at 20 μM Ca^{2+}) with an odorant pulse at concentrations high enough to bind all of the receptors. Twenty-five millisecond pulses of cineole at 1, 1.5, or 2 mM all produced the same response amplitude (Fig. 4B), indicating saturation of the receptors. When applied for 50 ms at these concentrations, the pulses produced responses exactly twice as large, indicating that the responses were within the linear range (i.e., no compression due to downstream transduction steps) with respect to their dependence on odorant duration. The relation between odorant duration and response amplitude at 2 mM cineole extrapolated to a time intercept near zero (Fig. 4B). A total of six experiments gave a time intercept of –3.2 to +8.1 ms (mean ± SD =

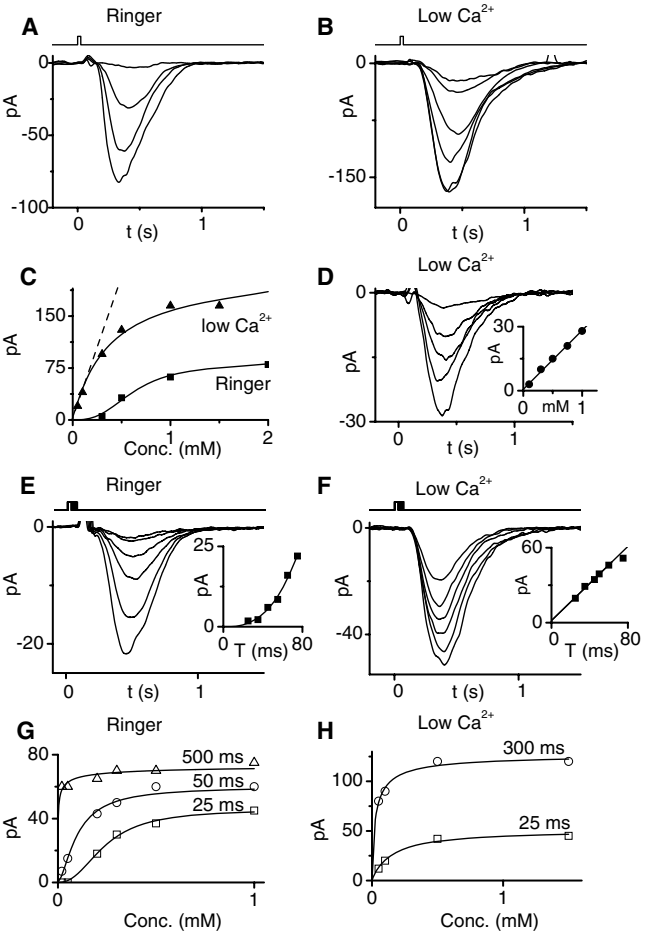

Fig. 1. Odorant-induced responses of an isolated frog ORN in normal and low (20 μM)–Ca^{2+} Ringer solutions. (**A** to **C**) Comparison of responses from the same cell in normal and low-Ca^{2+} Ringer solutions. (A) Normal Ringer solution. Responses to a 25-ms pulse of cineole at 300, 500, 1000, and 2000 μM, respectively. Each trace represents the average of two to five stimulus trials (five for each of the two smallest responses). (B) Low-Ca^{2+} Ringer solution. Responses to a 25-ms pulse of cineole at 50, 100, 300, 500, 1000, and 1500 μM, respectively. Each trace represents the average of two to five trials. (C) The dependence of the transient peak current on odorant concentration in (A) and (B) are plotted for comparison. The smooth curve for normal Ringer solution is a least-squares fit of the Hill equation, $I = I_{max}C^n/(C^n + K_{1/2}{}^n)$, where I is current response, I_{max} is maximum current, C is odorant concentration, $K_{1/2}$ is the concentration required to elicit half the maximum response, and n is the Hill coefficient. The curve is fit with I_{max} = 82 pA, $K_{1/2}$ = 625 μM, n = 2.8. The smooth curve in low-Ca^{2+} Ringer solution is fit with I_{max} = 217 pA, $K_{1/2}$ = 329 μM, n = 1. The dashed line indicates that the foot of the dose-response relation is linear. (**D**) Responses of a different cell in low-Ca^{2+} Ringer solution to a 25-ms pulse of cineole at 100, 300, 500, 750, and 1000 μM, respectively. Each trace represents the average of five stimulus trials. (**Inset**) Linear dose-response relation. (**E**) Responses of a different cell in normal Ringer solution to a 200 μM cineole pulse of different durations (25, 35, 45, 55, 65, and 75 ms, respectively). Each trace represents the average of 10 stimulus trials. (**Inset**) Least-squares fit of the equation $I \propto C^n$ (n = 2.8). (**F**) Responses of a different cell in low-Ca^{2+} Ringer solution to a 100 μM cineole pulse of different durations (25, 35, 45, 55, 65, and 75 ms, respectively). Each trace represents the average of 6 to 10 stimulus trials. (**Inset**) A linear-regression fit has a time intercept of −2 ms. Results similar to those in Fig. 1, B, D, and F, were obtained upon "clamping" the internal Ca^{2+} concentration during the olfactory response by replacing external Na^+ in the low-Ca^{2+} solution with the permeant guanidinium ion to simultaneously stop Ca^{2+} influx through the CNG channel and Ca^{2+} efflux through the Na-Ca exchanger (*11*, *24*). (**G** and **H**) Strong dependence of $K_{1/2}$ of the dose-response relation on the duration of stimulation by odorant. Each panel represents responses from a different cell. Each point is the average of 2, 5 or 10 stimulus trials. (G) Normal Ringer solution. Relation between response amplitude and odorant concentration with stimulus durations of 25, 50 , and 500 ms, respectively. The smooth curves are Hill-equation fits with I_{max}, $K_{1/2}$, and n of 75 pA, 1.5 μM, and 0.8 (500 ms); 61 pA, 99 μM, and 1.5 (50 ms); and 46 pA, 238 μM, and 2.3 (25 ms), respectively. Thus, by increasing the odorant duration from 25 to 500 ms, the $K_{1/2}$ decreases from 238 to 1 μM. (H) Low-Ca^{2+} Ringer solution. Dose-response relations from a different cell with 25- and 300-ms odorant duration, respectively. Smooth curves are Michaelis-equation (i.e., Hill equation with n = 1) fits, with I_{max} and $K_{1/2}$ of 121 pA and 24 μM (300 ms) and 45 pA and 128 μM (25 ms), respectively.

+2.3 ± 4.1 ms; the small positive mean value perhaps reflected slight measurement uncertainties). Thus, the odorant dwell-time on the receptor was at most on the order of 1 ms. Because it is so short-lived, the receptor-odorant complex is unlikely to activate a G_{olf} molecule. Even for rod phototransduction, known for its high amplification, one photoisomerized rhodopsin molecule will activate only 0.1 G protein (transducin) molecule in 1 ms (*12*, *18*). Indeed, even when rendered continuously bound to ligand by high odorant concentration (Fig. 4B), the receptor apparently still had a low probability of activating any G_{olf} in a time window up to 50 ms (up to at least 100 ms in other experiments); otherwise, concatenated binding events on the same receptor molecule would have produced overlapping domains of activation and a nonlinear relation between macroscopic response and odorant duration. In short, the brief odorant dwell-time leads to a low probability of activating G_{olf}, consistent with the constancy of the unitary event across cells. This interpretation does not depend on the detailed molecular mechanism for the receptor-G_{olf} interaction, either by diffusion (as with rhodopsin-transducin interactions) or by close-range interactions in a complex of signaling molecules. If a signaling complex exists, its purpose is unclear because of the low probability that the receptor-odorant complex will activate G_{olf}.

It is generally thought that one active G protein–coupled receptor (GPCR) molecule activates multiple downstream G protein/effector enzyme molecules, providing amplification. In rod phototransduction, one photoisomerized rhodopsin certainly activates many transducins before shutoff by phosphorylation and arrestin binding (*18*, *19*). We find that this is not necessarily so for olfactory transduction (and, by extension, perhaps some other ligand-activated GPCR pathways as well). The receptor-odorant complexes, at least those observed here, lasted <1 ms. Apart from a low probability of activating any G_{olf}, the complexes may be too short-lived to be phosphorylated by a G protein–coupled receptor kinase (GRK), whether or not this mechanism exists in ORNs (*20*–*22*). Our experiments indicate that, even if continuously bound to ligand, a receptor is not inactivated at least up to the order of 100 ms (otherwise

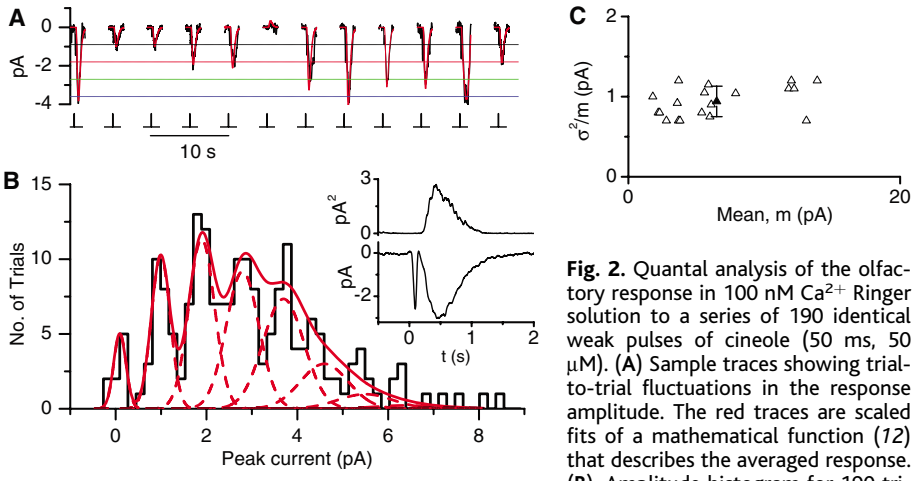

Fig. 2. Quantal analysis of the olfactory response in 100 nM Ca^{2+} Ringer solution to a series of 190 identical weak pulses of cineole (50 ms, 50 μM). (**A**) Sample traces showing trial-to-trial fluctuations in the response amplitude. The red traces are scaled fits of a mathematical function (*12*) that describes the averaged response. (**B**). Amplitude histogram for 190 trials. Bin-width is 0.2 pA. (**Inset**) Ensemble mean and variance as a function of time. Downward spike in the mean response indicates junction current introduced to mark the timing and duration of odorant stimulation (*12*). At the response peak, the mean current was 2.9 pA and the variance was 2.6 pA^2. These values give a unitary response of 0.9 pA and a mean quantal content (λ) of 3.2. The solid red curve is the Poisson distribution (*12*) with λ = 3.2, scaled by a unitary amplitude of 0.9 pA and blurred by Gaussian functions with σ_0 = 0.27 pA, σ_1 = 0.33 pA (*12*). The dashed profiles are Gaussians corresponding to failures and populations with quantal content of 1, 2, etc. (**C**) Results from 19 cells on the unitary amplitude in 100 nM Ca^{2+}, derived from σ^2/m. The values were all very similar and independent of *m*. Filled triangle and error bars: mean ± SD.

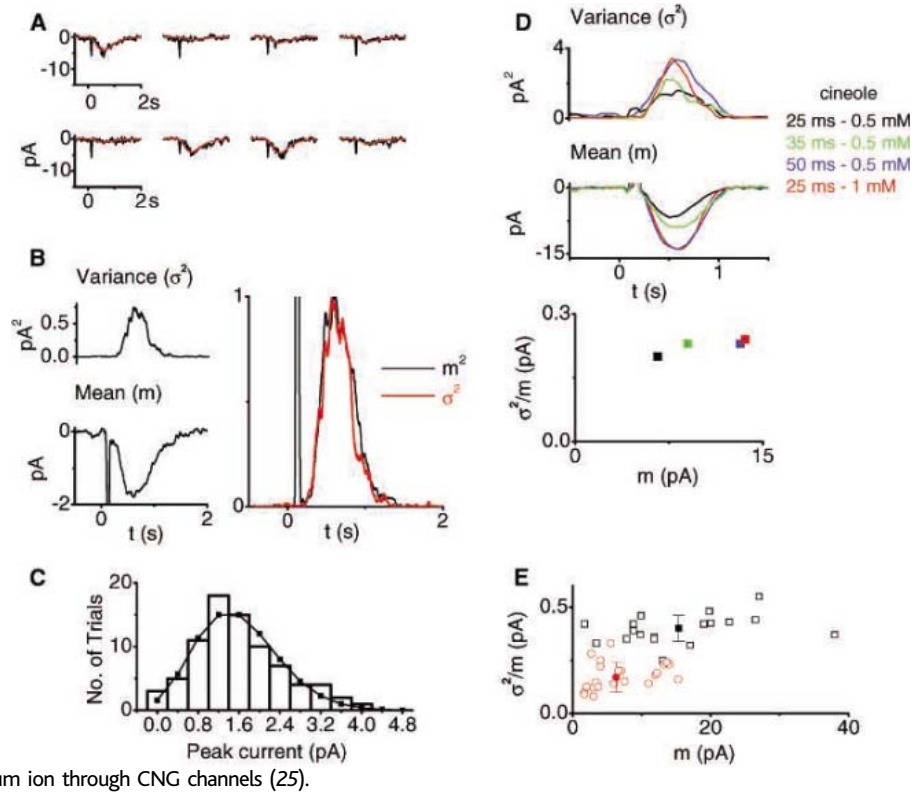

Fig. 3. Variance analysis of the olfactory response in Ringer solution containing 20 μM Ca^{2+}. (**A** to **C**) A series of 78 identical pulses of cineole (25 ms, 300 μM) was delivered to an ORN. (A) Eight sample traces showing trial-to-trial fluctuations in the response amplitude. The red traces are scaled fits of a mathematical function that describes the averaged response. Downward spike in each trace indicates junction current introduced to mark the timing and duration of odorant stimulation (*12*). (B) (Left) Ensemble variance and mean as a function of time from 78 trials. The downward deflection in the "mean" trace was the junction current. The variance (σ^2) and $(\text{mean})^2$ time courses overlap throughout. (C) The amplitude histogram was well described by the Poisson distribution calculated from the σ^2/m analysis (mean number of quanta = 4.0, quantal amplitude = 0.42 pA). (**D**) Variance/mean analysis of olfactory response from a different cell in four stimulus conditions, each with 20 identical cineole pulses. The value of σ^2/m is approximately constant at different *m* values. The Ringer solution contained guanidinium with a low concentration of Ca^{2+}. (**E**) Results of σ^2/m measurements, with cineole (27 cells), isoamylacetate (7 cells), or acetophenone (6 cells) as odorant. Black open squares show measurements in low-Ca^{2+} sodium Ringer solution. Red open circles show measurements in low-Ca^{2+} guanidinium Ringer solution. Corresponding filled symbols show mean ± SD (black: 0.40 ± 0.06 pA, 18 cells; red: 0.17 ± 0.07 pA, 22 cells). The smaller unitary response in guanidinium/low-Ca^{2+} solution reflects a smaller inward current carried by guanidinium ion through CNG channels (*25*).

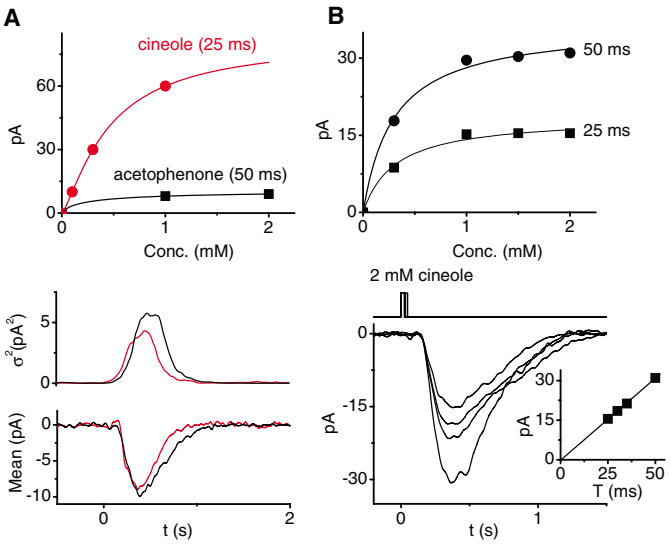

Fig. 4. (**A**) Unitary responses for two odorants with different potencies on the same cell are very similar. (Top) Relation between response amplitude and odorant concentration for acetophenone and cineole odorants. Each point represents the average of four to eight stimulus trials. Although the duration of acetophenone stimulation was twice as long as that for cineole, the response with all receptors bound by acetophenone was a factor of 7 less than the response to cineole. (Bottom) Variance/mean analysis of the unitary response to the two odorants. The quantal responses to the two odorants were similar (0.48 pA for cineole and 0.56 pA for acetophenone). Thirty trials each of 100 μM cineole at 25-ms duration and 2 mM acetophenone at 50-ms duration. The two stimuli were chosen to produce responses of comparable amplitudes. The slight difference in response kinetics for the two odorants was due to a change in cell condition during the experiment; this was not observed in other experiments. We chose this cell because of the large difference in efficacy between the two odorants. (**B**) Estimation of cineole dwell-time on the receptor. (Top) Relation between response amplitude and cineole concentration at two durations. Even when all receptors were bound (≥1 mM cineole), the response amplitude increased linearly with the odorant pulse duration. Each point represents the average of 3 to 20 stimulus trials. (Bottom) Complete data from the same experiment at a saturating cineole concentration of 2 mM and applied for four different durations. (**Inset**) Linear increase of the response with odorant duration. The time intercept of the linear-regression fit is near zero.

the stimulus duration-response relation in Fig. 4B would not have remained linear). Thus, phosphorylation and arrestin binding are unlikely to constitute the standard termination of olfactory responses. Possibly, phosphorylation is important for desensitization in situations of prolonged and intense stimulation.

A short-lived receptor-odorant complex does not preclude an overall high olfactory sensitivity. Repeated bindings of odorant molecules to the same receptor allow signal integration, especially if receptor phosphorylation does not occur (unlike in vision, where a photon acts only once and a photobleached pigment molecule is nonfunctional). The total rate of odorant-binding events is also amplified by orders of magnitude by the total number of receptor molecules on an ORN. The supralinear interactions occurring when unitary transduction domains overlap can further enhance sensitivity at intermediate odorant concentrations and durations. Finally, a high convergence of sensory input at the glomerulus (*23*) may boost sensitivity. The glomerulus is the synaptic plexus in the olfactory bulb that integrates signals from all ORNs expressing the same odorant receptor species. In principle, this convergence can increase indefinitely by simply expanding the surface area of the olfactory epithelium and therefore the number of ORNs expressing a given odorant receptor. This increase in convergence may explain why the olfactory sensitivity in many animals is much higher than it is in humans. Unlike the retinotopic map in vision, which imposes a functional limit on the degree of convergence from photoreceptors, no corresponding limitation exists in olfaction.

References and Notes

1. L. B. Buck, *Cell* **100**, 611 (2000).
2. D. Schild, D. Restrepo, *Physiol. Rev.* **78**, 429 (1998).
3. H. R. Matthews, J. Reisert, *Curr. Opin. Neurobiol.* **13**, 469 (2003).
4. A. Menini, C. Picco, S. Firestein, *Nature* **373**, 435 (1995).
5. G. Lowe, G. H. Gold, *Proc. Natl. Acad. Sci. U.S.A.* **92**, 7864 (1995).
6. G. H. Gold, G. Lowe, *Nature* **376**, 27 (1995).
7. S. Firestein, C. Picco, A. Menini, *J. Physiol.* **468**, 1 (1993).
8. D. A. Baylor, T. D. Lamb, K.-W. Yau, *J. Physiol.* **288**, 613 (1979).
9. T. D. Lamb, P. A. McNaughton, K.-W. Yau, *J. Physiol.* **319**, 463 (1981).
10. G. Lowe, G. H. Gold, *J. Physiol.* **442**, 147 (1991).
11. J. Reisert, H. R. Matthews, *J. Gen. Physiol.* **112**, 529 (1998).
12. Materials and methods as well as additional notes are available as supporting material on *Science* Online.
13. S. J. Kleene, *Neuroscience* **66**, 1001 (1995).
14. J. del Castillo, B. Katz, *J. Physiol.* **124**, 560 (1954).
15. S. Serizawa *et al.*, *Science* **302**, 2088 (2003).
16. J. W. Lewcock, R. R. Reed, *Proc. Natl. Acad. Sci. U.S.A.* **101**, 1069 (2004).
17. J. J. Tesmer, R. K. Sunahara, A. G. Gilman, S. R. Sprang, *Science* **278**, 1907 (1997).
18. Leskov *et al.*, *Neuron* **27**, 525 (2000).
19. K.-W. Yau, *Invest. Ophthalmol. Vis. Sci.* **35**, 9 (1994).
20. T. M. Dawson *et al.*, *Science* **259**, 825 (1993).
21. S. Schleicher, I. Boekhoff, J. Arriza, R. J. Lefkowitz, H. Breer, *Proc. Natl. Acad. Sci. U.S.A.* **90**, 1420 (1993).
22. K. Peppel *et al.*, *J. Biol. Chem.* **272**, 25425 (1997).
23. P. Mombaerts *et al.*, *Cell* **87**, 675 (1996).
24. K. Nakatani, K.-W. Yau, *Nature* **334**, 69 (1988).
25. K. Nakatani, K.-W. Yau, *J. Physiol.* **395**, 695 (1988).
26. We thank D. A. Baylor, P. A. Fuchs, J. S. Kauer, T. D. Lamb, J. Nathans, R. R. Reed, F. Rieke, D. T. Yue, and members of the Yau laboratory, especially J. Bradley and C.-Y. Su, for critique and discussions, V. Kefalov for help in initial experiments, and D. Chaudhuri for help in computations using MatLab. V.B. also thanks D. McClellen for instruction in scientific writing. This work was supported by Howard Hughes Medical Institute and grants from NIH (DC06904) and the Human Frontier Science Program.

Supporting Online Material
www.sciencemag.org/cgi/content/full/308/5730/1931/DC1
Materials and Methods
Figs. S1 to S4
References and Notes

18 January 2005; accepted 3 May 2005
10.1126/science.1109886

Allometry of Alarm Calls: Black-Capped Chickadees Encode Information About Predator Size

Christopher N. Templeton,[1]*† Erick Greene,[1] Kate Davis[2]

Many animals produce alarm signals when they detect a potential predator, but we still know little about the information contained in these signals. Using presentations of 15 species of live predators, we show that acoustic features of the mobbing calls of black-capped chickadees (*Poecile atricapilla*) vary with the size of the predator. Companion playback experiments revealed that chickadees detect this information and that the intensity of mobbing behavior is related to the size and threat of the potential predator. This study demonstrates an unsuspected level of complexity and sophistication in avian alarm calls.

Predation is a major cause of mortality for most species of animals, and many produce alarm signals when they perceive a potential predator (*1*). Alarm calls often differ in acoustic structure, depending on the situation in which they are produced (*2–5*). If a species is preyed upon by different predators that use different hunting strategies or vary in the degree of danger they present, selection can favor variation in alarm signals

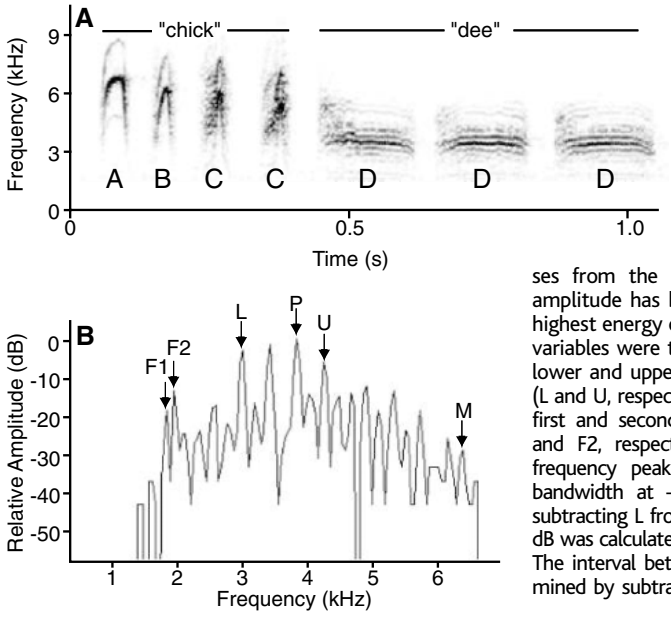

Fig. 1. Features of the "chick-a-dee" mobbing vocalization. (**A**) The call usually contains both "chick" sections (A, B, and C syllable types) and "dee" sections (D syllable types) (*11*). (**B**) Acoustic variables measured from power spectrum analyses from the center of a D note. The amplitude has been scaled relative to the highest energy overtone (dB = 0). Acoustic variables were the peak frequency (P), the lower and upper frequencies above –10 dB (L and U, respectively), the frequency of the first and second peaks above –30 dB (F1 and F2, respectively), and the maximum frequency peak above –30 dB (M). The bandwidth at –10 dB was calculated by subtracting L from U; the bandwidth at –30 dB was calculated by subtracting F1 from M. The interval between overtones was determined by subtracting F1 from F2.

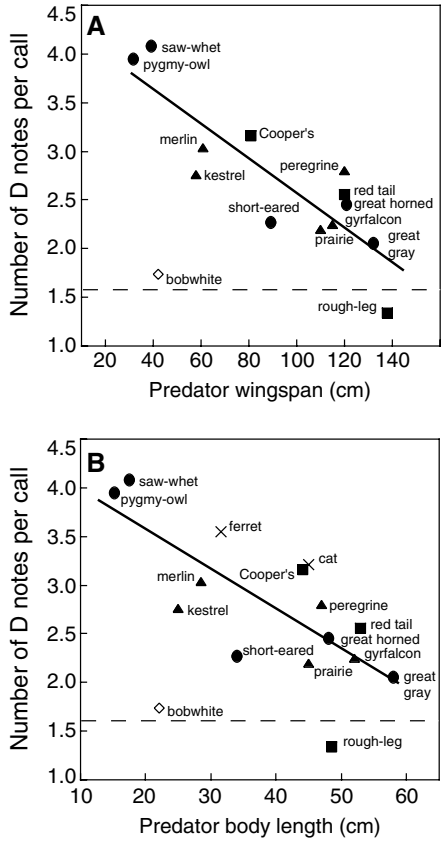

Fig. 2. Chickadees vary their mobbing calls in response to variation in predator body size. (**A**) Mean number of D syllables per call as a function of wingspan for raptors ($y = 4.4 – 0.02x$; $r^2 = 0.512$, $P < 0.0001$). (**B**) Mean number of D syllables per call as a function of body length for raptors and mammals ($y = 4.4 – 0.4x$; $r^2 = 0.361$, $P < 0.0001$). Each taxonomic group of raptors is represented by a different symbol (●, owl; ▲, falcon; ■, hawk; ×, mammal). A bobwhite quail (◇) was used as the procedural control. The dashed line displays the mean number of D notes per control trial without any stimulus.

that encode this information (*6*). Such variation in alarm signals can be used to transfer information about the type of predator [referential alarm call systems (*7*)], the degree of threat that a predator represents [risk-based systems (*8*)], or both (*9*, *10*).

In addition to discriminating among broad types of predators (e.g., raptor versus snake), discriminating among morphologically similar predators within a single type (e.g., different species of raptors) could also be adaptive if the predators vary in the degree of threat they pose. One species that is faced with numerous, morphologically similar predators is the black-capped chickadee (*Poecile atricapilla*). Chickadees are small, common songbirds that are widespread throughout North America. In the nonbreeding season, chickadees form flocks of six to eight birds (*11*). They use an elaborate system of vocalizations to mediate social interactions in these flocks (*12*, *13*) and to warn conspecifics about predators (*14*, *15*).

Chickadees produce two very different alarm signals in response to predators: When flying raptors are detected, chickadees produce a high-frequency, low-amplitude "seet" alarm call; in response to a perched or stationary predator, they produce a loud, broadband "chick-a-dee" alarm call that is composed of several types of syllables (*16*) (Fig. 1A). Whereas the "seet" alarm call functions to warn of flying predators, the "chick-a-dee" mobbing alarm call recruits other chickadees [and often many other species (*17*)] that harass, or mob, a perched predator. This "chick-a-dee" call is a complex vocalization that is also produced in many other situations and encodes information about food and identity (both individual and flock) in addition to information about predators (*11*).

We examined variation in the mobbing vocalizations and behavior of black-capped chickadees by conducting predator presentations and playback experiments with chickadees living under semi-natural conditions in large, outdoor experimental aviaries (*18*). We presented flocks of color-marked chickadees with 13 species of live, perched raptors and two species of live mammalian predators. The predators varied considerably in body size (e.g., factor of 20 difference in body mass between northern pygmy-owl and great horned owl), activity patterns, hunting strategies, and diet (Table 1). The raptors ranged from small, maneuverable predators whose diets include many small birds, to large, less maneuverable predators that eat few small birds. We also used two types of controls: a procedural control with a live bobwhite quail (*Colinus virginianus*); and no presentation, with observers present as they would be during predator presentations. During each predator presentation, two observers recorded chickadee vocalizations, noting the color band combination of each calling individual. By conducting controlled presentations of live predators to birds living under semi-natural conditions, we could isolate vocal responses to specific species of predators from other features such as the location, behavior, or movement pattern of the predator.

Spectrographic analyses of the more than 5000 "chick-a-dee" mobbing alarm calls we recorded (Fig. 1) revealed previously unsuspected levels of acoustic variation. The number of mobbing calls produced in response to each predator was highly variable [analysis of variance (ANOVA): $F_{16,34} = 5.17$, $P < 0.0001$], with the smaller, higher risk, predators eliciting significantly more calls than the larger predators or controls (Tukey's post hoc tests: $P < 0.05$). The total number of syllables per alarm call differed among predator treatments ($F = 3.05$, $P < 0.0001$). In particular, the average number of D syllables, or notes, per call differed significantly across predator treatments ($F = 7.771$, $P < 0.0001$). There was a strong inverse relationship between the number of D notes per alarm call and the wingspan of the raptors, with the smallest predators eliciting calls with the most D notes (Fig. 2A; $r^2 = 0.512$, $P < 0.0001$). There was also a strong inverse relationship between the number of D notes and predator body length when both the mammals and raptors were

[1]Division of Biological Sciences, University of Montana, Missoula, MT 59812, USA. [2]Raptors of the Rockies, Post Office Box 250, Florence, MT 59833, USA.

*Present address: Department of Biology, Box 351800, University of Washington, Seattle, WA 98195, USA.
†To whom correspondence should be addressed. E-mail: ctemple2@u.washington.edu

included in the analysis (Fig. 2B; $r^2 = 0.361$, $P < 0.0001$).

Many other acoustic features of these mobbing calls (Fig. 1) also varied in relation to the predator treatment. For example, in comparisons of mobbing calls given in response to a northern pygmy-owl and a great horned owl (small and large predators, respectively), the duration of the "dee" section (all D notes) was significantly longer (ANOVA: $F_{1,14} = 9.984$, $P = 0.003$), the interval between the "chick" and "dee" sections was significantly shorter ($F = 11.364$, $P = 0.001$), the first D note of each call was shorter ($F = 9.984$, $P = 0.003$), and the interval between the first and second D notes was also shorter in small predator alarm call variants ($F = 9.043$, $P = 0.004$). Calls that chickadees produced during the large predator presentations tended to have D notes that contained more high-energy peaks above –10 dB ($F = 2.855$, $P = 0.097$) spanning a wider bandwidth ($F = 2.719$, $P = 0.105$) than those produced during encounters with small predators. D notes elicited by large predators also tended to have more widely spaced overtones ($F = 3.385$, $P = 0.071$). No differences were observed in any of the other measured features ($P > 0.2$ for all).

Do these acoustic differences in mobbing calls transmit information about the potential predator to other chickadees? We conducted playback experiments (*18*) to test how chickadees reacted to the mobbing calls that they produced in response to different predators by broadcasting variations of the "chick-a-dee" alarm vocalization associated with different predators. We played mobbing calls that flock mates produced in response to a great horned owl (large predator), a northern pygmy-owl (small predator), and control calls of a pine siskin (*Carduelis pinus*). Chickadees exhibited longer and more intense mobbing behavior when they heard alarm calls recorded in response to a pygmy-owl than when they heard alarm calls recorded in response to a great horned owl or control vocalizations (Fig. 3). They produced significantly more "chick-a-dee" calls in response to playback of mobbing alarm calls elicited by a small predator than they did when presented with playbacks of mobbing calls elicited by a large predator or control vocalizations (Fig. 3A; Kruskal-Wallis $K = 11.50$, $P = 0.003$). Chickadees approached the hidden speaker more closely in response to the small predator mobbing call treatment than in response to the large predator mobbing call or control treatments ($K = 14.69$, $P = 0.001$); more individuals approached within 3 m (Fig. 3B; $K = 14.40$, $P = 0.001$) and within 1 m ($K = 11.34$, $P = 0.003$) of the speaker in response to the small predator alarm calls than in response to the large predator alarm calls or control vocalizations. After playback of small predator alarm calls, chickadees also mobbed for longer periods than they did after playback of large predator alarm calls and control sounds ($K = 12.69$, $P = 0.002$).

Previous studies have shown that animals produce different antipredator vocalizations for aerial and terrestrial predators. Most of these studies, however, have presented these two types of predators in different ways (*19–21*), potentially confounding the interpretation that prey distinguish between types of predators and not their location or

Table 1. Species presented to chickadee flocks. Length and wingspan were measured from animals used in experiments; mass (*26*) and diet information (*27–29*) were summarized from published accounts. The sex of each raptor used in the experiments is indicated in brackets.

Predator species	Mass (g)	Length (cm)	Wingspan (cm)	Time active	Primary diet
			Hawks		
Cooper's hawk (*Accipiter cooperii*) [F]	450	44	81	Day	Small birds
Red-tailed hawk (*Buteo jamaicensis*) [F]	1,080	53	120	Day	Small mammals, few birds
Rough-legged hawk (*B. lagopus*) [M]	990	49	138	Day	Small mammals
			Falcons		
American kestrel (*Falco sparverius*) [M]	117	25	58	Day	Inverts, small mammals, small birds
Merlin (*F. columbarius*) [F]	190	28	61	Day	Small birds
Peregrine falcon (*F. mexicanus*) [F]	720	47	120	Day	Medium-sized birds
Prairie falcon (*F. peregrinus*) [F]	720	45	100	Day	Small mammals, some birds
Gyrfalcon (*F. rusticolus*) [M]	1,400	52	115	Day	Medium-sized mammals and birds
			Owls		
Northern pygmy-owl (*Glaucidium gnoma*) [M]	70	15	31	Day	Small birds, small mammals
Saw-whet owl (*Aegolius acadicus*) [M]	80	17	39	Night	Small mammals, some small birds
Short-eared owl (*Asio flammeus*) [M]	350	34	89	Both	Small mammals
Great horned owl (*Bubo virginianus*) [M]	1,400	48	121	Night	Small to medium-sized mammals
Great gray owl (*Strix nebulosa*) [M]	1,080	58	132	Both	Small mammals
			Mammals		
Domestic cat (*Felis domesticus*)	15,000	45	—	Both	Birds, small mammals, insects
Ferret (*Mustela putorius*)	1,000	32	—	Day	Small mammals, eggs, some small birds
			Control		
Bobwhite quail (*Colinus virginianus*)	170	22	42	Day	Seeds, insects

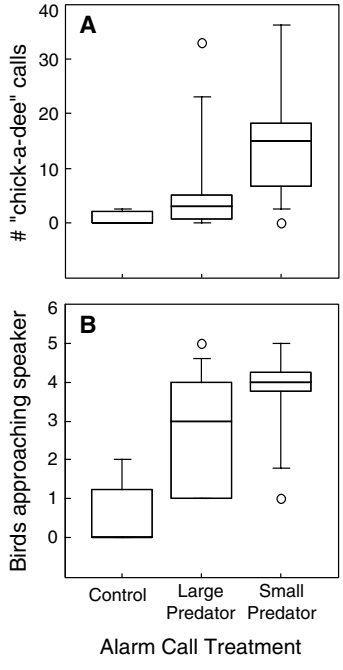

Fig. 3. Chickadees respond to predator-specific acoustic variations in their mobbing alarm calls. Two behavioral variables were used to quantify chickadees' responses to the three playback stimuli: control sounds (pine siskin calls), "chick-a-dee" calls produced in response to a large predator (great horned owl), and "chick-a-dee" calls produced in response to a small predator (northern pygmy-owl). (**A**) Boxplots (showing median, interquartile range (IQR), range, and outliers) of the number of "chick-a-dee" calls produced during the first 90 s after the start of each playback treatment. (**B**) Boxplots of the number of birds approaching within 3 m of the speaker after each treatment. All pairwise comparisons were significantly different (Mann-Whitney U, $P < 0.05$).

behavior. Our results show that chickadees do not vocally discriminate between raptors and mammals when they are presented in similar ways, and thus the "chick-a-dee" call does not refer specifically to the type of predator.

Instead, these vocal signals likely contain information about the degree of threat that a predator represents. Maneuverability (e.g., as measured by turning radius, or radial acceleration) is extremely important in determining the outcome of predator-prey interactions and is inversely related to wingspan and body size in birds (*22*, *23*). Body size may be a good predictor of risk for chickadees: Small raptors tend to be much more maneuverable than larger raptors and likely pose a greater threat to chickadees.

In addition to being one of the most subtle and sophisticated signaling systems yet discovered, this system is unusual in that it combines aspects of both referential and risk-based antipredator vocalization systems (*10*, *24*, *25*). To denote the presence of a rapidly moving predator (e.g., raptor in flight), chickadees produce a "seet" alarm call. When they encounter a stationary predator (e.g., perched raptor), they use the "chick-a-dee" mobbing call. These two vocalizations appear to be functionally referential to the type of predator encounter (i.e., each denotes a specific type of encounter). In addition, we have shown that subtle variation in the "chick-a-dee" mobbing call reflects the size of a specific predator, a characteristic of a risk-based system. Thus, chickadees convey information about predators at two different levels: A coarse level of encoding ("seet" or "chick-a-dee") signifies the type of predator encounter, and a fine level of encoding (variants of "chick-a-dee") signifies the degree of danger presented by that specific predator encounter.

The "chick-a-dee" vocalization is remarkably versatile; it is used in many different contexts and apparently conveys many different types of information. The fact that so much information can be transmitted by subtle variations in one type of vocalization raises some fascinating questions about how finely chickadees can discriminate between similar stimuli, and how they categorize different aspects of their environment.

References and Notes

1. J. W. Bradbury, S. L. Vehrencamp, *Principles of Animal Communication* (Sinauer Associates, Sunderland, MA, 1998).
2. P. Marler, *Nature* **176**, 6 (1955).
3. P. W. Sherman, *Science* **197**, 1246 (1977).
4. R. M. Seyfarth, D. L. Cheney, P. Marler, *Anim. Behav.* **28**, 1070 (1980).
5. C. S. Evans, L. Evans, P. Marler, *Anim. Behav.* **46**, 23 (1993).
6. M. D. Hauser, *The Evolution of Communication* (MIT Press, Cambridge, MA, 1996).
7. D. L. Cheney, R. M. Seyfarth, *How Monkeys See the World* (Univ. of Chicago Press, Chicago, 1990).
8. J. M. Macedonia, C. S. Evans, *Ethology* **93**, 177 (1993).
9. M. B. Manser, R. M. Seyfarth, D. L. Cheney, *Trends Cognit. Sci.* **6**, 55 (2002).
10. R. M. Seyfarth, D. L. Cheney, *Annu. Rev. Psychol.* **54**, 145 (2003).
11. S. M. Smith, *The Black-Capped Chickadee: Behavioral Ecology and Natural History* (Cornell Univ. Press, Ithaca, NY, 1991).
12. S. Nowicki, *Behav. Ecol. Sociobiol.* **12**, 317 (1983).
13. D. J. Mennill, L. Ratcliffe, P. T. Boag, *Science* **296**, 873 (2002).
14. M. S. Ficken, S. R. Witkin, *Auk* **94**, 156 (1977).
15. M. C. Baker, A. M. Becker, *Wilson Bull.* **114**, 510 (2002).
16. M. S. Ficken, R. W. Ficken, S. R. Witkin, *Auk* **95**, 34 (1978).
17. C. R. Hurd, *Behav. Ecol. Sociobiol.* **38**, 287 (1996).
18. See supporting data on *Science* Online.
19. E. Greene, T. Meagher, *Anim. Behav.* **55**, 511 (1998).
20. D. T. Blumstein, *Behaviour* **136**, 731 (1999).
21. A. Le Roux, T. P. Jackson, M. L. Cherry, *Behaviour* **138**, 757 (2001).
22. H. C. Howland, *J. Theor. Biol.* **47**, 333 (1974).
23. K. P. Dial, *Auk* **120**, 941 (2003).
24. C. S. Evans, *Perspect. Ethol.* **12**, 99 (1997).
25. D. T. Blumstein, *Evol. Commun.* **3**, 135 (1999).
26. D. A. Sibley, *The Sibley Guide to Birds* (Knopf, New York, 2000).
27. P. A. Johnsgard, *Hawks, Eagles, and Falcons of North America* (Smithsonian Institution Press, Washington, DC, 1990).
28. P. A. Johnsgard, *North American Owls: Biology and Natural History* (Smithsonian Institution Press, Washington, DC, ed. 2, 2002).
29. K. R. Foresman, *The Wild Mammals of Montana* (Allen, Lawrence, KS, 2001).

30. We thank K. Dial for discussions about scaling; J. Graham for statistical advice; C. Eldermire, N. Schwab, and C. Putnam for help with data collection; and D. Emlen, B. Walker, and M. Parker for helpful comments on the manuscript. Supported by donations from Marchie's Nursery, Caras Nursery, Swift Instruments, and the Birdwatcher's Country Store.

Supporting Online Material

www.sciencemag.org/cgi/content/full/308/5730/1934/DC1
Materials and Methods

17 December 2004; accepted 4 May 2005
10.1126/science.1108841

Nondenaturing Gel Electrophoresis Kit

The Native Next Gel Kit is an easy-to-use, nondenaturing gel electrophoresis kit that allows for superior resolution of proteins in their native conformation by an agarose-based gel format. The gel can be run with both basic and acidic proteins and is compatible will all supporting technology, such as protein immunoblotting, N-terminal sequencing, mass spectrometry, and matrix-assisted laser desorption ionization. The kit makes use of a heat-and-pour agarose that prevents exposure to the hazards associated with liquid acrylamide and allows for easier recovery of the protein following separation.

Amresco For information 800-448-4442 www.amresco-inc.com

Gene Knockout System

The TargeTron Gene Knockout System provides a robust and simple method for site-specific disruption of DNA sequences within a host cell genome. It performs permanent gene disruption in a nonrandom or targeted manner that does not require host recombination factors to mobilize. The technology makes use of the retrohoming ability of group II introns in order to "target" the exact position of gene disruption. An extensively validated TargeTron algorithm designs specific primer sets for use in polymerase chain reaction (PCR) mutation of the Targetron intron. The mutated intron is essentially "reprogrammed" to insert itself into the algorithm-predicted site of any user-defined gene. Ligation of the PCR product into a TargeTron vector is followed by transformation of the host cell. Expression results in a ribonucleoprotein complex that targets the intron to the precise insertion site within the host genome resulting in gene knockout.

Sigma-Aldrich For information 800-521-8956 www.sigma-aldrich.com

High-Speed cDNA Preparation

With the FastLane Cell cDNA Kit, it only takes 45 minutes to prepare first-strand complementary DNA (cDNA) directly from cultured cells. No RNA purification steps are necessary. The high-speed procedure makes it easy to perform real-time, two-step reverse-transcription polymerase chain reaction analysis of several samples within a few hours. The FastLane Cell cDNA Kit integrates rapid cell lysis, immediate RNA stabilization, elimination of genomic DNA, and efficient and sensitive reverse transcription. The simple workflow makes the kit suitable for applications such as validation of small-interfering RNA-mediated gene knockdown or snapshot analysis of gene expression in cells under different conditions.

Qiagen For information 800-426-8157 www.qiagen.com

Automated Detection of Nucleic Acids

The Vidiera NsD Nucleic Sample Detection Platform is for the fully automated, post-amplification detection of nucleic acids. The new platform for molecular pathology labs separates DNA molecules by capillary electrophoresis, with software features that deliver a high degree of productivity and flexibility. Vidiera NsD has the capacity to run two 96-well plates, and the second plate can be added while the first plate is running. The instrument significantly reduces the technician time required to separate nucleic acids for further analysis, running batches of eight samples in as little as 30 min. The Vidiera NsD is offered with accessories to assist high-complexity laboratories in developing assays in the fields of hematology, oncology, cardiovascular health, and inherited disorders.

Beckman Coulter For information 800-742-2345 www.beckmancoulter.com

Particle Size Analyzer

The SALD-3101 Laser Diffraction Particle Size Analyzer is designed for measurement of coarse or dense particles and offers a variety of sampling options for both wet and dry samples. It is suitable for use in a variety of applications, including pharmaceuticals, environmental, metals, minerals, and civil engineering. It seamlessly covers a wide measuring range from 0.05 to 3000 μm using a single measuring principle, a single optical system, and a single light source. The sampler incorporates a powerful vertical radial pump with a flow rate of 5000 cm^3/min to reliably circulate a range of particle sizes from microns to several millimeters. It can be equipped with an optional unit for fast switching between wet and dry samples. Users can choose from three types of injection nozzles with different dispersion power and three types of sample sucking methods.

Shimadzu For information 800-477-1227 www.ssi.shimadzu.com

Flash Unit

The Rapp OptoElectronic JML-C2 Flash Unit is a pulsed xenon light source that produces an intense flash of ultraviolet (UV) light for the photolysis of caged compounds in the specimen plane of a microscope. The unit offers a high-efficiency flash bulb with up to 200 J/pulse, UV anti-reflection coated quartz optics, and a 0.2–8 Hz repetition rate. The unit includes a 1.5-m quartz light guide, a built-in UV filter, and slots for optical filters, as well as an LED illumination tool for specimen alignment and a calibrated photodiode for lamp adjustment.

ASI/Applied Scientific Instrumentation For information 800-706-2284 www.ASImaging.com

Binding Measurement

The TransAM Flexi NFkB Kits make it simple to perform sequence-specific transcription factor analysis. They provide the flexibility to immobilize any oligonucleotide or polymerase chain reaction product in the provided 96-stripwell plate, which enables comparison of multiple transcription factor binding sites within a single kit. Flexi Kits can also provide validated antibodies, control oligonucleotides and cell extract, and reaction buffers.

Active Motif For information 877-222-9543 www.activemotif.com

Newly offered instrumentation, apparatus, and laboratory materials of interest to researchers in all disciplines in academic, industrial, and government organizations are featured in this space. Emphasis is given to purpose, chief characteristics, and availability of products and materials. Endorsement by *Science* or AAAS of any products or materials mentioned is not implied. Additional information may be obtained from the manufacturer or supplier by visiting www.science.labvelocity.com on the Web, where you can request that the information be sent to you by e-mail, fax, mail, or telephone.

ScienceCareers.org

Classified Advertising

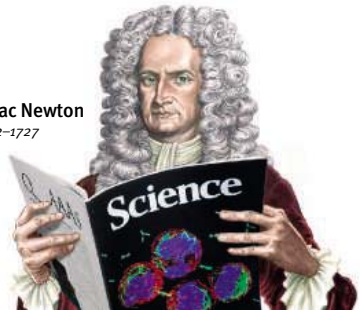

Isaac Newton
1642–1727

For full advertising details, go to **www.sciencecareers.org** and click on **How to Advertise,** or call one of our representatives.

United States & Canada

E-mail: advertise@sciencecareers.org
Fax: 202-289-6742

JILL DOWNING
(CT, DE, DC, FL, GA, MD, ME, MA, NH, NJ, NY, NC, PA, RI, SC, VT, VA)
Phone: 631-580-2445

KRISTINE VON ZEDLITZ
(AK, AZ, CA, CO, HI, ID, IA, KS, MT, NE, NV, NM, ND, OR, SD, TX, UT, WA, WY)
Phone: 415-956-2531

KATHLEEN CLARK
Employment: AR, IL, LA, MN, MO, OK, WI, Canada; Graduate Programs; Meetings & Announcements (U.S., Canada, Caribbean, Central and South America)
Phone: 510-271-8349

EMNET TESFAYE
(Display Ads: AL, IN, KY, MI, MS, OH, TN, WV; Line Ads)
Phone: 202-326-6740

BETH DWYER
(Internet Sales Manager)
Phone: 202-326-6534

Europe & International

E-mail: ads@science-int.co.uk
Fax: +44 (0) 1223-326-532

TRACY HOLMES
Phone: +44 (0) 1223-326-525

HELEN MORONEY
Phone: +44 (0) 1223-326-528

CHRISTINA HARRISON
Phone: +44 (0) 1223-326-510

JASON HANNAFORD
Phone: +81 (0) 52-789-1860

To subscribe to *Science*:
In U.S./Canada call 202-326-6417 or 1-800-731-4939
In the rest of the world call +44 (0) 1223-326-515

Science makes every effort to screen its ads for offensive and/or discriminatory language in accordance with U.S. and non-U.S. law. Since we are an international journal, you may see ads from non-U.S. countries that request applications from specific demographic groups. Since U.S. law does not apply to other countries we try to accommodate recruiting practices of other countries. However, we encourage our readers to alert us to any ads that they feel are discriminatory or offensive.

ScienceCareers.org
We know science AAAS

POSITIONS OPEN

RESEARCH ASSISTANT PROFESSOR

The Division of Rheumatology, Allergy, and Immunology of Virginia Commonwealth University seeks an Assistant Professor on the research/teaching track with experience in cell and molecular biology to join our faculty. Knowledge of mast cells is desirable. Working with the principal investigator, responsibilities will include research equipment maintenance, teaching, writing, and presentations. Candidates must be a Ph.D. or M.D./Ph.D. Interested candidates should send their curriculum vitae, letter of interest, and names of three references by July 24, 2005, to: **Dr. Lawrence Schwartz, Virginia Commonwealth University, Box 980263, Richmond, VA 23298-0263. E-mail: lbschwar@vcu.edu.**
VCU is an Equal Opportunity/Affirmative Action Employer. Women, minorities, and persons with disabilities are encouraged to apply.

ASSOCIATE DEAN FOR RESEARCH AND GRADUATE STUDIES
College of Veterinary Medicine
Auburn University

The College of Veterinary Medicine at Auburn University invites applications and nominations for the position of Associate Dean for Research and Graduate Studies. The Associate Dean reports directly to the Dean of the College, is a member of the administrative team of the College, and is responsible for managing the administrative aspects of the research and graduate studies programs in the College. The position is tenure track. The successful candidate will be an established scientist in veterinary medical and/or biomedical research with a strong record of scholarly achievement, peer recognition, and sustained extramural funding as a principal investigator. Excellent interpersonal communication skills, substantial experience in graduate education, demonstrated leadership and organizational abilities, and firsthand experience with a variety of funding sources which support veterinary or biomedical research are required. A terminal degree in biomedical sciences (Ph.D.) or veterinary medicine (D.V.M. or equivalent) is required. A Ph.D. degree is highly desirable. An additional veterinary medical or equivalent degree and previous administrative experience is preferred. The position is available September 1, 2005; review of applications will begin September 1, 2005, and continue until the position is filled. Please visit **website: http://www.vetmed.auburn.edu/index.pl/employment** for further information.

IMAGING/MICROSCOPY

A **RESEARCH ASSOCIATE** or **RESEARCH SCIENTIST** position is available for someone with experience in fluorescence microscopy and imaging to participate in or lead a collaborative research program aimed at developing novel methods for fluorescent imaging of molecular dynamics and associations in cells migrating cells in vitro and in vivo. A Ph.D. in a related discipline and familiarity with fluorescence microscopy and imaging is required. Rank and title will be commensurate with experience and scholarly achievements.

This position will be open until filled. Application material including current curriculum vitae, names and addresses of three references should be sent to:

Rick Horwitz
Department of Cell Biology
Box 800732
University of Virginia Health System
Charlottesville, VA 22908-0732
E-mail: horwitz@virginia.edu

The University of Virginia is an Equal Opportunity/Affirmative Action Employer.

POSITIONS OPEN

UNIVERSITY OF HYDERABAD
Central University Campus
Hyderabad-500 046, India

The University of Hyderabad (UOH) invites applications for **FACULTY POSITIONS** in various schools, departments, and centers.

Professors: 17, readers: 26, lecturers: 34.

For details visit **website: http://202.131.159.42/uoh/.**

Last date for receipt of applications online is July 10, 2005, for overseas candidates.

Registrar–UOH.

DIRECTOR
Laser Interferometer Gravitational Wave Observatory

The California Institute of Technology (Caltech) and Massachusetts Institute of Technology (MIT) have initiated a search for a new Director of the Laser Interferometer Gravitational Wave Observatory (LIGO). LIGO is a major scientific endeavor, funded by the National Science Foundation, and devoted to furthering our understanding of the universe through the observation of gravitational waves. The position will be for a term of five years, with the possibility of extension, beginning in 2006. The LIGO Oversight Committee welcomes applications and nominations for this position. It is recommended that applications be accompanied by curriculum vitae and other information bearing on the candidates' qualifications for the Directorship. Relevant qualifications include scientific stature, leadership capability, and management skills. Communication should be sent as soon as possible, preferably before August 15, 2005, and should be addressed to:

Emlyn Hughes
Chair, LIGO Oversight Committee
Kellogg Radiation Laboratory, MS 304-38
California Institute of Technology
Pasadena, CA 91125
E-mail: emlyn@caltech.edu

The California Institute of Technology and Massachusetts Institute of Technology are Affirmative Action/Equal Opportunity Employers, and encourage applications from women, minorities, veterans, and disabled persons.

UNIVERSITY OF MINNESOTA

The Department of Medicine and the Institute of Human Genetics (IHG) invite applications for the position of leadership of a joint Medical Genetics program. Ideally the successful candidate will qualify for an appointment as **ASSOCIATE** or **FULL PROFESSOR** with tenure. The Medical Genetics program is responsible for research in developing extramurally funded NIH programs in regards to genetics of complex diseases such as cancer, cardiovascular, autoimmune, or chronic pulmonary diseases. Research space for this position will be located in IHG space in the new Molecular and Cell Biology Building amongst faculty actively engaged in genetic research and resources are available to recruit additional faculty in related areas of medical genetics.

Successful candidates will hold an M.D., or M.D./Ph.D. and show evidence of: sustained extramural funding in an area of research regarding medical genetics or genetics of complex diseases; high potential for leadership of an academic program; high degree of collaboration with other scientists in related areas; and successful mentorship of graduate students, postdoctoral fellows, or junior faculty.

Interested candidates should submit their curriculum vitae and the names and addresses of three references to: **Harry T. Orr, Ph.D., 206 MMC, 515 Delaware Street, Minneapolis, MN 55455.** Applications will be reviewed immediately and accepted until position is filled.

The University of Minnesota is an Equal Opportunity Educator and Employer.

Positions @ NIH
THE NATIONAL INSTITUTES OF HEALTH

POSTDOCTORAL FELLOWSHIP IN FUNCTIONAL NEUROIMAGING UNIT ON INTEGRATIVE NEUROIMAGING

The National Institute of Mental Health (NIMH), a major research component of the National Institutes of Health (NIH) and the Department of Health and Human Services (DHHS), offers a two to five year post-doctoral fellowship at one of the premier research sites in the U.S., the 300 acre Bethesda campus of the NIH, near Washington D.C. which houses state-of-the-art neuroimaging facilities (MRI, PET and MEG) dedicated to research. The strong scientific environment and outstanding equipment resources at NIH make this a unique opportunity for an outstanding scientist. The position is open to 1) recent Ph.D.'s in psychology, cognitive neuroscience, neuroscience, neuropha**rmacology, computer science, or other applicable discipline or 2) M.D.'s with training in psychiatry, neurology, nuclear medicine, radiology or other relevant field.** The successful candidate will join a multidisciplinary team using neuroimaging to study genetic and neurochemical mechanisms of normal cognitive function as well as dysfunction in neuropsychiatric illnesses such as schizophrenia, those with genetic sources of cognitive dysfunction (e.g., Williams syndrome), and other conditions such as normal aging. Possible research areas include 1) neurofunctional substrate of higher cognitive function, particularly working memory and frontal lobe, 2) neurofunctional bases of neuropsychiatric illnesses, especially schizophrenia, 3) computational neuroscience (statistical and systems approaches), and 4) neurochemical underpinnings of higher cognitive function and dysfunction. Familiarity with computational and statistical methods for neuroimaging (e.g., Unix, C/C++, MatLab, SPM, AFNI) confers an advantage but is not absolutely required. Letter of interest, CV, and three reference letters should be sent to: **Karen Berman, M.D., NIH, Building 10, Room 4C101, 9000 Rockville Pike, Bethesda, MD 20892-1365 USA. (301)496-7603, or by e-mail to: karen.berman@nih.gov**.

The NIH Director's Wednesday Afternoon Lecture Series

Biomedical scientists around the world are invited to join us online to hear leading investigators present their latest results to the NIH Intramural Research community. Lectures may be viewed live at 3:00 p.m., EST (20:00 GMT) on Wednesdays, from September through June. Live webcasts can be viewed under "Today's Events" at: <http://videocast.nih.gov/>

The current schedule of lectures is available at: <http://www1.od.nih.gov/wals/schedule.htm>

Upcoming Lectures:

- June 22: Francis Chisari, Scripps University: To Kill or to Cure: Options in Host Defense against Viral Infections
- June 29: Stephen O'Rahilly, Cambridge University: Human Obesity and Insulin Resistance: Lessons from Experiments of Nature
- September 7: Adrian Krainer, Cold Spring Harbor Laboratories
- September 14: Solomon Snyder, Johns Hopkins University

The lecture series has archived more than 240 lectures since 1998. Archived lectures can be viewed under ""Wednesday Afternoon Lectures" at: <http://videocast.nih.gov/PastEvents.asp>

National Institute of Biomedical Imaging and Bioengineering

Scientific Director

The National Institute of Biomedical Imaging and Bioengineering (NIBIB) seeks a new Scientific Director to lead its intramural research program (DIR). The successful candidate will oversee a program which consists of the PET Radiology Research Group and the Imaging Physics Laboratory, with vacancies for two principal investigators and eight research fellows/staff scientists on board. The Scientific Director will help chart the future of a nascent intramural program of NIBIB. He/she will join an esteemed group of scientific directors from other Institutes and Centers of the National Institutes of Health and build partnership and collaborations in the NIH intramural community at large. The Scientific Director allocates an approximately $6 million (FY2005) budget to intramural laboratories in coordination with the Director, NIBIB. He/she will establish the Board of Scientific Counselors for the purpose of conducting quadrennial reviews of the intramural program. The Scientific Director will recruit new faculty/principal investigators to conduct research and training programs.

The successful candidate must have a Ph.D. and/or M.D. and an established record of outstanding research accomplishments, scientific leadership and service within the imaging or bioengineering research community. The Scientific Director also will supervise his/her own research laboratory, supported by the NIBIB intramural budget. For additional information please contact **Sheila Barrett, Administrative Officer, NIBIB, NIH, 31 Center Drive, Room 1C14, Bethesda, MD 20892, Phone: 301-451-0713 or Fax: 301-480-0679.**

Description of Duties and Responsibilities:

The incumbent leads and manages the NIBIB intramural research program (DIR) and in monitoring, coordinating, and evaluating all aspects of the program's progress in achieving its goals and objectives. The mission of the NIBIB is to improve human health by leading the development and accelerating the application of biomedical technologies. The Institute is committed to integrating the engineering and physical sciences with the life sciences to advance basic research and medical care. The DIR plays a key role in advancing the Institute's mission, particularly to advance knowledge in imaging and bioengineering research using a combination of basic, translational, and clinical science and to develop effective training programs in these fields.

WWW.NIH.GOV

NIDDK

NATIONAL INSTITUTE OF DIABETES AND DIGESTIVE AND KIDNEY DISEASES

Tenure-track Investigator
Mechanisms Of Obesity

With nation-wide responsibility for improving the health and well being of all Americans, the Department of Health and Human Services overseas the biomedical research programs of the National Institutes of Health (NIH) and those of NIH's Research institutes.

The Intramural Research Program of the National Institute of Diabetes and Digestive and Kidney Diseases (NIDDK), NIH/DHHS in Bethesda, MD seeks to recruit a tenure track scientist who will use cellular, molecular and/or genetic approaches to study the molecular mechanisms relevant to obesity. The investigator will be given resources and laboratory space to pursue a vigorous and effective research program. The position offers unparalleled opportunities for multi-disciplinary research and for interaction with a diverse group of outstanding scientists in the NIDDK and throughout the NIH. For information about the NIDDK, see **http://www.niddk.nih.gov.**

Candidates must have a Ph.D., M.D. or equivalent degree in the biomedical sciences, demonstrated research productivity, and capability of establishing an innovative and independent research program. Competitive salary and benefit packages are available. Applicants should send a curriculum vitae and list of publications, copies of three major publications, a plan for future research, and three letters of reference by **September 15, 2005 to Derek LeRoith, Chair of the Search Committee, c/o Renee Rabben, Diabetes Branch, NIH, Building 10, Room 8D12, 10 Center Drive, MSC 1758, Bethesda, MD, 20892-1758, Tel 301-496-6289, fax 301-402-4136, email rabben@mail.nih.gov**

NIDDK

NATIONAL INSTITUTE OF DIABETES AND DIGESTIVE AND KIDNEY DISEASES

Postdoctoral Fellowships
In Signaling Pathways And Disease

Postdoctoral Fellowships are available in the Metabolic Diseases Branch, NIDDK, NIH. The Branch is similar to a small academic department and has excellent laboratory facilities. The intramural program of the NIH offers an outstanding research environment and has been rated by *The Scientist* as one of the top places for Postdocs to work. The Branch is located on the main intramural campus of the NIH in Bethesda, Maryland, a 20-minute ride from Washington, D.C. Applications are invited from individuals of the highest caliber who have obtained a Ph.D., or M.D. degree within the last 5 years. Positions are available in the following areas:

Regulation of *GNAS* imprinting and role of the stimulatory G protein $G_s\alpha$ in metabolic regulation

Postdoctoral positions are available to study the mechanisms of *GNAS* and $G_s\alpha$ imprinting in mouse models and in patients with *GNAS* imprinting defects. We are also studying the role of $G_s\alpha$ and other *GNAS* gene products in metabolic regulation using several germline and tissue-specific *GNAS* knockout mouse models **(Lee S. Weinstein, MD, leew@amb.niddk.nih.gov)**

Function of tumor suppressor *HRPT2*

A postdoctoral position is available to study the novel tumor suppressor gene, *HRPT2*, recently implicated in parathyroid cancer and the familial cancer syndrome HPT-JT (hyperparathyroidism-jaw tumor syndrome). We are studying parafibromin, the protein encoded by *HRPT2*, in both mammalian and invertebrate models systems with the aim of elucidating the biological pathway(s) critical for its tumor suppressor function. A strong background in molecular biology and/or signal transduction is required. **(William F. Simonds, MD, wfs@helix.nih.gov)**

Applicants must have an advanced degree (M.D., Ph.D., or equivalent). Salary and benefits will be commensurate with the experience of the applicant. **Interested candidates should send a letter stating their interests, their curriculum vitae, list of publications, and the names of three references to the appropriate individual by e-mail or to Building 10, Room 8C-101; 10 Center Dr MSC 1752; National Institutes of Health; Bethesda, MD 20892-1752.**

The
NATIONAL RESEARCH COUNCIL
OF THE NATIONAL ACADEMIES
announces

Postdoctoral Research Awards
at the
Department of Homeland Security

Awards will be offered for research in biological forensics; foreign animal and zoonotic diseases; detection analysis; biosensor development; food protection and safety; epidemic modeling; nanotechnology; decontamination; chemical and biological threat agents; radiation detection; DNA diagnostics; and atmospheric dispersion. Awards are for one year, possibly renewable, at the following locations:

DHS Centers of Excellence:
- **University of Southern California**
- **University of Minnesota**
  - **North Dakota State University-Partner**
  - **Georgia Institute of Technology-Partner**
  - **Michigan State University-Partner**
  - **University of Tennessee-Partner**
  - **University of Wisconsin at Madison-Partner**
- **Texas A & M University**
  - **University of Texas Medical Branch-Partner**
  - **University of California at Davis-Partner**

National Laboratories Homeland Security Activities:
- **Bechtel Nevada**
- **Lawrence Livermore National Laboratory**
- **Oak Ridge National Laboratory**
- **Pacific Northwest National Laboratory**

Other Federal Partners:
- **National Institute of Standards and Technology**

Eligibility:	**Ph.D. recipients within five years of the doctorate at the time of application; US citizenship required**
Stipend:	**$55,000 per annum**
Benefits:	**relocation, health insurance coverage, limited professional travel**
Duration:	**one year with possible renewal**
Deadlines:	**Aug 1, Nov 1, Feb 1, May 1**

Instructions on how to apply are available on the NRC Web site at **www.national-academies.org/rap**
Questions should be directed to the NRC at 202-334-2760 (tel) or rap@nas.edu

Contact at DHS:
Laura Petonito
Tel: 202-254-5840
E-mail: laura.petonito@dhs.gov

THE NATIONAL ACADEMIES
Advisers to the Nation on Science, Engineering, and Medicine

Faculty Position in Microbial Genomics
University of Illinois at Urbana-Champaign

Applications are invited for a position in microbial genomics in the Departments of Food Science and Human Nutrition and Animal Sciences as part of the campus interdisciplinary initiative in genomic biology, and more specifically, the molecular bioengineering of biomass conversion theme associated with the Institute for Genomic Biology (IGB). The position is at the Associate or Full Professor level. It is expected that the successful candidate will continue the development of an internationally recognized research program, direct graduate students and postdoctoral fellows, advise and interact with undergraduate students, contribute to the teaching needs of the departments in appropriate areas, compete effectively for private and public research funds, and participate in the public service mission of the departments. Applicants should have a Ph.D. and evidence of established externally funded research programs. Of particular interest are applications from individuals with research experience in industrial microbial genomics. The University of Illinois at Urbana-Champaign is a world-class institution with quality academic units including a center of excellence in biotechnology and a national supercomputing center. Successful candidates will be provided with excellent laboratory facilities, and substantial start-up funds. The position will be available January 16, 2006.

Applicants should submit a curriculum vitae with a complete list of publications, a concise summary of research accomplishments and future plans, and provide contact information for three references. Applications in the form of a single PDF file should be submitted to: **http://www.traill.uiuc.edu/jobsearch/microbial/**. To ensure full consideration, applications must be received by **August 15, 2005**. Questions can be directed to **Dr. Hans P. Blaschek**, Chair of the Search Committee, at **217-333-8224** or **blaschek@uiuc.edu**. Additional information about the Departments and University can be found at **http://www.fshn.uiuc.edu** and **http://www.ansci.uiuc.edu**.

The University of Illinois is an Affirmative Action, Equal Opportunity Employer.

RBLX
RECEPTOR BIOLOGIX, INC.

Signal Transduction Scientist
PhD level Scientist with at least three years postdoctoral experience in the area of receptor tyrosine kinase signal transduction.

GLP Assay Development Scientist
PhD level Scientist with 2-5 years of laboratory assay experience in biotech, pharmaceutical or diagnostic industry; experienced in GLP/GMP compliance and product release. Req. optimization of cell-based bioassays and ELISA, proficient in tissue culture and bioassay techniques,

Process Scientist
Ph.D. Level Scientist with 5 yrs. protein purification development experience in biotech. Req. GLP/GMP experience, hands-on, proficient in purification techniques bench to production scale.

Senior Research Associate
BS/MS level Scientist, cell biology/biology 2-5 yrs. experience in assay design and performance. GLP/GMP experience desirable, hands-on with current technology experience required.

Receptor BioLogix Inc., based in South San Francisco, is a biopharmaceutical company focused on developing a newly discovered class of protein therapeutics to treat cancer and autoimmune diseases. Receptor BioLogix's lead clinical product is Dimercept™, a broad-spectrum anticancer agent that represents a new class of receptor modulators called Intron Fusion Proteins™.

The successful candidates will join a strong group of molecular and cellular biologists.

Please send C.V. to:
db@receptorbiologix.com

Receptor BioLogix is an Equal Opportunity Employer.

Job opportunity in statistical modelling in marine biology

The Modelling Division of the **Marine Research Institute in Reykjavík, Iceland**, has a vacancy in the field of statistical modelling of marine populations with an emphasis on marine mammals and capelin in Icelandic waters. The position is within a two-year research project funded by the European Union.

PhD degree required, with emphasis on quantitative analysis and modelling in biological sciences. Programming ability (preferably C++), knowledge of Linux and expertise with a statistical package is required as is the ability to formalise models and document results.

Applications will be reviewed beginning August 1, 2005. Salary starts at 250000 Ikr/month ($47000/yr).

Send letter of application, resume, and names, addresses, and phone numbers of three referees or inquiries by electronic mail to: Gunnar Stefansson, Marine Research Institute (gunnar@hafro.is).

Links:

- **Marine Research Institute -** http://www.hafro.is
- **Recent projects by the MRI Modelling Division -** http://www.hafro.is/dst2

ETH

Eidgenössische Technische Hochschule Zürich
Swiss Federal Institute of Technology Zurich

Scientist with Postdoc experience in insect behaviour

The **ETH Applied Entomology Group** investigates insect-plant relationships from the molecular to the agroecosystem level, in particular as a basis for more sustainable pest and crop management (www.em.ipw.agrl.ethz.ch). A position with a several years perspective is open for a creative and cooperative scientist with strong Postdoc experience in insect behaviour and ecology.

Responsibilities include (1) research together with graduate and undergraduate students using state-of-the-art techniques, and (2) participation in teaching and administration. Languages spoken in the group are mainly English and German.

Send curriculum vitae, a list of methods, and addresses with phone numbers of three references to Prof. Dr. Silvia Dorn, Applied Entomology, ETH, CH - 8092 Zürich, Switzerland.

Email: silvia.dorn@ipw.agrl.ethz.ch

JOHNS HOPKINS
UNIVERSITY

Dean of the Zanvyl Krieger School of Arts & Sciences

The Johns Hopkins University invites inquiries, nominations, and applications for the position of James B. Knapp Dean of the Zanvyl Krieger School of Arts and Sciences (KSAS). The Dean is the chief executive and intellectual leader of the School, shaping its vision, generating resources in support of the mission, and managing operations. The Krieger School of Arts and Sciences has a full-time faculty of approximately 300, 2,900 undergraduate students, 1,000 graduate students, and a growing part-time graduate student population at several locations in the greater Baltimore-Washington area. The School covers a wide range of fields and specialties in its 23 departments in the humanities, social sciences, and natural sciences, as well as a number of interdepartmental programs and centers. Sharing the same campus and many of the same facilities, the Krieger School of Arts and Sciences and the Whiting School of Engineering have a close collaborative relationship, and the Dean of KSAS also works collaboratively with each of the other academic divisions of the University. A member of the AAU, Johns Hopkins ranks first among U.S. universities in receipt of federal research and development funds.

The Dean has responsibility for and authority over the School's programs and budget within the context of a highly decentralized organizational structure. The University seeks an individual of distinguished accomplishment to work with the faculty in leading a School with a tradition of excellence in research, teaching, and service. Candidates should have demonstrated skills in academic leadership, administration, and fund raising. Additional information about the position and the University is available at www.jhu.edu or their home page http://www.jhu.edu/ksas/; candidates are strongly encouraged to review this information before preparing their materials.

Inquiries, nominations and applications are invited. Candidates should provide a cover letter describing their interest in and qualification for the position, along with a curriculum vitae and the names and contact information for five references; references will not be contacted until candidates have been notified. All inquiries and materials will be treated as confidential. We are being assisted in this search by Dr. Jean Dowdall and Elizabeth Bohan; inquiries and application materials may be sent to them at JohnsHopkinsKSAS@wittkieffer.com. Materials that cannot be sent by email may be mailed to Witt/Kieffer, 2015 Spring Road, Suite 510, Oak Brook, IL 60523. Our consultants can be reached by phone at (630) 575-6131.

The Search Committee will begin reviewing nominations and applications on July 31, 2005. The University expects to fill this position by December 1, 2005.

The Johns Hopkins University is an Equal Opportunity, Affirmative Action Employer

WITT / KIEFFER

THE INTERNATIONAL ATOMIC ENERGY AGENCY SEEKS A UNIT HEAD (Mass Spectrometry)

The IAEA, an independent United Nations organization headquartered in Vienna, Austria, with 138 Member States and a staff of 2200, serving as the global focal point for international co-operation in the safe and peaceful use of nuclear energy, is seeking a Unit Head for its Mass Spectrometry Unit in the Safeguards Analytical Laboratory (Seibersdorf, about 45 km from Vienna). **This individual will be responsible for supervising and providing essential technical support to the nuclear and environmental TIMS (Thermal Ionization Mass Spectrometry) laboratories through daily contacts with the mass spectrometry staff.**

If you have at least:

- ***An advanced university degree in experimental physics, electronics or analytical chemistry, with specialization in nuclear sciences;***
- ***10 years working experience in inorganic isotopic analysis by mass spectrometry including 2 years in electronic faultfinding and maintenance of TIMS and SIMS instrumentation***
- ***Experience in the measurement of uranium and plutonium by TIMS (desirable)***
- ***Supervisory skills,***

you may wish to apply for this position. To do so*, please submit an on-line application** at *http://www.iaea.org/About/Jobs* ***before 11 July 2005, quoting the vacancy notice no. **2005/039**.

Benefits: The IAEA offers a stimulating multicultural working environment in the beautiful and culturally rich city of Vienna, Austria, with easy access to Europe-wide attractions. The post offers: **tax free remuneration; rental subsidy; 6 weeks annual vacation;** medical insurance coverage; a staff retirement plan; full coverage of removal expenses for staff member, family, and personal effects; additional allowance for installation expenses; assistance with finding housing and schools in Vienna; financial assistance with the education of dependent children; and paid travel to the home country for the staff member and family every other year.

INTERNATIONAL ATOMIC ENERGY AGENCY

Our Goal: to facilitate the safe contribution of nuclear technologies to peace, health and prosperity throughout the world, while ensuring that no technology or material under our oversight or provided with our assistance is used to further any military purposes.

DIRECTOR OF RESEARCH PROGRAMS
Shriners Hospitals for Children

Shriners Hospitals for Children, a system of 18 pediatric orthopaedic and four pediatric burn centers located throughout North America, seeks an experienced scientist for a full time position as Director of Research Programs at the Shriners International Headquarters in Tampa, Florida.

In this key role, you will provide oversight for basic science, clinical and outcome research. The successful candidate should have a Ph.D. and/or an M.D. degree, with at least 2 years of post-doctoral research training in an internationally recognized laboratory. Additional degrees and/or completed coursework in Business Administration, Management, Fiscal Control, or Leadership also required.

Candidate should have at least 15 years successful experience in Research or R&D administration/management in academia or pharmaceutical/biotech industry, with a minimum of 10 years of experience in both intellectual property/copyright areas and university-industry contracts. Extensive skills in fiscal management, budget control, editing and preparing research materials, and an in-depth knowledge of organizational principles, medical and scientific terminology, and resource management essential. The professional we seek will be an accomplished investigator with a history of independent funding and research, an extensive list of publications in peer-reviewed professional journals, with demonstrated leadership and organizational abilities. Advanced computer proficiency and the experience with regulatory agencies are also necessary. Superior administrative and interpersonal skills are vital.

For a complete position description and other information, please contact

Peter F. Armstrong, MD, FRCSC, FACS, FAAP
Director of Medical Affairs
Shriners Hospitals for Children
2900 Rocky Point Drive
Tampa, FL 33607
Phone: 813-281-8160
Fax: 813-281-8113
email: parmstrong@shrinenet.org

www.shrinershq.org
eoe • m/f/v/d • dfw

Shriners Hospitals for Children

CAMS
Center for Advanced Modeling and Simulation

The Idaho National Laboratory (INL) is one of the U.S. Department of Energy's premier research and development laboratories.

We are seeking an individual with a proven record in computer modeling and simulation to lead the activity to establish the INL Center for Advanced Modeling and Simulation (CAMS). Through CAMS the INL will develop next generation modeling and simulation tools to support and grow the lab's programs in nuclear and other advanced energy systems, national security, and science and technology. The individual selected to lead CAMS will implement and refine the development plan for CAMS; build partnerships with other laboratories, universities, and industrial partners; and work with the INL technical staff to position the laboratory to exploit advances in high performance computing. This position requires a demonstrated record of accomplishment and publication, and a Ph.D. in engineering, computer science, or physical science.

Please apply online at www.inl.gov, and reference posting number 1890.
Equal Opportunity Employer M/F/D/V.

INL Idaho National Laboratory

Executive Director

Centenary Institute of Cancer Medicine and Cell Biology

The Centenary, an independent medical research organisation, is one of Australia's premier immunology and molecular medicine institutions with an excellent record of attracting funding. The Centenary accommodates up to 150 research and support staff, currently nine research groups, five in Immunology and one each in Gene Therapy, Liver Biology, Molecular Cardiology and Cancer Drug Resistance. Centenary is equipped with state of the art support facilities including a SPF level 2 animal house, a PC3 laboratory for work on human pathogens, flow cytometry, and a microinjection service.

The challenge for the Executive Director is to provide strong leadership, strategic direction, motivation to the organization and develop the Centenary's research profile globally. Your input will include mentoring staff; interacting with government, funding bodies, and the general community; and attracting peer reviewed research funds to continue your internationally recognised research.

The successful applicant will bring to this role excellent leadership, communication, negotiation, planning, and interpersonal skills; an internationally exceptional track record of basic and/or clinical research relevant to the Centenary's vision.

The Executive Director will be appointed to the position of Professor in the Faculty of Medicine at the University of Sydney and offered an appropriate appointment at the Royal Prince Alfred Hospital.

Terms, conditions and salary will be competitive and commensurate with the qualities sought in a successful applicant.

More information is available on our website
http://www.centenary.org.au/p/employ/director
or contact Dr Nick Pearce **Tel:** 612 9565 6190,
email: n.pearce@cenint.org
Closing Date is August 31 2005

Applications are invited for a

Full Professorship in Physical Chemistry

starting **1 September 2006** at the
Department of Chemistry and Biochemistry (DCB),
University of Bern, Switzerland.

Candidates should have a strong track record of internationally recognized research in experimental Physical Chemistry in the condensed phase, with relevance to materials chemistry and/ or the life sciences. Specific areas of interest include (but are not limited to) scanning probe methods, (nano)electrochemistry, fundamental processes at electrodes, electrocatalysis, molecular electronic devices, nano- and chemomechanical systems, transport processes through membranes.

The research areas of the Department of Chemistry and Biochemistry (**www.dcb.unibe.ch**) are "Physical and Materials Chemistry" and "Molecular Foundations of Biological Processes". The successful candidate is expected to contribute to the teaching of physical chemistry at the BSc, MSc and PhD levels.

The University of Bern is an equal opportunity employer and strives to increase the number of women in the faculty. Qualified female researchers are especially encouraged to apply.

Applications, including curriculum vitae, publication list, copies of the 5 most important publications, an outline of research plans and teaching experience should be sent to the address below by **15 September 2005**.

Prof. P. Messerli, Dekan der Phil.-nat. Fakultät, Universität Bern, Sidlerstr. 5, CH-3012 Bern, Switzerland.

For further information contact Prof. S. Leutwyler
(tel: +41 (0)31 631 4479; email: **leutwyler@iac.unibe.ch**).

Computational Chemistry and Biology Opportunities at D. E. Shaw Research and Development

Extraordinarily gifted computational chemists, biologists, and other computational scientists are sought to join a rapidly growing New York-based research group that is pursuing an ambitious, long-term strategy aimed at fundamentally transforming the process of drug discovery.

Candidates should have world-class credentials in computational chemistry, biology, or physics, or in a relevant area of computer science or applied mathematics, and must have unusually strong research skills. Relevant areas of experience might include protein structure prediction, the computation of protein-ligand binding affinities, the study of biologically important systems using molecular dynamics and/or Monte Carlo simulation, and the application of statistical mechanics to biomolecular systems—but specific knowledge of any of these areas is less critical than exceptional intellectual ability and a demonstrated track record of achievement. Current areas of interest within the group include molecular dynamics simulation of functionally significant globular and membrane proteins, the prediction of protein structures and binding free energies, structure- and ligand-based drug design, characterization of protein-protein, protein-nucleic acid and protein-lipid interactions, and the development of algorithms for biomolecular simulations.

This research effort is being financed by the D. E. Shaw group, an investment and technology development firm with approximately $15 billion in aggregate capital. The project was initiated by the firm's founder, Dr. David E. Shaw, and operates under his direct scientific leadership.

We are eager to add both senior- and junior-level members to our world-class team, and are prepared to offer above-market compensation to candidates of truly exceptional ability. Please send your CV (including list of publications, thesis topic, and advisor, if applicable) to sciencemag-cc@desrad.deshaw.com.

D. E. Shaw Research and Development, L.L.C. does not discriminate in employment matters on the basis of race, color, religion, gender, national origin, age, military service eligibility, veteran status, sexual orientation, marital status, disability, or any other protected class.

D E Shaw & Co

USDA ARS Agricultural Research Service
www.ars.usda.gov

The U.S. Department of Agriculture (USDA)-Agricultural Research Service (ARS), Corn Insects and Crop Genetics Research Unit in Ames, Iowa, is seeking an innovative scientist to conduct basic and applied research on genomics of soybean and related legumes. The incumbent will serve as an independent investigator and as a team member on a diverse interdisciplinary team. The focus of the research will be resistance to soybean rust and emerging diseases. The incumbent will develop methods of approach and is responsible for organizing, conducting, interpreting, and reporting assigned portions of the research results upon completion. Ph.D. preferred. U.S. Citizenship required. Comprehensive benefits package includes paid annual and sick leave, life insurance, health insurance, and a savings and investment plan, in addition to a Federal retirement plan. Salary commensurate with experience ($60,576 – 93,643).

For further information please contact **Dr. Randy Shoemaker** at **515-294-6233** or **rcsshoe@iastate.edu**. Vacancy announcements and application information can be obtained by ARS DIAL-A-VACANCY at 301-504-1482, **Janae Lentz 515-663-7277**, or the ARS website at **www.ars.usda.gov/hrd/jobs/index.htm**. Applications in response to this ad must be postmarked by **August 1, 2005** and reference vacancy announcement number **ARS-X5W-0296**.

The USDA is an Equal Opportunity Provider and Employer.

Ferring Research Institute Inc. (FRI Inc.) is the San Diego-based research division of Ferring Pharmaceuticals (**www.ferring.com**), an established and stable biopharmaceutical company devoted to identifying, developing and marketing innovative drugs in the fields of urology, obstetrics and gynecology, gastroenterology and endocrinology. FRI Inc. is expanding its efforts to discover new treatments in these and related therapeutic areas.

Research Scientist I (code: RSIRL05SC) – In Vivo Pharmacology
Requirements include a PhD in Pharmacology or related, or a DVM or DVM/PhD. Must have experience with rodent surgery, in vivo techniques, and knowledge of integrative biology, animal physiology, pathophysiology and PK/PD relationships. Experience with comparative medicine, data acquisition and analysis a plus. Must be able to move between therapeutic areas, interact with colleagues from related disciplines. Responsibilities include designing, analyzing and documenting major experiments, investigating feasibility using a wide variety of scientific principles, managing research staff, and writing reviews/literature for conferences and future projects.

Research Associate III (code: RAIIISA05SC) – Fertility/OBGYN
Requirements include a BS in animal physiology or related field with preference to 2-3 yrs animal surgery or MS in similar field with 1yr animal surgery and 1yr animal handling experience, AALAS cert., pharm. research/drug discovery, in vivo techniques, and data analysis experience preferred. Experience in animal behavior monitoring, compound formulation, drug administration techniques, biological samples collection, technical knowledge in ex-vivo and cell-based functional assays preferred.

All candidates for the above positions must be detail-oriented, have strong communication and multitasking skills, and have the ability to work independently and as a member of a team. Also must be proficient with MS Excel/Word.

Ferring Research Institute Inc. offers competitive compensation and benefits packages. Apply by sending a cover letter and resume to: **Ferring Research Institute Inc., 3550 General Atomics Court, 2-442 (include job code), San Diego, California, 92121, Fax: 858-455-3190 or email: jobs2005@ferring.com.**

BIOLOGIST
FULL TIME ACADEMIC POSITION
UNIVERSITY OF CALIFORNIA, SAN FRANCISCO

The candidate will establish an active and independently funded research program and teach professional and graduate students. He/she will interact with the basic science as well as the clinical faculty of the School of Medicine in relevant research and teaching endeavors. The candidate must have a demonstrated expertise in connective tissue research at the cellular and molecular level with particular interest in bone or cartilage biology.

The incumbent will provide leadership in molecular cell and/or developmental biology research, be an active member of the Department of Orthopaedic Surgery Research Committee, advise interested and committee faculty and residents in their research activities, provide lectures to faculty and residents and part of the Department of Orthopaedic Surgery basic science core curriculum.

Applicants must have Ph.D. (foreign training/experience acceptable). Applicants should have in computational and experimental methods. The candidate will have demonstrated involvement in quality research through accepted or published writings in peer-reviewed journals. Applicant must have extensive and comprehensive expertise in comparative anatomy, vertebrate embryology, craniofacial development, skeletal biology and evolution. The applicant should have experience of academic orthopaedic performance demonstrate his/her abilities in teaching and research efforts.

Send curriculum vitae and names of references to:
Dr. Theodore Miclau
San Francisco General Hospital
Department of Orthopaedic Surgery
1001 Potrero Avenue, 3A36
San Francisco, 94110-0842

UCSF is an Affirmative Action/Equal Opportunity Employer. The University undertakes affirmative action to assure equal employment opportunity for underutilized minorities and women, for persons with disabilities and for Vietnam-era veterans and special disabled veterans.

Science
AAAS

Life Science Editor for *Science*

Join the dynamic team at *Science* as a full time associate editor for the biological sciences in our Washington, DC, USA or Cambridge, UK office. We are looking for a life scientist with broad interests, a lively curiosity, and experience in cutting-edge research in one or more of the following fields: evolutionary genomics, evo-devo, microbial ecology, biological chemistry, systems biology, bioinformatics, computational or quantitative biology, and neuroscience. Responsibilities include managing the review, selection, and editing of manuscripts, soliciting reviews and special issues, and fostering contacts and communication with the scientific community. Editors are expected to travel to scientific meetings. A Ph.D., postdoctoral experience, and multiple publications are required. Previous editorial experience is not necessary.

For consideration, send a resume and cover letter, along with salary requirements, to:

AAAS
Human Resources Department
Suite #101
1200 New York Avenue
Washington, DC 20005

Applications can also be sent by e-mail to **hrtemp@aaas.org** or Fax to **202-682-1630**. Visit us at: **www.aaas.org**.

Nonsmoking work environment. EOE.

Forschungszentrum Karlsruhe
in der Helmholtz-Gemeinschaft

Das Forschungszentrum Karlsruhe in der Helmholtz-Gemeinschaft Deutscher Forschungszentren ist eine der größten Forschungseinrichtungen in Europa. Es wird von der Bundesrepublik Deutschland und dem Land Baden-Württemberg gemeinsam getragen, um wichtige Forschungsaufgaben im öffentlichen Interesse durchzuführen.

Das Zentrum ist natur- und ingenieurwissenschaftlich ausgerichtet, arbeitet multiprogrammatisch und interdisziplinär und hat sich im internationalen Wettbewerb als eines der bedeutenden nationalen Forschungszentren der Bundesrepublik Deutschland etabliert. Forschungsschwerpunkte des FZK sind die Bereiche Energie und Umwelt, Nano- und Mikrosysteme unter Einbeziehung der Regenerativen Medizin sowie Struktur der Materie.

Das frühere Kernforschungszentrum hat sich strategisch neu ausgerichtet und erfolgreich zu einem großen, multidisziplinären Forschungszentrum entwickelt. Die Aufgaben des Zentrums wurden in den letzten Jahren auf die Lösung komplexer Fragestellungen konzentriert, die langfristig angelegte Forschung und die Mitwirkung exzellenter Mitarbeiter und Mitarbeiterinnen aus unterschiedlichen Fachdisziplinen erfordern. Der Schwerpunkt der Arbeiten liegt bei Natur- und Ingenieurwissenschaften – von der Grundlagenforschung bis hin zur Entwicklung zukunftsfähiger und nachhaltiger Technologien für die industrielle Anwendung unter Einschluss sozialwissenschaftlicher Arbeiten. Wichtiger Bestandteil der strategischen Positionierung des Zentrums ist die Einbindung in die Helmholtz-Gemeinschaft innerhalb der deutschen Forschungslandschaft. Das Forschungszentrum verfügt über eine leistungsfähige wissenschaftliche Infrastruktur. Es pflegt intensive Kooperationen mit den Universitäten und widmet sich gezielt der Förderung des wissenschaftlichen Nachwuchses.

Das Forschungszentrum Karlsruhe hat zurzeit ein jährliches Budget von ca. 350 Mio. € und beschäftigt rund 3.800 Mitarbeiter und Mitarbeiterinnen. Weitere Informationen sind im Internet unter **www.fzk.de** zu entnehmen.

Zum 1. Oktober 2006 ist die Stelle des/der

Wissenschaftlichen Vorstandsvorsitzenden/ Geschäftsführers/-führerin

neu zu besetzen.

Der Wissenschaftliche Vorstand verantwortet die wissenschaftliche Ausrichtung des Forschungszentrums. Der/die künftige Vorstandsvorsitzende repräsentiert das Zentrum und seine Forschung nach außen, insbesondere an der Schnittstelle von Wissenschaft und Politik, kennt das deutsche und europäische Wissenschaftssystem und ist unternehmerisch orientiert. Er/sie soll die weitere Schärfung des Profils und die strukturelle Weiterentwicklung des Zentrums im Rahmen der programmorientierten Förderung der Helmholtz-Gemeinschaft und im internationalen Wettbewerb vorantreiben.

Die zu besetzende Position erfordert überzeugende Führungseigenschaften, Entscheidungskraft, Kontaktfreude sowie die Bereitschaft und Fähigkeit zu Kommunikation und Motivation. Ein anerkanntes wissenschaftliches Profil ist ebenso erforderlich wie umfassende Management-Erfahrungen mit komplexen Organisationen sowie eine ausgewiesene Kompetenz in der Vermittlung von Forschung und Wissenschaft. Erwartet werden insbesondere die Fähigkeit zur konzeptionellen Planung, Gestaltungs- und Durchsetzungsfähigkeit sowie Erfahrungen in der internationalen Zusammenarbeit.

Die Bestellung erfolgt für die Dauer von fünf Jahren. Eine Wiederbestellung ist möglich. Die Vergütung entspricht internationalen Maßstäben.

Die Mitglieder der Helmholtz-Gemeinschaft haben sich die Förderung von Frauen in Führungspositionen zum Ziel gesetzt. Bewerbungen von Frauen werden daher ausdrücklich begrüßt.

Bitte richten Sie Ihre Bewerbung mit aussagefähigen Unterlagen innerhalb einer Frist von 6 Wochen nach Erscheinen dieser Anzeige:

An den
Vorsitzenden des Aufsichtsrats der
Forschungszentrum Karlsruhe GmbH
- Herrn MinDir Dr. Hermann Schunck -
z. Hd. Frau Dr. Beatrix Vierkorn-Rudolph
- persönlich -
im Bundesministerium für Bildung und Forschung
53175 Bonn

PEW Latin American FELLOWS PROGRAM in the BIOMEDICAL S·C·I·E·N·C·E·S

The Pew Latin American Fellows Program in the Biomedical Sciences provides support for young scientists from Latin America for post-doctoral training in the United States.

The sixteenth class of Fellows will be selected in 2006. An award of $50,000 will be provided as a salary stipend for the fellow during the period of training (2 years) and will be administered by the sponsoring U.S. institution. The sponsoring institution is required to supplement the salary stipend with at least $5,000 a year and to provide full medical benefits for the fellow. Following the two year fellowship, the Program will issue an additional $35,000 award to the sponsoring institution to purchase equipment and supplies for the fellow to establish a laboratory in his or her home country.

Applicants must have held a Ph.D. and/or M.D. degree, or equivalent, for no more than five years as of July 1, 2006. Applicants who received their degree from schools in the U.S., Canada or Europe will not be accepted. Applicants may not have had previous post-doctoral training outside of Latin America, nor may they have begun a post-doctoral position in the U.S. prior to July 1, 2005. Applicants are not required to have a commitment of a position and laboratory space after the fellowship. However, applicants must submit a written statement of intent to return to Latin America. Fellows must accept a position and have confirmed laboratory space in Latin America by the end of the fellowship period in order to obtain the $35,000 portion of the award.

Fellows will be selected on the basis of their promise as outstanding investigators, as well as the scientific merit of their research proposal, their record of training and how well their interests coincide with the laboratory of their sponsor in the United States. If potential applicants need assistance with the identification of an appropriate sponsoring laboratory in the United States, they may contact the Program Office before August 1, 2005. The program will accept applications from Mexico, Central and South America. Applications may be obtained from the Regional Committee contact listed here for each country or from our website at: **www.pewlatinfellows.com**

The application deadline is September 30, 2005. Winners will be notified in April 2006 and the fellowship should begin no later than August 2006.

APPLICATION DEADLINE IS SEPTEMBER 30, 2005

ARGENTINA
Ana Belén Elgoyhen, Chair
Instituto de Investigaciones en Ingeniería Genética y Biología Molecular
Phone: (5411)(4) 783-2871
Fax: (5411)(4) 786-8578
E-mail elgoyhen@dna.uba.ar

BRASIL
Patricia T. Bozza, Chair
Fundacao Oswaldo Cruz
Laboratorio de Imunofarmacologia
Phone: (5521) 2598-4492 Ext. 221
Fax: (5521) 2590-9490
E-mail: pbozza@ioc.fiocruz.br

CHILE
Manuel Kukuljan, Chair
Universidad de Chile
Instituto de Ciencias Biomédicas
Phone: (562) 678-6707
Fax: (562) 777-6916
E-mail: kukuljan@neuro.med.uchile.cl

MEXICO
Mario Zurita, Chair
Universidad Nacional Autónoma de México
Instituto de Biotecnología
Phone: (52)(555) 622-7659
Fax: (52)(777) 317-2388
E-mail: marioz@ibt.unam.mx

All Other Countries
Silvia Montano de Jiménez
The Pew Latin American Fellows Program
3333 California Street, Suite 410
San Francisco, CA 94118
Phone: (415) 476-5116
Fax: (415) 502-4992
E-mail: montano@thecenter.ucsf.edu

The University of Ottawa Heart Institute is recruiting a leader in atherosclerosis research to fill the position of

MERCK FROSST CANADA CHAIR IN ATHEROSCLEROSIS

The Heart Institute is the largest cardiac care centre in Eastern Ontario and is establishing a major focus in the area of genomic approaches to the study of cardiac disease. The Institute seeks a candidate at the level of Associate or Full Professor with expertise in areas such as epigenetics, genetic modifiers of Mendelian disorders, the study of complex traits and cardiovascular genomics.

The individual holding the chair will be an established investigator holding a PhD, MD or MD/PhD degree and will be based at the University of Ottawa Heart Institute. The mandate of the Chair is to carry out leading research in keeping with the vision and objectives of the University of Ottawa Heart Institute. The University of Ottawa biomedical research community is one of the fastest growing in Canada and the city provides a unique environment with great outdoor and cultural activities.

Please forward applications to:
Dr. Ruth McPherson
Professor of Medicine
Chair, Research Sub Committee
University of Ottawa Heart Institute
40 Ruskin Street
Ottawa, Ontario K1Y4W7
Fax: 761-5281

Creighton UNIVERSITY Medical Center

School of Medicine
Department of Microbiology and Immunology
Chair, Professor-Tenure Track

Creighton University School of Medicine invites applications and nominations for Chair of the Department of Microbiology and Immunology. Information about the department can be found at **http://mmi.creighton.edu**. The school is seeking an individual with leadership ability and administrative experience who will work with faculty, other chairs, students, and senior administration to promote excellence in meeting all missions of the department, school, and university. The major responsibilities of the Chair are to promote high quality scholarship by faculty and students, provide leadership in creating and implementing a vision to enhance existing programs and develop new initiatives, and to oversee teaching and research in the department.

Applicants should have a Ph.D. and/or MD. The successful candidate must have a record of distinguished research accomplishments highlighted by publications in peer-reviewed journals, and a research program supported by ongoing extramural funding. A strong commitment to mentoring in order to promote professional growth and development of faculty in the department, and to establishing collaboration with faculty in other basic and clinical science departments is essential.

The School of Medicine is one of nine schools or colleges at Creighton University including professional schools of Business, Law, Nursing, Dentistry, Pharmacy and Health Professions, and a Graduate School. Founded in 1878, Creighton University is a Catholic, Jesuit institution with an enrollment of approximately 6725 students. It is consistently ranked as one of the finest comprehensive universities in the nation by U. S. News and World Report and regularly appears in Best Buys in American Colleges.

Applications will be accepted until the position is filled.

A *Curriculum Vitae* and letter of application that includes a description of administrative and teaching experiences, current and future research activities and funding sources, and the names and contact information of three references may be submitted by mail or e-mail to: **John A. Yee, Ph.D., Professor, Chairman, Microbiology and Immunology Search Committee, Department of Biomedical Sciences, School of Medicine, Creighton University, 2500 California Plaza, Omaha, NE 68178; jayee@creighton.edu**.

Women and minority candidates are encouraged to apply.
Creighton University is an Equal Opportunity, Affirmative Action Employer.

POSITIONS OPEN

CENTER FOR MEMBRANE BIOLOGY
Case Western Reserve University

The newly established Case Center for Membrane Biology (CMB) invites applications for nontenure-track faculty positions at the **ASSISTANT PROFESSOR** level. The Center, based in the Department of Pharmacology at the Case School of Medicine, serves as an interdisciplinary bridge for basic and clinical investigations throughout the University, its hospital systems, and the City of Cleveland. Superb physical and fiscal resources have been provided to the CMB for creation of a world-class program. We are seeking highly motivated individuals with expertise in two-photon microscopy and cell biology to support research and teaching programs integral to the Center's mission. In the near future the Center anticipates announcing opportunities for tenure-track faculty positions as well. We offer a competitive compensation package, the chance to join this new program at its outset and influence its future direction and choice of state-of-the-art research facilities. A Ph.D. or other appropriate terminal degree(s) and three years post-degree experience are required. Submit curriculum vitae, a brief statement of research interest(s), three representative reprints, and the names, addresses, e-mails, and telephone numbers of three references electronically, addressed to: **Krzysztof Palczewski, Ph.D., c/o e-mail: michael.maguire@cwru.edu.**

In employment, as in education, Case Western Reserve University is committed to Equal Opportunity and World Class Diversity.

POSTDOCTORAL FELLOW sought to join pulmonary biology group at Columbia University studying mouse alveolar epithelial ion transport using in vivo physiologic models. Qualified individuals will have at least one year of experience with small animal surgery (mice) and physiologic models. Familiarity with general laboratory techniques and strong communication and writing skills required. Interested individuals should contact: **Dr. P. Factor** at **e-mail: phf2103@columbia.edu.** *Columbia University is an Affirmative Action/Equal Opportunity Employer.*

POSITIONS OPEN

Western University OF HEALTH SCIENCES
The discipline of learning. The art of caring.

PART/FULL-TIME MEDICAL SCHOOL INSTRUCTIONAL FACULTY

The Western University of Health Sciences, College of Osteopathic Medicine of the Pacific (COMP) is looking for part-time/full-time faculty in the areas of gross anatomy, cell biology, molecular biology, biochemistry, genetics, pharmacology, and medical statistic for first and second year medical students. Experienced medical school teaching professionals need only apply. Salary is commensurate with the number of hours taught and the qualifications of the applicants. Transportation and housing can be provided, if necessary, for applicants not located in the general area of Los Angeles, California. COMP is located in Los Angeles County; freeway minutes from the mountains, deserts, and Pacific Ocean. Please write to: **Nissar A. Darmani, Ph.D.** at **e-mail: ndarmani@westernu.edu.**

The Department of Medicine at the University of California San Francisco (UCSF) is recruiting physician-scientists engaged in translational research. Candidates must have an M.D. or M.D./Ph.D. degree and demonstrated potential to lead a first-rate and independent research program. Board certification in internal medicine is required. Appointments will be made at the **ASSISTANT/ASSOCIATE PROFESSOR** level in the In-Residence series, depending upon qualifications. The candidate will also become a member of the graduate program in Biomedical Sciences. Please send curriculum vitae to:

Joseph M. McCune, M.D., Ph.D.
Chair Search Committee
Gladstone Institute of Virology and Immunology
1650 Owens Street
San Francisco, CA 94158

UCSF is an Affirmative Action/Equal Opportunity Employer. The University undertakes affirmative action to assure equal employment opportunity for underutilized minorities and women, for persons with disabilities, and for Vietnam-era veterans and special disabled veterans.

POSTDOCTORAL RESEARCH POSITION
Protein microarrays and human host-pathogen interactions

The U.S. Army Medical Research Institute of Infectious Diseases (USAMRIID) in Frederick, Maryland, has a research appointment available for a highly motivated and qualified candidate with a Ph.D. or M.D. and zero to five years relevant post-graduate experience. Responsibilities include developing new protein microarray platforms and validating analytical assays. Stipend is competitive and will be commensurate with experience. *U.S. citizenship or permanent residence status required.* To apply, please forward a cover letter and curriculum vitae to: **Oak Ridge Institute for Science and Education (ORISE), Maryland, Attn: Kim Myers (e-mail: kim.myers3@us.army.mil).** Please reference project #MRMC 02-05.

Two NIH-funded **POSTDOCTORAL POSITIONS** are available immediately at Florida International University (FIU) Department of Chemistry and Biochemistry to study transcription-coupled DNA supercoiling and to study structure-activity relationship of metalloproteins. A Ph.D. is required. Strong background in biochemistry, molecular biology, microbiology, bio-inorganic chemistry, or protein chemistry is preferred. If interested in transcription-coupled DNA supercoiling, please send curriculum vitae and three reference letters to: **Dr. Fenfei Leng** at **e-mail: lengf@fiu.edu.** If interested in metalloprotein chemistry, please send curriculum vitae and three reference letters to: **Dr. Xiaotang Wang** at **e-mail: wangx@fiu.edu. Website: http://www.fiu.edu/~lengf.** *FIU is an Equal Opportunity/Affirmative Action Employer.*

POSITIONS OPEN

THE CHINESE UNIVERSITY OF HONG KONG

The Department of Biochemistry invites applications for the post(s) of **ASSOCIATE PROFESSOR(S)/ASSISTANT PROFESSOR(S)** (Reference 05/110(665)/2). Applicants should have (i) a Ph.D. degree in biological sciences; (ii) postdoctoral research experience; and (iii) a demonstrated record of research accomplishments. The appointees will (a) teach undergraduate and postgraduate courses (including advanced courses in their specialty); (b) work on either neuroscience/stem cell research; or fermentation, medical biotechnology/bioengineering; (c) capitalize on the well-established infrastructure in the Department for independent research in their fields of expertise, and collaborate with the present research teams; (d) supervise postgraduate students; and (e) participate in administration. For information about the Department, please visit **website: http://www.bch.cuhk.edu.hk.** Appointments will initially be made on a fixed-term contract basis for two to three years, with prospect for renewal or a longer-term appointment thereafter subject to mutual agreement. Salary will be highly competitive, commensurate with qualifications and experience. The University offers a comprehensive fringe benefit package, including medical care, plus a contract-end gratuity for appointments of two years or longer and housing benefits for eligible appointees. Further information about the University and the general terms of service for appointments is available at **website: http://www.cuhk.edu.hk/personnel.** The terms mentioned herein are for reference only and are subject to revision by the University. Please send full resume, copies of academic credentials, a publication list, and/or abstracts of selected published papers, together with names, addresses, and fax numbers/e-mail addresses of three references to whom applicants' consent has been given for their providing references (unless otherwise specified), to: **Personnel Office, The Chinese University of Hong Kong, Shatin, New Territories, Hong Kong (fax: 852-2603-6852)** on or before 23 July 2005. The Personal Information Collection Statement will be provided upon request. Please quote the reference number and mark Application–Confidential on cover.

Two **RESEARCH SCIENTIST** positions are available in the area of atherosclerosis and intracellular signaling in vascular disease.

(1). To investigate niacin, high-density lipoprotein (HDL) metabolism and atherosclerosis. A highly motivated individual with Ph.D. or M.S. and experience in cellular/molecular biology, in-vivo animal studies, and receptor assays, is encouraged to apply.

(2). To investigate intracellular signaling pathways involved in atherogenic lipoprotein-mediated cellular responses in vascular and glomerular cells. Motivated candidate with Ph.D. and experience in cell signaling and protein phosphorylation, receptor biology, cellular transfection, is encouraged to apply. *Applicants should be U.S. citizens or have a valid U.S. visa.* Please send resume to: **Dr. Moti L. Kashyap** (for position one) or **Dr. Vijay Kamanna** (for position two), **Department of Veterans Affairs Healthcare System, 5901 East 7th Street (151), Long Beach, CA 90822. E-mails: moti.kashyap@med.va.gov** or **vaijinath.kamanna@med.va.gov.**

POSTDOCTORAL FELLOWSHIP IN PSYCHIATRIC GENETICS
Johns Hopkins University School of Medicine

A Postdoctoral Fellowship is available for the study of epigenetic factors in bipolar disorder and major depression, focusing on high throughput approaches to allele-specific gene expression and methylation analysis. The candidate should be a recent recipient of a Ph.D. or M.D./Ph.D. with good publication(s) in genetics or genomics. Please send curriculum vitae and names and e-mail addresses of three references to: **Drs. Andrew P. Feinberg and James Potash, Johns Hopkins University School of Medicine** at **e-mails: afeinberg@jhu.edu** and **jpotash@jhmi.edu.** *Johns Hopkins University is an Equal Opportunity/Affirmative Action Employer.*

POSITIONS OPEN

POSTDOCTORAL AND CLINICAL FELLOWSHIPS
at the
National Institutes of Health
U.S. Department of Health and Human Services

Website: http://www.training.nih.gov

NIH is dedicated to building a diverse community in its training and employment programs.

The University of Wisconsin-Madison School of Pharmacy is seeking exceptional candidates at the rank of **ASSISTANT, ASSOCIATE,** or **FULL PROFESSOR** in the area of pharmacology, toxicology, or related pharmaceutical sciences. The successful candidate will have a Ph.D. or M.D. and be expected to establish an independent and externally funded research program, supervise graduate students, and teach pharmacology at the professional, graduate, and undergraduate levels. This University has a strong history of collaborative and interdisciplinary research excellence in the biological sciences. We seek individuals whose scientific interests complement existing faculty strengths. Areas of research interest include, but are not limited to, developmental biology, development and application of unique model organisms, impact of small molecules upon human disease, neuroscience, chemical genetics, toxicology, and/or pharmacology.

Refer to **website: http://www.ohr.wisc.edu/pvl/pv_050727.html** for further details.

Please send curriculum vitae, statement of research interest, and three letters of recommendation to: **Pratima Sharma, 777 Highland Avenue, Madison, WI 53705-2222.**

Unless confidentiality is requested in writing, information regarding the applicants must be released upon request. Finalists cannot be guaranteed confidentiality.

The University of Wisconsin is an Equal Opportunity Employer.

Columbia University-Department of Surgery is seeking an **ASSOCIATE RESEARCH SCIENTIST,** preferably with a Pharm.D. background, to direct the clinical research effort in the Center for Liver Disease and Transplantation. The candidate must have experience and expertise in designing and executing clinical research projects, including protocol development, institutional review boards process, budgets, and collection of specimens and data. Knowledge and experience in hepatitis and liver transplant research protocols are also required. The appropriate candidate must be extremely well organized and versed at data acquisition and analysis, as well as having computerized database management skills.

Candidates should mail curriculum vitae to: **Robert S. Brown, Jr., M.D., M.P.H., 622 West 168th Street, PH 14 Center, New York, NY 10032.**

Columbia University is an Equal Opportunity/Affirmative Action Employer.

MEDICAL WRITERS

Accel Health, an internationally recognized medical education agency that prepares publications and other educational materials for its pharmaceutical company clients, is currently seeking medical writers. The ideal candidate will have an advanced degree (Pharm.D., Ph.D., or M.D.). The positions' core responsibilities are the production of a variety of educational products, written in clear and scientifically accurate prose. Candidates must enjoy writing and display outstanding writing skills. They must be able to integrate information quickly and work to tight deadlines in a team environment. Interfacing with people is an essential component of the job, requiring excellent interpersonal skills. All positions are based in New York City. Competitive salary, full benefits. If interested, please send resume to **e-mail: serena_stanley@accelhealth.com.**

POSITIONS OPEN

TENURE-TRACK FACULTY POSITION IMMUNOLOGY

The George Washington University Medical Center is expanding its program in the Department of Microbiology, Immunology, and Tropical Medicine (**websites: http://www.gwumc.edu/microbiology** and **http://www.gwumc.edu/immunology**) as part of its growing commitment towards basic science research with a particular focus on infectious disease, cancer, and cardiovascular biology. We are now seeking applicants for a tenure-track position at the **ASSISTANT/ASSOCIATE PROFESSOR** level. Although the selected candidate must come with extramurally funded research in any area of immunology, we are particularly interested in recruiting an investigator in the area of host-pathogen interactions. The successful candidate will be expected to complement existing strengths within the Department of Microbiology, Immunology, and Tropical Medicine including: molecular parasitology, retrovirology, host-pathogen interactions, inflammation, and/or vaccine development. Faculty candidates will be required to participate in graduate and medical student immunology teaching responsibilities.

Required: A Ph.D., M.D., or M.D./Ph.D. with postdoctoral training in microbiology, immunology, or infectious disease, an extramurally funded research program in immunology, and interest in teaching. Preferred qualifications: Demonstrated interest and expertise in the area of host-pathogen interactions.

The George Washington University Medical Center has extensive core facility support including The Catherine Birch McCormick Genomics Center, state-of-the-art flow cytometry core facility, barrier animal facility, and a BSL-3 laboratory, and enjoys close collaborative ties with investigators at Children's National Medical Center, The Institute for Genomic Research, and the NIH.

Review of applications will begin on September 20, 2005, and will continue until the position is filled. To apply send or e-mail curriculum vitae, a one- to two-page statement outlining research and teaching interests, and the names of three references to:

David Leitenberg, M.D., Ph.D.
Department of Microbiology, Immunology, and Tropical Medicine
The George Washington University
Ross Hall, Room 411
2300 I Street, N.W.
Washington, DC 20037
Telephone: 202-994-9475
Fax: 202-994-9420
E-mail: dleit@gwu.edu

The George Washington University is an Equal Opportunity/Affirmative Action Employer.

ANATOMIST (CHAIR)

The American University of the Caribbean (AUC), a 25-plus-year-old accredited medical school with over 3,000 graduate physicians is pleased to announce an opening for the Chair of Anatomy, Ph.D., and/or M.D. Rank is commensurate with experience.

We seek an individual with experience and expertise, who both enjoys and is dedicated to teaching. The courses in anatomy and/or histology/embryology are team taught, and active research is in place. Individuals familiar with U.S. medical education and evaluation systems are encouraged to apply. All lectures are in English, with PowerPoint formats preferred. Anatomy laboratories are ongoing.

The majority of the basic science AUC faculty is drawn from North America and the European Union. Clinical clerkships occur in the United States, United Kingdom, and Ireland.

AUC (**website: http://www.aucmed.edu**) is in a new, up-to-date facility on the delightful island of St. Maarten, in the Netherlands, Antilles, some three hours by air from Miami, Florida.

Interested parties should send their curriculum vitae, and the names of three references with coordinates, to: **B. Salafsky, Ph.D., Dean, Basic Sciences** via **e-mail: buzs@aucmed.edu.**

POSITIONS OPEN

USDA ARS Agricultural Research Service
www.ars.usda.gov

SUPERVISORY RESEARCH FOOD TECHNOLOGIST/RESEARCH CHEMIST/GENETICIST (PLANTS), GS-1382/1320/440-14/15, GS-14 ($85,123.00 to $110,662.00 per year), GS-15 ($100,129.00 to $130,173.00 per year), U.S. Department of Agriculture, Agricultural Research Service.

Soft Wheat Quality Research Laboratory, Wooster, Ohio. The incumbent will serve as the Research Leader of the Soft Wheat Quality Research Laboratory (SWQL). The mission of the SWQL is to evaluate quality of soft wheat breeding lines and cultivars to ensure maintenance and/or improvement of milling and baking quality, and develop new or improved methods for measuring and predicting quality. The assignment will identify genetic and environmental influences on the improvement of wheat quality that could increase the domestic and exported value-added potential of the soft wheat crop. The incumbent will be responsible for planning, organizing, enhancing, and maintaining the creativity and productivity of the unit; provide supervision over scientists and support personnel assigned to the unit; hire personnel and manage the human, fiscal, and physical resources; serve as the Unit fund holder; provide technical information and consultation as well as ensure the proper interpretation and reporting of scientific research results and information. As Research Leader, conducts individual and team research aimed at developing and improving procedures and methods that practically and quickly identify and evaluate new and important wheat and flour quality parameters. A degree in food technology, microbiology, biology, chemistry, physics, genetics, or a related discipline or field of biological or physical science is required as described in the announcement. For details and application directions, visit the **website: http://www.afm.ars.usda.gov/hrd** and refer to announcement ARS-X5W-0136. To receive a printed copy by mail, **telephone: 301-504-1482.** *U.S. citizenship and pre-employment background investigation required.* Application must be postmarked by July 29, 2005. Opening date: June 20, 2005. Closing date: July 29, 2005. *USDA/ARS is an Equal Opportunity Employer and Provider.*

ASSISTANT/ASSOCIATE/FULL PROFESSOR
Forest Hydrology–Search Extended

The School of Forestry and Wildlife Sciences at Auburn University invites nominations and applications for the position of Assistant/Associate/Full Professor, forest hydrology. This is a 12-month, tenure-track position with 90 percent research and 10 percent teaching responsibilities. Review of applications will begin October 31, 2005. For details, see **website: http://www.forestry.auburn.edu** or contact: **Dr. Graeme Lockaby, Chair, Search Committee** at **telephone: 334-844-1054, fax: 334-844-1084,** or **e-mail: lockaby@auburn.edu.** *Affirmative Action/Equal Opportunity Employer. Women and ethnic minorities are encouraged to apply.*

SOFTWARE ENGINEER–Proteomics: Design, develop, implement software tools for computational analysis of proteomics data. Requirements: M.S. in physics-field (astrophysics, biophysics, or geophysics) or equivalent; and six months work/academic experience designing and implementing dynamic websites, writing software in support of scientific research, developing database-driven web applications, and specific experience with Linux, Apache, Perl, MySQL, C, and XML. Full-time; Seattle, Washington. Resume to: **Institute for Systems Biology, 1441 N. 34th Street, Seattle, WA 98103** or **e-mail: hr@systemsbiology.org.**

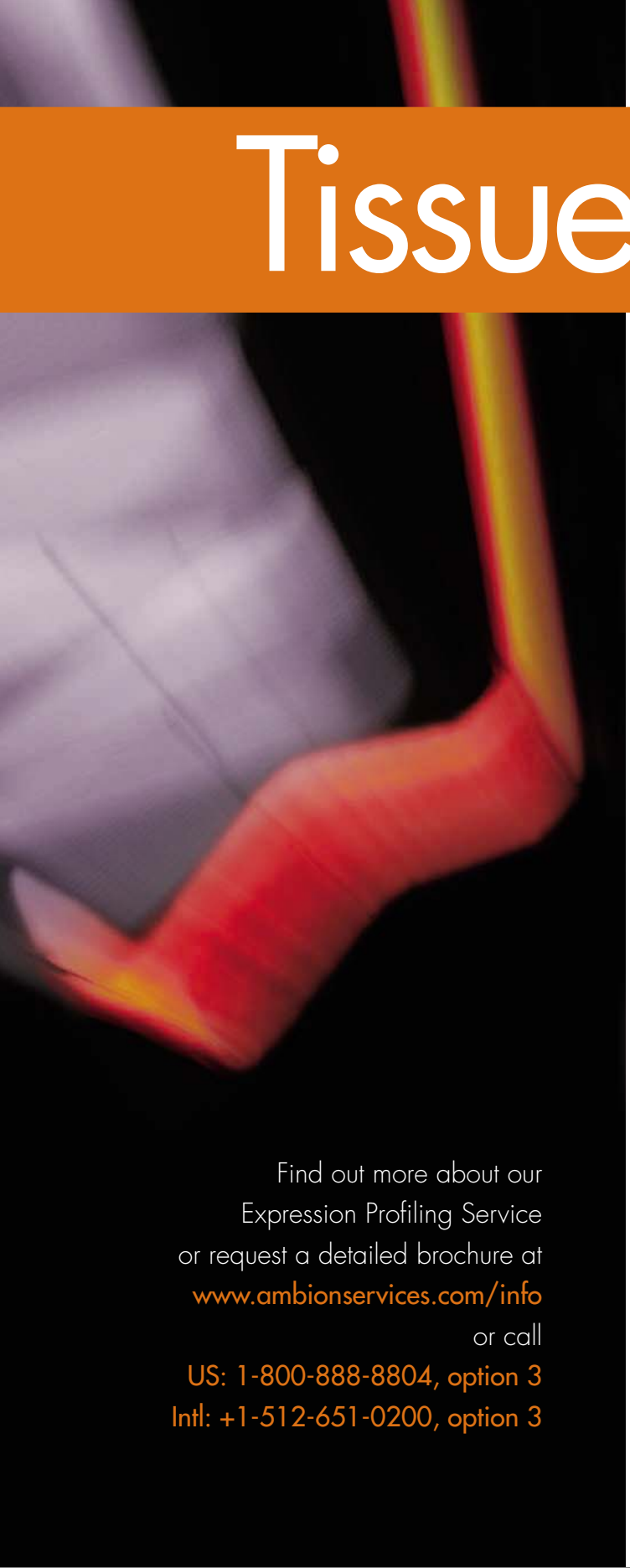

Tissue to Data

Available* from Ambion®– The RNA Company®: Gene Expression Profiling Service for Affymetrix® GeneChip® Arrays

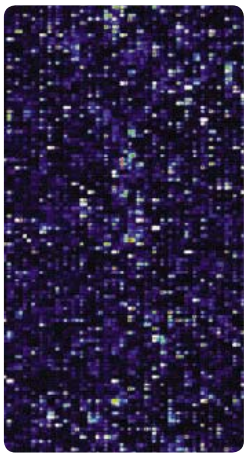

From simple data analysis, to complete experimental design, Ambion Services has one over-riding goal: Maximize meaningful data from microarrays.

Ambion Services includes consultation with a team of highly experienced array and informatics scientists, as well as comprehensive data analysis capabilities.

Ambion Services will work with you to provide the most informative, economical and stress-free approach to undertake and complete your microarray experiments.

Expression Profiling Service currently not available in Japan

Find out more about our Expression Profiling Service or request a detailed brochure at www.ambionservices.com/info or call US: 1-800-888-8804, option 3 Intl: +1-512-651-0200, option 3

Ambion® Services